

University of St Andrews



Full metadata for this thesis is available in
St Andrews Research Repository
at:

<http://research-repository.st-andrews.ac.uk/>

This thesis is protected by original copyright

Investigations into a macrosegregated,
differentiated, dolerite dyke,
northern Skye, Scotland.

Investigations into a mannequin
determined, police type
Northern type, Southern

TL B468

This thesis is dedicated to
my mother, Hilda Kyle.



Acknowledgements

I would like to thank my supervisor, C.H. Donaldson, for suggesting this project, and for his advice, support and patience whilst waiting for its completion. The technical staff at St. Andrews: A. Calder, A. Mackie, D. Herd, J. Allen, R. Batchelor, S. Allison and S. Harvey are thanked for their assistance, as is Gilbert Chalmers for figure preparation. Margaret Hanlin is greatly thanked for childminding my daughter Innes, allowing me to continue my studies.

Special thanks must go to my husband, Phil Leighton for his support and to my father for continuous encouragement and fiscal contributions.

Abstract.

The Mystery Dyke is a differentiated dolerite sheet intruded along hexagonal joints of the Bornaskitaig leaf of the Little Minch Sill Complex (L.M.S.C.), northern Skye. Near-vertical banding parallel to the margins and approximately symmetrical about the median plane is displayed along the exposed 65m length of the dyke. A complete half-transect across the northern part of the dyke, comprising 11 bands distinguished on the basis of modal and textural differences has been obtained. The bands however may change progressively laterally along strike with certain amygdaloidal bands bifurcating both vertically and along strike. Bands of particular interest contain comb-layered olivine- and plagioclase or pyroxene. In the northern part, olivine- and plagioclase are the common comb-layered minerals, while to the south comb-layered pyroxene is more abundant.

Petrographically, the normally porphyritic dyke is diverse, with comb-layering, ophitic, poikiliophitic and trachytic textures and chills developed. Whole-rock analyses of the bands indicate that the dyke consists of three distinct chemical groupings which have a general affinity with the L.M.S.C. picrodolerite analyses of Gibson (1988).

Variation in whole-rock and mineral analyses across the banding may be progressive or abrupt. Comb-layered olivine- and plagioclase have restricted compositions with forsterite content increasing into the bands, towards the centre of the dyke. This suggest that supercooling of magma declined through the growth of these bands (or the melt became magnesium-rich).

The dyke is multiple in type, although the compositional variations are not so great as to merit the term composite. A provisional model of cogenetic pulses of melt plus crystal-mush over a short time period, from a vertically layered, shallow-level chamber similar to that proposed by Gibson and Jones (1991) as the source for the Little Minch Sill Complex is proposed.

Declaration.

I, Alison Helena Kyle hereby certify that this thesis has been composed by myself, that it is a record of my own work, and that it has not been accepted in partial or complete fulfilment of any other degree or professional qualification.

Signed

Date 14th October, 1993.

I certify that the candidate has fulfilled the conditions of the Resolution and Regulations appropriate to the Degree of MSc.

C.H. Donaldson - Supervisor
14 October, 1993

Copyright.

In submitting this thesis to the University of St. Andrews I understand that I am giving permission for it to be made available for use in accordance with the regulations of the University Library for the time being in force, subject to any copyright vested in the work not being affected thereby. I also understand that the title and abstract will be published, and that a copy of the work may be made and supplied to any *bona fide* library or research worker.

Contents

Acknowledgements.....	i
Abstract.....	ii
Declaration.....	iv
Contents.....	v
<u>Chapter 1. Igneous Layering and the "Mystery Dyke".</u>	1
1.0 Introduction	1
1.1 Previous Study of the "Mystery Dyke".....	3
1.2 Regional Geological History.....	4
1.3 Methods and Aims of the Study.....	6
1.4 Note on Geological Site Preservation.....	8
<u>Chapter 2. Field Geology.....</u>	9
2.0 Introduction and External Contact Relations.....	9
2.1 Joint Patterns.....	12
2.2 Curved Concentric Lamination.....	13
2.3 Internal Contacts and Subdivisions of the Dyke.....	14
2.4 The Marginal Unit.....	15
2.5 The Intermediate Unit.....	16
2.6 The Central Unit.....	19
2.7 Typical Cross-Sections from the Three Segments of the Mystery Dyke.....	22
2.7.1 The Northern Segment of the Mystery Dyke.....	22
2.7.2 The Middle Segment of the Mystery Dyke.....	25
2.7.3 The Southern Segment of the Mystery Dyke.....	27
2.8 Possible Extension to the Mystery Dyke.....	29
2.9 Summary.....	30
<u>Chapter 3 Petrography.....</u>	32
3.0 Introduction.....	32
3.1 Discussion of Textural Terminology.....	33
3.2 The Outer Marginal Sub-Unit.....	34
3.3 The Inner Marginal Sub-Unit.....	36
3.3.1 Band 9/174'.....	41
3.4 The Intermediate Unit.....	43
3.5 The Central Unit.....	51
3.6 Internal Variation in Crystal Diameter.....	55
3.7 The Sill.....	55
3.8 Summary.....	58
<u>Chapter 4 Mineral Chemistry.....</u>	62
4.0 Introduction.....	62
4.1 The Study Objectives.....	63
4.2 Olivine.....	64
4.2.1 Phenocrysts.....	64
4.2.2 Matrix.....	66

4.2.3 Comb-Textured Olivines.....	67
4.3 Minor Element variation within Olivine.....	68
4.4 Comparison of Sill and Dyke Olivine.....	69
4.5 Clinopyroxene.....	71
4.5.1 Phenocrysts.....	71
4.5.2 matrix.....	73
4.5.3 Comb-Textured Pyroxene.....	73
4.5.4 Ophitic Pyroxene.....	75
4.6 Minor Element Variation within Pyroxene.....	77
4.7 Plagioclase Feldspar.....	80
4.7.1 Phenocrysts.....	81
4.7.2 Matrix.....	82
4.7.3 Comb-Textured Crystals.....	82
4.8 Sill and Dyke Plagioclase Feldspar Comparison.....	83
4.9 Oxide Minerals.....	84
4.10 Sill and Dyke Oxide Mineral Comparison.....	86
4.11 Accessory Minerals.....	88
4.12 Summary.....	88

Chapter 5 Geochemistry of the Mystery Dyke.....94

5.0 Introduction.....	94
5.1 Major Element Variation with Distance across the dyke.....	100
5.2 Harker-type Plots of the Major Minerals.....	104
5.3 Trace Element Variation with Distance across the dyke.....	105
5.4 Harker-type Plots of the Trace Elements.....	110
5.5 Normative Mineralogy.....	111
5.6 Computer Modelling.....	116
5.7 Relationships between bands in the Southern Segment of the dyke.....	121
5.8 The Relationship between the "Mystery Dyke", Little Minch Sill Complex and the Skye Main Lava Series..	123
5.9 Summary.....	125

Chapter 6 Petrogenesis.....129

6.0 Introduction.....	129
6.1 Direction and Type of Flow.....	130
6.2 Cooling Time and Propagation of the dyke.....	131
6.3 Variation in Band/Unit Thickness.....	133
6.4 Mineral Layering across the dyke.....	134
6.5 Textural Implications.....	135
6.6 Comb-Layering.....	137
6.7 Relationship between Amygdales (zeolite) and Pyroxene.....	143
6.8 Olivine and Melt Equilibrium Compositions.....	146
6.9 Mineral Chemistry.....	147
6.10 Whole-rock Geochemistry.....	151
6.11 Magma evolution in a chamber beneath the dyke....	153
6.12 Relationship between the Dyke and Sills.....	156
6.13 Petrogenetic Processes.....	158

6.14 Summary.....	175
Appendix 5.1.....	177
References.....	180

CHAPTER 1

IGNEOUS LAYERING AND THE "MYSTERY DYKE".

1.0 Introduction.

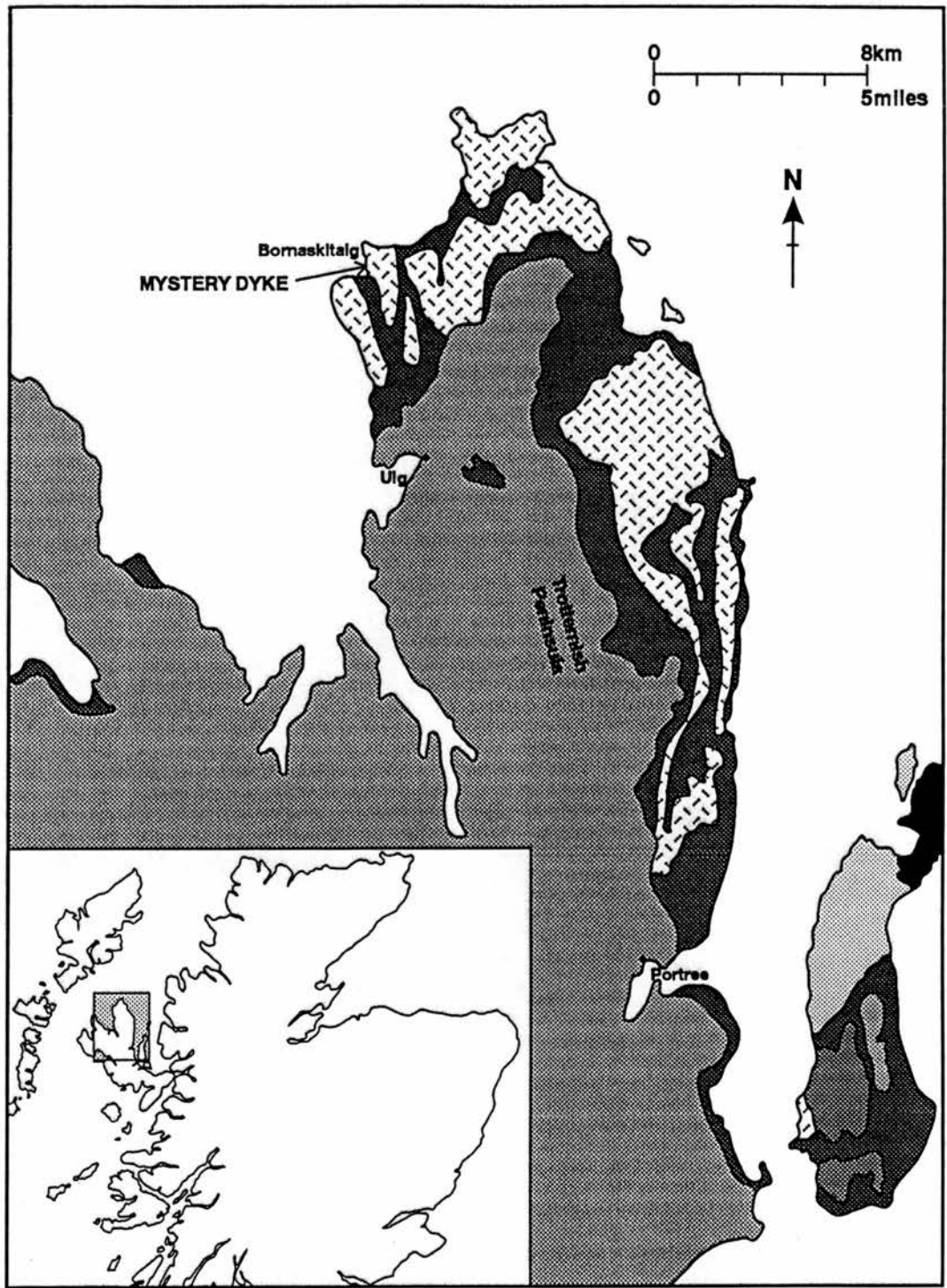
A feature of fascination for most igneous petrologists is layering in igneous intrusions. This has been described within numerous major intrusions ranging in composition from ultrabasic, through basic to acidic, eg Skaergaard (Wager and Deer 1939, McBirney and Noyes 1979), Rhum (Wager and Brown 1951), Bushveld (Hall 1932) and the Nunarssuit Intrusive Complex, Greenland (Harry and Pulvertaft 1963), and also less commonly within minor intrusions, eg a kimberlite dyke at Kimberley, South Africa (Donaldson and Reid 1982), the Dawros ultramafic intrusion, Connemara, Eire (Wager and Brown 1968) and the Eilean Mhuire Sill of the Shiant Isles (Drever 1953). This layering may be cryptic (detectable only by changes in mineral compositions) or modal or textural (both types normally being visible to the naked eye). The origin of layering has been discussed by many authors and is still a controversial issue (Irvine 1979, 1982).

An unusual textural layering developed within some layered bodies consisting of columnar crystals in a

parallel arrangement is commonly referred to as "comb-layering". This thesis presents the results of a reconnaissance study of a differentiated, intricately comb-layered, dolerite dyke in northern Skye. The aim is to understand the origin of the layering and the transport processes within the melt responsible for the modal contrasts existing between layers.

The so-called "Mystery Dyke" is of Tertiary age and is situated on the western coast of the Trotternish Peninsula, the Isle of Skye, Scotland (Figure 1.1). The exposed portion of the dyke measures less than two metres wide by approximately 67 metres. It has near-vertical banding approximately conformable with the walls of the dyke and approximately symmetrical about a central unit. The dyke has intruded one of the Tertiary, alkaline, dolerite-picrodolerite sills that make up the Little Minch Sill Complex (Gibb & Gibson 1989) which has intruded into the Jurassic, Greater Estuarine Series sandstones, shales and shelly limestones.

The dyke was discovered by Dr T. Simkin in the early 1960's, whilst he was investigating the sill complex as a research student under the supervision of Dr H.I. Drever. Dr Drever named the intrusion the "Mystery Dyke" as he knew of no dyke on Skye with comparable layering (Drever 1969). In fact, other layered, differentiated dykes do occur on Skye, in the Strathaird and Sleat peninsulas (Harker 1904, Platten and Watterson 1969). The seven



TERTIARY :

-  GRANITE
-  LITTLE MINCH SILL COMPLEX (L.M.S.C.)
-  SKYE MAIN LAVA SERIES (S.M.L.S.)

PRE-TERTIARY :

-  MESOZOIC SEDIMENTARY ROCKS
-  TORRIDONIAN SEDIMENTARY ROCKS
-  LEWISIAN GNEISSES

Figure 1.1
LOCATION OF THE "MYSTERY DYKE"
AND REGIONAL GEOLOGY OF THE
ISLE OF SKYE, SCOTLAND

dykes noted by Platten and Watterson (1969) are similar in several aspects to the "Mystery Dyke", except that the latter has a more complex zoning pattern across its width. Nonetheless, the name given to this minor intrusion by Drever has become the accepted name, as shown by Bell and Harris (1986).

1.1 Previous Study of the "Mystery Dyke".

Unpublished work completed by other workers includes a map of the banding and an "aerial" photographic sequence along the length of the dyke by Simkin. The photographs were produced during 1982 with the use of a stepladder to give the necessary height. Collections of rock samples by both Drever and Simkin are held at the University of St. Andrews and the Smithsonian Institution, Washington. Drever and Johnston (1972) briefly described the banding and aspects of the crystallographic relationships between the elongate minerals in the comb layers. Drever also described an excursion to the "Mystery Dyke" in the Geologist's Association Guide No. 13, The Tertiary Igneous Geology of the Isle of Skye (1969). During 1985, a St Andrews undergraduate student, David Walker investigated the mineralogy of two selected samples using the electron

microprobe, during a four-week Carnegie Vacation Scholarship and produced an unpublished report.

1.2 Regional Geological History.

Igneous activity commenced during the late Cretaceous in Greenland (Anderton et al 1979), but did not spread to the Isle of Skye until the Tertiary. This activity was related to the opening of the Atlantic Ocean between Greenland and Europe along the Reykjanes Ridge (Upton 1988), possibly as a result of uprise of hot mantle plume near East Greenland (White 1988). Four phases of igneous activity affected the Inner Hebrides (Judd 1874, Geikie 1897, Richey 1961, Anderson and Dunham 1966, Donaldson 1983, Emeleus 1983 and Bell and Harris 1986).

The earliest phase involved the extrusion of the plateau lavas in northern and central Skye, which have an age of approximately 60 Ma (Mussett 1986) and are assumed to have been fed by dolerite dykes. The second phase involved the emplacement of the central intrusion complexes of the Cuillins and the Red Hills at approximately 59-58 Ma (Mussett 1986).

In the third phase, a mafic sill complex intruded the plateau lavas and the underlying Mesozoic rocks in northern Skye. Total sill thickness is approximately

250 metres (Bell and Harris 1986), with individual sills up to 90 metres (Simkin 1965). Anderson and Dunham (1966) state that five distinct rock types are found within the sill complex. These include picrite and picrodolerite (Ru Bornaskitaig and Kilmuir Sills), crinanite and teschenite variants (Rhuba Hunish) and dolerite (The Kilt Rock). The sills in the vicinity of the Mystery Dyke are picrite and picrodolerite. Simkin (1965, 1967) noted differentiation within some of these sills.

In the final event numerous dykes were intruded, radiating from the central intrusion complexes and having an age of approximately 58-50 Ma (Evans et al 1973). Individual dykes are usually less than 2 metres across, are almost vertical and strike north-west to south-east. Most are basalt or dolerite in composition (Bell and Harris 1986). The Mystery Dyke could be one of these late dykes or it could be directly related to the sill complex. This matter is considered further via the chemistry of the dyke and that of the host sill in Chapter 5.

1.3 **Methods and Aims of the Study.**

This reconnaissance study of the "Mystery Dyke" was conducted to acquire geochemical, petrological and mineralogical data from a transect across this small, differentiated intrusion. The conditions of solidification must have been different from the conditions under which the majority of dolerite dykes in Skye consolidated, to allow the complex banding to develop. One possibility to be investigated is that this difference may result from the dyke development being related to the host sill complex.

The origins of differentiation and comb-layering within this small body have general petrological implications as well as importance in understanding the "Mystery Dyke". Differentiation of this small body is shown to have happened quickly (Chapter 6), thus if this rate of differentiation can be shown to occur in larger layered intrusions, the understanding of these large bodies can benefit from studies on smaller bodies such as this.

The study was largely laboratory-based due to restrictions imposed by employment. Field observations were made on five short visits. The dyke was mapped to produce a record of the present-day exposure. This mapping involved measurement of the banding across the dyke at intervals of one foot along the length of the dyke. (Imperial measurements were used to allow ease of

comparison with previous work by Drever and Simkin.) A drill-coring machine was used on one occasion to obtain a small diameter, near-horizontal core through the dyke, from the sill across 75% of the dyke width. The whole dyke was examined in the field which proved it to be very complicated and variable in petrology (Chapters 2 and 3). Time constraints required that investigations be largely confined to the less-banded northern portion with a brief comparative study of the less-banded southern section. (The middle segment is the area exhibiting the most complex banding and comb layering.)

As the dyke is approximately symmetrical about a central band, a large sample was taken (from the northern segment) that covered over one half of the dyke from the contact with the sill. Each band was cut from the sample for analysis. Laboratory methods included: thin section analysis for mineral modal compositions and textures; X-ray fluorescence for whole-rock geochemistry of the bands; crystal compositions were analysed using a Jeol microprobe; and crystallographic data was obtained from orientated sections on the Universal Stage. The data was then compared with other partial transects of the "Mystery Dyke", as well as with data for other comb-layered bodies. From this, a mode of emplacement and solidification history is proposed.

1.4 Note on Geological Site Preservation.

Over the five-year duration of my visits to the Mystery Dyke, the intrusion has been publicised by various methods eg An Excursion Guide to Geology the Isle of Skye by Bell and Harris (1986). The site is now regularly visited by groups of geologists. The destruction being caused by visiting collectors is considerable. As this very small intrusion is of special interest to igneous petrologists, it may be beneficial (even essential) to preserve the remaining outcrop with a voluntary ban on sampling, except where research is to be carried out on the samples collected.

The remainder of this thesis is concerned with the field relations (Chapter 2), petrography and textures (Chapter 3), mineral chemistry (Chapter 4), geochemistry of the layering (Chapter 5) and the development of the dyke (Chapter 6).

CHAPTER 2
FIELD GEOLOGY.

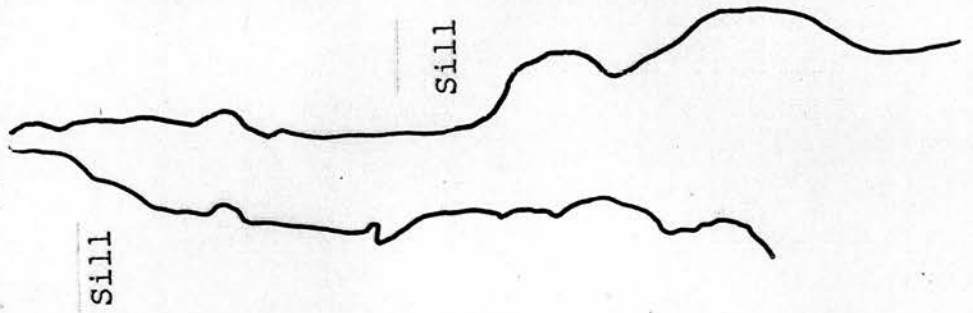
2.0 Introduction and External Contact Relations.

The "Mystery Dyke" is exposed in a wave-cut platform, between a cobble beach to the south and a cliff face to the north (Plate 2.1). It can be traced along the top of the cliff for a short distance by two small insignificant exposures visible through the overburden. It has intruded a hexagonally jointed picrite sill (part of the Trotternish Sill Complex) which is concordant with the Jurassic country rock. North of Bornaskitaig (GR NG405727), the underlying micaceous sandstone dips 10° to 048° , whereas south from Duntulm Castle (GR NG407334), the Jurassic shales and shelly limestones have a regional dip of 16° to 231° . All compass readings are given as magnetic readings.

The dark grey, fine-grained dolerite dyke strikes approximately north-south, but locally deviates in a zigzag fashion, following the cooling joints of the sill. The dyke measures approximately 200' (61m) in length by an average 3' (1m) across. The dyke is approximately

Plate 2.1 General View of the Mystery
Dyke exposure, looking South.

Plate 2.2 Irregular contact of sill and
dyke at 183', showing possible
xenolith of sill.





vertical, the dip varying from 83° to the west through vertical to 71° to the east.

The vertical exposure is very restricted compared to horizontal exposure. Vertical exposure is visible as the dyke lies approximately 2' (0.6m) below Mean High Water Springs (M.H.W.S.) to the south and cuts the cliff face to the north, the top of the cliff being approximately 15' (4.6m) above M.H.W.S.. At intervals along the length of the dyke, vertical faces are present, the maximum height variation being approximately 3' (1m) at 163'-168', with several localities exhibiting a height variation of 1-2' (0.3m-0.6m) eg 100' and 50'.

A detailed map of the present day (1990) exposure was produced (Figure 2.1). This involved the measurement of each band where visible, across the width of the dyke at 1' (0.3m) intervals along the length of the dyke. The distances that are quoted along the length of the dyke follow the deviations in the Central Unit, and are therefore not "true" distances along the strike of the intrusion as measured in a straight line as by Simkin (unpublished). Imperial units were used along the length of the dyke to aid comparison of the results of this work with previous work on the dyke. The exposure is not complete as shown in Figure 2.1, and where the exposure is obscured, the junction between two bands has been estimated.

The banding across the "Mystery Dyke" can be divided into three units which are visible in the field. One unit in particular makes the dyke conspicuous; the Central Unit. On either side of this Central Unit outwards to the dyke margins lie the Intermediate Unit and the Marginal Unit. Previous workers (Drever and Johnston and Simkin) have referred to the Intermediate Unit as the Middle Facies. This term has not been used in this study, to avoid confusion with the Central Unit. The aforementioned workers used the term facies as the collective name for a group of bands, whilst the term "unit" has been used in this study. As the character of the subdivisions within the unit may differ greatly, this precludes the use of the term facies.

The petrographic character of each Unit may change with distance along the dyke: the dyke has been subdivided into three segments along its length at the most appropriate positions. The northern segment is considered to be that portion of the dyke north of 110': the middle segment lies between 110' and 44': and the southern segment is that portion south of 44'. A generalised sketch of the dyke (Figure 2.2) shows the important features discussed with reference to cross sections within each segment (174', 92' and 43').

The contact of the sill and the dyke is irregular and nonplanar, both vertically and horizontally. Vertically, it is irregular and in places this results in

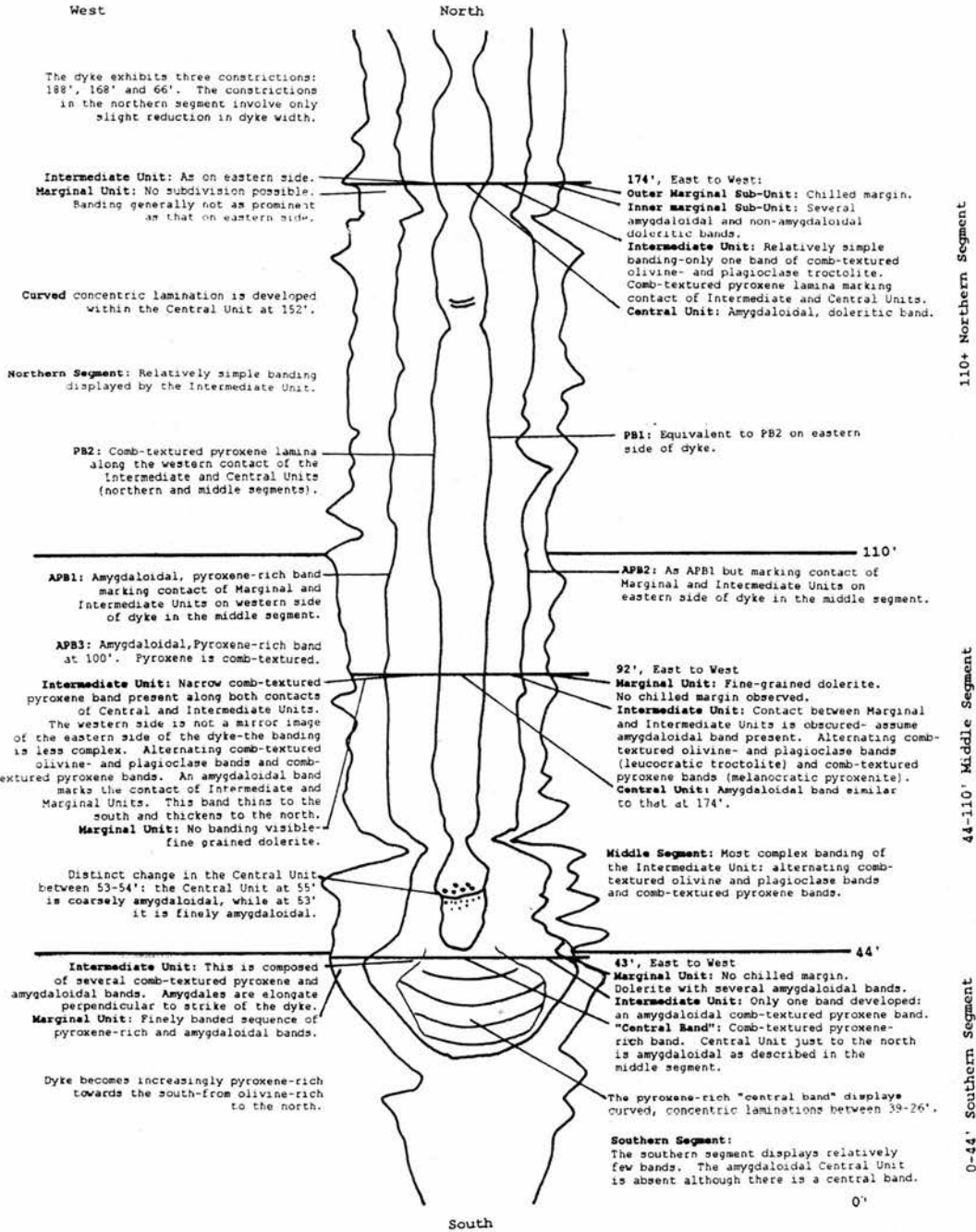


Figure 2.2 Some Important Features of the Mystery Dyke.

a tongue of dyke material protruding into the sill, e.g. 183' and 158' (Plates 2.2, 2.3 and 2.4). At the former distance (Plate 2.2), the sill lenticle enclosed by the dyke may be a xenolith, but present exposure does not permit further comment. The horizontal section is more regular, with the dyke being approximately symmetrical about the Central Unit, although in places, the angularity of the contact and any half-width variation from margin to Central Unit is slightly offset, eg at the constriction at 66' (Plate 2.5 and Figure 2.1). However, towards the south, the contact with the sill and the bands on one side of the dyke may be smoothly curving, whilst on the opposite side they may be angular. This is well displayed at 34' (Plate 2.6).

2.1 Joint Patterns.

In several locations, the Mystery Dyke and the sill exhibit concordant joint patterns with some fractures cutting the sill and the complete width of the dyke. At 152', both dyke and sill are cut by a set of fractures with an approximate strike of 051° , whilst at 155', three vertical joints in the dyke strike 050° , whilst they are slightly offset in the adjacent sill, striking 058° , with the two joints nearest to the contact with the sill becoming part of the hexagonal cooling joint system of

Plate 2.3 General view of the zig-zag,
angular contact of sill and dyke at 158',
and banding in the dyke.

Plate 2.4 Detailed view of the zig-zag,
angular contact of sill and dyke at 158',
showing angular deviation of the
amygdaloidal bands in the Marginal Unit
decreasing with distance from the contact.

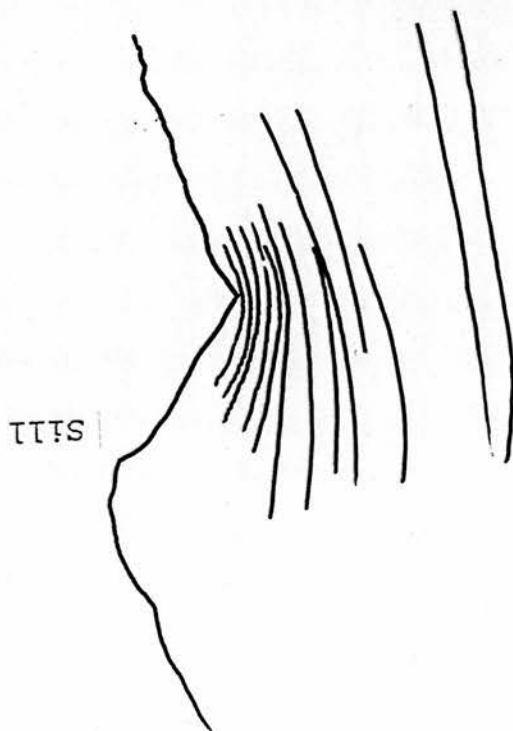
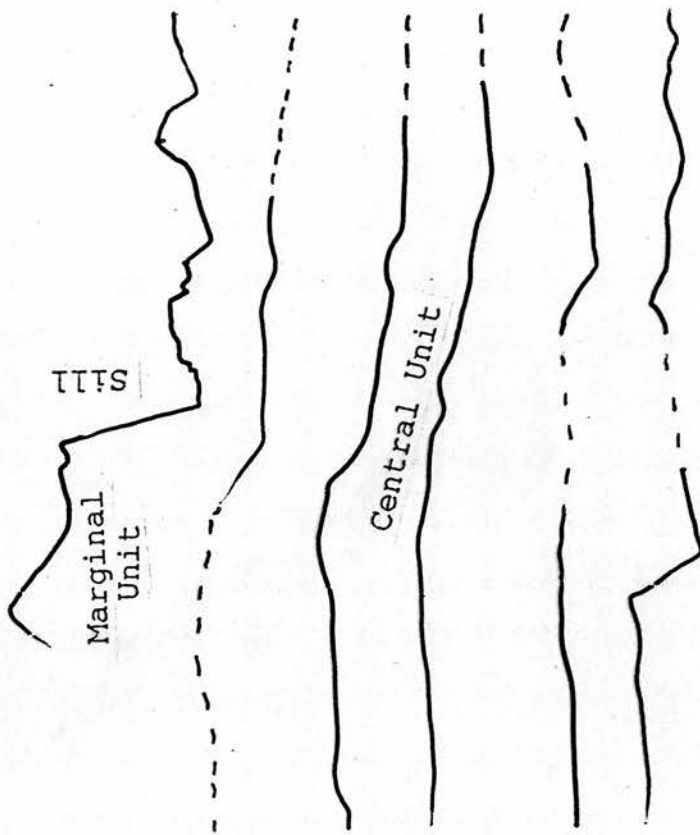




Plate 2.5 View of the constriction of the dyke at 66' showing the skewed, offset angularity of the banding in the dyke and of the sill and dyke contact. (Simkin, 1963)

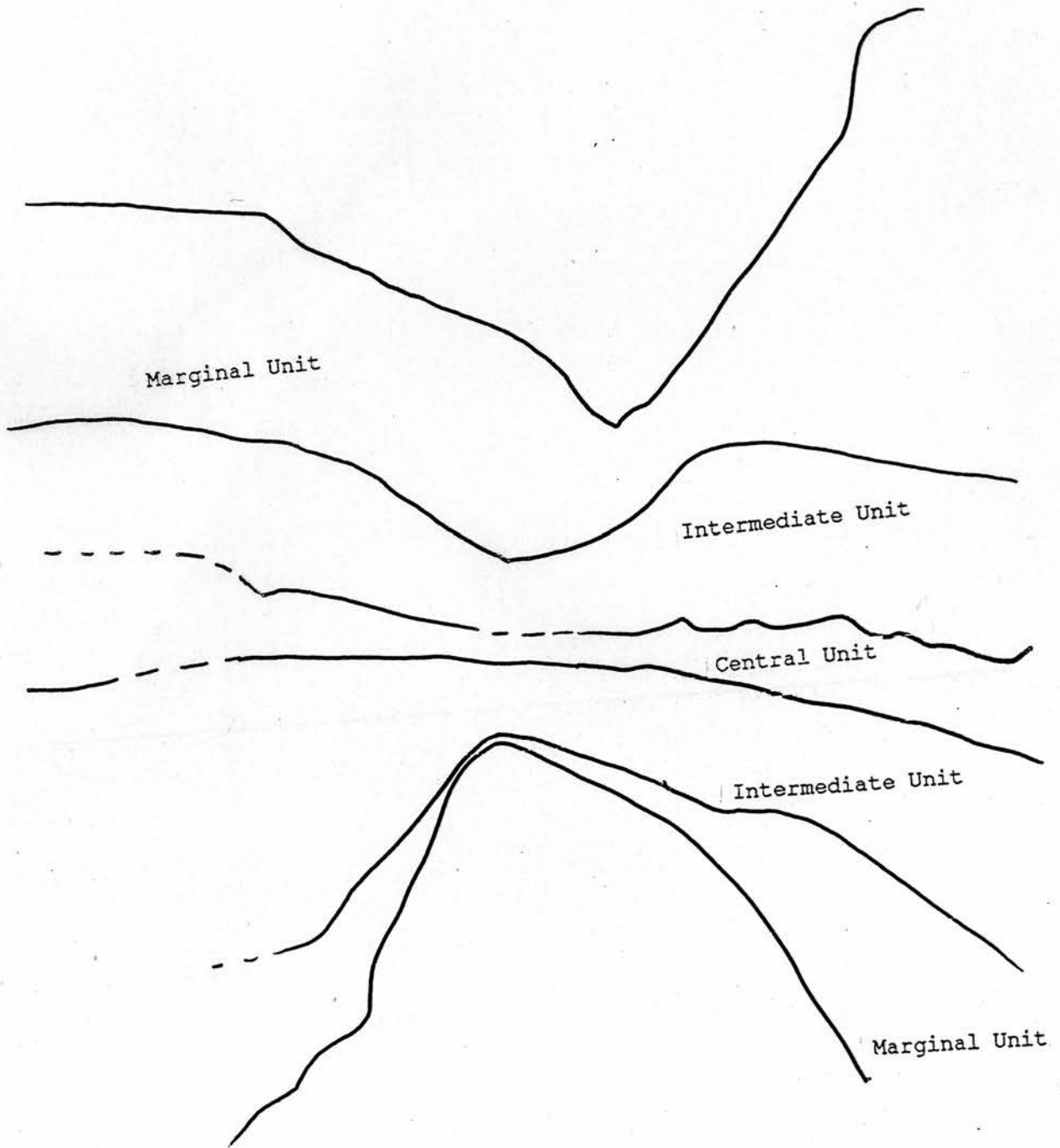




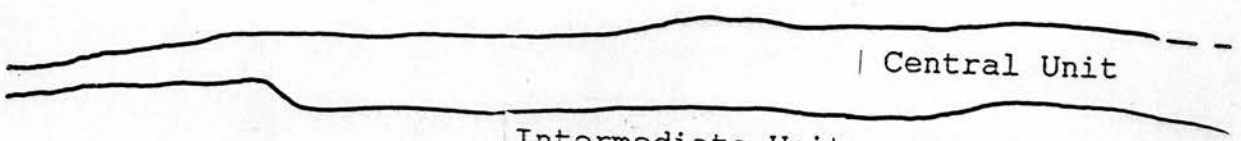
Plate 2.6 The contact of the sill and dyke may be angular on one side, but smoothly curving on the other, as at 34'. The banding in the dyke is curvilinear across the width of the dyke. (Simkin, 1963)

Plate 2.7 Banding visible in the field at 174', and sample collection area.

Marginal Unit

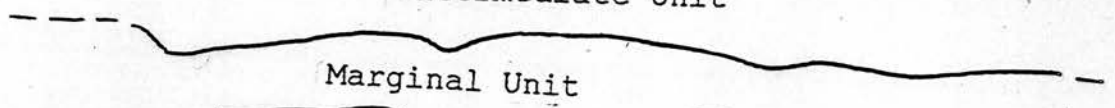


Intermediate Unit



Central Unit

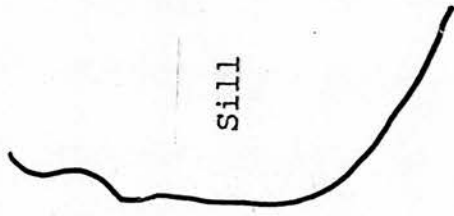
Intermediate Unit



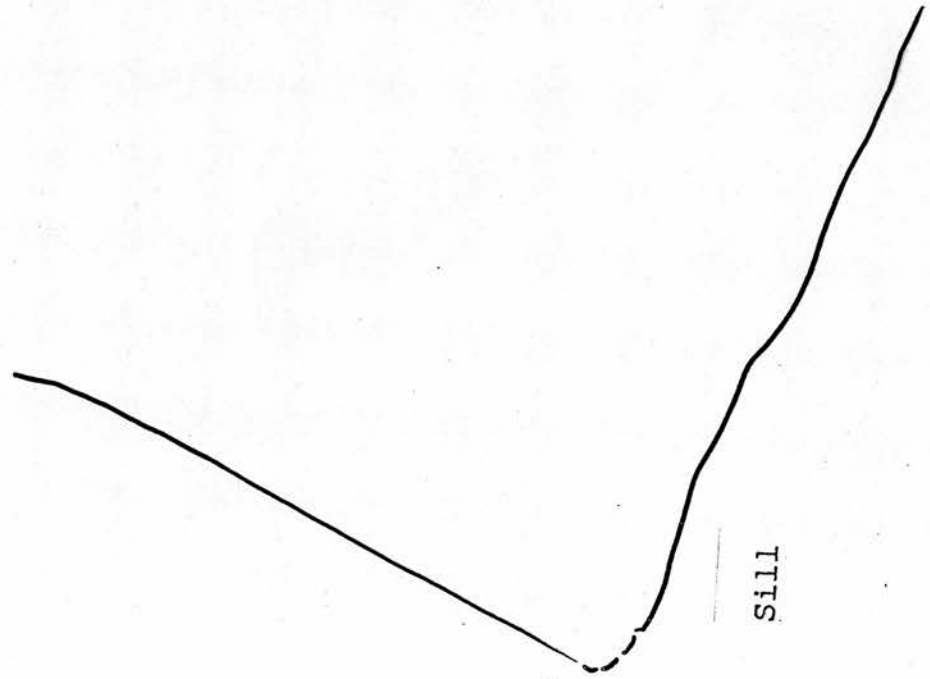
Marginal Unit



Sill



Sill



Sill



the latter. At 139', there is a vertical as well as horizontal exposure exhibiting jointing. Here there is no displacement of the joints as they cross from the sill into the dyke. The joints strike 049° , and dip 80° to 152° , the strike varying slightly to a maximum of 060° . Not all joints are continuous across both dyke and sill, as shown at 160-161', where two sets of joints within the dyke are not obvious within the sill. Since a portion of the joints cut both sill and dyke, the sill must not have completed solidification prior to the intrusion of the dyke.

2.2 Curved Concentric Lamination.

This feature occurs within two areas of the exposed dyke. In the "Central Band" between 26-39', in the southern segment of the dyke, it is highlighted by numerous veins of small amygdaloids. Within the Central Unit at 151-152', in the northern segment, it is highlighted by non-amygdaloidal horizons in the amygdaloidal Unit.

It exhibits a smooth curve convex to the south, and at 39' curves vertically upwards, i.e. a lobate form. At 38' it has a radius of 20cms, whilst at 28', the radii of curvature are 28cms along the strike of the dyke by 30.5cms across the dyke. Here, the "Central Band"

appears to narrow southwards, while the curved laminations appear more pronounced, and have a wider radius.

At 152', the banding appears to be a continuation of the joints developed within the adjacent bands of the dyke. These concentrically banded areas are highlighted by the presence of non-amygdaloidal horizons upto 5mm in thickness within curved bands of amygdaloidal material. Towards the middle of this unit, the amygdales are lathe-shaped and strike approximately perpendicular to the strike of the dyke, whereas close to the contacts of this unit, the amygdales are elongate parallel to the contacts of the unit and strike of the dyke.

2.3 Internal Contacts and Subdivisions of the Dyke.

Figure 2.1 displays the complex banding exposed between 1986 and 1990, with a generalised view shown in Figure 2.2. The Central Unit for the northern and middle segments of the dyke is conspicuously amygdaloidal. If this unit continues into the southern segment it is non-amygdaloidal.

The Intermediate Unit displays the greatest variation in textures and layers visible in the field. In the northern segment, it is olivine- and plagioclase feldspar comb-layered and contains relatively few bands.

In the middle segment, the unit exhibits a complex pattern of olivine- and plagioclase comb-layers alternating with pyroxene comb-layers, while the unit is pyroxene comb-layered in the southern segment (Figures 2.1 and 2.2).

The Marginal Unit has been subdivided into the Outer and Inner Marginal Sub-Units. This subdivision is not always immediately apparent in the field. The Outer Marginal Sub-Unit forms the outermost horizon along the length of the dyke, contains no macroscopic amygdales and is visibly chilled in places, whilst the Inner Marginal Sub-Unit contains many narrow amygdaloidal bands. The contact between these two sub-units is taken as the outer contact of the outermost amygdaloidal band.

2.4 The Marginal Unit.

In this section both Outer and Inner Marginal Sub-Units will be treated together. This unit has an average width of 20cms varying from a minimum of 3cms at 65' to a maximum of 48cms at 64', and is composed of many bands of doleritic composition. At 174', a hand specimen of this unit can be sub-divided into nine bands (Plate 2.7), while the number of bands visible in the field is reduced due to the weathered appearance of the rock, and only slight variations differentiating bands.

The bands at 174' will be described later in this chapter. A chilled margin is developed along the contact with the sill and is most prominent at 184', 150' and 100', although it is not well developed along the whole length of the dyke (Figure 2.1). The width of this chilled margin extends for approximately 3.5cms at 174' (Plate 2.7).

Where the dyke width increases, protruding into the sill, the change in dyke thickness is accommodated by the Marginal Unit, especially in the Inner Marginal Unit, with only the outer bands showing a change in strike, the amount of change decreasing with distance into the dyke eg. 34', 150', 153' and 158' (Figure 2.1 and Plates 2.3 and 2.4). At such sites, the amygdaloidal bands remain approximately of constant thickness, whilst the non-amygdaloidal material between them varies in thickness, compensating for the variation in thickness of the dyke.

2.5 The Intermediate Unit.

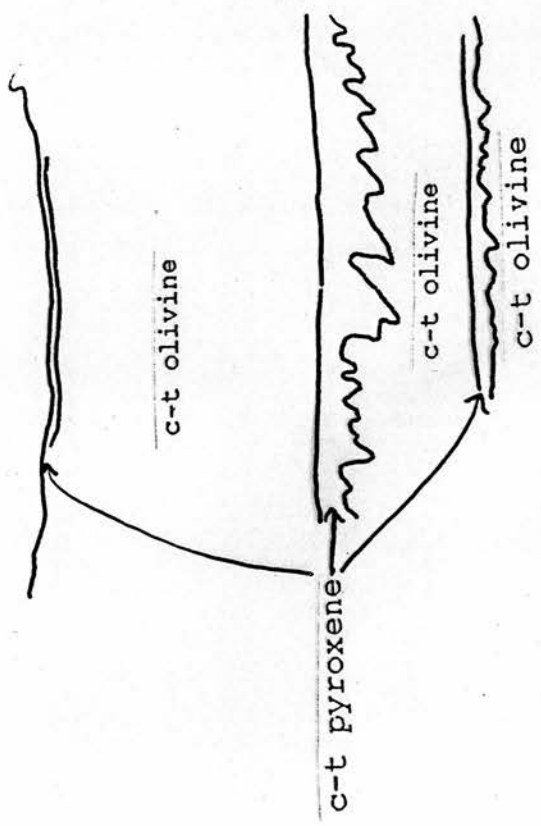
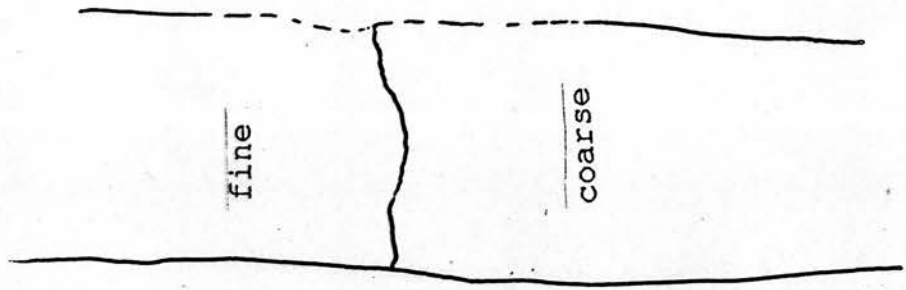
The Intermediate Unit contains comb-layers and only a few amygdaloidal bands (Figures 2.1 and 2.2). The contact between the Marginal and the Intermediate Unit is taken as the inner contact of the innermost amygdaloidal band (APB1 in Figure 2.2) within the northern segment which can be traced southwards to the southern segment.

Amygdaloidal bands are found in the Intermediate Unit in all segments of the dyke, with the maximum number being present in the middle segment. The minimum width of the Intermediate Unit is approximately 6cms at 81' and the maximum is 38cms at 108', with the unit having an average thickness of 27cms (Figures 2.1 and 2.2). The number of bands, their mineral constitution and textures that make up this unit vary with distance along the dyke. This unit is resistant to weathering and forms two parallel upstanding ridges running the length of the dyke.

A striking feature of the Intermediate Unit is the comb-textured bands present along most of its length. The bands may be either olivine- and plagioclase-rich (troctolitic) or pyroxene-rich (pyroxenitic). The weathered troctolitic bands are green whilst the pyroxenitic bands remain black. To the north, olivine and plagioclase are dominantly the combed minerals, whilst to the south, the comb-layering is developed predominantly by pyroxene. Around 90', the banding consists of olivine- and plagioclase comb-layers alternating with pyroxene comb-layers (Figure 2.1 and Plate 2.8). Crystals within the comb-layers are elongate and branch towards the centre of the dyke. The long axes of the pyroxene crystals curve upwards and at 13' curve towards the north. Both the olivine and plagioclase comb-texture crystals curve towards the north, with the olivine comb-textured crystals undulating upwards. There is an angular discontinuity between the

Plate 2.8 Alternating bands of comb-textured olivine- and plagioclase, and comb-textured pyroxene in the Intermediate Unit at 90', in the Middle Segment.

Plate 2.9 Abrupt variation in amygdale diameter at 55' in the Middle Segment of the dyke. To the north, the amygdales are large and round (3-5mm diameter), while to the south, they are small and irregular in shape (1-2mm diameter).





elongation directions of the olivine and pyroxene crystals in adjacent troctolitic and pyroxenitic bands displaying comb-texture. This feature is similar to the refraction of a light beam at an interface. At 40', this deflection is approximately 35° .

The character of a band may vary with distance along the dyke. The amygdaloidal bands in the northern segment of the dyke become progressively pyroxene-rich (comb-textured) amygdaloidal bands and then pyroxene comb-textured bands devoid of amygdales towards the south (Figure 2.2, APB1 and APB2). Traced southwards these bands change from doleritic to pyroxenitic in composition. At 100', the innermost amygdaloidal band on the western side of the Intermediate Unit, has 2mm thick comb-textured pyroxene along its innermost margin. This comb-textured band thins to the north where it disappears, but thickens to the south at the expense of the amygdaloidal band, as the overall thickness of these layers remain approximately constant, as displayed at 94' (Figure 2.2, APB3).

The amygdaloidal-pyroxene comb-textured bands bifurcate and rejoin both horizontally and vertically, and have a tendency to thicken towards the south. It is not always possible to follow the bands as they terminate and reappear along the strike of the dyke (possibly continuing at another horizon not presently exposed). The most consistent comb-layered band is pyroxenitic and

delineates the contact between the Central Unit and the Intermediate Unit (Figures 2.1 and 2.2 -PB1). This band (PB1) is present even in the northern segment of the dyke, where the other pyroxenitic bands of the south (APB1 & 2) are actually amygdaloidal dolerite.

In the southern segment, the amygdaloidal bands may contain either large or small amygdales. Both varieties may be present within the layering across the strike of the dyke, as at 6' and 13'. At 13' there are laminations of coarsely amygdaloidal (2-3mm diameter) and finely amygdaloidal (1mm diameter) material, together with laminations of comb-textured pyroxene. The coarsely amygdaloidal layer ends abruptly.

2.6 The Central Unit.

The contact between the Intermediate Unit and the Central Unit is taken as the inner side of the narrow comb-textured pyroxene band that is developed along the length of the dyke (PB1 -see above and Figure 2.2). The pyroxene comb-textured band is assumed to be present even where it is not visible due to lack of exposure. The amygdaloidal Central Unit is of approximately constant width (c22cms) along its length with three exceptions. It narrows considerably at 66' and 186' to 5cms, and at 168' to 6cms. The whole dyke narrows markedly at 66',

unlike the other constrictions, where it is only the Central Unit that narrows (Figures 2.1, 2.2 and Plate 2.5). The maximum thickness of this unit is 40cms, at 92'. The Central Unit is not present along the whole length of the dyke, and its termination is taken as the boundary between the middle and southern segments of the dyke (Figures 2.1 and 2.2).

The size and shape of the amygdales within the Central Unit varies along the length of the dyke. This change may be sudden, as around 55', where to the north, the Central Unit contains large amygdales and to the south, numerous small amygdales (Plate 2.9). At 51', the Central Unit contains many small amygdales (1mm diameter), elongate parallel to the strike of the dyke, but there is also lamination perpendicular to the strike of the dyke composed of non-amygdaloidal material. These non-amygdaloidal bands may bifurcate. At 49', very fine amygdaloidal material within the amygdaloidal unit forms lenticles upto 11cms across (East-West) by 4cms up-down the dyke (North-South), from which veinlets of amygdales (upto 10cms in length) disseminate, almost parallel to the strike of the dyke. At the 66' constriction, there are fewer, large amygdales (c4mm across) with less total volume of amygdales than at 54' (4% compared to 6%).

At 100', the Unit contains very large amygdales e.g. 2.0: 0.4: 0.5 cms -length: width: height which respectively are parallel to the strike, perpendicular to

the strike, and vertical. Here, the amygdales decrease in size towards the contacts of the band. At 156', many of the amygdales are elongate along the strike of the dyke (136°). At the western contact, the amygdales measure 0.3 by 0.2cm, in the middle 0.2 by 0.2cm and 0.8 by 0.4cm, and towards the eastern contact 0.5 by 0.2cm and 2.0 by 0.4cm. By contrast at 152', it is the larger vesicles that are situated close to the contacts, some partially infilled with zeolite. Some are circular, others elongate, with their long axes striking 035° and 083°.

2.7 Typical Cross-Sections from the Three Segments of the Mystery Dyke.

One typical cross-section from each of the three segments along the length of the dyke are described below; 174', 92' and 43' (Figures 2.1 and 2.2). Their constitution is summarised below.

2.7.1 The Northern Segment of the Mystery Dyke.

The Northern segment is comparatively simple in terms of the banding visible in the field. A typical section from the Northern segment was taken as 174' (Plate 2.7). Here, the dyke has a width of 108cms, and a section from East to West includes:

- 3.0cms Outer Marginal Sub-Unit
- 27.5cms Inner Marginal Sub-Unit
- 20.0cms Intermediate Unit
- 12.0cms Central Unit
- 20.0cms Intermediate Unit
- 22.0cms Marginal Unit (Inner and Outer Sub-Units indistinguishable).

The Outer Marginal Sub-Unit.

This is the most easterly band, in contact with the Trotternish Sill Complex. This dark grey rock is considered a chilled margin due to its very fine crystal

size. No phenocrysts or amygdales are visible with the naked eye.

The Inner Marginal Sub-Unit.

This is composed of several amygdaloidal or fine-grained, grey, doleritic bands. In contrast to the Outer Marginal Sub-Unit, macroscopic olivine phenocrysts are visible to the naked eye. The amygdales are irregularly shaped and infilled with zeolite. A sample obtained and later analysed in the laboratory was divided into eight bands, however in the field, due to its weathered condition it was noted only as one band which contained varying amounts of amygdales across its width.

The Intermediate Unit.

Here, the Intermediate Unit is relatively simple, comprising of only one band of comb-textured olivine- and plagioclase feldspar, together with a narrow pyroxene comb-textured lamina. However, a lamination dissects the band 6cms away from the Central Unit. This band differs in colour from the Marginal Unit due to the green weathering of the comb-textured olivine. Highlighting the contact between the Intermediate and Central Units is the narrow (0.5cms) lamina of comb-textured pyroxene (Figure 2.2 -PB1). No phenocrysts are visible in the field, although the comb-textured olivines can be seen. This band is more resistant to weathering than the

remaining bands and is physically upstanding compared to adjacent bands.

The Central Unit.

The band that constitutes the Central Unit is noticeably different from all others. It is extremely amygdale-rich (12%), with the white zeolite- and calcite-infilled amygdales irregularly orientated, in the dark grey, fine-grained matrix.

The Intermediate Unit.

The Intermediate Unit on the Western side of the dyke is comparable to that on the East. The lamination noted 6cms from the contact with the Central Unit on the eastern side of the dyke is present at a distance of 5.5cms from the Central Unit on the western side of the dyke.

The Marginal Unit.

No distinction is possible between Inner and Outer Marginal Sub-Units at this locality due to poor exposure. The Outer Marginal Sub-Unit at 175' and 173' is approximate to that on the Eastern side of the dyke.

2.7.2 The Middle Segment of the Mystery Dyke.

The banding within the Middle Segment of the dyke is the most complex, for the Intermediate Unit displays petrologic changes both along and across the dyke. A section at 92', was chosen for description. The total width of the dyke here is 110cms, although the Marginal and Intermediate Units are not fully exposed. (Figures 2.1 and 2.2). In the middle section of the dyke, the contact between the Marginal and Intermediate Units on the eastern side of the dyke is taken as the inner contact of the amygdaloidal band (APB2) as shown in Figure 2.2. The section is from East to West.

17.5cms approx. Marginal Unit.

21.0cms approx. Intermediate Unit.

39.5cms Central Unit.

16.5cms Intermediate Unit.

14.0cms Marginal Unit.

The Marginal Unit.

The Marginal Unit is fine grey dolerite, with no distinction between Inner and Outer Sub-Units.

The Intermediate Unit.

There is not a complete exposure of the Intermediate Unit, with the outer 4.5cms not being recorded in detail due to the weathered nature of the exposure. The remaining portion of the Unit consists of 10 bands.

Bands 1, 5, 7 and 9 have widths of 3.0, 1.5, 1.7 and 2.7cms respectively (Figures 2.1 and 2.2). These are leucocratic, comb-textured olivine- and plagioclase bands. Bands 6, 8 and 10 are melanocratic, comb-textured pyroxene bands, of 0.4, 1.0 and 0.4cms widths respectively (Figures 2.1 and 2.2). The remaining bands include Bands 2, 3 and 4. Band 2 is an amygdaloidal and pyroxene-rich band (0.6cms), the pyroxene not being comb-textured, Band 3 (5.0cms) is leucocratic and unusual in that it contains comb-textured olivine-, plagioclase- and pyroxene, whilst Band 4 is an amygdaloidal, dolerite band of 0.5cms.

The Central Unit.

The amygdaloidal, central band is similar in appearance to that described at 174'.

The Intermediate Unit.

The Intermediate Unit on the western side of the dyke does not mirror that on the eastern side. The total width of the Unit is less and there are only four bands developed. A comb-textured pyroxene lamina (0.3cms) highlights the contact between the Central and Intermediate Units. The comb-textured olivine- and plagioclase bands of 4.8 and 11.5cms are separated by a comb-textured pyroxene band of 0.8cms (Figures 2.1 and 2.2).

There are no amygdaloidal bands on the west side of the dyke here, nor is the complex alternating pattern of comb-textured olivine and pyroxene developed to the same extent as on the eastern side of the dyke.

The Marginal Unit.

The Marginal Unit is a fine-grained dolerite and does not exhibit banding, with no distinction between Inner and Outer Marginal Sub-Units.

2.7.3 The Southern Segment of the Mystery Dyke.

The southern segment displays relatively few bands. The Central Unit does not appear to be present, as there is no amygdaloidal central band although there is a definite "central band". The total width of the dyke at 43' is 90.8cms (Figures 2.1 and 2.2).

The section from East to West includes:

- 30.0cms Marginal Unit.
- 19.0cms Intermediate Unit.
- 11.0cms "Central band".
- 19.0cms Intermediate Unit.
- 11.0cms Marginal Unit.

The Marginal Unit.

This band is a fine-grained, grey dolerite. It contains several amygdaloidal laminae which have a strike parallel to that of the dyke. It is not possible to distinguish Outer and Inner Marginal Sub-Units.

The Intermediate Unit.

The Intermediate Unit in the Southern Segment consists of an amygdaloidal- comb-textured pyroxene band.

The "Central Band".

The "central band" consists of a very fine-grained pyroxene-rich band. Less than two feet further north, the amygdaloidal Central Unit is still present.

The Intermediate Unit.

The Intermediate Unit is composed of several bands of comb-textured pyroxene with some of the bands being enriched in amygdales. The amygdales are infilled with zeolite and calcite and are elongate across the width of the dyke. The amygdales measure 0.3-0.8cms across the dyke by 0.1-0.2cms along the strike of the dyke.

The Marginal Unit.

The Marginal Unit comprises a finely banded sequence of amygdaloidal bands and pyroxene-rich bands, with no distinction of Outer and Inner Sub-Units.

2.8 Possible Extension to the Mystery Dyke.

Following the approximate strike of the Mystery Dyke northwards over the headland of Ru Bornaskitaig to Uamh Oir, (GR NR372720) at a distance of approximately 700 metres, a 1 metre wide doleritic dyke was discovered. This dyke had intruded along the hexagonal cooling joints of the sill, and exhibits no evidence of banding or comb layering. At this location on the foreshore, the dyke has been preferentially eroded, resulting in a gully.

2.9 Summary.

Field evidence has been presented to support the proposal of the subdivision of the Mystery Dyke into three major units (Marginal, Intermediate and Central), and three segments (Northern, Middle and Southern). The sill had cooled sufficiently to allow the development of hexagonal cooling joints to have developed (the planes of weakness along which the dyke intruded), and to chill the intruding dyke magma, but was still sufficiently warm to allow the development of some of the cooling joints to cut both dyke and sill with no deflection. This short time period may allow the dyke to have acted as a feeder dyke for a higher level sill. Due to the absence of obvious chill features within the dyke, the intrusion of the magma was accomplished within a short time span.

Inferred flow direction of the magma in the dyke was investigated following examination of the elongation direction of the vesicles and phenocrysts (Wada 1992, Shelley 1985). It was assumed that the downstream side of an elongate crystal or vesicle would face towards the centre of the flow. (Nakamura 1972, Blanchard et al 1979). Elongation of the amygdales varies both along the length of and across the width of the Central Unit of the dyke.

The elongation directions of the amygdales indicate a flow from the north, possibly with increased speed towards the centre of the dyke (amygdales parallel to the

strike close to the contact with the Intermediate Unit but perpendicular to the strike in the middle of the Central Unit). These elongation directions of the amygdales could also however reflect pressure on the dyke after the intrusion pressure decreased. The lobate form of the curved concentric lamination at 39' suggests the magma flowed from the North with some vertically upward element. This direction is in agreement with the conclusions reached by previous workers (Drever and Johnston and Simkin). The morphology of the dyke in the Southern segment and the textures present eg the curved concentric banding confirms this direction of dyke propagation.

The variation in rock type and texture both along and across the width of the dyke is seen as possible evidence of intrusion of magma of varying compositions and crystal content over a short period of time, with changes in the controlling conditions during the development of the dyke.

CHAPTER 3

PETROGRAPHY

3.0 Introduction.

The dyke exhibits a range of textures and variation in mineral proportions, both laterally and longitudinally. It is doleritic in composition with olivine, clinopyroxene and plagioclase feldspar as essential minerals. Accessory minerals include zeolite, calcite, spinel, haematite, nepheline and apatite. Table 3.1 shows modal analyses for the dyke, with sill data (this study) included for comparison. The dyke is holocrystalline and normally porphyritic with areas of poikilitic, ophitic and subophitic textures; comb-texture and trachytic texture are also developed. Crystallographic orientation of the olivine was determined utilising a four-axis Leitz Universal Stage.

3.1 Discussion of Textural Terminology.

Various names have been used to describe the relatively unusual texture, in which elongate crystals

Table 3.1

Modal Analyses of the Mystery Dyke and Sill.

Unit:	O.M.S-U.	I.M.S-U.						
Band/Dist.	1/174'	2/174'	3/174'	4/174'	5/174'	6/174'	7/174'	8/174'
Ol. Phen.	16.0	15.5	5.7	7.6	2.1	6.1	4.9	0.2
Ol. Gms.	20.1	14.8	11.7	9.5	10.0	9.4	10.0	11.6
Ol. C-T.	0.0	0.0	0.0	0.0	0.0	0.0	0.0	0.0
Cpx. Phen.	0.0	0.9	0.9	1.0	1.2	1.1	1.4	1.0
Cpx. Gms.	9.7	17.0	30.5	25.1	29.5	21.4	27.0	26.0
Cpx. C-T.	0.0	0.0	0.0	0.0	0.0	0.0	0.0	0.0
Cpx. Oph.	0.0	0.0	0.0	0.0	0.0	0.0	0.0	0.0
Plag. Phen	10.1	10.0	10.3	11.6	8.2	8.5	3.0	1.6
Plag. Gms.	28.4	22.4	25.6	30.1	37.2	45.4	37.6	46.8
Plag. C-T.	0.0	0.0	0.0	0.0	0.0	0.0	0.0	0.0
Opaque	12.9	13.4	12.2	11.8	8.1	5.7	6.8	7.6
Zeolite	2.6	5.7	2.5	3.2	3.7	2.0	8.8	3.2
Calcite	0.1	0.3	0.5	0.1	0.0	0.5	0.5	0.2
Nepheline	0.1	0.0	0.0	0.0	0.0	0.0	0.0	0.0
	100.0	100.0	99.9	100.0	100.0	100.1	100.0	98.2
Total Ol.	36.1	30.3	17.4	17.1	12.1	15.5	14.9	11.8
Total Cpx.	9.7	17.9	31.4	26.1	30.7	22.5	28.4	27.0
Total Plag	38.5	32.4	35.9	41.7	45.4	53.9	40.6	48.4

I.M.S-U.	I.U.	I.U.	C.U.	O.M.S-U.	I.U.	I.U.	I.U.	I.U.
9/174'	10/174'	*10a/174'	11/174'	151'	150'a	150'b	150'c	150'd
1.0	0.0	2.4	7.9	24.3	0.0	0.0	0.0	0.0
8.0	4.4	3.9	1.6	15.5	7.8	1.2	0.5	0.4
0.0	21.7	10.4	0.0	0.0	16.7	19.4	28.3	15.4
0.0	0.0	0.1	11.2	0.0	0.0	0.0	0.0	0.0
25.2	4.7	5.4	20.0	1.8	2.0	0.7	1.0	3.0
6.8	0.0	0.0	0.0	0.0	0.0	0.0	0.0	4.8
0.0	7.2	16.4	0.0	0.0	15.8	18.2	10.8	10.4
3.4	0.0	0.0	14.2	10.0	0.0	0.0	0.0	0.0
39.8	51.5	25.0	20.0	32.8	37.8	41.5	30.7	27.6
0.0	5.5	27.7	0.0	0.0	11.0	13.0	25.2	30.1
6.2	2.9	3.2	8.8	15.8	5.8	2.9	2.1	3.5
9.6	2.1	5.5	12.4	0.0	3.3	3.1	1.4	4.0
0.0	0.2	0.1	0.7	0.0	0.0	0.0	0.0	0.8
0.0	0.0	0.0	3.2	0.0	0.0	0.0	0.0	0.0
100.0	100.2	100.2	100.0	100.2	100.2	100.0	100.0	100.0
9.0	26.1	16.7	9.5	39.8	24.5	20.6	28.8	15.8
32.0	11.9	21.9	31.2	1.8	17.8	18.9	11.8	18.2
43.2	57.0	52.7	34.2	42.8	48.8	54.5	55.9	57.7

*10a/174' modal analysis of thin sections along the strike of the comb-textured crystals to allow comparison with data from 150'.

Table 3.1 cont.

C.U.	O.M.S-U.	C.U.	"C.Band"	I.U.	Sill	Sill
150'e	100'	54'	40'	40'	151'	100'
7.2	6.8	12.9	0.0	0.0	40.2	58.7
0.6	16.3	2.9	7.0	7.8	0.5	1.4
0.0	0.0	0.0	0.0	0.0	0.0	0.0
7.9	0.0	8.1	0.0	0.0	0.3	0.0
22.1	1.8	19.9	45.9	28.4	1.7	0.0
0.0	0.0	0.0	0.0	12.0	0.0	0.0
0.0	0.0	0.0	0.0	0.1	14.7	11.1
26.7	11.0	15.4	0.1	0.2	0.5	1.1
8.7	41.8	16.9	31.4	38.8	39.7	24.3
0.0	0.0	0.0	0.0	0.0	0.0	0.0
7.2	22.5	11.4	14.9	12.2	2.5	3.3
19.2	0.0	12.6	0.6	0.4	0.0	0.0
0.4	0.0	0.0	0.1	0.0	0.0	0.0
0.0	0.0	0.0	0.0	0.0	0.0	0.0
100.0	100.2	100.1	100.0	99.9	100.1	99.9
7.8	23.1	15.8	7.0	7.8	40.7	60.1
30.0	1.8	28.0	45.9	40.5	16.7	11.1
35.4	52.8	32.3	31.5	39.0	40.2	25.4

are orientated almost perpendicular to the planes of layering, resembling the teeth of a comb. Wager and Brown (1951) described this texture in the Rhum intrusion as "harrisitic", a term with geographical connotations. Poldervaart & Taubeneck (1959) introduced "Willow Lake-type Layering", again a term with geographical significance. Loomis (1963) introduced "combed layering" and "combed texture" implying that the texture is similar to something that has been combed.

Wager & Brown (1967) used the term "crescumulate" to describe the texture where there is an upward growth of elongate crystals from the floor of a magma chamber. Their definition is restricted to horizontally layered intrusions. Irvine (1987) redefined crescumulate to allow it to be applicable to growth in any direction.

Moore & Lockwood (1973) recommended "comb layering" as a more acceptable name. Irvine (1987) defined comb layering as layers in which the main minerals occur as elongate blades or prisms, orientated normal (or at high angles) to the layering planes. This definition will be used in this thesis.

Comb layering has been reported in rocks of varying compositions, from ultramafic through to granitic by Loomis (1963), Batemann et al (1963), Wager and Brown (1967), Drever and Johnston (1967), Moore and Lockwood (1973), Shannon et al (1982), Donaldson and Reid (1982) and Petersen (1985a,b). Such elongate, branching crystals have been found in volcanic, hypabyssal and

plutonic environments (Wager and Brown 1951, Poldervaart and Taubeneck 1959, Preston 1963, Platten and Watterson 1969, Drever and Johnston 1972 and Bryan 1972).

Olivine morphology is related to cooling rate and melt composition (Donaldson 1976). Hollow, hopper-shaped crystals were produced from mafic melts with cooling rates of 2.5 to 15°C/h and elongate crystals at cooling rates of 15 to 40°C/h.

The petrography of the dyke is described below from margin to core (Outer Marginal Sub-Unit to Central Unit).

3.2 The Outer Marginal Sub-Unit.

a). In hand specimen the chilled margin is dark grey, very fine grained with occasional olivine phenocrysts visible with the aid of a hand lens. Samples from 174', 151' and 100' (Figure 2.2 and Plates 3.1-3.3) were studied.

b). In thin section the chilled margin is microcrystalline, with average grain size increasing with distance from the contact. At the contact the groundmass crystals average 0.01mm diameter increasing to 0.02mm within 5mm from the contact. The dyke matrix crystals average 0.2mm in diameter. The chilled margin contains phenocrysts of olivine and feldspar (Plate 3.4, Table 3.1).

Plate 3.1 Hand specimen of sample 174' showing locations
of vertical serial thin sections.



10 cm

Plate 3.2 Hand specimen of 151' showing the contact of the Marginal Unit and sill. Veinlets of amygdales can be seen highlighting the banding in the Marginal Unit.

Plate 3.3 Hand specimen from 100' showing the contact of the Marginal Unit and sill.



2 cm

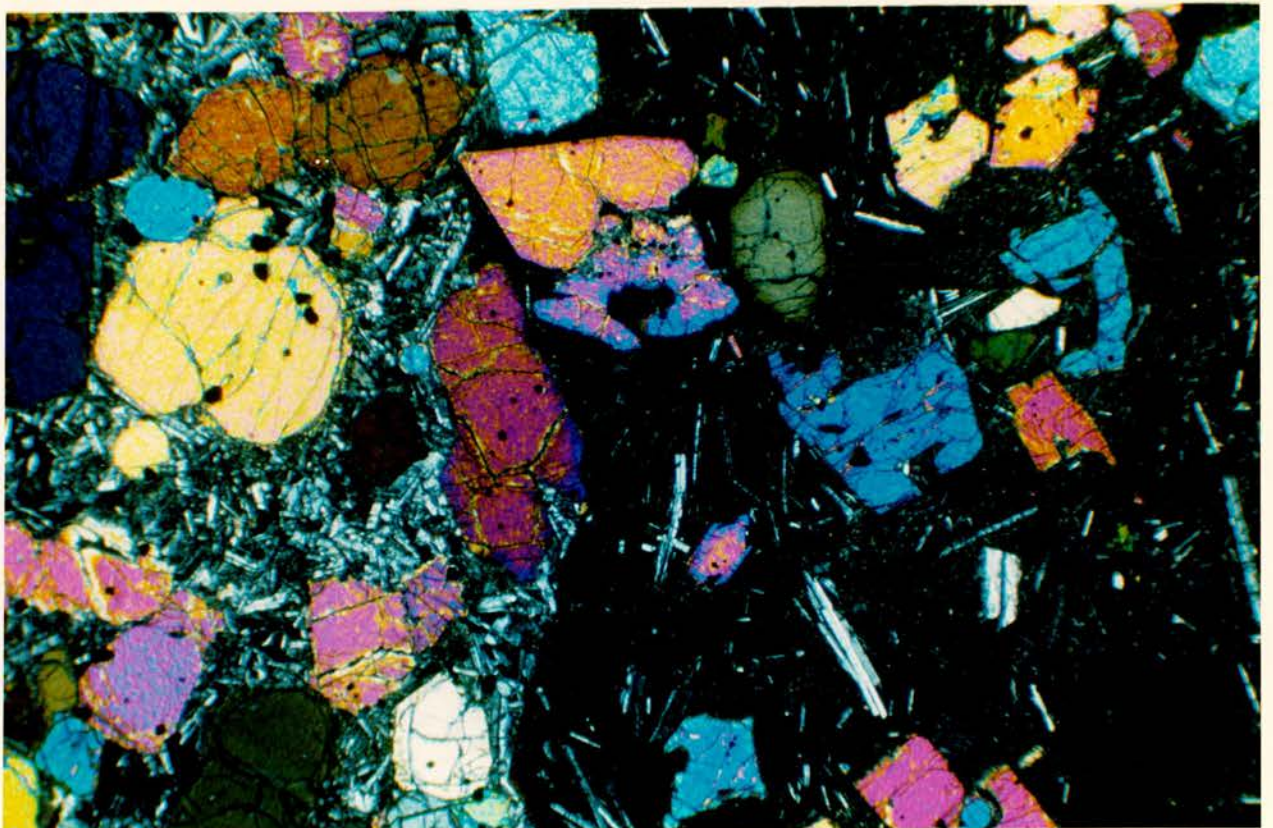
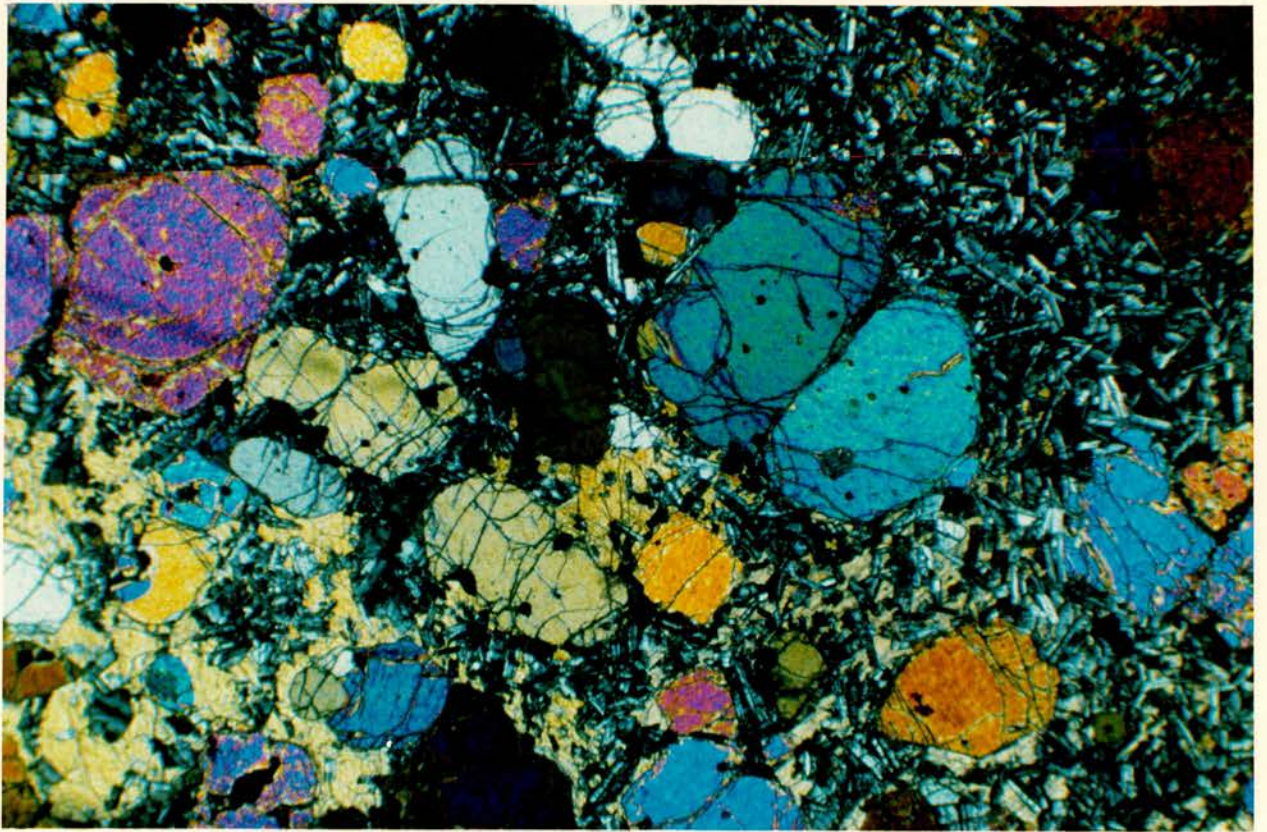


2 cm

MD10C

Plate 3.4 Contact of sill and dyke at 100', showing embayed (skeletal) olivine phenocrysts and plagioclase phenocrysts aligned parallel to the contact of the chilled margin. Some plagioclase crystals appear to be bent. The zoned rims to the olivine phenocrysts are discernible. The coarsening of the groundmass is visible to the left-side of the view. XN x25

Plate 3.22 Microphotograph of a typical area of sill, adjacent to the dyke, 100', showing euhedral and subhedral olivine phenocrysts surrounded by areas enriched in matrix feldspar and ophitic pyroxene. XN x25



Olivine.

Olivine phenocrysts range from 0.3-0.4mm diameter and exhibit both euhedral and subhedral habits. Close to the contact subhedral crystals show embayments, the hollows of which are filled with matrix crystals (Plate 3.4). Phenocrysts may also form glomerocrysts, with crystals showing closely-related crystallographic orientations. The abundance of olivine phenocrysts within this sub-unit could mean that some originated in the adjacent olivine-rich sill. This possibility is investigated further in Chapter 4.

Figure 3.1 displays the orientation of the crystallographic axes of olivines across sample 174'. Groupings of axes have been shown where appropriate. Figure 3.1a exhibits all the crystallographic axes of the crystals, while Figure 3.1b displays only axes of elongation of the crystals. Fourteen olivine phenocrysts were analysed from the Outer Marginal Sub-Unit. Clustering of the c axes around the centre of the stereogram indicates a near-horizontal strike, parallel to the sides of the walls of the dyke. Small groups of the a and b axes are also shown. Phenocrysts are preferentially elongate along the c or a axes. Figures 3.3 and 3.4 show the crystallographic axes and the direction of strike for olivines in the Marginal Unit.

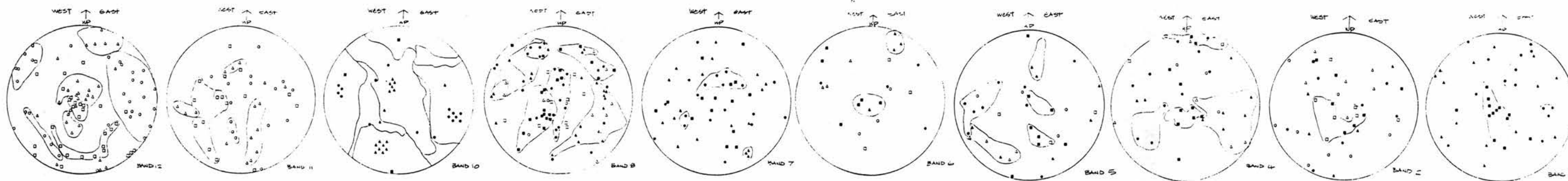


Figure 3.1a Stereograms showing crystallographic axes of olivine crystals per band, 174'.

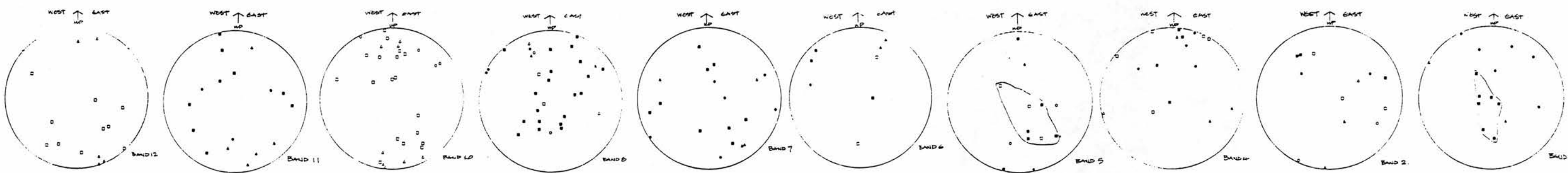


Figure 3.1b Stereograms showing axes of elongation for olivine crystals (and dendrites) analysed per band, 174'.

LEGEND

PHENOCRYSTS

- - a
- ▲ - b
- - c

MATRIX

- - a
- △ - b
- - c



Figure 3.1ci Stereogram showing crystallographic axes of single comb-textured olivine in Band 12/174'

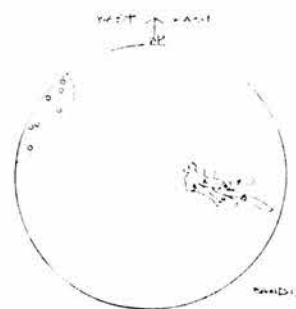


Figure 3.1cii Stereogram showing crystallographic axes of elongation for single comb-textured olivine crystal in Band 12/174'.

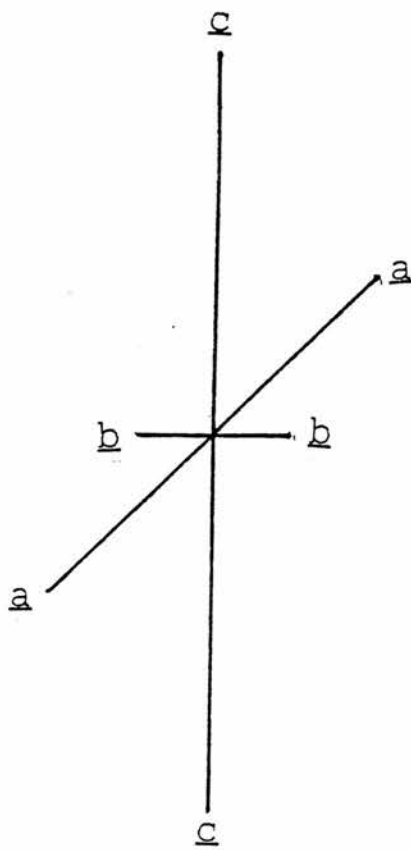


Figure 3.3 Diagrammatic representation of the crystallographic axes orientations of olivine in the Marginal Unit (174').

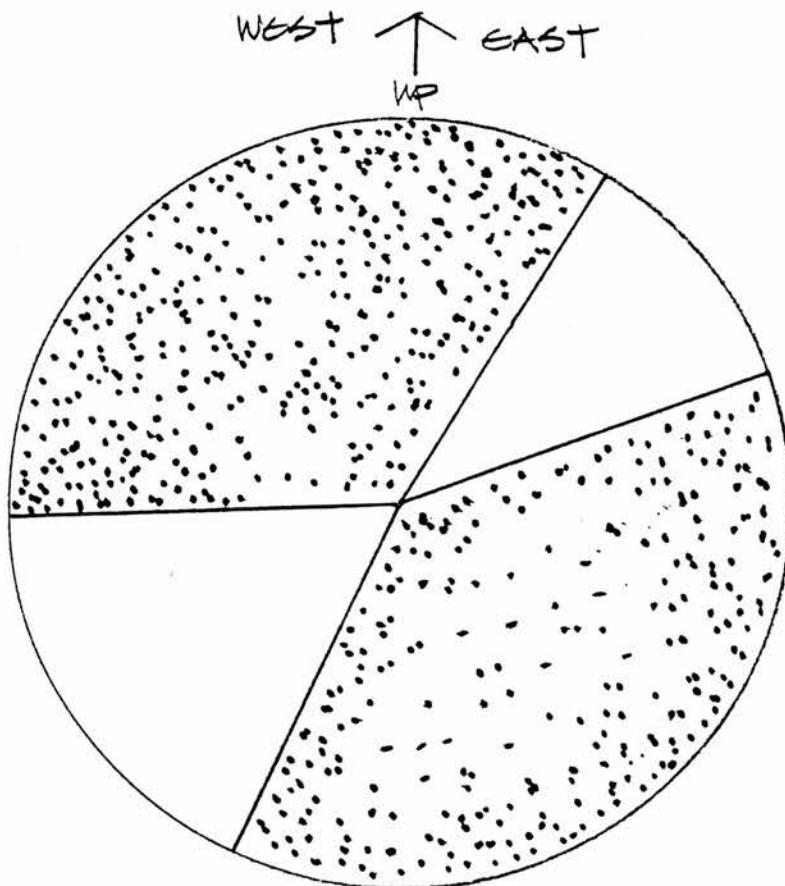


Figure 3.4 Diagrammatic representation of the direction of strike of the elongation axes of the olivine crystals in the Marginal Unit (174').

Pyroxene and Plagioclase feldspar.

A small amount of anhedral matrix pyroxene is present (Table 3.1). Plagioclase shows multiple albite twinning, with some showing a ragged ± 01 edge to the crystal. Many of the feldspar laths appear to be curved or broken. Feldspar phenocrysts range in size from 0.3-1.0mm. Many of the feldspars are aligned parallel or sub-parallel to the contact with the sill, displaying trachytic texture, while other matrix feldspars cluster (Plate 3.4).

Accessory Minerals.

The chilled margin contains abundant cubic opaques (Table 3.1) with a maximum diameter of 0.1mm, which are present both as groundmass crystals and enclosed within the olivine phenocrysts. The contact between the dyke and sill at 100' is marked by a very fine-grained horizon up to 0.4mm wide containing elongate (skeletal?) opaques orientated perpendicular to the contact.

3.3 The Inner Marginal Sub-Unit.

a). A serial vertical transect of thin sections was obtained for 174' (Plate 3.1). As stated in Chapter 2, this sub-unit has been subdivided into 8 bands (Bands 2-9), on the basis of variations in the volume of amygdales

observed in the hand specimen obtained. A sample from 151' was also analysed (Plate 3.2).

b). The Inner Marginal Sub-Unit (with the exception of Band 9/174') will be discussed as a complete unit, with variations being noted where applicable. Band 9/174' will be discussed separately due to its distinct petrographical character. This sub-unit is porphyritic, with the volume and size of phenocrysts varying within individual bands. Many bands display trachytic texture with crystals aligned parallel to the strike of the dyke (Plate 3.5). Other notable textures include the tangential orientation of crystals around the olivine phenocrysts in Bands 2-4/174', and veining in Bands 3,5-8/174'. Comb-textured pyroxene occurs within the sample from 151'.

Olivine.

Olivine is present as both phenocrysts and matrix crystals across Bands 2-8/174'. There is a decline in total modal olivine across Bands 2 to 9/174' (Table 3.1 and Figure 3.2). The phenocrysts are generally euhedral or subhedral, although there are skeletal olivine phenocrysts in Band 2/174'. No zoning is obvious within the outermost bands until Band 7/174', (approximately 16cms into the dyke) where a rim is optically visible. In section phenocrysts range in diameter from 2mm by 1mm (Band 2/174') and 1.5mm by 1mm (Band 7/174') to microphenocrysts with a diameter of 0.5mm by 0.3mm (Band

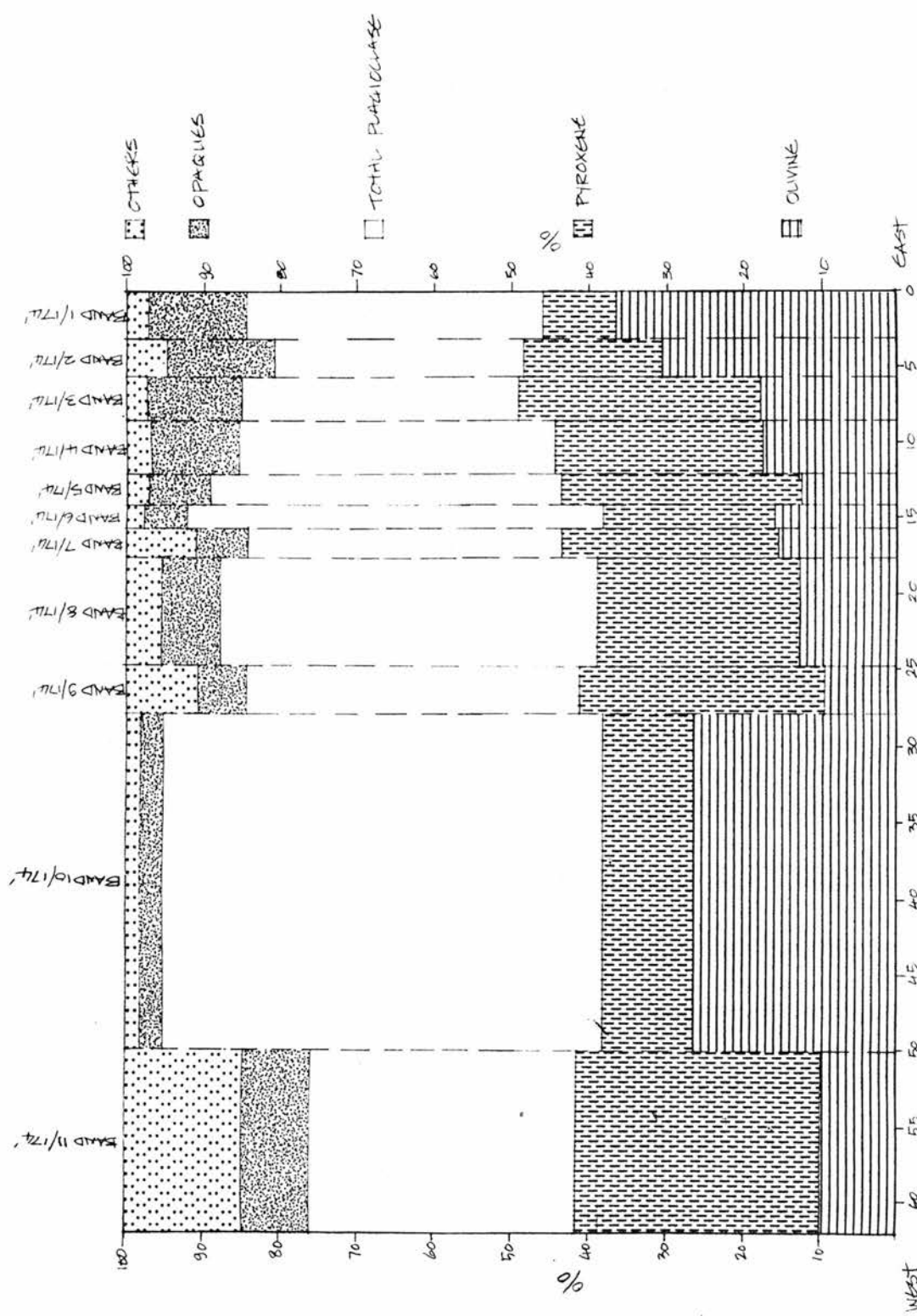
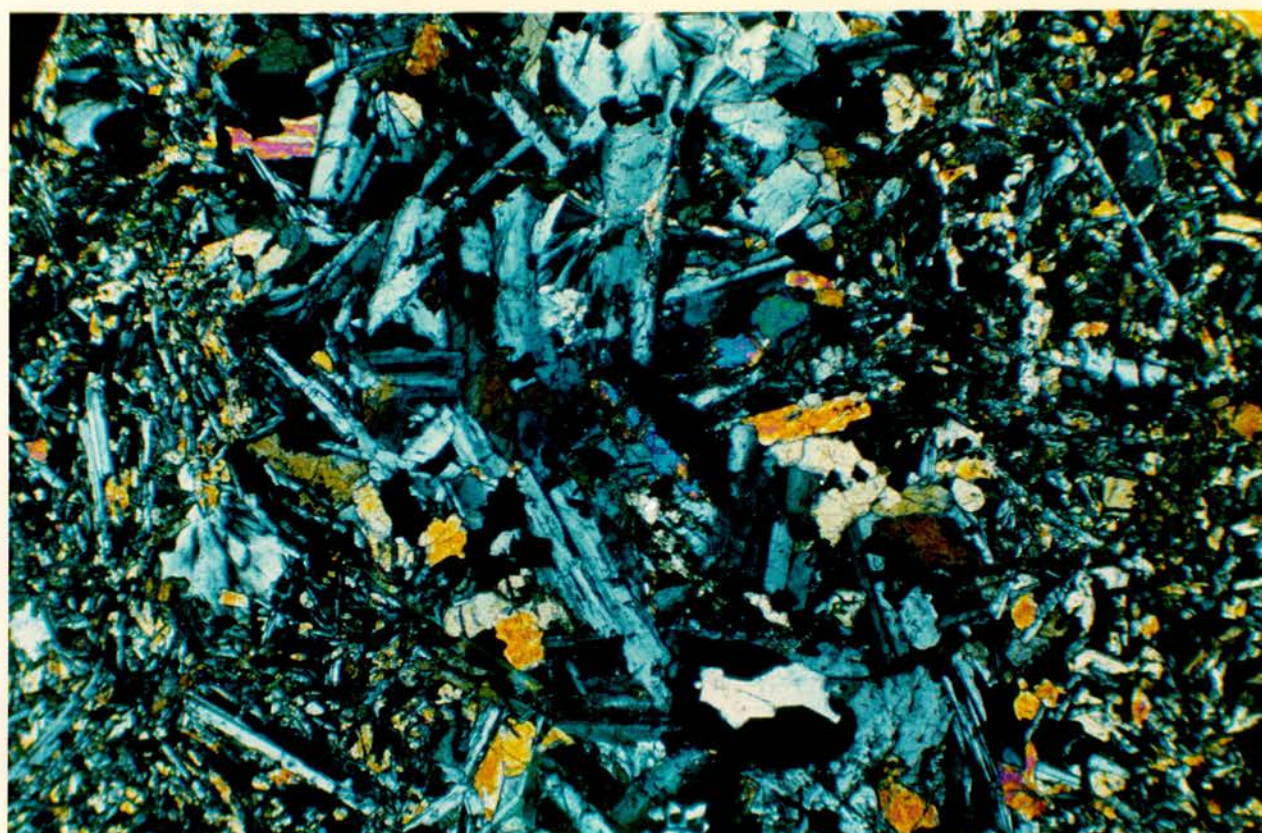
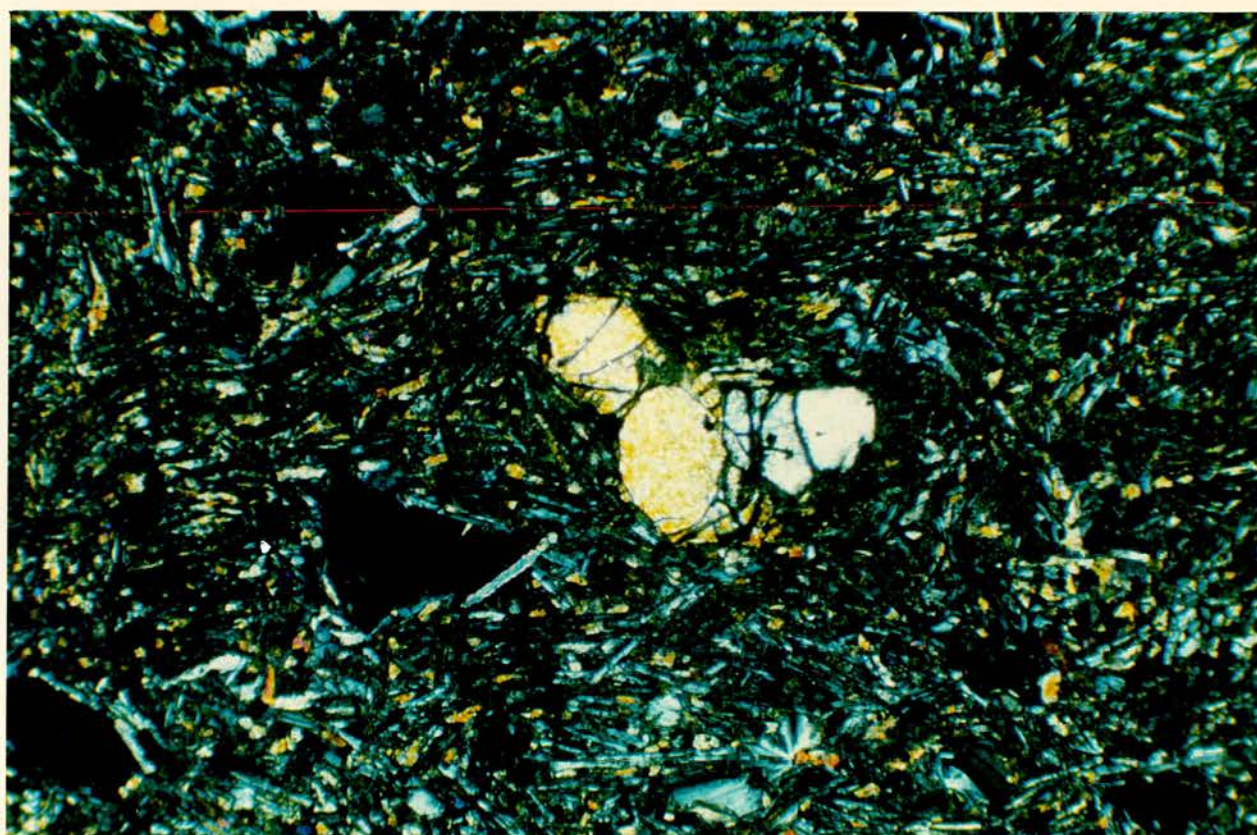


Figure 3.2 Modal Olivine, Pyroxene, Plagioclase Feldspar and Opaques for the sample 174' transect.

Plate 3.5 Typical view of the Inner Marginal Sub-Unit at 174', showing euhedral and subhedral olivine phenocrysts, vesicles and zeolite-filled amygdales. XN x50

Plate 3.6 Photomicrograph of veining in the Marginal Unit, 151', showing large plagioclase crystals and zeolite-filled amygdales in the centre of the vein and pyroxenes at the edges, orientated perpendicular to the strike of the vein. XN x50



2/174') and 0.3mm^2 (Band 5/174'). These smaller phenocrysts are usually subhedral. In Bands 3-8/174' the microphenocrysts exhibit glomeroporphyritic texture. Band 2/174' has the highest modal phenocrystic olivine content of the Inner Marginal Sub-Unit (16%).

Groundmass olivine may be euhedral, subhedral or anhedral, with some in Band 8/174' having zoned rims. With the exception of Band 2/174' (15%), there is little variation in matrix olivine content across the Inner Marginal Sub-Unit, which has an average modal content of 10-11%. The average matrix crystal diameter varies from 0.05mm to 0.1mm across Bands 2-6/174', increasing in Band 7/174' to 0.2mm.

Orientations of phenocrystic and groundmass olivines were analysed from Bands 2,4,5,6 and 8/174' using the Universal Stage, whereas only phenocrysts were analysed from Band 7/174'. A total of 85 phenocrysts and 32 matrix olivines were analysed. In some Bands the optic axes exhibit clustering eg Band 8/174' (the b and c axes), in Bands 2 and 6/174', the c axes form a group and Band 4/174', clusters of a, b and c axes are depicted (Figure 3.1a).

In all bands, the olivines (both phenocrysts and groundmass) are preferentially elongate along the c axes (Figures 3.1b and 3.3). In Band 2/174' the largest group of crystals are orientated with their long axes sub-horizontally across the strike of the dyke.

Bands 4-6/174' show elongation axes which are approximately vertical, parallel to the walls of the dyke (Figure 3.1b). Band 7/174' shows variation with distance across the band; the outer area containing a greater proportion of crystals with approximately vertical strike compared to further into the band, where horizontally elongate crystals, plunge predominantly to the south and towards the walls of the dyke. Olivines in Band 8/174' are approximately vertical.

Pyroxene.

The Inner Marginal Sub-Unit contains predominantly matrix pyroxene with Bands 2-8/174' containing approximately 1% micro-phenocrystic pyroxene. These have an average diameter of 0.2mm to 0.5mm and are generally subhedral but may be euhedral or anhedral. Matrix pyroxenes are predominantly subhedral with an average diameter of 0.05mm to 0.2mm. In Bands 6-8/174' a high proportion of the matrix pyroxenes enclose numerous minute opaques and in Band 8/174', have a zoned rim. Many groundmass pyroxenes are elongate across the dyke (along the c axis). Pyroxene exhibits sector zoning and ophitic texture in areas where it wholly and partially encloses plagioclase matrix laths.

The sample from 151' exhibits comb-textured pyroxene. In a horizontal section they occur as dispersed, disjointed dendrites upto 10mm long. The dendrites are not curved as in the Intermediate Unit, but

may exhibit slightly changing optical and elongation directions across a thin section.

Plagioclase Feldspar.

Plagioclase is present as phenocrysts and matrix crystals. Total modal feldspar increases across Bands 2-6/174' (32-54%) and then decreases. Modal phenocrystic feldspar varies from 3% (Band 8/174') to 12% (Band 4/174'- Table 3.1). Phenocrysts may exhibit simple or repeated albite twinning, and range in size from 2.0mm by 0.3mm to 0.5 by 0.1mm, the average length of the laths being approximately 1mm. Many phenocrysts in Band 4/174' exhibit trachytic texture sub-parallel to the dyke walls. Others show interpenetrant relationships with adjacent feldspars.

Modal groundmass feldspar increases across the sub-unit (22-47% in Bands 2 and 8/174' respectively- Table 3.1). Matrix feldspars frequently exhibit simple albite twinning, with lath length ranging from 0.05mm to 0.5mm. Groundmass feldspars exhibit trachytic texture in all bands, although its development is variable (Plate 3.7).

Accessory Minerals.

Opagues are present in varying amounts (6-13%), the least in Band 6, the most in Band 2/174' (Table 3.1). They occur as both angular grains and amorphous, round "blobs" and are found in the groundmass, within crystals and associated with amygdales. Those within crystals

tend to be angular or subangular, while near to amygdales they are amorphous. Matrix opaques tend to be angular.

Zeolite and calcite are the predominant minerals found in the amygdales varying from 3% in Band 6/174' to 9% in Band 7/174'. Amygdales in the Inner Marginal Sub-Unit are either elongate with irregular form (measuring approximately 4mm by 1mm) or are small, round amygdales (0.5mm to 0.7mm diameter). These amygdales may be sufficiently abundant and concentrated to form veinlets as in Band 8/174', which may measure 2mm by 0.6mm.

All Bands contain veins (Table 3.2), which are predominantly composed of plagioclase, pyroxene, zeolite and opaques, and have a strike similar to that of the dyke (Plate 3.6). The veins may be up to 1mm wide and may have small branches budding from them. Both plagioclase and pyroxene are elongate across the veins; the latter measure 0.2mm in length and are significantly larger than adjacent plagioclase crystals in the dyke.

3.3.1 Band 9/174'.

In hand specimen this appears similar to the remainder of the Inner Marginal Sub-Unit, but has modal concentrations and textures sufficiently distinct to be considered separately (Tables 3.1 and 3.2). It contains comb-textured pyroxene and more zeolite-filled amygdales.

Olivine is present only as groundmass crystals which are euhedral or subhedral, with zoned rims. These range

Table 3.2

Textural Comparison within the Mystery Dyke.

Unit:	Band No.	Band width Cms	Olivine:		Pyroxene:		Plagioclase:		Textures:				
			C-T Phen.	C-T Phen.	Ophit	Phen.	C-T Phen.	C-T	Trach	Amygd	Phen	Vein-Chill	
		174'							ytic	aloidal	ing		
O.M.S-U.	1	2.8	*				*					*	
I.M.S-U.	2	2.6	*				*			*	*	*	
I.M.S-U.	3	3.0	*				*		*	*	*	*	
I.M.S-U.	4	3.4	*				*		*	*	*	*	
I.M.S-U.	5	2.2	*				*		*	*	*	*	
I.M.S-U.	6	1.5	*				*		*	*	*	*	
I.M.S-U.	7	1.9	*				*		*	*	*	*	
I.M.S-U.	8	7.3	*				*		*	*	*	*	
I.M.S-U.	9	3.1		*			*	*	*	*	*	*	
I.U.	10	22.1	*		lam	*	*		*				
C.U.	11	12.0		*			*			*	*		
I.U.	12		*		lam		*		*				
I.U.	156'		*		lam	*	*		*	*		*	
C.U.	156'			*			*				*		
O.M.S-U.	151'		*				*			*	*	*	*
I.M.S-U.	151'		*	*		*	*	*	*	*	*	*	*
I.U.	150'		*	*	*		*		*	*	*	*	
C.U.	150'		*			*	*			*	*	*	
O.M.S-U.	100'		*				*				*	*	*
C.U.	54'		*			*	*			*	*	*	
I.U.	40'			*			*	*	*	*	*	*	*
"C.Band"	40'						*	*	*	*	*	*	*

Key:

O.M.S-U. Outer Marginal Sub-Unit

I.M.S-U. Inner Marginal Sub-Unit

I.U. Intermediate Unit

C.U. Central Unit

* present

lam present in lamina

from 0.05mm to 0.1mm in diameter. Comb-textured pyroxene occurs as "simple" dendrites, 4-5mm in length which curve up to 4° along their length. The term "simple" is applied because the dendrite has only one or two branches developed from the spine of the comb unlike the comb-textured pyroxenes in the lamina adjacent to the Central Unit (Band 12/174'). The dendrites are zoned along their length. These crystals have a very irregular contact with adjacent crystals, which in places has almost developed subophitic texture. Groundmass pyroxene crystals may be subhedral, euhedral or anhedral. They exhibit a zoned rim and an average diameter of 0.1mm, with their long axes frequently orientated parallel to the trachytic texture of the plagioclase.

Plagioclase is present as both phenocrysts and matrix crystals. The former average 1.5mm and the latter 0.2mm in length. The phenocrysts are elongate oblique to the strike of the dyke, exhibit repeated albite twinning and may form glomerocrysts. Groundmass plagioclase exhibits trachytic texture in which trains of crystals form curves between the pyroxene dendrites, convex to the walls of the dyke.

Opaque minerals have modal concentrations intermediate to the remainder of the Inner Marginal Sub-Unit and the Intermediate Unit (Table 3.1). They range in diameter from 0.05mm to 0.1mm and may form clusters.

3.4 The Intermediate Unit.

a). Samples of the Intermediate Unit were obtained from 174', 168', 156', 150' and 40' (Plates 3.1, 3.8-3.9). The Intermediate Unit at 40' will be considered separately, as its modal and textural features are different from the Intermediate Unit elsewhere in the dyke (see Tables 3.1 and 3.2).

b). This unit contains many textures including ophitic, poikilophitic and subophitic (Plate 3.10), intergranular, trachytic and comb-texture. It displays comb-texture along the length of the dyke with the complexity of the comb-textured banding increasing in the middle segment of the dyke (Plates 3.11-3.14). With the exception of the comb-textured lamina adjacent to the Central Unit, the northern segment contains only comb-textured olivine- and plagioclase, while in the middle segment bands of comb-textured olivine and plagioclase alternate with comb-textured pyroxene. The southern segment contains predominantly comb-textured pyroxene. Matrix crystal diameter decreases from an average 0.1mm to 0.05mm in the comb-textured pyroxene lamina adjacent to the Central Unit. Discussion about this fine-grained, comb-textured lamina is given later in this chapter.

Thin sections from 150' were prepared only from horizontal slices across the strike of the dyke (ie along the strike of the comb-textured crystals). Thus modal results are not an accurate reflection of true

Plate 3.7 Trachytic texture developed by the plagioclase crystals in the Marginal Unit at 151'. The trachytic texture is parallel to the strike of the dyke, convex to the centre of the dyke between the "simple" comb-textured pyroxene dendrites. XN x50

Plate 3.10 Ophitic texture of pyroxene in the Intermediate Unit, 174'. The pyroxene oikocrysts wholly or partially enclose the smaller plagioclase chadacrysts, which are displaying trachytic texture parallel to the strike of the dyke. XN x50

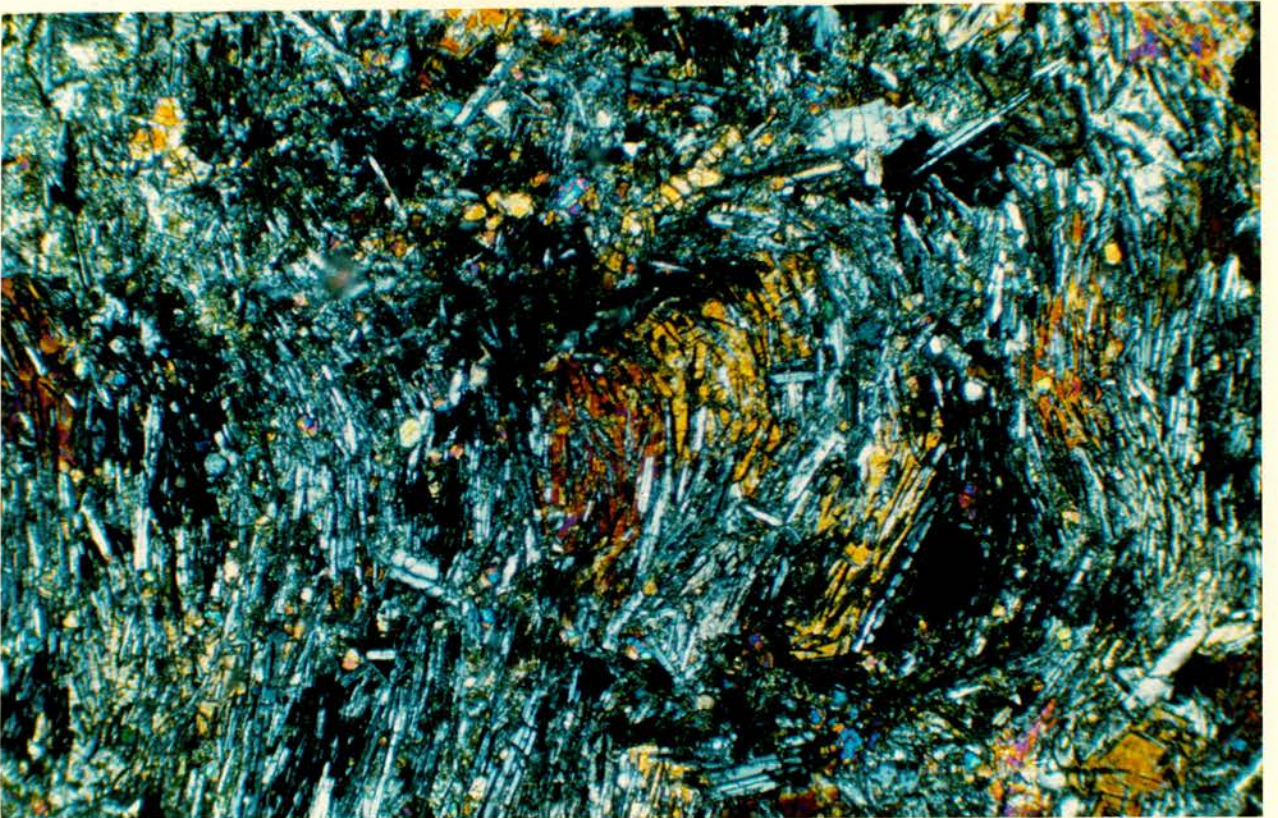
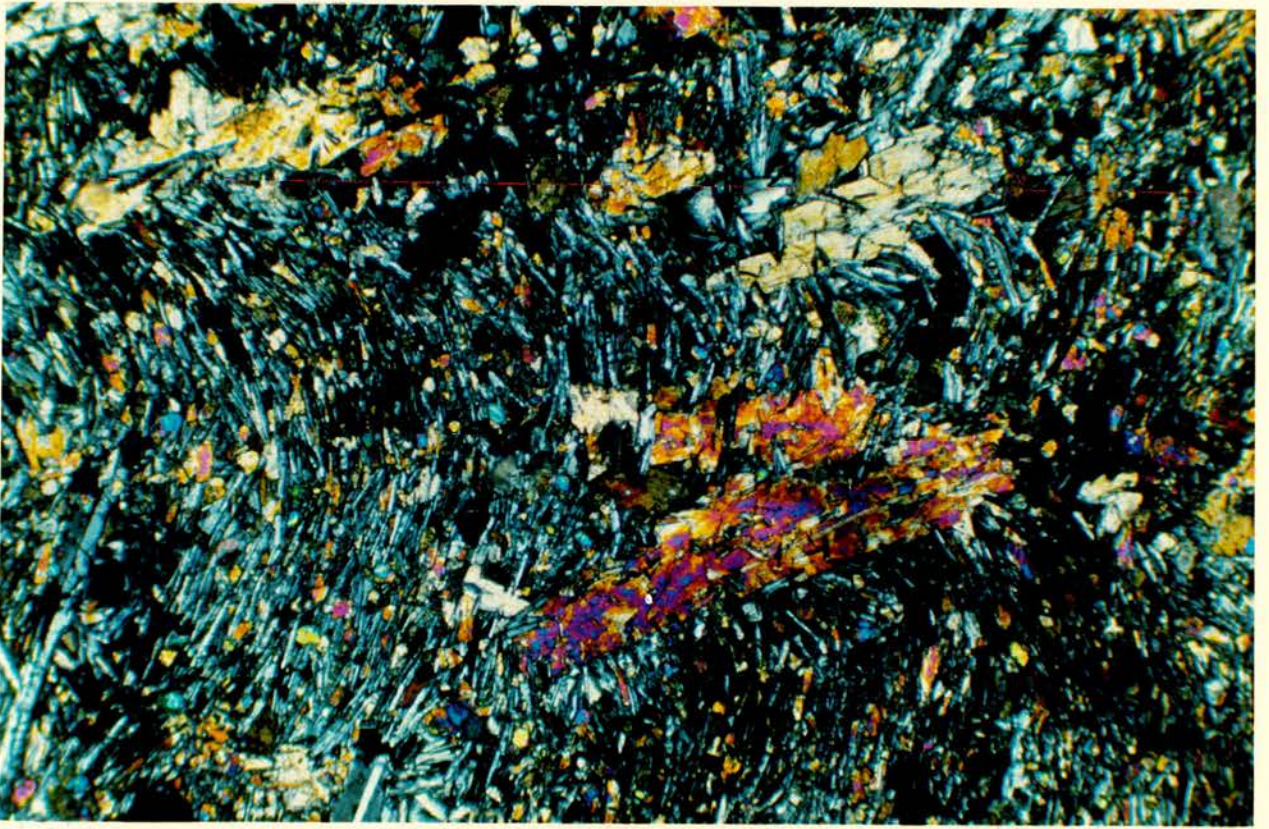


Plate 3.8 Hand specimen from the Intermediate and Central Units, 150' showing location of thin sections.



2 cm

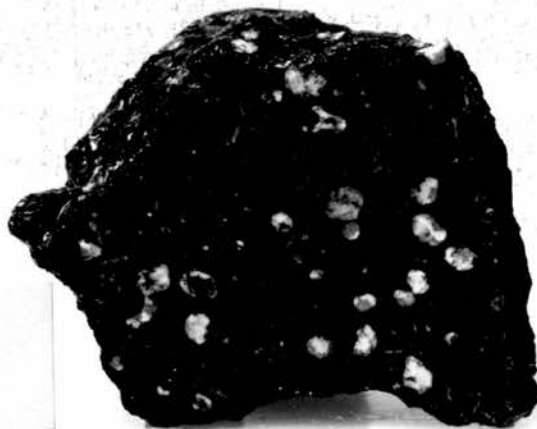
Plate 3.9 Hand specimens from 40'.

Left: "Central Band". **Right:** Intermediate Unit.

Plate 3.16 Hand specimen from the Central Unit, 54'.



2 cm



2 cm

Plate 3.11 General view of comb-textured olivine- and plagioclase in Band 12/174'. XN x 50

Plate 3.12 Comb-textured pyroxene in the Intermediate Unit, 156', showing sector-zoning along the branches. XN x15.

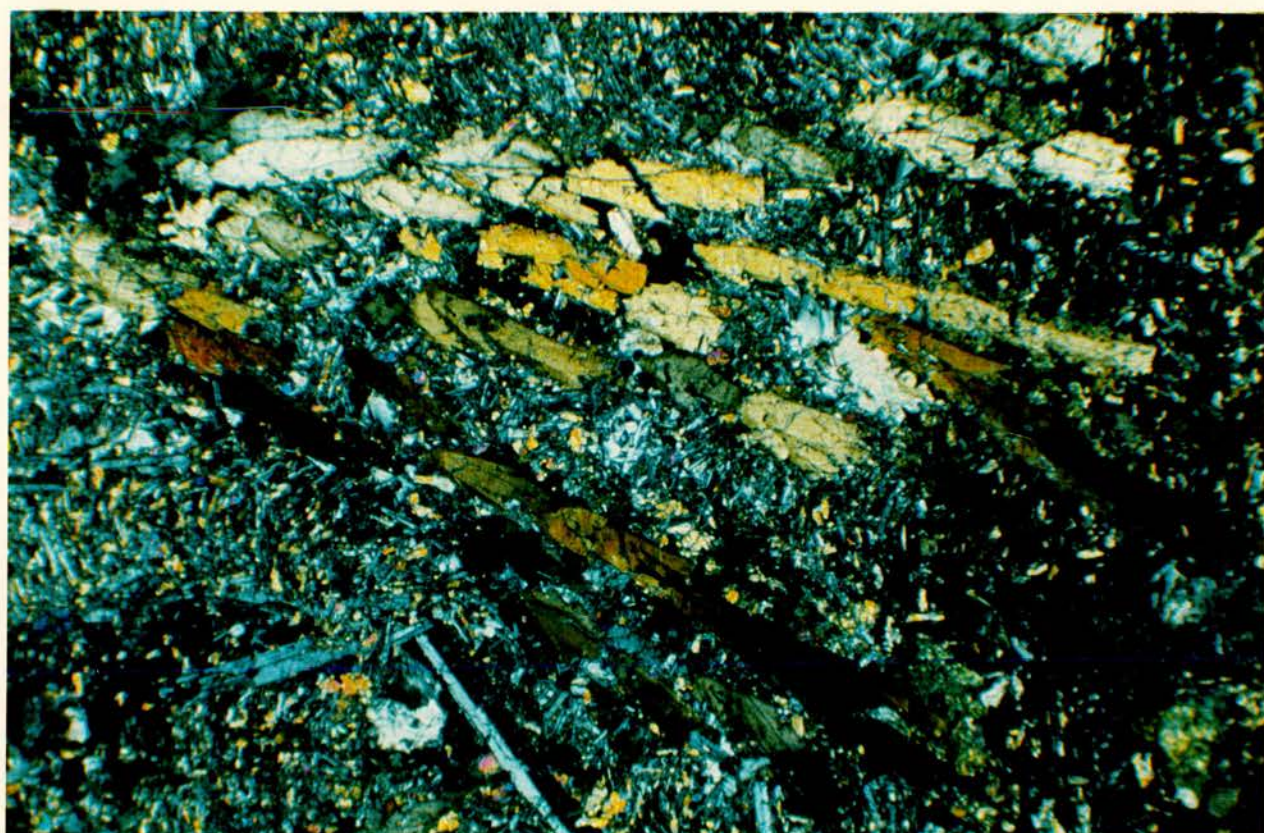
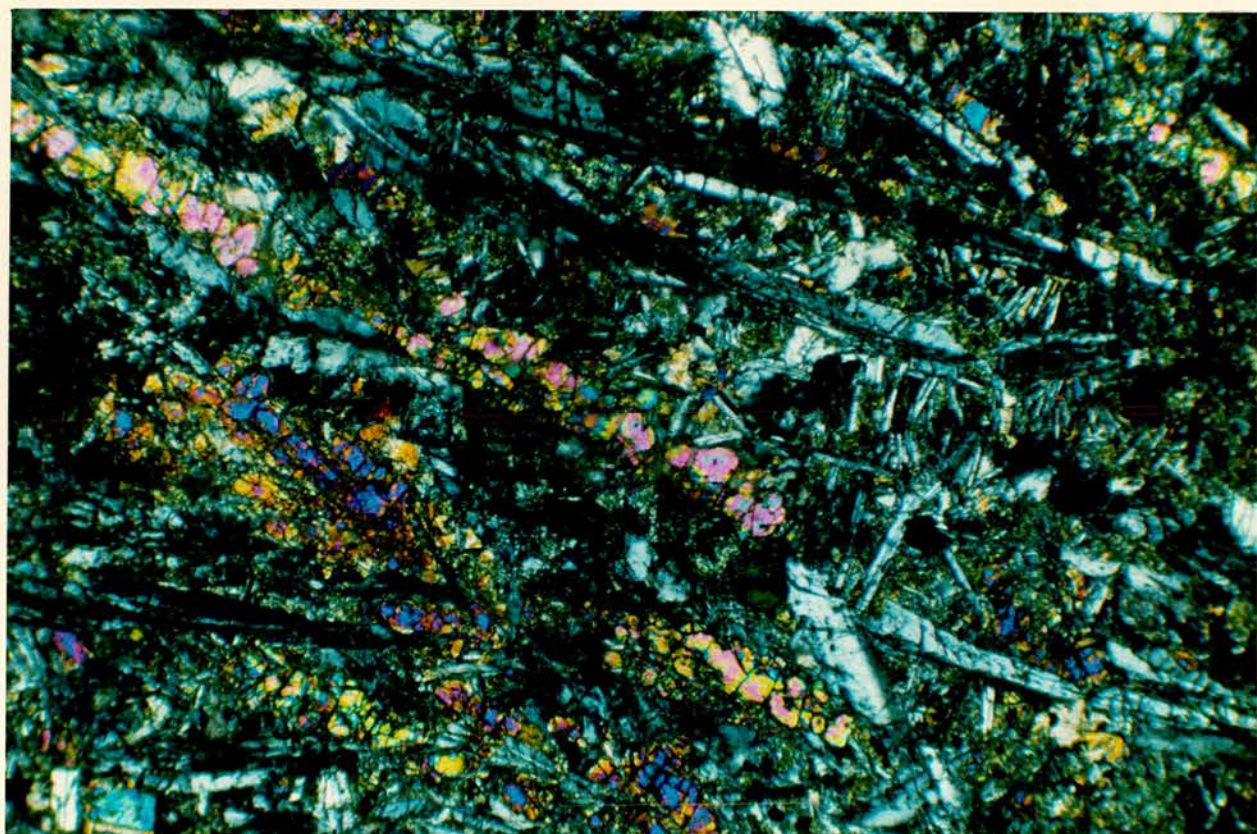
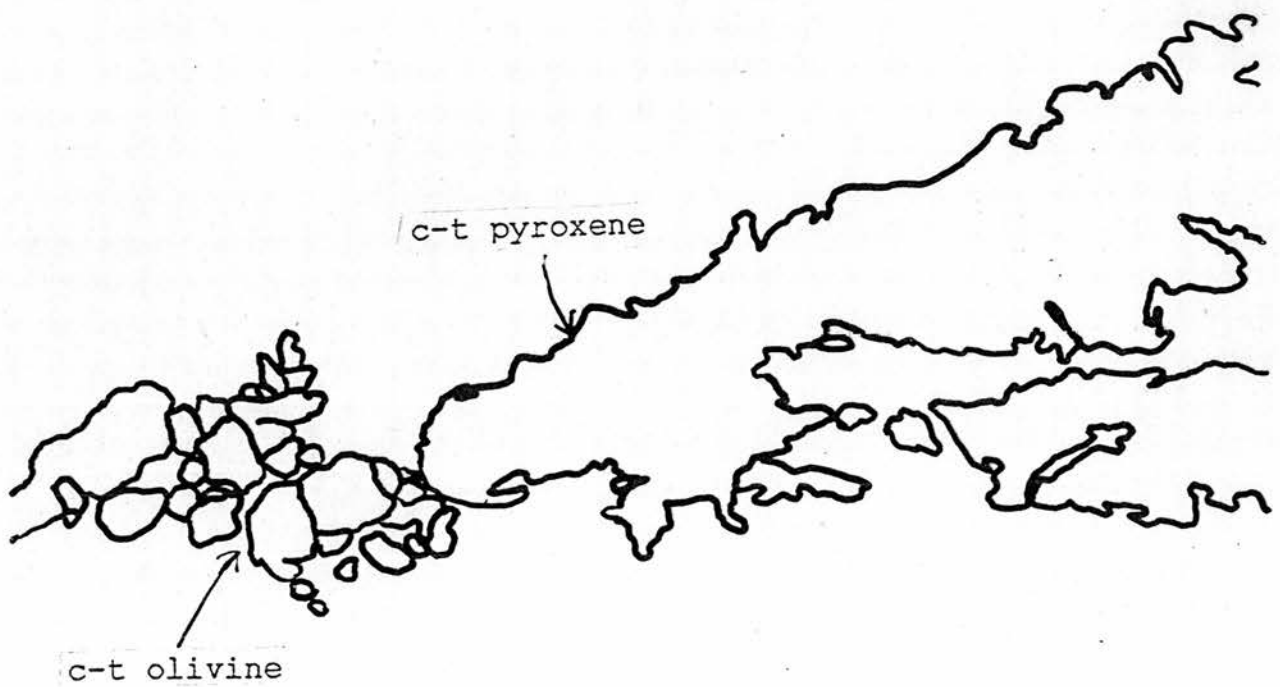
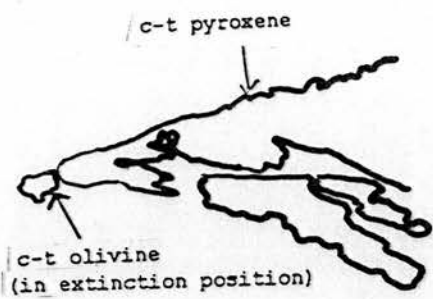
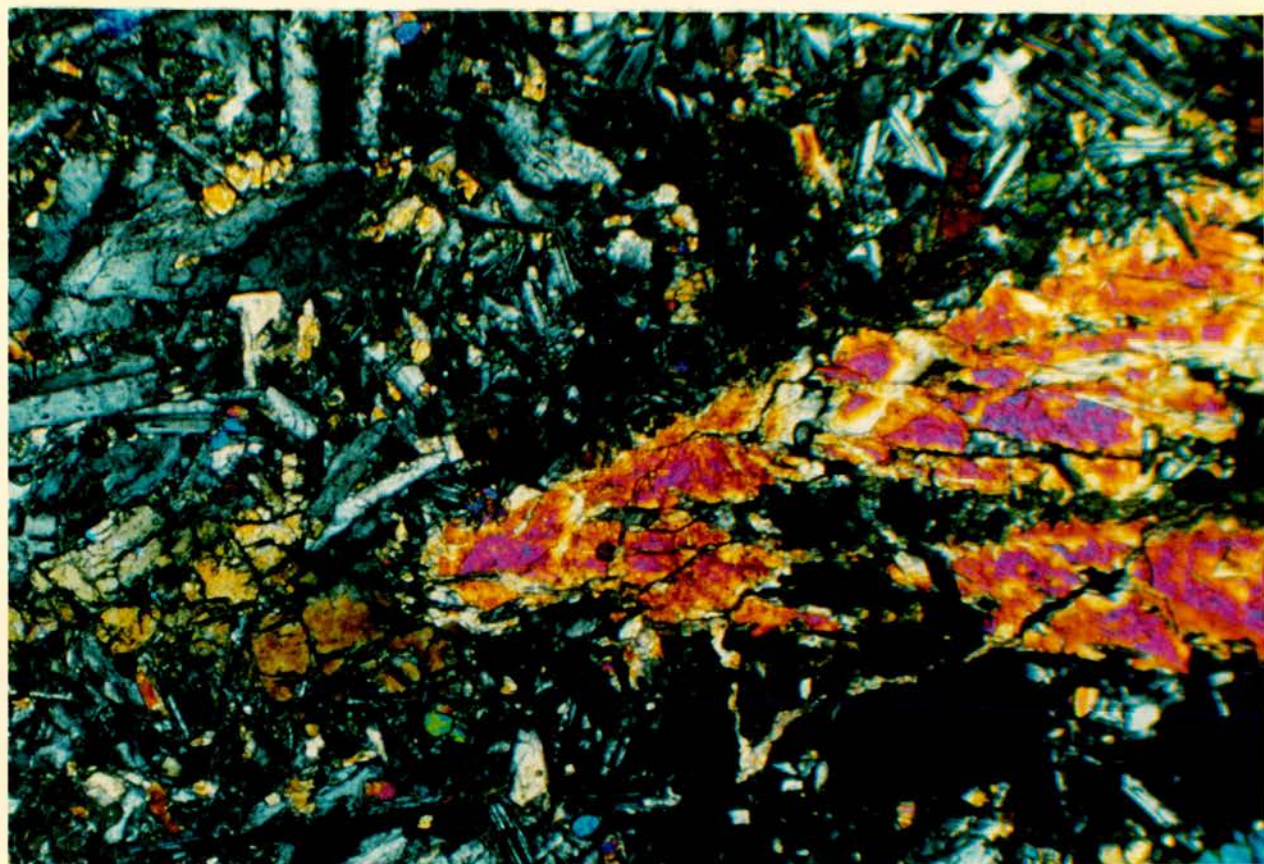
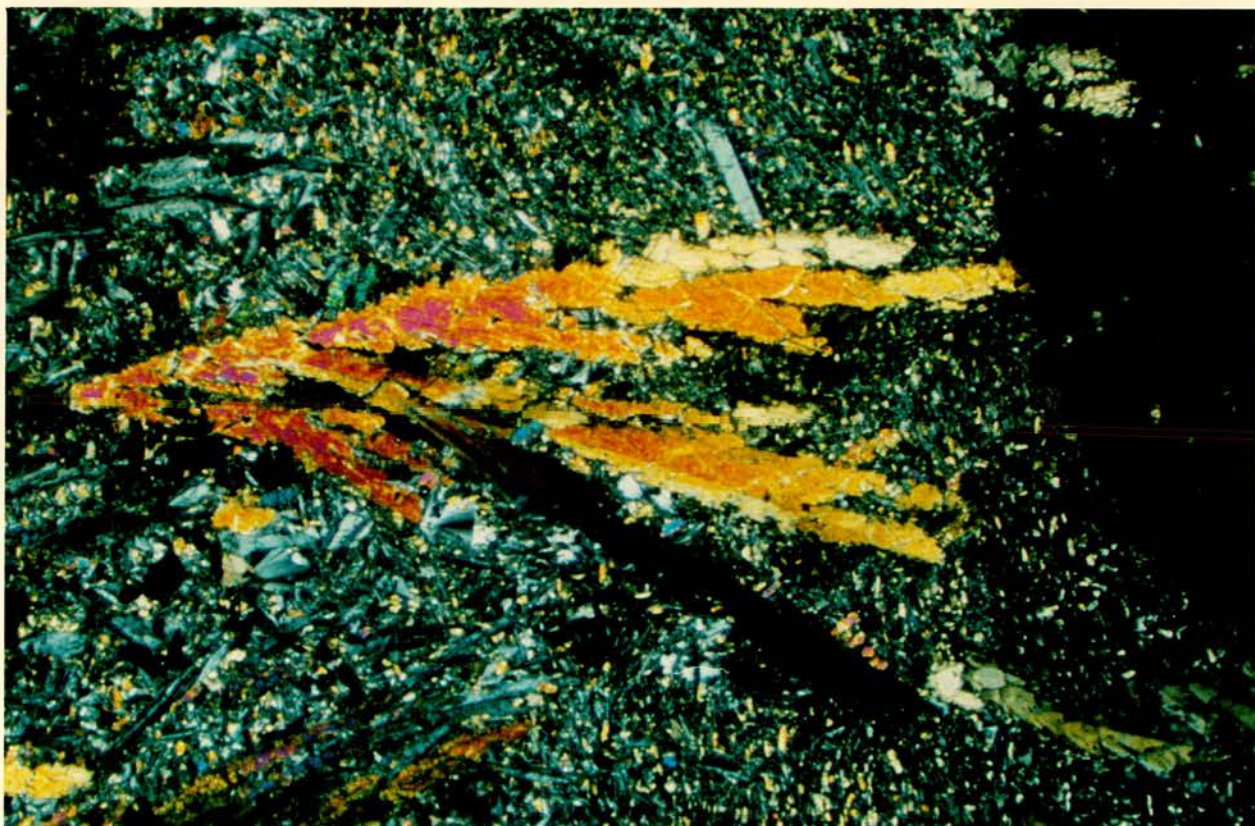


Plate 3.13 General view of comb-textured olivine and pyroxene in the Intermediate Unit, 150'. Comb-textured olivine is in extinction position. Area of the close-up photograph is highlighted. XN x 15

Plate 3.14 Close up of contact between comb-textured pyroxene on a comb-textured olivine crystal. XN x 50





concentrations, although since all sections are of identical orientation, they allow comparison amongst themselves, and with *10a/174' in Table 3.1 (which represents the modal analysis of Band 10/174' along a similar strike).

Modal comb-textured olivine and plagioclase increases with distance into the Intermediate Unit (Table 3.1) but decreases close to the Central Unit.

Olivine.

Olivine is present as euhedral, subhedral, anhedral and intergranular matrix crystals and columnar comb-textured crystals. Much has been altered to bowlingite or serpentinised. A general view of comb-textured olivine is shown in Plate 3.11. Olivine dendrites may be 2-3cms in length and branch towards the centre of the dyke. Some of these crystals appear to be anchored to a plagioclase crystal. The width of the dendrite diminishes with length. In some parts of the dyke, dendrites have relatively few branches, whereas in other areas branches are more numerous and complicated. The dendrites have grown upwards oblique to the vertical, and at 174' the complex dendrites extend towards the north, while less complicated dendrites can show a southwards inclination. Viewed along the strike of the dendrite, the crystals are approximately 2-4mm in diameter, anhedral or subhedral in shape, and form long columnar crystals. Cross-sections show the comb-textured

crystals to be euhedral or subhedral, with an average diameter of 0.1mm, having an elongate, flattened tape-like form (cf Walker 1985). Figure 3.5 shows general comb-textured olivine crystal morphology. The average diameter of intergranular matrix crystals is 0.05mm, these being subhedral, rather rounded crystals.

Comb-textured olivines were studied with the aid of the Universal Stage to determine crystallographic orientation of the crystals. A total of 109 crystals from 15 dendrites from Band 10/174' were analysed, together with 43 crystals from 5 dendrites in Band 12/174'. Isolated matrix crystals were also analysed. Band 10/174' (Figure 3.1a) displays groupings of the a, b and c crystallographic axes, which may overlap. The well defined groups in Band 10/174' show the a axes lying approximately horizontally across the dyke, plunging both north and southwards (Figure 3.1a). The b axes lie approximately vertical, parallel to the walls of the dyke and again may plunging either to the north or south. Band 12/174' shows similar clustering of the a axes, which lie across the dyke, with the b axes near vertical, while the c axes show a more scattered grouping.

The comb-textured crystals are preferentially elongate along the c axes with only a minority elongate to the a axes (Figure 3.1b). Individual crystals are orientated with their long axes vertical, parallel to the walls of the dyke.

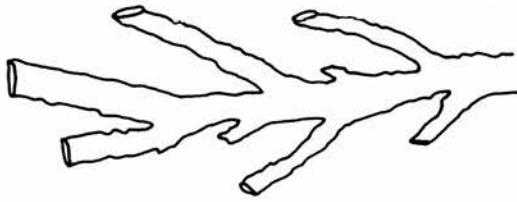


Figure 3.5
Morphology of comb-textured olivine.

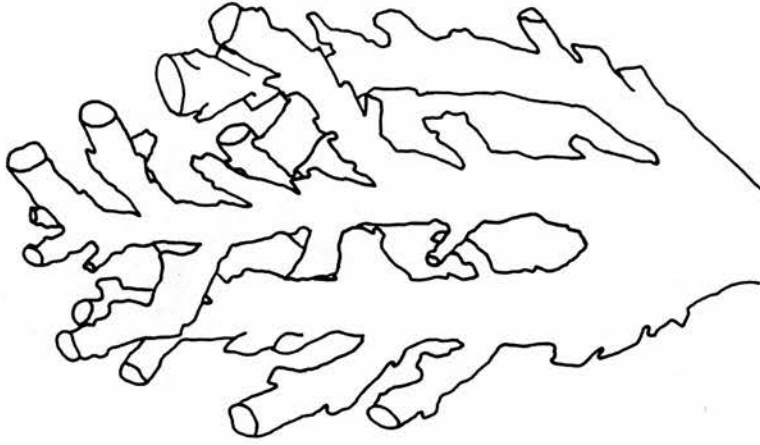


Figure 3.7
Morphology of comb-textured pyroxene.

Segments of the dendrite show almost identical crystallographic orientation. The dendrites are horizontally elongate along the a axes, perpendicular to the individual crystals that compose the dendrite (Figure 3.1 and 3.6).

This feature is well-exhibited by a dendrite analysed in Band 12/174' and depicted in Figure 3.1c. The segments of the dendrite are numbered, and their axes show close groupings on the stereograms. The dendrite is nearly horizontal having grown eastwards towards the centre of the dyke. This is parallel to the a axes, while crystals within the dendrite (segments 1 and 6), show the fastest axis of growth to have been the c axis.

The fastest growth (elongation) direction of the comb-textured olivines was the a axis, across the strike of the dyke (east-west), while the slowest growth direction was parallel to the b axis (which strikes horizontally along the strike of the dyke). This is shown graphically in Figure 3.1c. Walker (1985) states that the comb-textured olivines in the area of the dyke he investigated were elongate parallel to the a axes, flattened along the c axes, with the b axes parallel to the dyke walls.

Pyroxene.

Pyroxene is present as subhedral and anhedral crystals as small matrix crystals, comb-textured dendrites and oikocrysts. The dendrites may be 5mm in

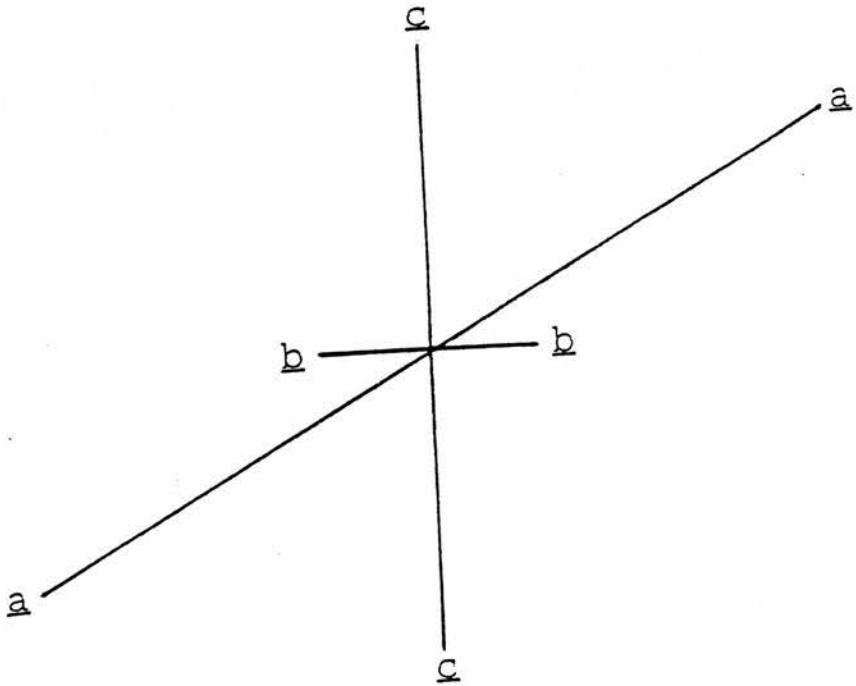
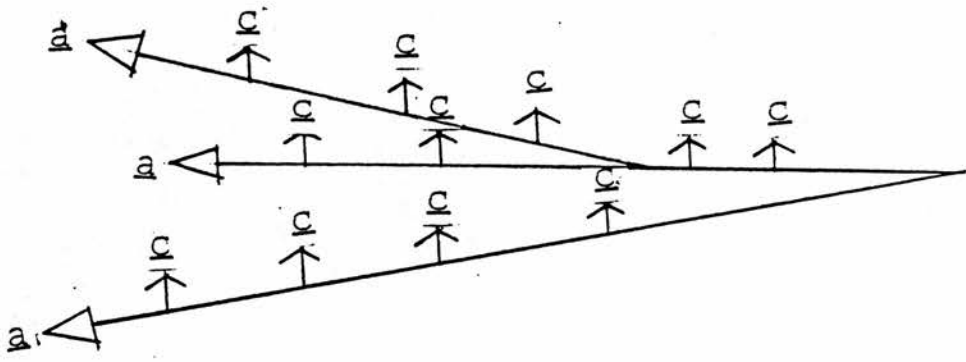


Figure 3.6 Orientation and crystallographic axes of the comb-textured olivines (174').

length and are frequently curved. A general view of comb-textured pyroxene is shown in Plate 3.12. Comb-textured pyroxenes in the lamina at the contact of the Intermediate and Central Units at 174' contain narrow bands of opaques parallel to the edges of the crystals. Comb-textured pyroxenes exhibit complex sector zoning, having high- and low-CaO sectors (see Chapter 4). The crystals are approximately equidimensional when viewed perpendicular to the length of the dendrite, with an approximate diameter of 0.25mm in the lamina in Band 10/174'. Several adjacent crystals have a similar crystallographic orientation suggesting the presence of one crystal connected at levels not seen in the thin section. Figure 3.7 illustrates a possible comb-textured pyroxene crystal morphology. Comb-textured pyroxenes in a thin section parallel to the strike of the dyke and perpendicular to the elongation direction of the crystals exhibit two cleavage traces intersecting at approximately 90° indicating that this section cuts the a and b axes. This indicates that the crystals are elongate along the c axis, with approximately equidimensional a and b axes.

In the northern segment, where the olivine-rich band becomes pyroxene-rich, there is normally a close relationship between the olivine and pyroxene comb-textured crystals (Plates 3.13-3.14). There may be an overlap of 0.5-4.0mm of comb-textured pyroxene and olivine. Where there is an overlap of these comb-

textured minerals, they are normally in close contact, actually touching each other or possibly separated by a single groundmass plagioclase. If the two minerals are in contact, the pyroxene may frequently establish growth along the elongation of the comb-textured olivine, with the latter continuing along the edge of the pyroxene dendrite. At 150', the two minerals exhibit a complex relationship, with a pyroxene dendrite being in contact with two olivine combs that continue along either side of it, for a distance of 4mm. As the comb-textured pyroxene has developed branches, comb-textured olivine has continued to develop between the branches, although it may no longer be present along the outer edge of the pyroxene.

Matrix pyroxenes measure approximately 0.1mm in diameter. The volume of matrix pyroxene increases in the comb-textured pyroxene lamina adjacent to the Central Unit (cf Walker 1985). These matrix crystals are elongate parallel to the plagioclase crystals, perpendicular to the strike of the dyke. Ophitic, subophitic and poikilophitic textures are also developed within the Intermediate Unit, with pyroxene oikocrysts wholly or partially enclosing the olivine or feldspar chadacrysts (Plate 3.10). The irregularly shaped oikocrysts decrease in diameter across Band 10/174' from 1mm adjacent to the Intermediate Unit to 0.5mm adjacent to the Central Unit.

Plagioclase Feldspar.

Walker (1985) states that plagioclase displays three habits: interstitial, elongate and "inter-olivine". The comb-textured plagioclase (Walker's elongate feldspar) has developed within the troctolitic bands, and also rarely present within the pyroxenitic bands. The elongate, comb-textured plagioclase may be curved or bent in appearance. Plate 3.11 shows a general view of comb-textured plagioclase. The majority consist of a single lath, although in places, there are several branches developed. At 156', there are single, curved laths up to 1.5mm long, as well as multi-branched crystals up to 3mm in length. These multi-branched crystals have a central lath with minor branches either side of it. The simple, single lath comb-textured plagioclase increases slightly in width towards the centre of the dyke. They may exhibit simple albite twinning.

Interstitial groundmass plagioclase exhibits simple albite or repeated twinning. Matrix plagioclase exhibits trachytic texture (which maybe curved) as chadacrysts in the ophitic pyroxene oikocrysts. The average dimensions of the interstitial matrix plagioclase is 0.2mm by 0.1mm.

The "inter-olivine" plagioclase is found between comb-textured olivine and more rarely, comb-textured plagioclase. These small feldspars (0.1-0.2mm in length) are elongate perpendicular to that of the comb-textured crystals. The texture may continue between

several adjacent dendrites. The trachytic texture parallels the walls of the dyke and may be curving, with the arc convex to the centre of the dyke.

The Intermediate Unit at 40'.

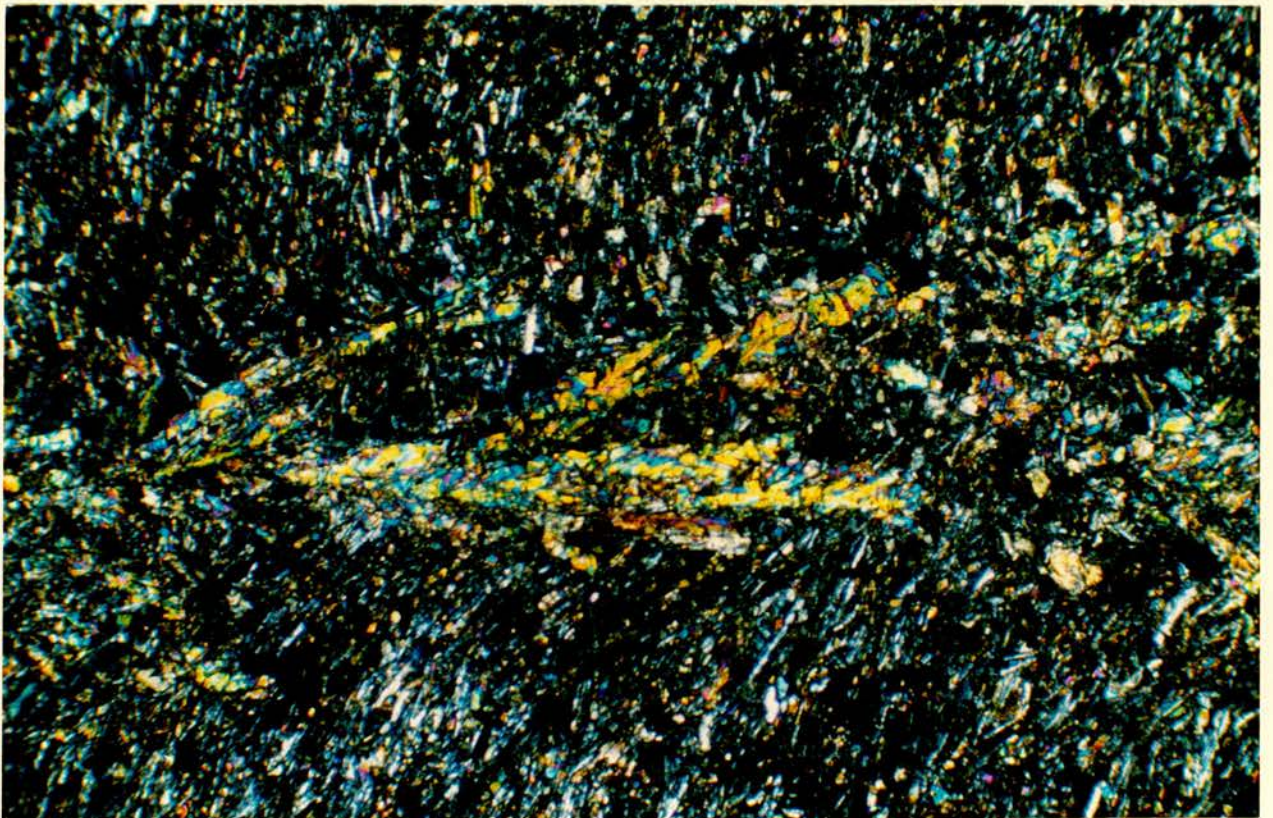
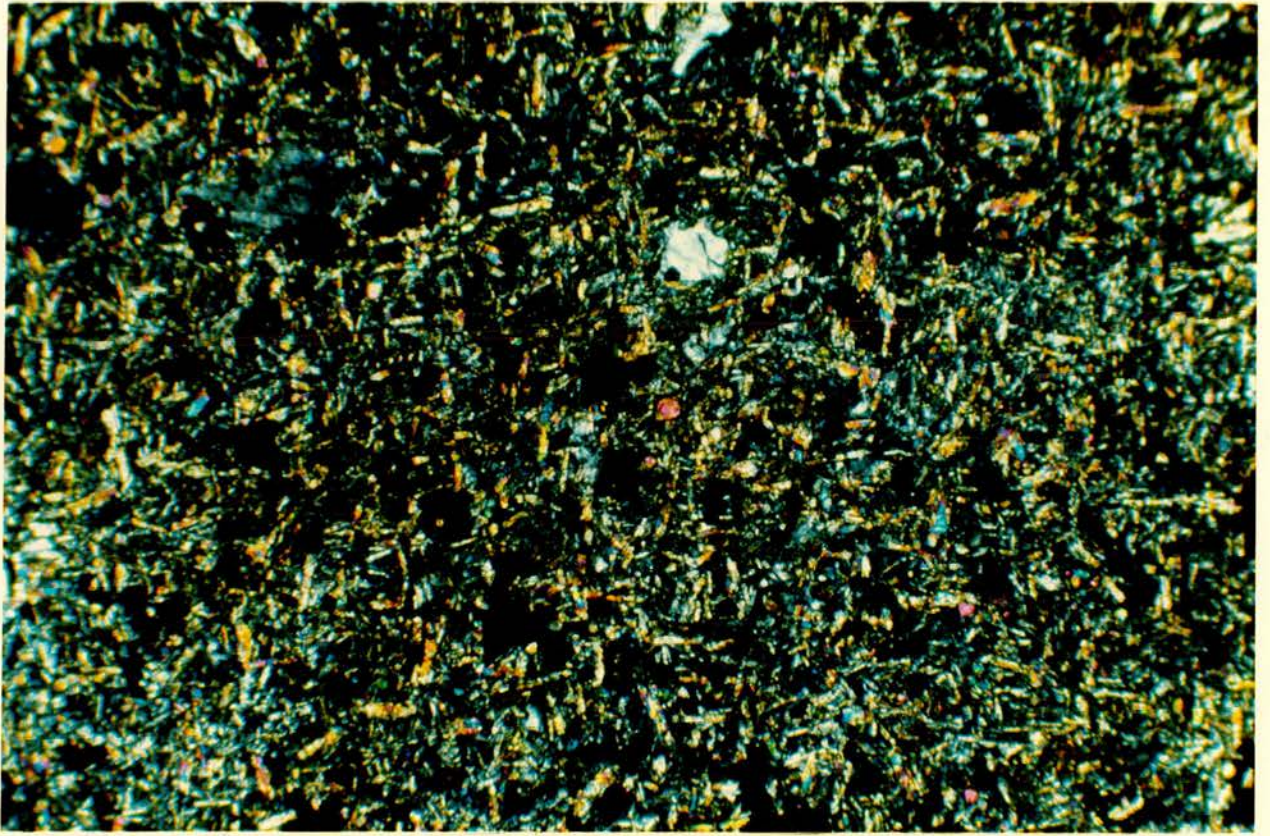
Three thin sections (one orientated horizontally, another vertically parallel to the strike of the dyke and a third vertically perpendicular to the walls of the dyke) were prepared both for the Intermediate Unit and the "central band" at 40'. This sample of Intermediate Unit from the southern segment of the dyke is an amygdaloidal rock with comb-textured pyroxene and trachytic texture (Table 3.2). Modally (Table 3.1) this sample is depleted in olivine and feldspar and enriched in pyroxene and opaques relative to the Intermediate Unit elsewhere in the dyke. It shows trachytic texture with plagioclase aligned parallel to the dyke walls but has no ophitic pyroxene (Plate 3.15, Table 3.2). Groundmass crystals exhibit little variation in diameter between 40' and samples from further north.

Olivine is only found as subhedral or anhedral groundmass crystals, averaging 0.05mm to 0.1mm in diameter and elongate parallel to the trachytic texture of the plagioclase.

Pyroxene forms comb-textured crystals and subhedral or anhedral groundmass crystals. The comb-textured pyroxene forms narrow dendrites 5-20mm long, that are slightly disjointed along their length. They have a

Plate 3.15 Photomicrograph of the Intermediate Unit at 40' in the southern segment, showing comb-textured pyroxene and trachytic texture developed by the groundmass plagioclase crystals. XN x 50

Plate 3.21 General view of the "Central Band", 40'. Unlike the Central Units elsewhere in the dyke, it is non-porphyrific. XN x 50



very feathery appearance and interdigitate with adjacent crystals. The spine of the dendrite shows uniform extinction, while branches show extinction at varying orientations indicating some variation of crystallographic orientation. In cross-section the pyroxene is occasionally euhedral, but normally subhedral or anhedral, with a diameter of 0.05mm to 0.1mm. Groundmass pyroxene may be elongate parallel to the trachytic texture of the feldspars, ie perpendicular to the comb-textured pyroxenes.

Plagioclase is present as phenocrysts as well as groundmass crystals. Phenocrysts may be up to 1.5mm in length and lie parallel or perpendicular to the trachytic texture, which parallels the walls of the dyke. The matrix feldspar has an average lath length of 0.1-0.2mm. The trachytic texture may be curved in places, being convex to the walls of the dyke, and may curve around amygdales. The amygdales are elongate and lie parallel to the strike of the comb-textured pyroxenes and may measure 3mm by 1mm. Some form disjointed veinlets. Many contain opaques which cluster around the periphery of the amygdales. The opaques are angular, (which may be due to several small crystals clustering together) and measure 0.1mm to 0.3mm in diameter.

3.5 The Central Unit.

a). Hand specimens were obtained from 174', 156', 150' and 54' together with a sample from the "central band" at 40' (Plates 3.1, 3.8, 3.16).

b). A prominent feature of all these samples (with the exception of 40') is the abundance of amygdales: the majority infilled with zeolite and calcite (Plate 3.17-3.18, Table 3.2). The Central Unit is an inequigranular, microcrystalline dolerite. The sample from 40' will be described separately due to its individual features.

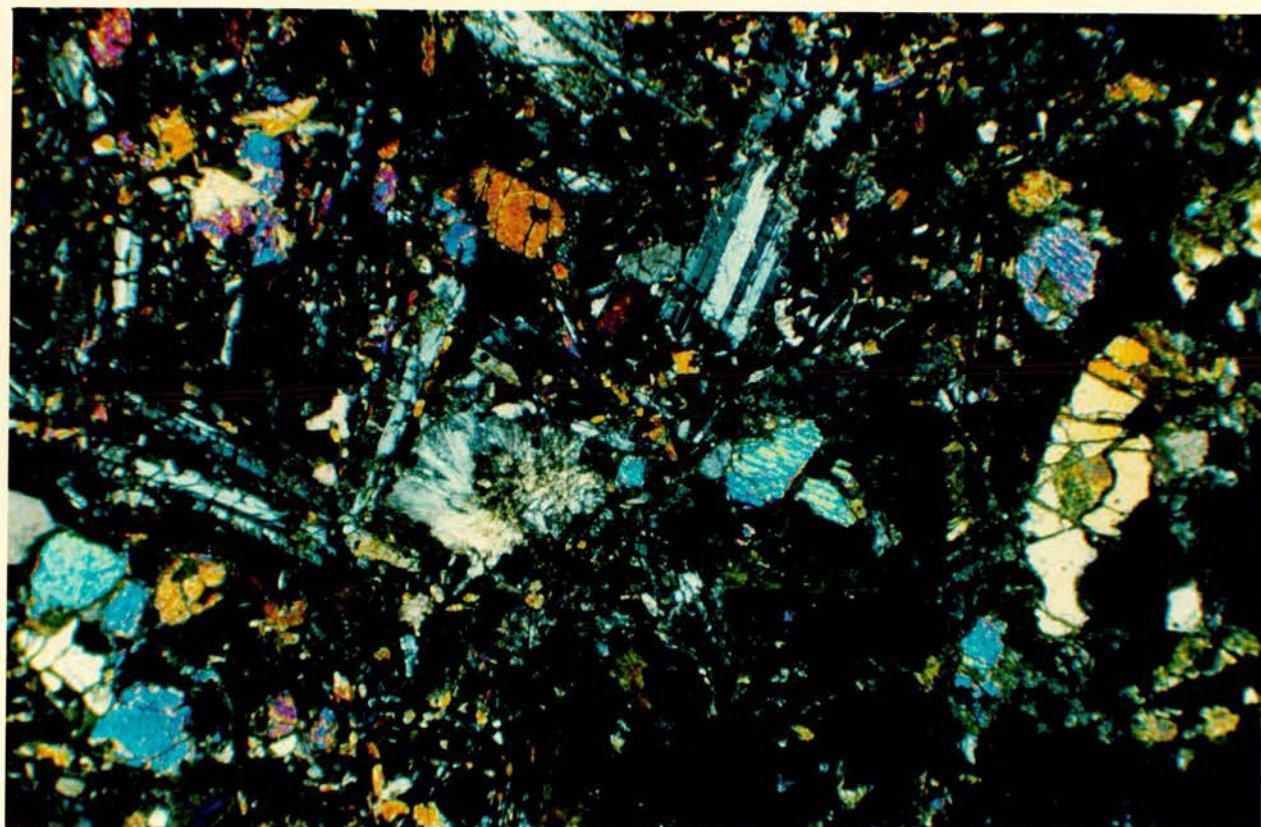
Total modal pyroxene content is similar for all samples, with total feldspar content also varying little (Table 3.1). Olivine content exhibits the greatest variation of the essential minerals, and ranges from 8% to 16% in 150' and 54' respectively. The volume of opaque minerals is comparable along the length of the dyke varying from 7% to 11% (150' and 54' respectively).

Olivine.

Olivine phenocrysts may be euhedral or subhedral, with an average 43% of the olivine phenocrysts enclosing opaque minerals. The phenocrysts exhibit glomeroporphyritic texture, with the c axes showing approximately similar orientations. At 54' some phenocrysts are simple skeletons exhibiting embayments. The phenocrysts vary in diameter from 0.5 by 0.3mm to microphenocrysts of 2.0 by 1.5mm, with all sizes being

Plate 3.17 Photomicrograph of the Central Unit, 174'
with subhedral olivine and twinned plagioclase
phenocrysts with zeolite-filled amygdales. XN x 15

Plate 3.18 Photomicrograph of the Central Unit, 54' in
the middle segment of the dyke. XN x 15



present along the length of the dyke. The groundmass crystals vary in size from 0.2 by 0.1mm to 0.3 by 0.3mm.

Twenty one olivine phenocrysts and one matrix crystal were analysed with the Universal Stage. Figure 3.1a shows no large groupings of any crystallographic axes although small groups are highlighted in Figure 3.1a. Olivines in the Central Unit may be elongate along the c,b or a axes respectively as shown in Figure 3.1b, with crystals having variable dip with none lying horizontally along the strike of the dyke.

Pyroxene.

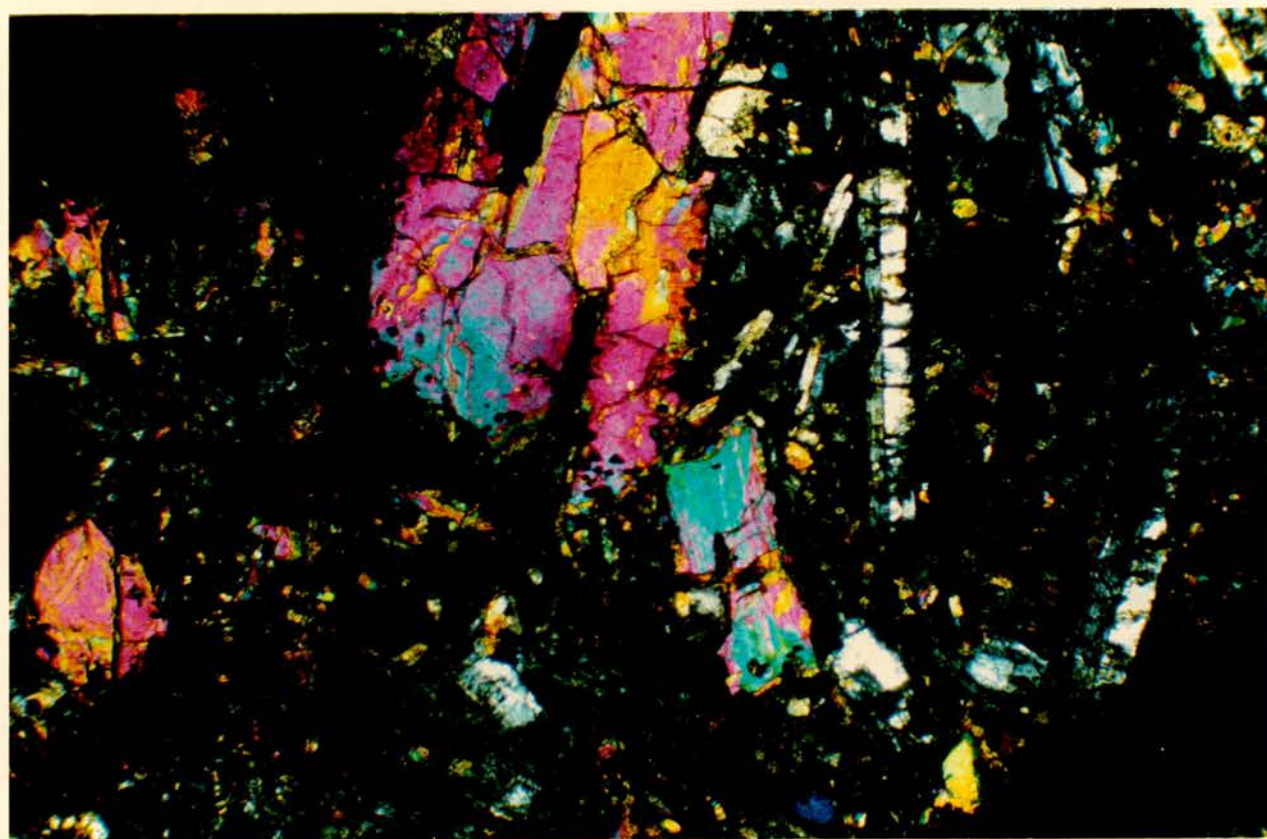
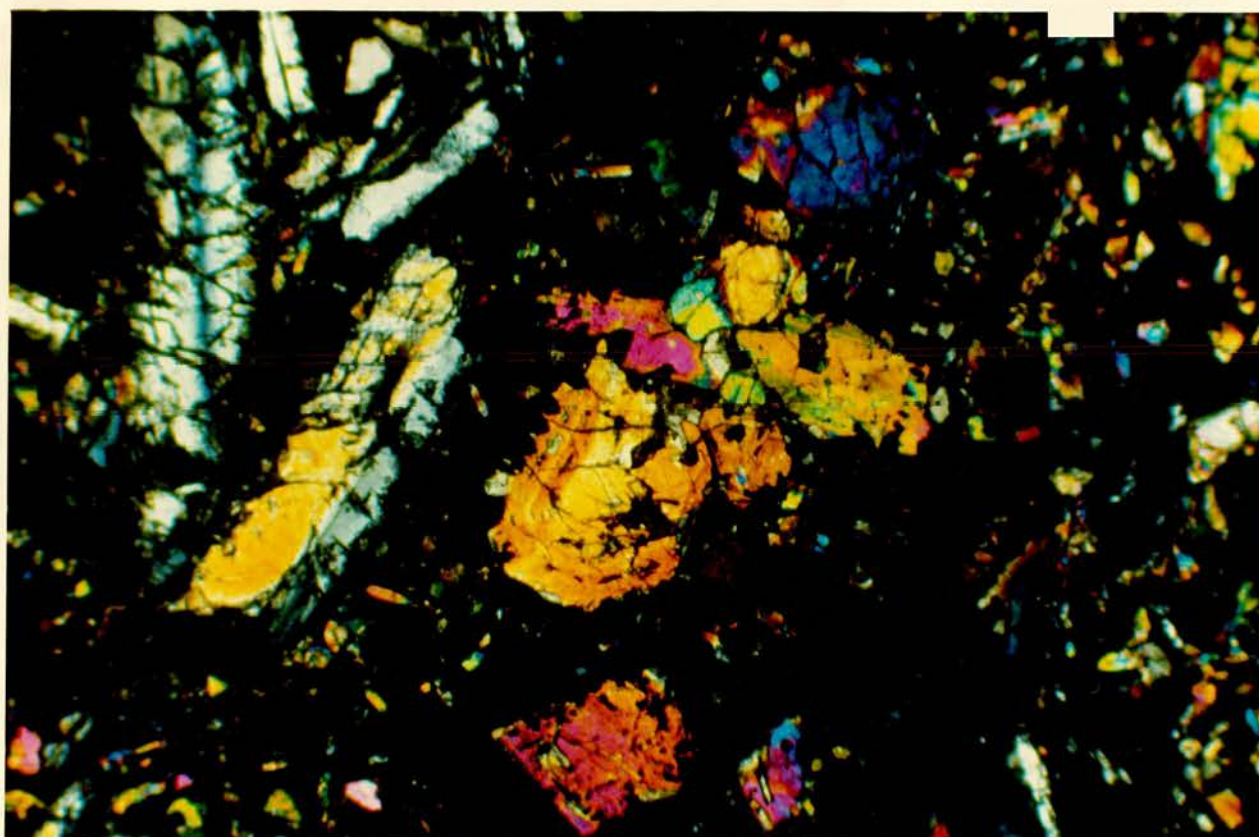
Pyroxene phenocrysts are usually euhedral or subhedral and frequently exhibit glomeroporphyritic texture. The phenocrysts show normal zoning with a narrow rim or complex sector zoning, the latter sometimes being hourglass sector zoning (Plates 3.19-3.20). 174' contains slightly smaller phenocrysts (0.3 by 0.2mm to 0.5 by 0.4mm), compared to 150' and 54' which contain phenocrysts averaging 1.0 by 1.5mm diameter. Matrix crystals are predominantly subhedral, and range from 0.1 by 0.05mm to 0.2 by 0.2mm in diameter.

Plagioclase Feldspar.

Plagioclase phenocrysts display albite twinning which may be simple or repeated, with some crystals being interpenetrant. Phenocrysts vary in size from 1mm by 0.3mm to 4mm by 1.3mm. Some large phenocrysts at 150'

Plate 3.19 Hourglass sector zoning in
pyroxene microphenocryst in the Central
Unit at 174'. XN x50

Plate 3.20 Oscillatory- and sector zoned
pyroxene phenocryst in the central Unit,
174'. XN x50



enclose anhedral pyroxene groundmass crystals. Matrix feldspars have an average size of 0.4 by 0.1mm. At 174', groundmass feldspars within 2mm of the contact with the Intermediate Unit display trachytic texture.

Accessory Minerals.

Accessory minerals include opaques and zeolite. The abundant opaque minerals (7-9 modal%) are of angular habit and average diameter of 0.1mm. They are found around the periphery of phenocrysts, within phenocrysts or as isolated groundmass crystals. The zeolite occurs within amygdales and displays a radial, fibrous texture. The amygdales may be irregular or rounded, varying in size from 2mm² to 0.5mm by 0.3mm.

The "Central Band" at 40'.

The "Central Band" at 40' is amygdaloidal and composed solely of groundmass crystals in which the feldspars exhibit trachytic texture parallel to the dyke walls (Plate 3.21). Olivines are equidimensional, subhedral or anhedral with diameters of 0.05mm to 0.1mm and occasionally zoned rims. Pyroxenes are elongate, subhedral or anhedral with a diameter of 0.05mm to 0.1mm and parallel the trachytic texture of the feldspars. No zoning of pyroxene is evident.

Plagioclase laths measure 0.05mm to 0.15mm in length, and exhibit simple albite twinning. The ends of

the crystals may be irregular. In close proximity to the veins the plagioclase forms slightly larger crystals.

This band contains veins parallel to the walls of the dyke. The thickness of which increases with distance into the dyke, from 0.3mm to 0.35mm. They are composed of interlocking plagioclase crystals with an average diameter of 0.2mm, which have grown across the vein, together with zeolite and calcite crystals, and accessory olivine and pyroxene.

3.6 Internal Variation in Crystal Diameter.

There is a decrease in matrix crystal size within the comb-textured pyroxene lamina adjacent to the Central Unit. This lamina contains abundant opaques, groundmass pyroxene, and feldspars displaying trachytic texture parallel to the strike of the dyke. Average groundmass crystal size in the comb-textured olivine layer is approximately twice that of groundmass crystals within the comb-textured pyroxene lamina (0.1mm compared to 0.05mm respectively). The Central Unit contains groundmass crystals of greater diameter than the Intermediate Unit.

3.7 The Sill.

a). In hand specimen the sill is a dark grey-green, coarse-grained rock. Abundant olivine phenocrysts give the rock a "sugary" texture.

b). The picrite sill contains abundant olivine phenocrysts. Both the sill and dyke contain the same essential minerals, although in varying amounts (Table 3.1). Table 3.3 displays only the total olivine, pyroxene, plagioclase and opaques for the sill complex. Data for the dyke is included for comparative purposes. The groundmass of the sill is rich in plagioclase feldspar, which may form patches up to 4mm in diameter. Pyroxene exhibits poikilitic texture, enclosing or partially enclosing olivine and feldspar. A general view of the sill adjacent to the dyke is shown in Plates 3.4 and 3.21.

Olivine.

Olivine is present predominantly as phenocrysts. Modal total olivine of the sill adjacent to the dyke at 151' and 100' is 41% and 60% respectively (Table 3.1). The latter is in close agreement with the typical modal olivine content of the sill at Bornaskitaig (60%- Gibson 1988) and the T.S.C. (59%- Gibson 1988) (Table 3.3). Olivine crystals may be euhedral, subhedral or anhedral. The larger ones (3mm by 1.5mm) being usually euhedral or subhedral, while the smaller ones (1mm by 0.7mm) normally subhedral or anhedral. The olivines exhibit

Table 3.3

**Comparison of modal proportions from the
Little Minch Sill Complex.**

Modal %	Sill adjacent to dyke:		"Typical"	Bornaskitaig
	151'	100'	Analysis	Analysis
			(Gibson 1988)	
Olivine	40.7	60.1	58.6	60.0
Pyroxene	16.7	11.1	10.8	9.8
Plagioclase	40.2	25.4	28.7	30.0
Opagues	2.5	3.3	2.0	0.2

glomeroporphyritic texture, with adjacent crystals having similar crystallographic orientations. No zoning of the phenocrysts was noted. The olivines contain opaques, which may be associated with cracks within the crystals.

Pyroxene.

Pyroxene forms ophitic crystals which totally or partially enclose both olivine and plagioclase. Modally there is little variation in pyroxene content (17% and 11% for 151' and 100' respectively) comparable with the typical mode of 10% for the Bornaskitaig sample (Gibson 1988). The pyroxene crystals may be isolated or cluster between two olivine phenocrysts. A vertical section from 151' contained several crystals that exhibited two cleavage traces, indicating that many of the crystals have a horizontal c axis, parallel to the dyke wall.

Plagioclase Feldspar.

Plagioclase is predominantly found as matrix crystals of approximately 0.1mm by 0.05mm size arranged tangentially around the olivines. Modally, the samples analysed contained 40% and 25% plagioclase (151' and 100' respectively, Table 3.3). This variation is due to the differing olivine content of these two samples. The T.S.C. typical analysis of 29% (Gibson 1988), is comparable. Some larger crystals (microphenocrysts)

measure 0.5mm by 0.2mm. The smaller crystals have single albite twinning, while the larger ones exhibit multiple albite twinning. Occasional crystals also exhibit a zoned rim.

Accessory Minerals.

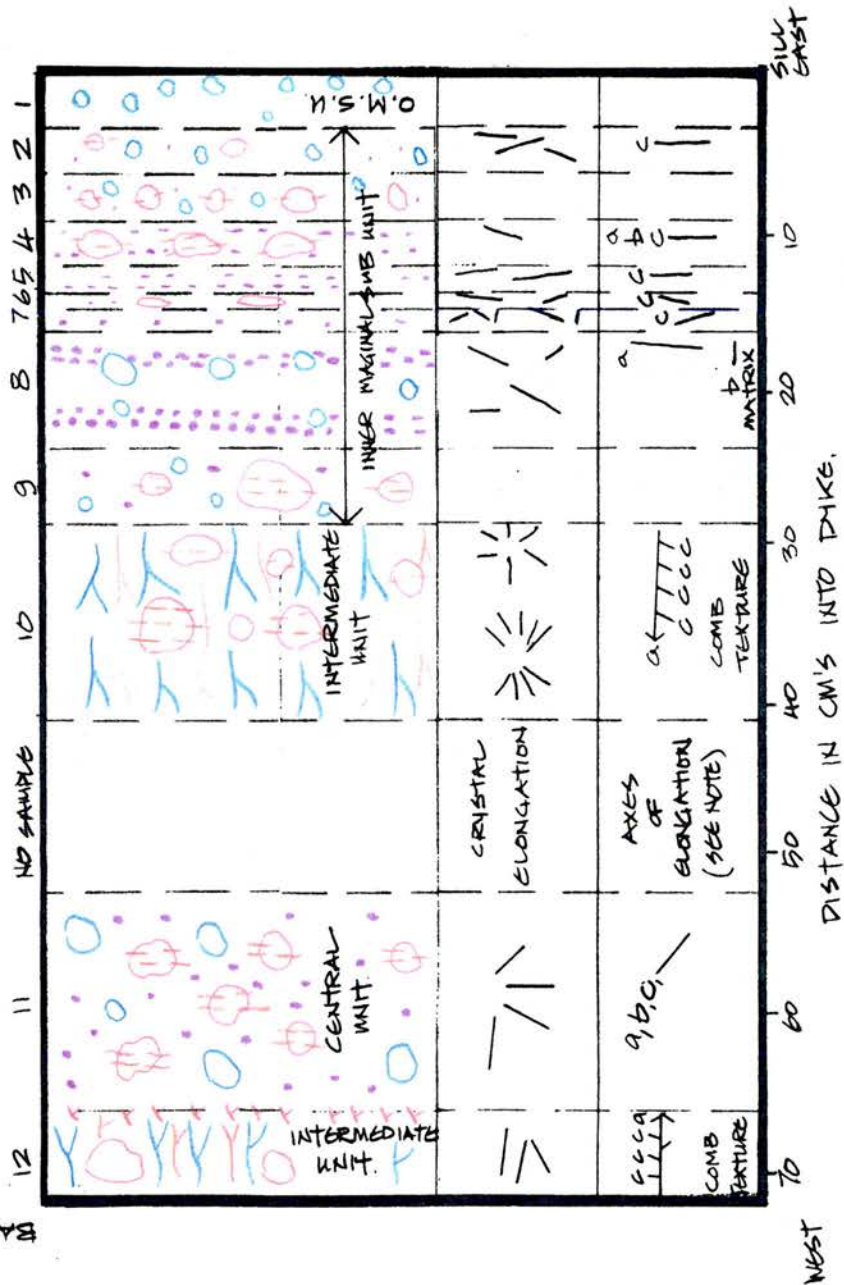
Other minerals in the sill include opaque minerals, which occur as either groundmass crystals or enclosed by other minerals, normally olivine. Modally, the samples from 151' and 100' contain 3% opaques. This compares to 2% and less than 1% quoted by Gibson (1988) (Table 3.3). The opaques enclosed within olivines measure approximately 0.2mm in diameter, while those in the groundmass 0.1mm. They may be either square, anhedral or elongate, with the latter measuring 1mm by 0.1mm.

3.8 Summary.

The essential minerals of the dyke, together with the two generations of olivine growth, purplish augite and absence of orthopyroxene and pigeonite indicate that the magma forming the dyke is alkali in composition.

Modal and textural variation across the dyke is displayed in Tables 3.1, 3.2 and Figures 3.1-2 and 3.8.

1030



NOTE: AXES OF ELONGATION - ALL REFERENCES ARE TO PHENOCRYSTS UNLESS STATED OTHERWISE.

- OLIVINE
- PIROXENE
- PLAGIOCLASE
- AMPHIBOLES

Figure 3.8 Summary figure to show textures, orientation of crystallographic axes and axes of elongation of olivines across the dike at 174'.

The chilled margin at 100' varies from that at 174' (Table 3.1) being relatively enriched in plagioclase and opaques and relatively depleted in olivine and pyroxene. The distinction of the Outer and Inner Marginal Sub-Units in field specimens is supported by the modal proportions of minerals and textures (Tables 3.1, 3.2 and Figures 3.1, 3.2). Band 2/174' is an intermediate between the Outer and Inner Marginal Sub-Unit. Texturally, it is identical to the remainder of the Inner Marginal Sub-Unit (Table 3.2), but modally (Table 3.1) it exhibits similarities with the Outer Marginal Sub-Unit.

O'Hara (1968) stated that if a magma chamber was replenished by a batch of primitive magma, this may trigger eruption of porphyritic magma. This possible explanation for phenocrystic variation across the banding will be investigated further in Chapter 6.

Table 3.2 and Figure 3.8 display the textures of the Inner Marginal Sub-Unit, while Figure 3.2 shows modal proportions graphically. There is lateral variation between 174' and 151' (Tables 3.1 and 3.2). The Inner Marginal Sub-Unit at 151' contains comb-textured and phenocrystic pyroxene. No comb-textured pyroxene was seen in Bands 2-3/174' at a comparable distance into the dyke. At 151', the Outer Marginal Sub-Unit is comparable with the Inner Marginal Sub-Unit at 174' (Table 3.2). This suggests changing crystallisation conditions along the dyke, causing textures to develop in different units at different distances along the dyke.

Comb-textured pyroxene has also developed within the Inner Marginal Sub-Unit in Band 9/174'. Variation in habit and length of the pyroxene dendrites within the Inner Marginal Sub-Unit and the Intermediate Unit may reflect slightly different crystallisation conditions.

All three essential minerals display comb-textured growth in the Intermediate Unit. Samples from the northern segment exhibit similar textures and modal proportions (Tables 3.2 and 3.1), while the sample from the southern segment displays different textures and modal proportions (Tables 3.2 and 3.1).

The Central Unit at 54' is dissimilar with regard to the textures and modal mineralogy to the "Central Band" at 40' (Plates 3.18 and 3.21). The Intermediate Unit and "Central Band" at 40' are similar modally (Table 3.1), although different texturally (Table 3.2), suggesting changing crystallisation conditions.

The Universal Stage analyses of the olivine crystals show trends across the width of the dyke. The Marginal Unit as a whole exhibits approximately vertical elongation of olivine crystals, shown graphically in Figures 3.1, 3.3-3.4. Olivines in the Outer Marginal Sub-Unit are elongate along the c or a axes, either vertically or horizontally, parallel to the dyke walls.

Comb-textured olivine within the Intermediate Unit show dendrites horizontally elongate along the a axis, with growth towards the centre of the dyke. Individual crystals within the dendrites are vertically elongated

along the c axis, as are the groundmass olivines analysed within Band 10/174'. In Band 12/174' the comb-textured crystals exhibit a southward plunge. The dendrites are elongate along the a axis, but each branch is at a slightly different crystallographic orientation to adjacent ones (Figure 3.6). In each of these dendrites, the individual crystals are almost vertical, elongate along their c axis (Figures 3.1, 3.6). Comb-textured pyroxene is also elongated along its c axis. Adjacent crystals in the thin section cut perpendicular to the elongation direction of the dendrite, show slight deviation in the orientation of the crystallographic axes (non-crystallographic branching).

The mineral chemistry and whole-rock geochemistry are investigated in Chapters 4 and 5 and will discuss aspects of the banding and minerals in greater depth.

CHAPTER 4

MINERAL CHEMISTRY.

4.0 Introduction.

The mineral chemistry of the major constituent minerals of the dyke and adjacent sill were analysed using a Jeol JcXA -733 Superprobe operated at an accelerating voltage of 15 Kv and probe current of 20 nA. The beam diameter and penetration were set to one micron, with raw data corrected using the ZAF program of JEOL. Reproducibility is 1wt% relative. Polished thin sections were prepared from several samples from the dyke (174', 150', 100', 54' and 40') and two samples of sill. Figure 2.2 and Plates 3.1, 3.6, 3.3, 3.8 and 3.7 detail locations of samples and thin sections.

Serial sections of sample 174' were investigated in detail for variation in mineral chemistry across the banding (Plate 3.1). All band contacts from the eastern side of the dyke were investigated with the exception of the contact between Bands 10 and 11/174' (the Intermediate and Central Units respectively), the contact between these units being analysed from a sample from the western side (Bands 12 and 11/174' respectively). It has been assumed that minerals from comparable bands

either side of the dyke would be temporally equivalent and by extension, chemically equivalent.

Sample 150', across the eastern contact of the Intermediate and Central Units (the non-investigated portion of 174') allowed end to end analyses of single comb-textured olivines (Plate 3.6).

The middle segment of the dyke is represented by a sample of the Central Unit at 54' (Plate 3.8). The southern segment was studied with a sample of the Intermediate Unit and central band from 40' (Plate 3.7).

The sill and dyke contact was studied using the 100' sample (Plate 3.3). The mineral chemistry of the sill was also studied using a sample obtained 25' from the dyke at 105'.

4.1 The study objectives were:

To define, compare and contrast the chemical composition of the principal minerals, both across the width and along the length of the dyke, and to test for relationships between mineral texture and composition. From analysis of internal variations within the dyke petrogenetic inferences are made. In addition the relationship of the dyke to the Little Minch Sill Complex and the Skye Main Lava Series was investigated.

4.2 Olivine.

Phenocryst, matrix and comb-textured olivine were analysed. Table 4.1 details representative olivine analyses of each band in the dyke and of the sill. The compositional range for the dyke is Fo₈₈ to Fo₄₆ with data displayed as a histogram (Figure 4.1) to show trends in composition. Figure 4.2 is a comparative diagram detailing compositional ranges of olivine, pyroxene and plagioclase across a synthetic east-west traverse. The most forsteritic cores per band are shown in Figure 4.3, both phenocryst and matrix where applicable, while Figure 4.4 shows olivine composition at each distance studied.

4.2.1 Phenocrysts.

Maximum forsterite content of phenocryst cores varies only slightly across and along the length of the dyke (Fo₈₈ in Band 1/174' to Fo₆₂ in Band 8/174' -Figures 4.1-4.4) with the exception of Band 9/174'. Phenocrysts exhibit continuous normal zoning, with a maximum variation of 27% Fo within the Central Unit at 174'.

Due to apparent lack of variation along the length of the dyke (Figures 4.1 and 4.2), all analysed samples are described in a margin to centre synthetic traverse. The transect at 174' (Figures 4.1, 4.2 and 4.4) shows a general decline in magnesium content of the cores towards the centre of the dyke. There is a slight increase in the mean phenocryst core composition from Band 4/174' to

Table 4.1
Representative Olivine Analyses from the dyke and sill.

Band	174/1	174/2	174/3	174/4	174/5	174/6	174/7	174/8	174/9	174/10
* Unit	O.M.S-U.	I.M.S-U.	I.U.							
Distance across dyke in Cms	2.88	4.15	7.85	9.80	13.38	15.46	16.23	19.11	25.51	28.49
	phen core	c-t core								
SiO ₂	39.83	39.03	39.79	39.74	39.88	39.35	39.74	39.34	36.41	37.55
FeO t	12.92	14.94	14.00	15.50	12.45	16.28	15.15	15.71	30.69	27.52
MnO	0.11	0.15	0.20	0.22	0.18	0.24	0.22	0.21	0.57	0.44
MgO	46.44	45.24	45.76	44.69	46.88	44.12	45.18	44.23	31.58	34.05
CaO	0.30	0.31	0.28	0.27	0.24	0.28	0.25	0.24	0.47	0.40
Cr ₂ O ₃	0.03	0.00	0.05	n.d.	0.06	0.00	0.02	0.09	0.02	0.00
NiO	0.29	0.27	0.29	n.d.	0.31	0.16	0.23	0.26	0.06	0.07
Total:	99.92	99.92	100.37	100.42	100.00	100.43	100.80	100.08	99.79	100.02

	Atoms per 4 Oxygens									
Si	0.99	0.98	0.99	0.99	0.99	0.99	0.99	0.99	0.99	1.00
Fe t	0.31	0.31	0.29	0.32	0.26	0.34	0.32	0.33	0.70	0.61
Mn	0.00	0.00	0.00	0.00	0.00	0.01	0.00	0.00	0.01	0.01
Mg	1.69	1.70	1.70	1.67	1.74	1.66	1.68	1.66	1.28	1.35
Ca	0.01	0.01	0.01	0.01	0.01	0.01	0.01	0.01	0.01	0.01
Cr	0.00	0.00	0.00	n.d.	0.00	0.00	0.00	0.00	0.00	0.00
Ni	0.01	0.01	0.01	n.d.	0.01	0.00	0.00	0.01	0.00	0.00

Fe %	84.43	84.37	85.35	83.71	87.03	82.85	84.16	83.38	64.71	68.80
Fa %	15.57	15.63	14.65	16.29	12.97	17.15	15.84	16.62	35.29	31.20

* Unit abbreviations:
O.M.U. Outer Marginal Sub-Unit
I.M.U. Inner Marginal Sub-Unit
I.U. Intermediate Unit
C.U. Central Unit

174/11	174/12	150a	150b	150c	150d	150e	100	54	40	40
C.U.	I.U.	I.U.	I.U.	I.U.	I.U.	C.U.	O.M.S-U.	C.U.	C.U.	I.U.
61.82	63.79	33.29	37.17	41.62	41.89	49.64	0.31	52.76	55.91	78.32

phen core	gas core	c-t core	c-t int.	c-t core	c-t core	phen core	phen core	phen core	gas core	gas core
38.64	38.77	38.21	37.68	38.59	38.22	38.93	39.78	40.15	35.20	36.54
20.32	23.48	25.42	24.99	22.64	23.77	18.92	15.88	15.59	38.01	32.99
0.29	0.42	0.43	0.38	0.26	0.28	0.22	0.30	0.18	0.75	0.57
40.90	38.71	35.45	36.68	37.60	37.57	42.04	44.77	44.46	24.26	29.63
0.30	0.41	0.39	0.43	0.44	0.41	0.31	0.27	0.26	0.51	0.43
0.00	0.02	0.03	n.d.	0.01	n.d.	0.02	n.d.	0.00	0.02	0.01
0.12	0.06	n.d.	n.d.	0.14	n.d.	0.19	n.d.	0.26	0.09	0.01
100.56	101.86	99.92	100.15	99.68	100.25	100.63	101.00	100.90	98.84	100.18

0.99	1.00	1.01	0.99	1.01	1.00	0.99	0.99	1.00	1.01	1.00
0.44	0.50	0.56	0.55	0.50	0.52	0.40	0.33	0.33	0.91	0.76
0.01	0.01	0.01	0.01	0.01	0.01	0.01	0.01	0.00	0.02	0.01
1.56	1.48	1.40	1.44	1.47	1.46	1.60	1.67	1.65	1.04	1.21
0.01	0.01	0.01	0.01	0.01	0.01	0.01	0.01	0.01	0.02	0.01
0.00	0.00	0.00	n.d.	0.00	n.d.	0.00	n.d.	0.00	0.00	0.00
0.00	0.00	n.d.	n.d.	0.01	n.d.	0.00	n.d.	0.01	0.00	0.00
78.19	74.61	71.31	72.29	74.74	73.81	79.83	83.41	83.58	53.21	61.57
21.81	25.39	28.69	27.71	25.26	26.19	20.17	16.59	16.42	46.79	38.43

Sill 100' Sill 105'6"

phen core	phen core
39.66	39.03
17.73	18.43
0.27	0.27
43.14	41.94
0.37	0.37
0.05	0.03
0.27	0.20
101.49	100.27

0.99	1.00
0.37	0.39
0.01	0.01
1.61	1.59
0.01	0.01
0.00	0.00
0.01	0.00

81.26 80.23
18.74 19.77

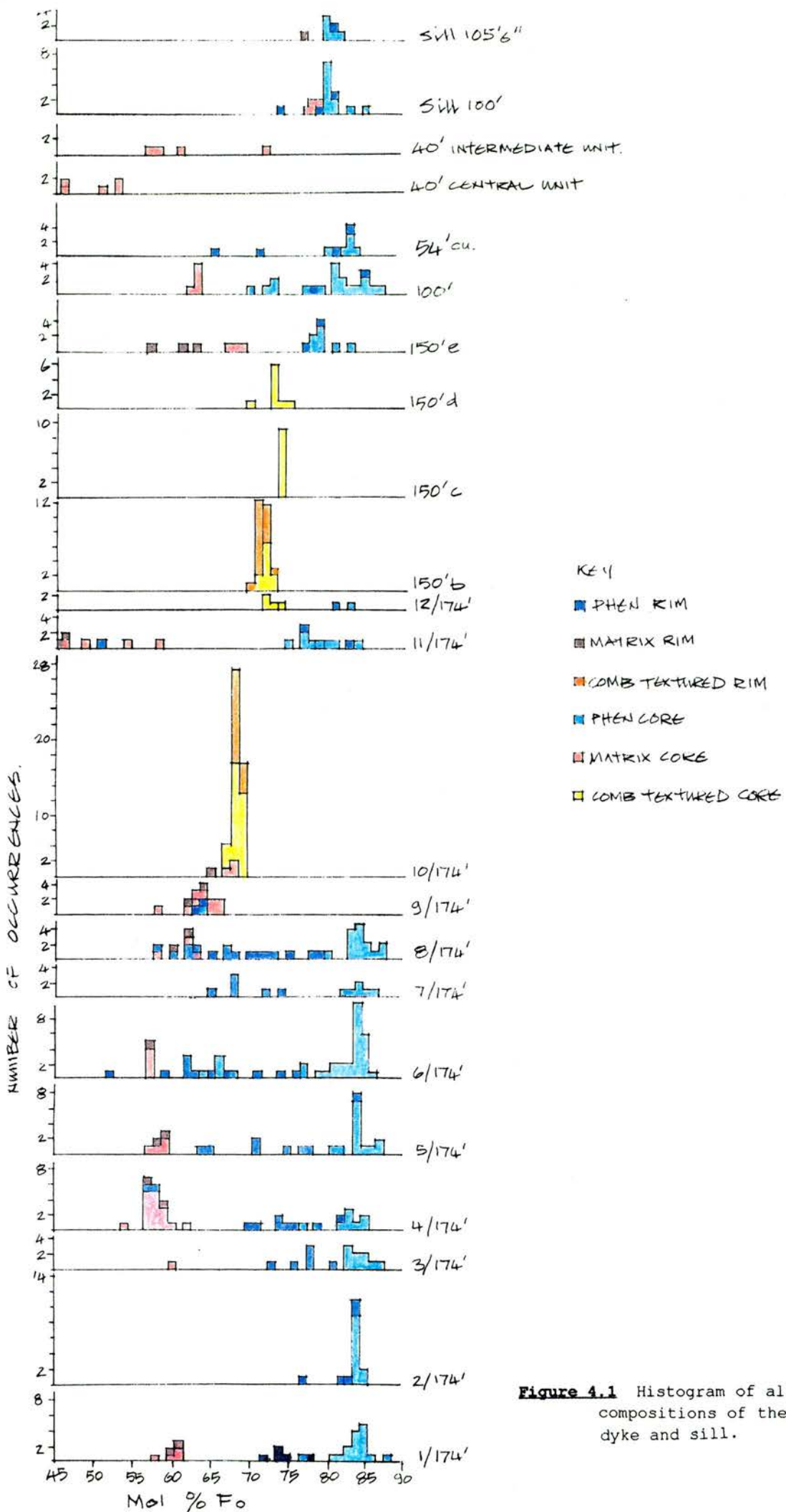
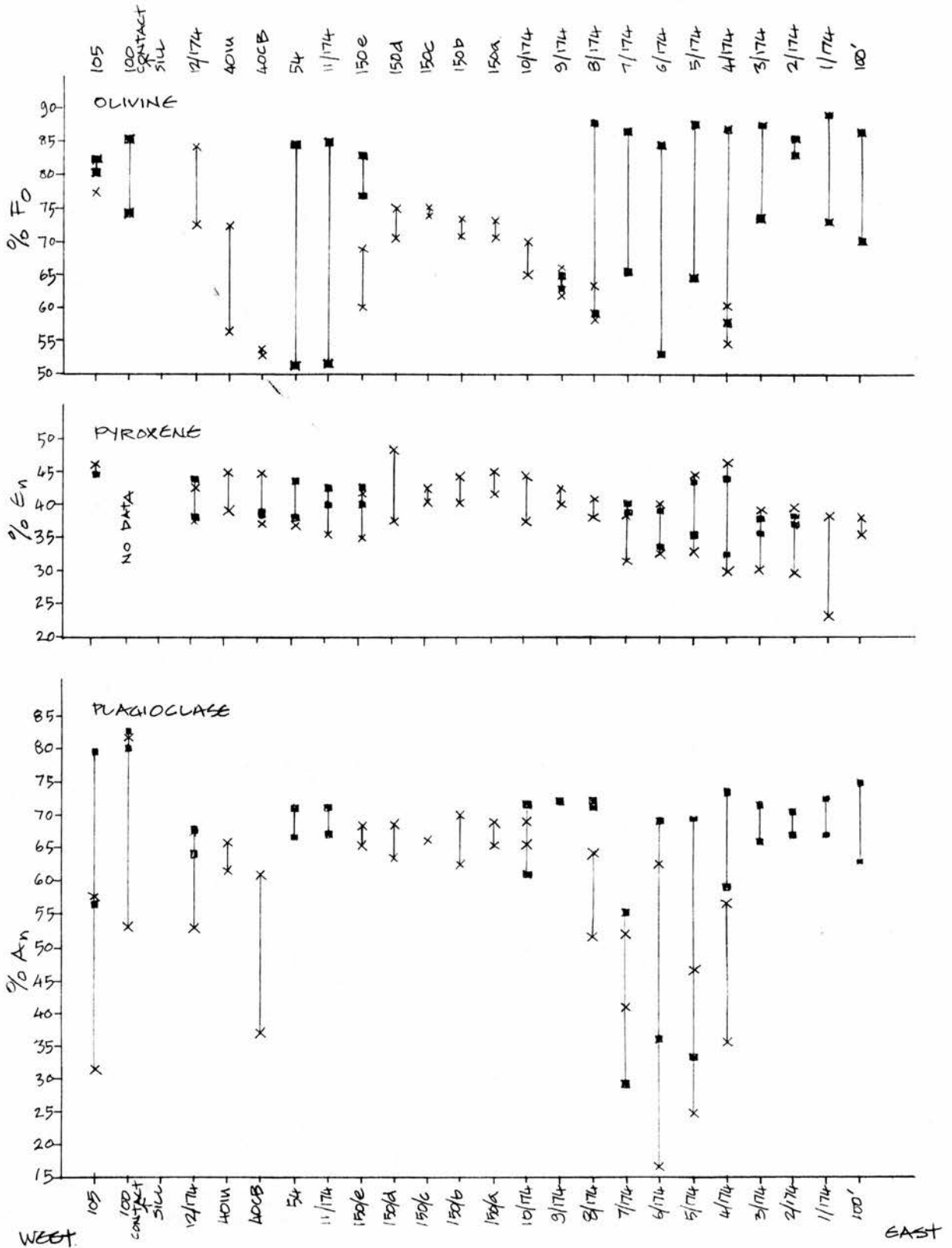


Figure 4.1 Histogram of all olivine compositions of the dyke and sill.



- PHENOCRYSTS
- x GROUND MASS CRYSTALS

Figure 4.2 Variation between olivine, pyroxene and plagioclase feldspar phenocryst and groundmass crystal compositions per analysed area of the dyke and sill.

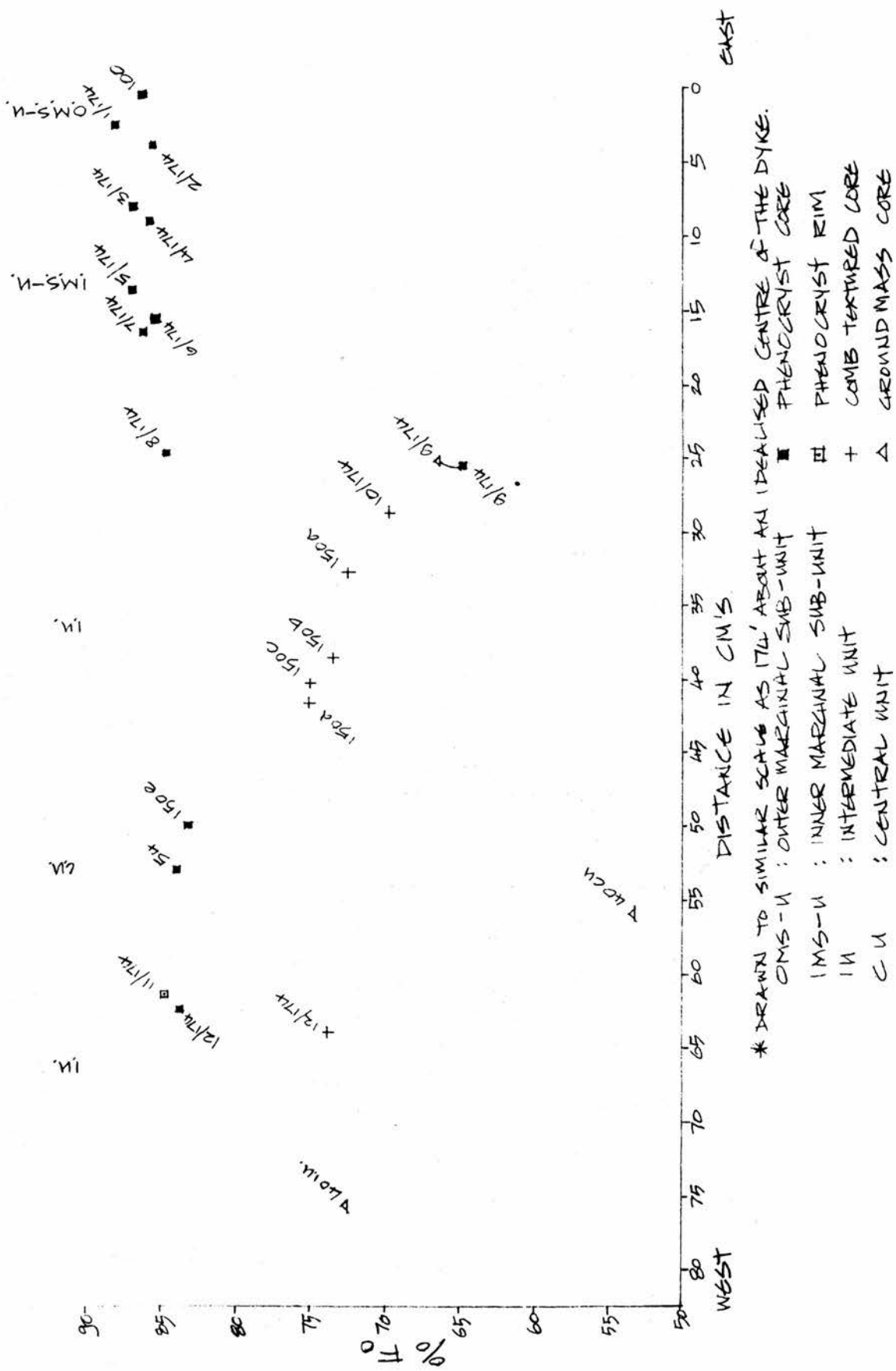


Figure 4.3 The most forsterite-rich olivine per area analysed. Matrix olivine is represented in areas studied that do not contain olivine phenocrysts (Bands 10 and 12/174', 150'a-d and 40')

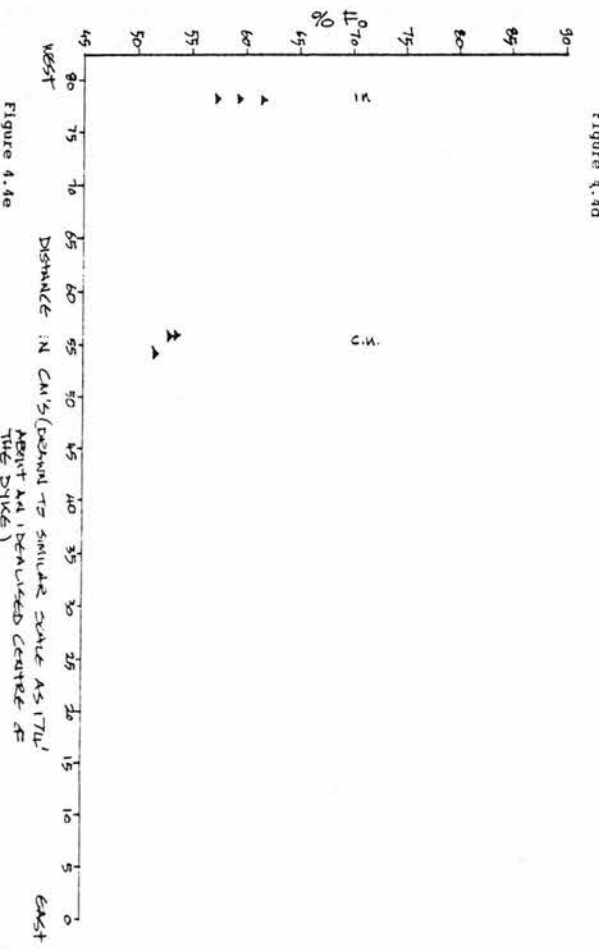
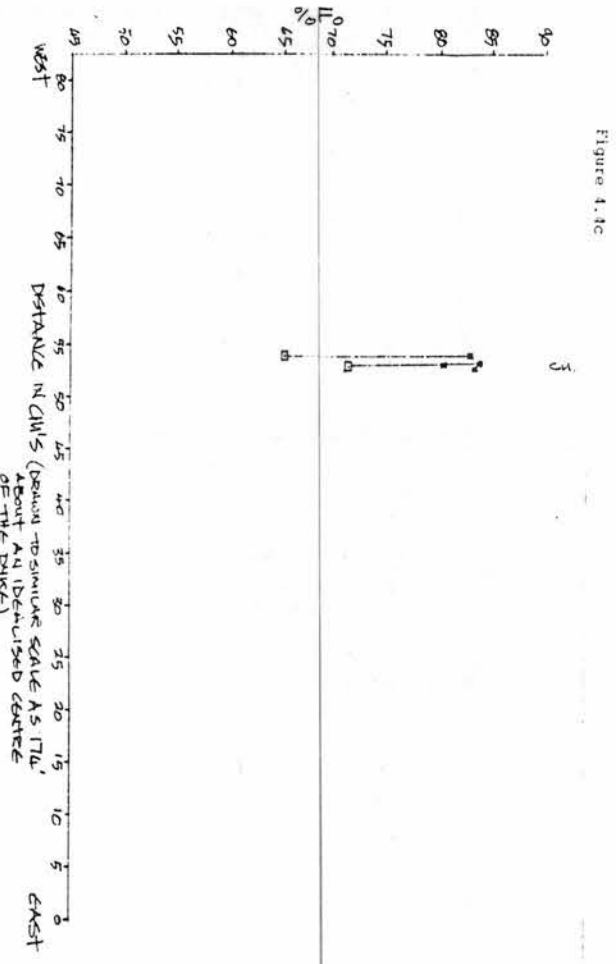
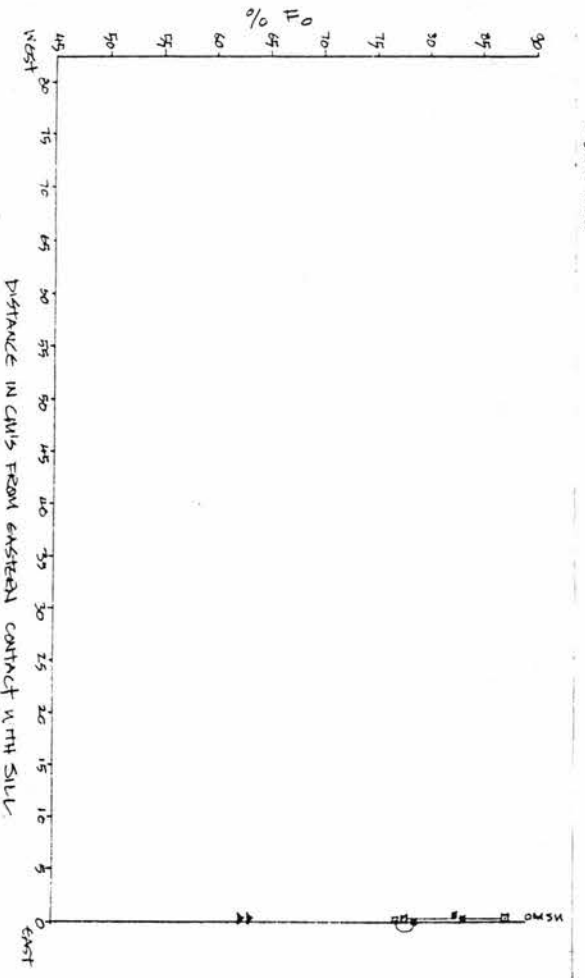
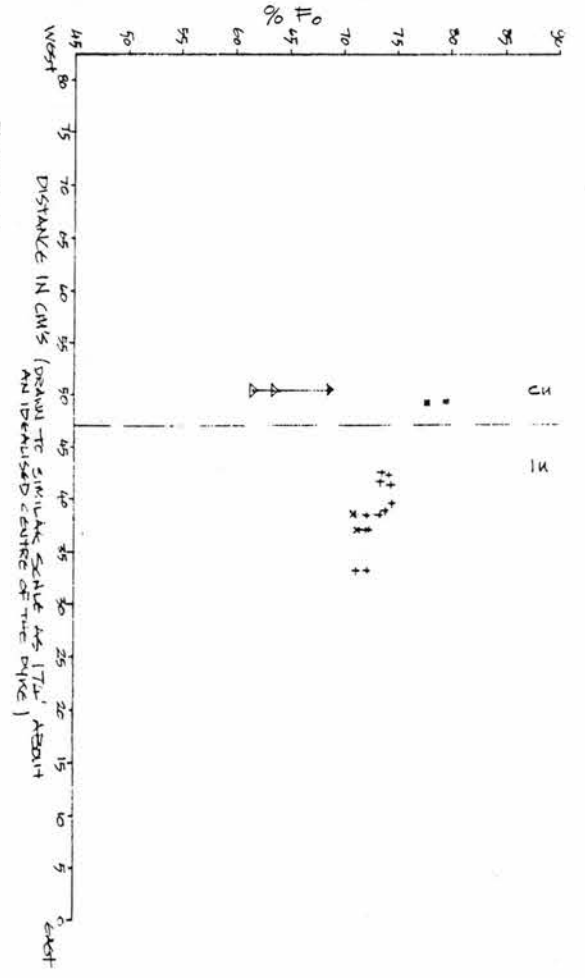
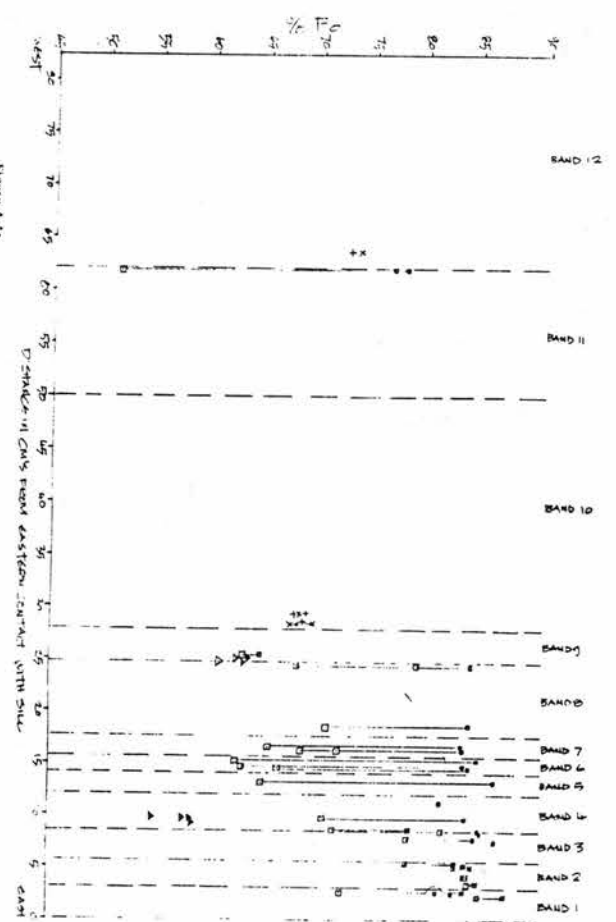
Figure 4.4 Variation in olivine composition per transect analysed.

- a) 174'
- b) 150'
- c) 100'
- d) 54'
- e) 40'

Legend for Figures 4.4, 4.9 and 4.19

- PHENOCRYST CORE
- PHENOCRYST RIM
- ▲ MATRIX CORE
- △ MATRIX RIM
- + C-t CORE
- X C-t RIM
- OPHTIC CORE
- OPHTIC RIM

CENTRE OF SYMBOL DENOTES
POINT ON GRAPH.



Band 5/174'. Wilson (1989) states that an increase in forsterite composition may be due to crystallisation in stationary magma, when crystallising crystals release latent heat, thereby increasing the temperature at which the next crystals form. Band 8/174' shows two groups of phenocrysts, one comparable with the phenocrysts in the remainder of the dyke, while the other group which continues into Band 9/174' has a composition of Fo₆₅ to Fo₆₀ (Figures 4.1 and 4.4). The phenocrysts are euhedral or sub-euhedral with the lower-forsterite group represented by smaller phenocrysts in Band 8/174'. This is in agreement with observations on Hawaiian lavas by Maaloe et al (1989), who state that forsterite content of olivine phenocrysts decreases with decreasing size. The above authors also state that in a slowly cooling magma chamber, all phenocrysts have uniform compositions, while the later-formed phenocrysts have a smaller size range and slightly lower forsterite content due to crystallisation at slightly lower temperatures during rapid cooling during ascent of magma.

Close to the contact with the sill, phenocrysts are either unzoned or zoned with a core to rim variation of 10% Fo (Figures 4.1 and 4.4). With increasing distance into the dyke, phenocrysts have increased compositional zoning. However, Band 5/174' contains both unzoned and zoned phenocrysts with upto 23% Fo variation between core and rim (Fo₈₇-Fo₆₄). The Central Unit at 150' contains unzoned phenocrysts of approximately Fo₈₀, while those in

the Central Unit at 174' and 54' are zoned from a similar core composition to Fo₇₀-Fo₅₀.

4.2.2 Matrix.

Groundmass olivine crystals exhibit a wide range of compositions. Cores vary from Fo₇₂ in the Intermediate Unit at 40' to Fo₄₆ in Band 11/174' and the "central band" at 40' (Figures 4.1, 4.2 and 4.4). The groundmass crystals exhibit a very narrow rim showing slight normal, continuous zoning, the maximum variation (6% Fo) being in the Central Unit of 150'.

Two groups of matrix crystals are visible: all those analysed from 174' (with the exception of Band 11) and 150' lie between Fo₇₃-Fo₅₅ with Band 11/174' showing a range of Fo₅₈-Fo₄₆. These two groups can also be seen at 40', where the matrix crystals in the Intermediate Unit fall between Fo₇₂-Fo₅₇, while those in the "central band" have a composition of Fo₅₄-Fo₄₆. Matrix crystals in the Central Unit (150') do not belong to the lower forsterite group as expected, but the high forsterite group of the Marginal and Intermediate Units. This may indicate a change in the composition and temperature of the magma of the Central Unit between 174' and 150'.

In Band 4/174', matrix crystals are comparable with the most iron-rich of the zoned phenocryst rims (Figures 4.1, 4.2 and 4.4), indicating that phenocryst rims had equilibrated with the magma. The matrix crystals in Band 8/174' have a similar Fo content to the more iron-

rich group of phenocrysts, and become increasingly magnesium-rich across Band 9/174', with some more magnesium-rich than the phenocrysts (Figures 4.1 and 4.4). This increase in magnesium content continues into Band 10/174' where matrix crystal analyses cluster at the lower end of the comb-textured compositional range.

4.2.3 Comb-Textured Olivines.

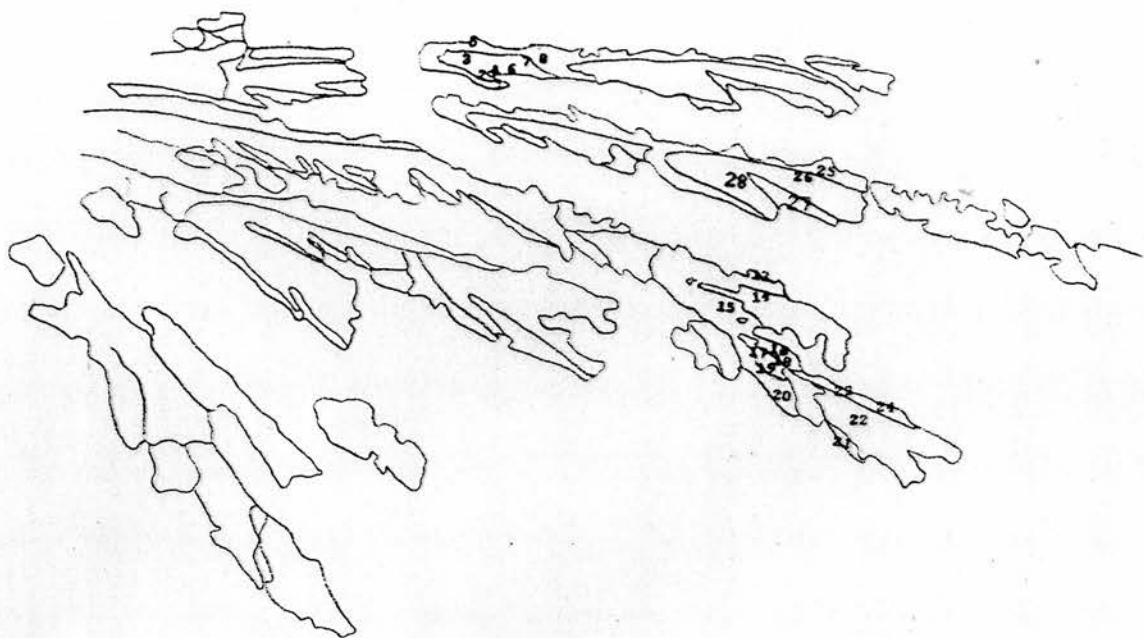
Comb-textured olivine was only sampled from the northern segment of the dyke (174' and 150') and no compositional variation between these were found.

Comb-textured olivines exhibit very slight normal zoning: the maximum variation of 2% Fo is found along the length of branches on the dendrite, with no variation along the length of the spine (Plate 4.1).

Core composition ranges from Fo₇₅ at 150' to Fo₆₇ in Band 10/174', with olivines in this band being more iron-rich than those analysed in Band 12/174'. Comb-textured olivines in Band 10/174' have a composition similar to and slightly more magnesium-rich than matrix crystals in the band and Band 9/174'. Core magnesium content increases towards the centre of the dyke from a maximum Fo₇₀ in Band 10/174' to Fo₇₅ in crystals in close proximity to the Central Unit at 150', although a slight decrease was noted in crystals in immediate contact with the Central Unit (Band 12/174' and 150'). This composition is equivalent to that of the most iron-rich phenocryst in the Central Unit in the northern segment.

Plate 4.1 Microphotograph of a comb-textured pyroxene dendrite in Band 12/174' showing variation in birefringence and points of microprobe analyses. PPL. x 15

Plate 4.2 Microphotograph of a comb-textured pyroxene dendrite in Band 12/174' showing zoning. XN. x 15





Walker (1985) gives the range of compositions for comb-textured olivines analysed from a sample at 74' as Fo₇₂-Fo₅₈. He found the least magnesian crystals were those furthest from the centre of the dyke, with forsterite content rising steeply initially, then levelling off towards the centre of the dyke (Figure 4.5). He also found no compositional variation along the spine of a dendrite. These results are comparable to the results of this study. Variation across a band but lack of any along the spine of individual comb-textured crystals suggests any chemical variation must be occurring due to changing magma composition.

4.3 Minor Element Variation within Olivine.

Several elements have notable relationships with the magnesium-iron ratio of the olivines. Nickel shows a positive correlation with magnesium, while manganese shows a negative correlation (Figure 4.6). These findings are in agreement with previous studies (Simkin and Smith 1970 and Gibson 1988). Simkin and Smith (1970) related CaO content of olivine to crystallisation environment; olivines containing below 0.1 wt% CaO were considered to be from plutonic environments indicating slow equilibrated crystal growth, while olivines with excess of this figure were considered hypabyssal or

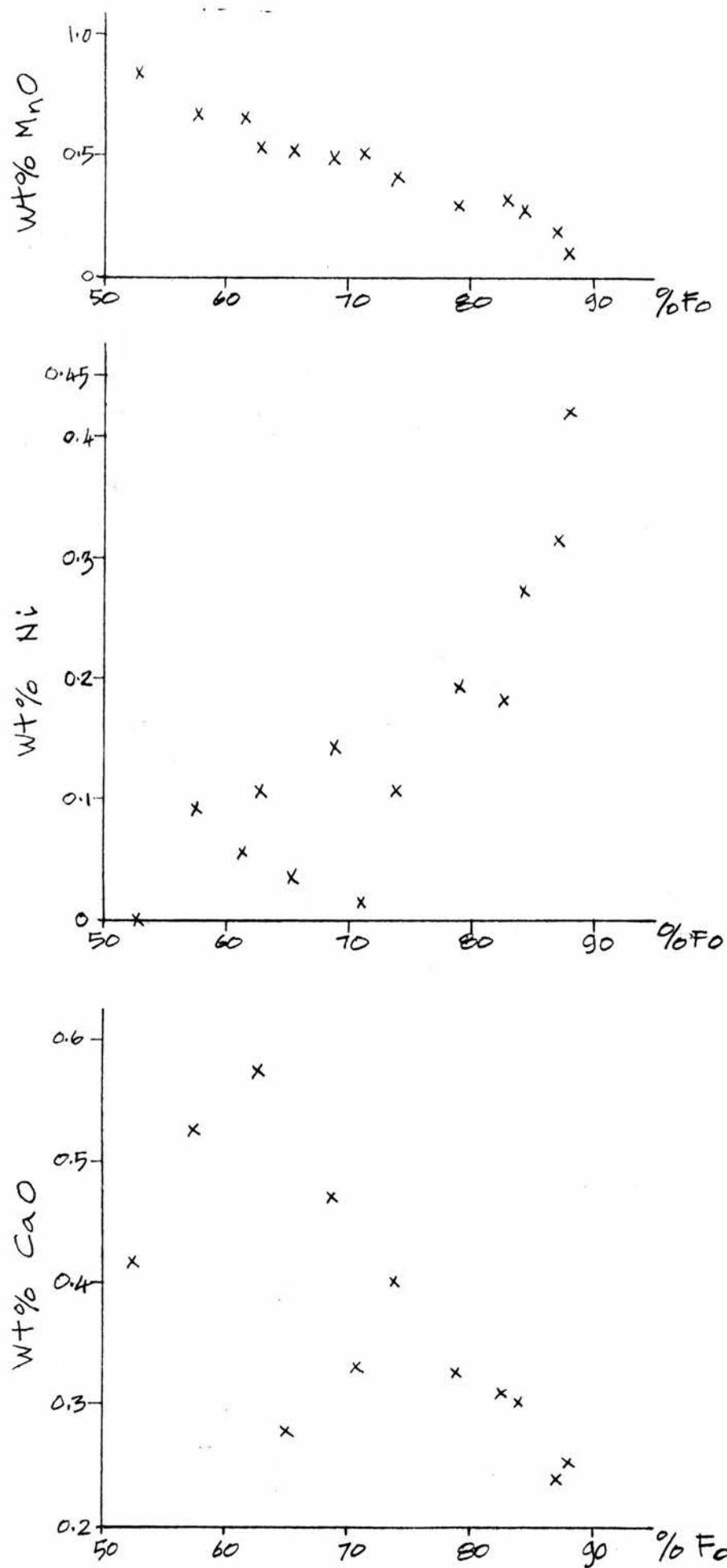


Figure 4.6 Variation of MnO, Ni and CaO with variation in forsterite content of olivine.

extrusive. Analysed olivines contain an average 0.3 wt% CaO suggesting non-equilibrated crystal growth in a high crustal location.

4.4 Comparison of Sill and Dyke Olivine.

Phenocryst core compositions within the sill range from Fo₈₅ to Fo₈₀, compared to Fo₈₈-Fo₇₆ in the chilled margin of the dyke (Figure 4.1). Zoning is continuous and normal with up to 11% Fo variation (Fo₈₅ to Fo₇₄). Sill phenocrysts show wider rims than those in the dyke, indicative of a slower cooling history.

Sill matrix crystals have a compositional range of Fo₇₉-Fo₇₇, slightly in excess of those of the dyke. Gibson (1988) states olivines throughout the L.M.S.C. have a compositional range of Fo₈₂-Fo₂₂, although phenocrysts (this study) have higher forsterite content. Representative analyses of olivines (Gibson 1988) are given in Table 4.2, together with analyses (this study).

Olivines in the sill contain 0.3-0.4 Wt% CaO, similar to dyke olivines, suggesting crystallisation at a comparable, high level location. Table 4.3 shows the ranges of oxide content for phenocryst cores and for all crystals analysed in the dyke and sill complex. The minimum and maximum content of selected elements for all

Table 4.2
Representative analyses of olivine
per principal lithology of the T.S.C.
 (Gibson 1988)

	Picro- dolerite	Marginal Picrite	Picrite	Crinanite
Wt%				
SiO ₂	38.66	39.10	39.05	35.80
FeO t	24.32	20.96	16.89	34.88
MnO	0.26	0.29	0.34	0.31
MgO	35.15	38.11	42.39	25.77
CaO	0.55	0.64	0.52	0.58
NiO	0.10	0.11	0.26	0.19
Total:	99.04	99.21	99.45	97.53

	Atoms per 4 Oxygens			
Si	1.03	1.01	1.00	1.01
Fe t	0.54	0.45	0.36	0.83
Mn	0.01	0.01	0.01	0.01
Mg	1.39	1.46	1.61	1.09
Ca	0.02	0.02	0.01	0.18
Ni	0.00	0.00	0.01	0.00
Fo %	72	76	82	43
Fa %	28	24	18	57

Table 4.3
Comparative data for olivine chemistry of sill and dyke

wt%	FeO	MnO	MgO	CaO	NiO
Dyke: Phen. core Minimum	11.43	0.10	31.58	0.20	0.17
Dyke: Phen. core Maximum	30.69	0.57	47.71	0.56	0.45
Dyke: All crystal data-					
Minimum	11.43	0.00	20.18	0.20	0.00
Maximum	39.17	0.94	47.71	*0.60	0.45
Sill: Phen. core Minimum	14.35	0.21	41.94	0.28	0.11
Sill: Phen. core Maximum	18.92	0.36	45.98	0.38	0.37
Sill: All crystal data					
Minimum	14.35	0.14	38.42	0.28	0.11
Maximum	23.72	0.36	45.98	0.38	0.37
(this study)					
Sill (all crystals):					
Picrite: Minimum	16.08	0.20	39.56	0.18	0.09
Maximum	20.13	0.63	41.56	0.39	0.40
Picrodolerite: Minimum	23.05	0.13	24.52	0.48	0.00
Maximum	36.32	0.81	35.78	0.88	0.42
Crinanite Minimum	16.74	0.19	15.85	0.50	0.00
Maximum	46.42	0.96	40.32	0.82	0.58
(Gibson 1988)					

* One matrix analysis (Band 4, 174') contains 1.98 wt % CaO

crystals are given as a comparative aid to interpretation of analyses by earlier workers.

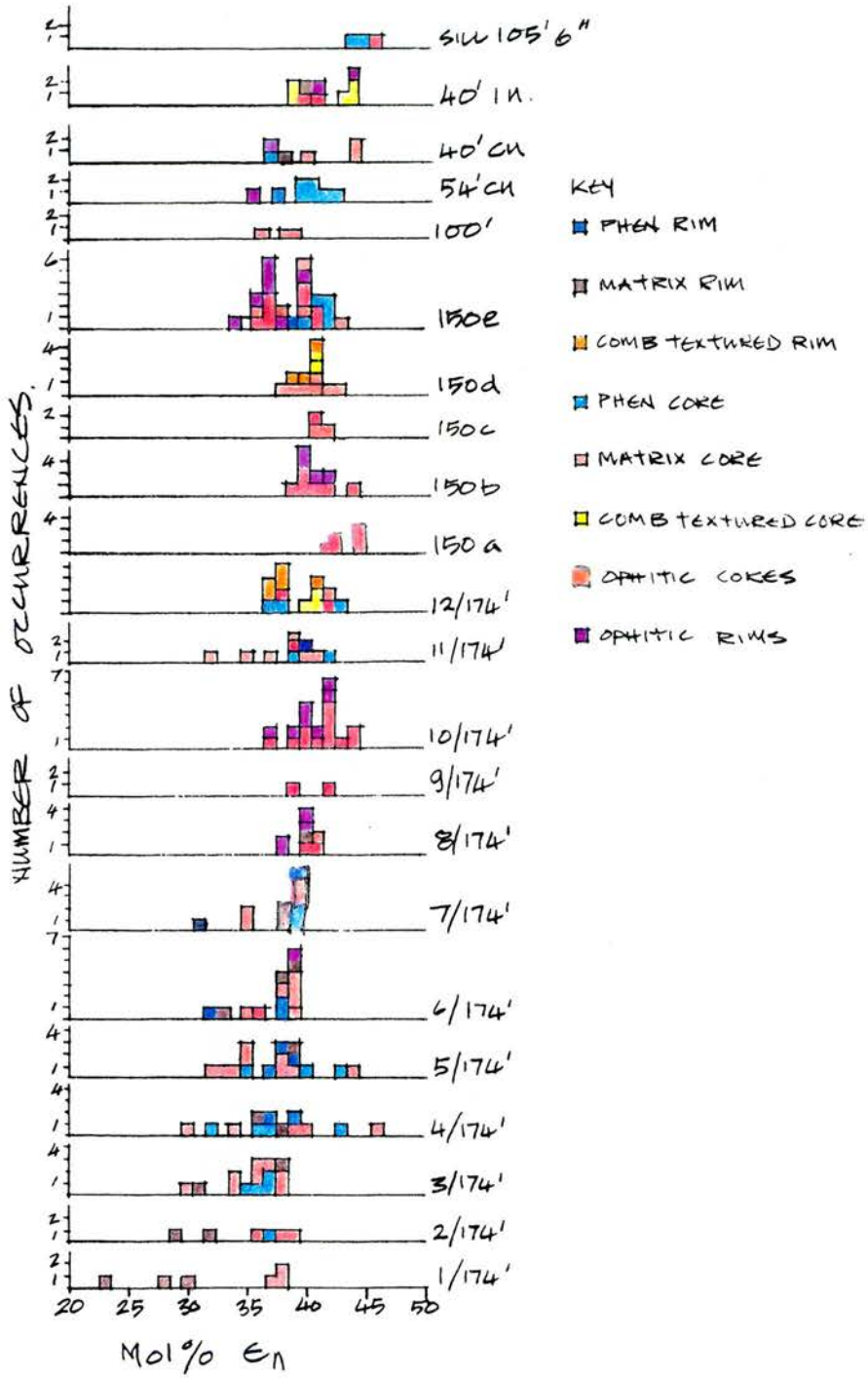
Olivine phenocrysts in the dyke contain less iron and manganese and more magnesium compared to those in the sill, although their maximum FeO and minimum MgO contents lie within the limits of olivines analysed from the sill (Gibson 1988) (Table 4.3). The CaO and Ni of dyke phenocrysts lie within the range of those from the sill complex. Excepting FeO and MgO, major elements show comparability between sill and dyke olivines.

Insufficient mineral chemistry data was obtained for the S.M.L.S. for comparison with dyke or sill complex.

4.5 Clinopyroxene.

Pyroxenes are of augite, diopside and hedenbergite compositions. The nomenclature of pyroxenes follows the recommendations of the Subcommittee on Pyroxenes, I.M.A. (1988). Figure 4.7 shows composition of pyroxenes as a histogram. There is little variation in core composition across the dyke, with the magnitude of compositional variation diminishing with distance into the dyke. Maximum zoning is found in matrix crystals of the Outer Marginal Sub-Unit, while there is overlap of core and rim compositions in the Central Unit. Figures 4.2 and 4.8-4.9 illustrate the limited compositional

Figure 4.7 Histogram of all pyroxene compositions of the dyke and sill.



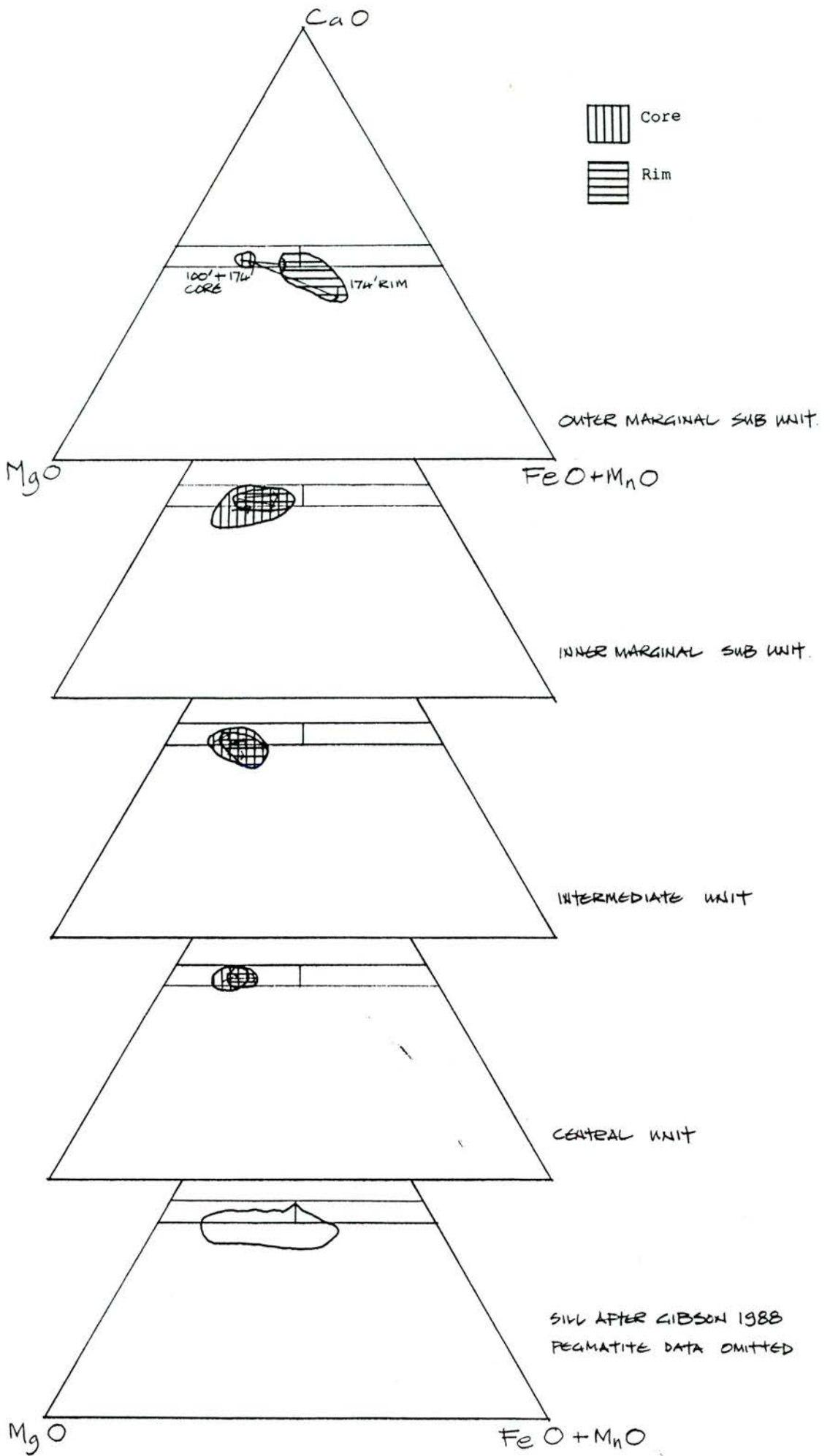


Figure 4.8 Pyroxene compositions per Unit of dyke and the sill.

Figure 4.9 Variation in pyroxene composition per area transect analysed:

- a) 174'
- b) 150' Legend as for Figure 4.4
- c) 100'
- d) 54'
- e) 40'

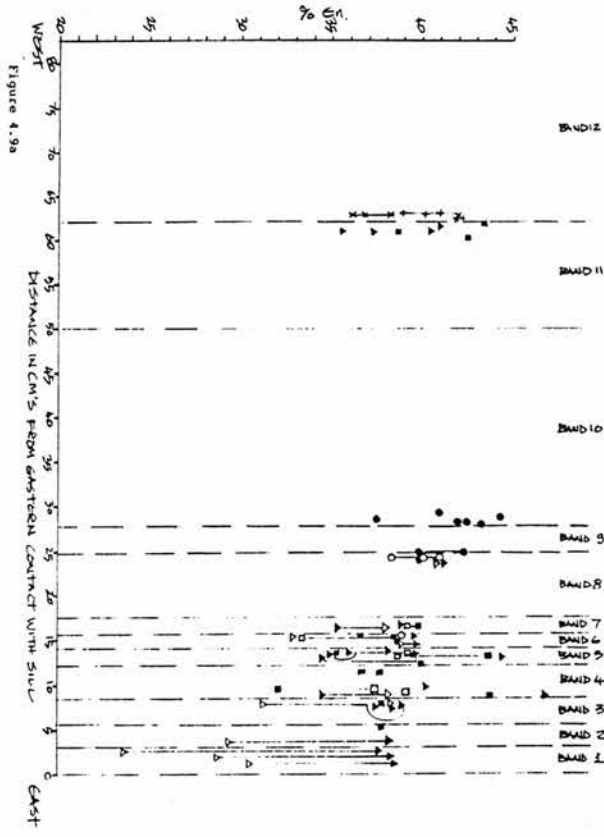


Figure 4.9a

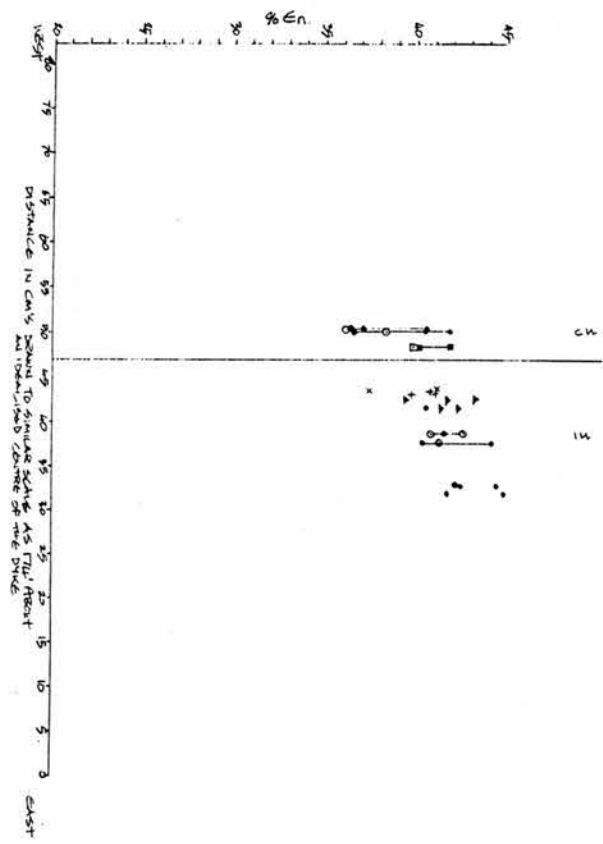


Figure 4.9b



Figure 4.9c

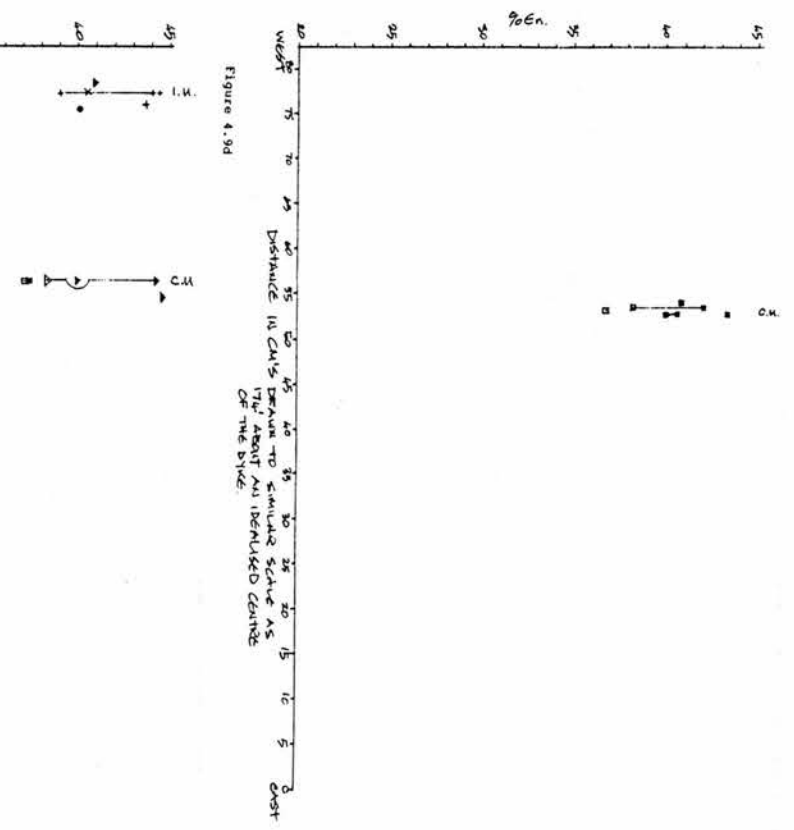


Figure 4.9d

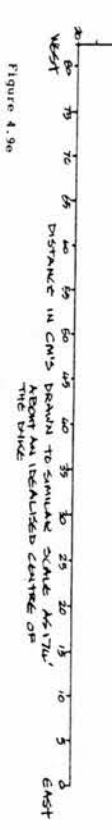


Figure 4.9e

variation within the dyke. Table 4.4 contains representative analyses of both dyke and sill pyroxenes.

Augite exhibits the greatest textural variation of the essential minerals, with phenocrysts, matrix, comb-textured and ophitic crystals analysed. Iron shows maximum variation from Fs_{38} to Fs_{10} , magnesium varies from En_{47} to En_{24} , and calcium from Wo_{48} to Wo_{42} . The maximum ferrosilite content is exceptional (a matrix rim analysis) with phenocryst cores ranging from Fs_{23} to Fs_{11} , any reference to composition therefore, will be with comment to enstatite content, as this ratio shows the most significant variation.

4.5.1 Phenocrysts.

Phenocryst cores lie between En_{43} and En_{32} , both analyses from Band 4/174'. No obvious patterns of compositional variation is seen along the length, or across the width of the dyke (Figures 4.2, 4.8 and 4.9), although within-crystal variation does occur.

The phenocrysts are variably zoned across the dyke with both normal and reverse zoning. Maximum reverse zoning of 5 Mol.% magnesium is found in Band 4/174', with those in Bands 5-6/174' being normally-zoned. Phenocrysts analysed in the Central Unit display little compositional variation and only slight normal zoning towards the rims, where it is continuous and normal.

4.5.2 Matrix.

Table 4.4
Representative Pyroxene analyses from the dyke and sill.

Band	1/174'	2/174'	3/174'	4/174'	5/174'	6/174'	7/174'	8/174'	9/174'	10/174'
* Unit	O.M.S-U.	I.M.S-U.	I.M.S-U.	I.M.S-U.	I.M.S-U.	I.M.S-U.	I.M.S-U.	I.M.S-U.	I.M.S-U.	I.U.
Distance	2.01	5.47	7.85	11.62	13.61	14.95	16.96	24.26	24.77	29.29
across dyke in Cms										
	gas core	phen core	oph core	oph core	oph core					
SiO ₂	51.86	46.53	46.54	51.61	49.46	47.51	50.46	50.55	48.50	48.74
TiO ₂	0.82	2.42	2.30	0.98	1.31	2.07	1.18	1.15	1.45	1.52
Al ₂ O ₃	2.12	6.90	6.25	1.93	1.94	5.95	2.25	2.34	5.04	4.82
FeO ^t	9.27	8.56	8.37	9.96	12.58	8.94	9.19	8.57	6.83	7.74
MnO	0.25	0.15	0.13	0.32	0.18	0.21	0.13	0.16	0.18	0.01
MgO	13.11	12.36	12.41	12.96	11.96	13.05	13.46	14.11	14.11	13.88
CaO	22.19	21.49	21.93	21.93	20.67	21.76	21.70	21.49	21.41	21.73
Na ₂ O	0.57	0.52	0.49	0.58	0.37	0.38	0.47	0.48	0.32	0.39
Cr ₂ O ₃	0.00	0.13	0.07	0.00	0.00	0.05	0.00	0.00	0.69	0.01
NiO	0.00	0.07	0.08	0.00	0.03	0.00	0.08	0.00	0.01	0.00
Total:	100.19	99.13	98.57	100.28	98.50	99.92	98.92	98.85	98.52	98.85
Atoms per 6 Oxygens										
Si	1.94	1.76	1.78	1.93	1.91	1.79	1.91	1.91	1.83	1.84
Ti	0.02	0.07	0.07	0.03	0.04	0.06	0.03	0.03	0.04	0.04
Al	0.09	0.31	0.28	0.09	0.09	0.26	0.10	0.10	0.22	0.21
Fe ^t	0.29	0.27	0.27	0.31	0.41	0.28	0.29	0.27	0.22	0.24
Mn	0.01	0.01	0.00	0.01	0.01	0.01	0.00	0.01	0.01	0.00
Mg	0.73	0.70	0.71	0.72	0.69	0.73	0.76	0.79	0.79	0.78
Ca	0.89	0.87	0.90	0.88	0.86	0.88	0.88	0.87	0.87	0.88
Na	0.04	0.04	0.04	0.04	0.03	0.03	0.04	0.03	0.02	0.03
Cr	0.00	0.00	0.00	0.00	0.00	0.00	0.00	0.00	0.02	0.00
Ni	0.00	0.00	0.00	0.00	0.00	0.00	0.00	0.00	0.00	0.00
Fs Mol. %	15.20	14.67	14.36	16.29	20.92	14.89	15.03	13.99	11.50	12.83
En Mol. %	38.26	38.04	37.77	37.77	35.20	38.71	39.38	41.05	42.33	41.01
Wo Mol. %	46.54	47.28	47.87	45.94	43.88	46.40	45.60	44.95	46.18	46.15

*Unit abbreviations:

O.M.S-U. Outer Marginal Sub-Unit
I.M.S-U. Inner Marginal Sub-Unit
I.U. Intermediate Unit
C.U. Central Unit

11/174'	12/174'	150a	150b	150c	150d	150e	100	54	40	40	Sill
C.U.	I.U.	I.U.	I.U.	I.U.	I.U.	C.U.	O.M.S-U.	C.U.	C.U.	I.U.	105'6"
61.12	62.44	32.87	38.67	41.83	43.63	48.65	0.19	52.78	56.30	78.39	
phen core	oph core	oph core	oph core	gas core	ot core	phen core	gas core	phen core	gas core	gas rim	phen core
46.41	49.53	51.51	49.70	48.81	49.81	48.77	48.69	48.61	48.19	48.90	50.49
1.93	1.49	0.79	1.01	1.32	1.57	1.70	1.41	1.27	1.90	1.46	1.15
6.04	3.42	2.89	4.04	5.02	3.69	5.07	3.95	4.87	4.96	5.71	3.71
7.62	8.59	5.94	6.65	6.78	8.32	8.38	9.14	6.85	8.35	6.91	5.45
0.14	0.20	0.18	0.12	0.07	0.20	0.11	0.17	0.10	0.13	0.07	0.14
12.86	14.24	15.43	14.21	14.05	13.90	13.69	13.07	14.19	13.49	13.78	15.37
22.36	21.80	22.03	22.49	22.36	21.56	21.79	22.25	22.22	21.48	22.15	21.73
0.40	0.34	0.31	0.41	0.40	0.41	0.41	0.70	0.39	0.42	0.38	0.35
0.19	0.12	0.48	no data	0.85	0.04	0.23	no data	0.46	0.21	0.70	1.00
0.00	0.04	no data	no data	0.09	0.01	0.00	no data	0.00	0.04	0.03	0.07
97.95	99.76	99.56	98.62	99.74	99.52	100.15	99.38	98.96	99.17	100.08	99.45
1.78	1.86	1.91	1.87	1.82	1.87	1.82	1.85	1.83	1.82	1.82	1.87
0.06	0.04	0.02	0.03	0.04	0.04	0.05	0.04	0.04	0.05	0.04	0.03
0.27	0.15	0.13	0.18	0.22	0.16	0.22	0.18	0.22	0.22	0.25	0.16
0.24	0.27	0.19	0.21	0.21	0.26	0.26	0.29	0.22	0.26	0.21	0.17
0.00	0.01	0.01	0.01	0.00	0.01	0.00	0.01	0.00	0.00	0.00	0.00
0.73	0.80	0.85	0.80	0.78	0.78	0.76	0.74	0.80	0.76	0.76	0.85
0.92	0.88	0.88	0.91	0.90	0.87	0.87	0.90	0.90	0.87	0.88	0.86
0.03	0.03	0.02	0.03	0.03	0.03	0.03	0.05	0.03	0.03	0.03	0.02
0.01	0.00	0.01	no data	0.03	0.00	0.01	no data	0.01	0.01	0.02	0.03
0.00	0.00	no data	no data	0.00	0.00	0.00	no data	0.00	0.00	0.00	0.00
12.70	13.89	9.90	10.97	11.21	13.70	13.82	15.00	11.32	13.93	11.54	8.98
38.62	41.00	44.27	41.69	41.42	40.82	40.19	38.23	41.72	40.13	41.04	45.14
48.68	45.11	45.83	47.34	47.38	45.48	45.99	46.77	46.96	45.94	47.42	45.88

The compositional range of matrix crystals is En_{46} to En_{23} . Normal and reverse zoning is present. The chilled margin (174' and 100') contains only matrix pyroxene. Core compositions remain approximately constant (En_{39} - En_{36}) across the outer 5cms of the dyke, the crystals being normally zoned, with core to rim variation diminishing with distance into the dyke (Figures 4.7 and 4.9). Matrix crystals in Band 4/174' display the greatest variation in core composition (En_{46} - En_{30}), the variation lessening across Bands 5-7/174'. In Band 5/174' the rim compositions of reversely zoned matrix crystals are comparable to rims of normally zoned phenocrysts, suggesting that surfaces of both crystal types had reached chemical equilibrium with the melt. No compositional variation between matrix, comb-textured or ophitic crystals was found.

Walker (1985) describes matrix pyroxenes with compositions broadly similar to those in this study. He found interstitial matrix crystals contained the least iron of all pyroxenes analysed, while this study found ophitic crystals to be equally low in iron. The sample from 74' examined by Walker (1985), does not contain ophitic pyroxene.

4.5.3 Comb-textured Pyroxene.

Comb-textured pyroxene was analysed from the narrow lamina marking the contact between the Intermediate and Central Units at 174' and 150' and from the Intermediate

Unit at 40' (Figure 4.10). Figure 4.10a displays the pyroxene compositions of Walker (1985). There is little variation of core composition from En₄₄ to En₃₇ along the length of spines of comb-textured crystals or along branches (Figure 4.10b). These directions relate to the \underline{c} and perpendicular to the \underline{c} crystallographic axis direction. Composition varies from En₄₄ to En₃₅, with cores slightly more magnesian than rims. The former lie between En₄₄-En₃₇, the latter En₄₁-En₃₅.

Walker (1985) gives a range of Ca/Ca+Mg+Fe+Mn *100 ratios of 49-42 for one crystal at 74' comparable to ratios of 48-44 (174'), 47-44 (150') and 47-43 (40'). He does not give details of core and rim analyses, but in this study, the cores have a lower Ca/Ca+Mg+Fe+Mn ratio (Figure 4.11). Rims show enrichment of TiO₂ and Al₂O₃ compared to cores (Figures 4.12-4.13).

Walker (1985) subdivided dendritic pyroxenes into high- and low-Ca pyroxenes, although there is a near-continuous trend on his graph. This overlap was also noted in this study (Figure 4.10). Subdivision into high- and low-Ca pyroxenes for each sample studied is possible, but there is little evidence of subdivision overall due to overlap of the high- and low-Ca groups with distance along the dyke. Subdivision is also noticeable in figures relating to the Ca/Ca+Mg+Fe+Mn *100 ratios, TiO₂ and Al₂O₃ content (Figures 4.11-4.13). Walker (1985) states zoning of the comb-textured crystals with reference to calcium indicates a core of high

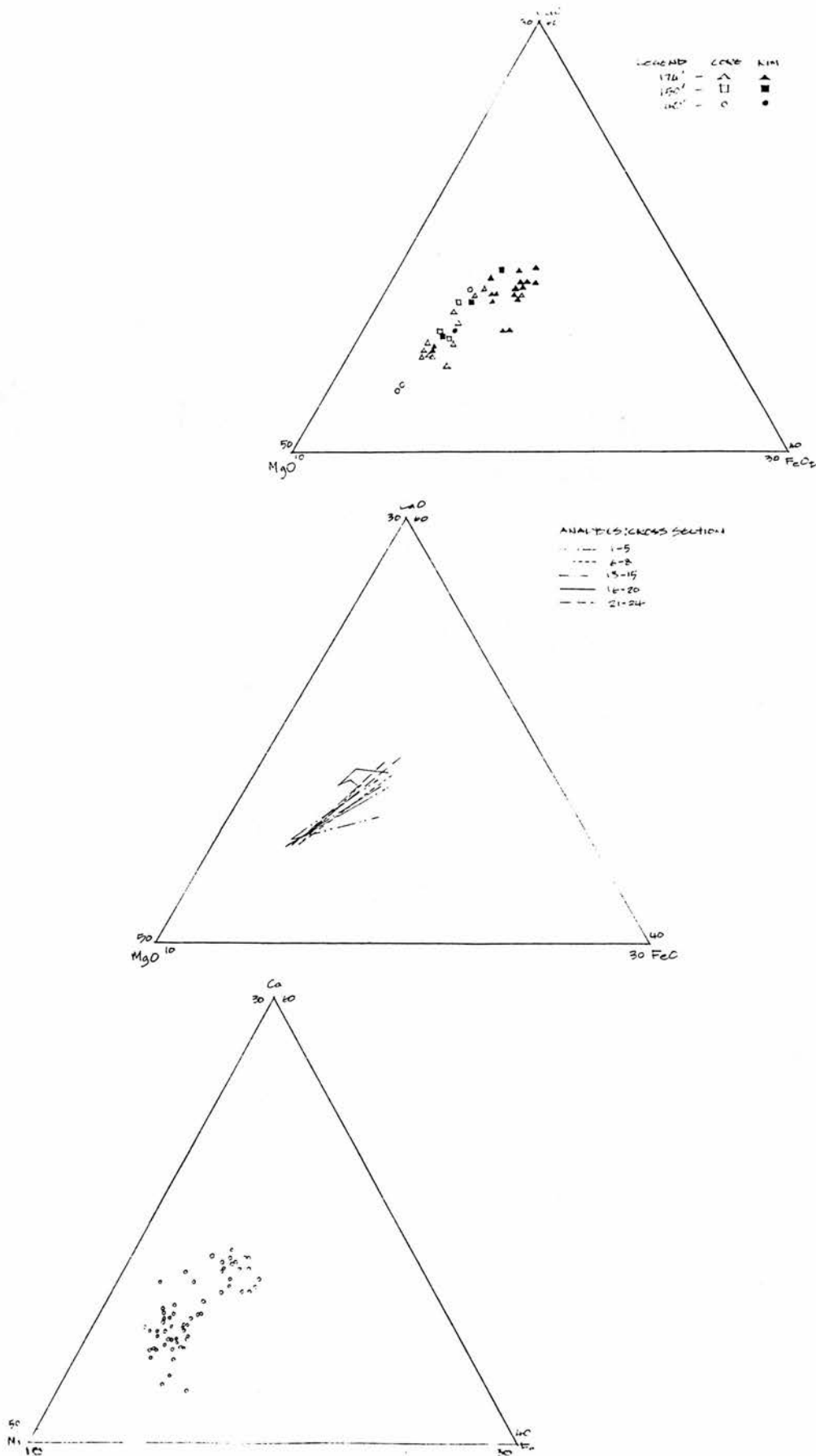


Figure 4.10 Chemical composition of comb-textured pyroxene from 174', 150' and 40'.

Figure 4.10a Chemical composition of transects across one comb-textured pyroxene from 174'

Figure 4.10b Chemical composition of comb-textured pyroxene from 74' (Walker 1985).

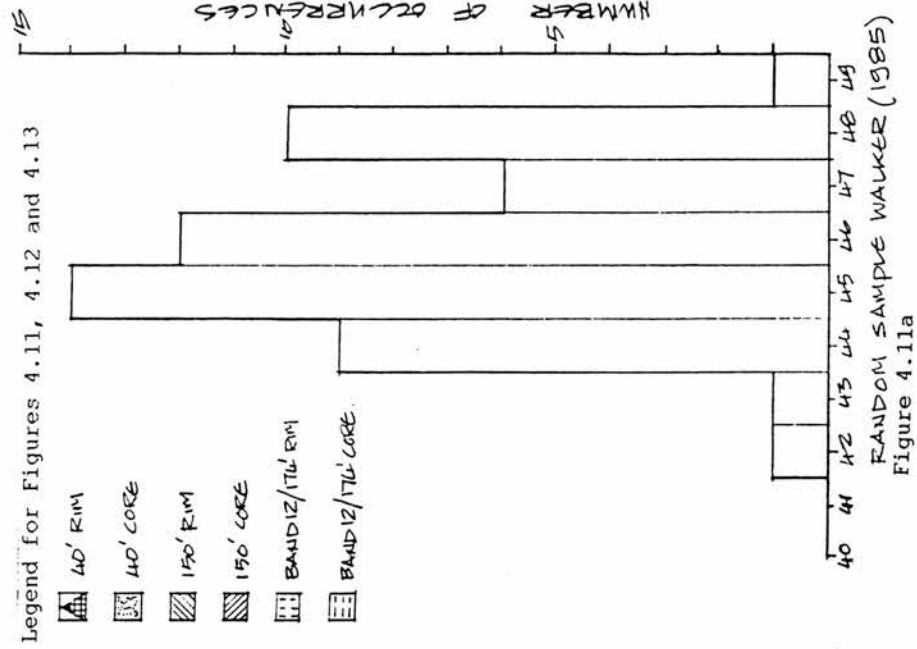


Figure 4.11a
RANDOM SAMPLE WALKER (1985)

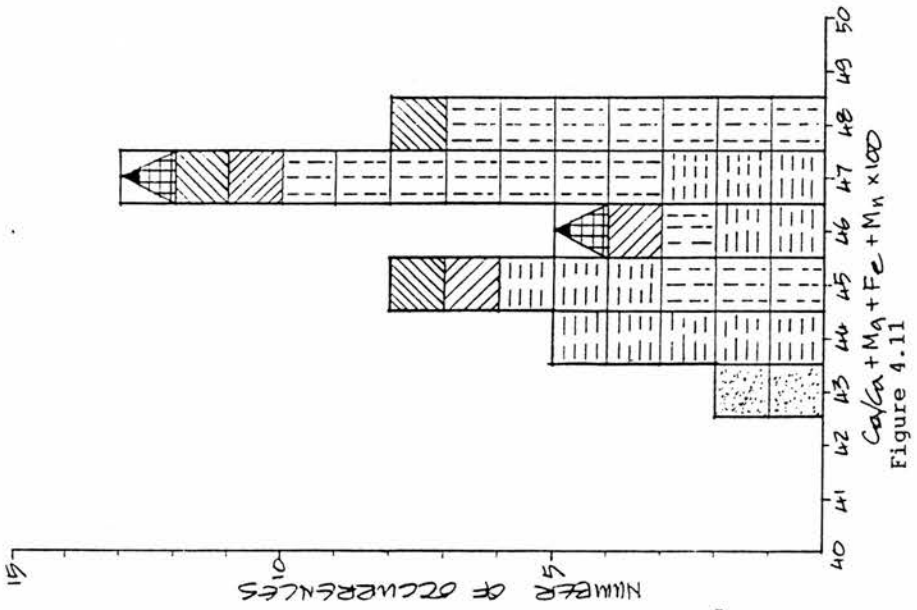


Figure 4.11
Ca/(Ca+Mg+Fe+Mn) x 100

Figure 4.11 Histogram of the Ca/Ca+Mg+Fe+Mn*100 ratio for comb-textured pyroxene from 174', 150' and 40'.

Figure 4.11a Histogram of the Ca/Ca+Mg+Fe+Mn*100 ratio for comb-textured pyroxene from 74' (Walker 1985).

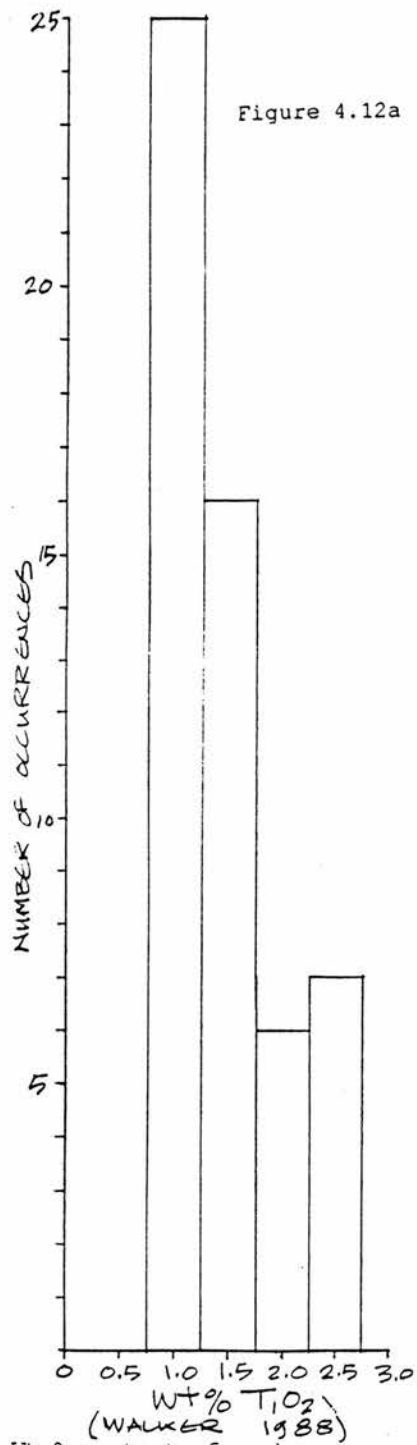
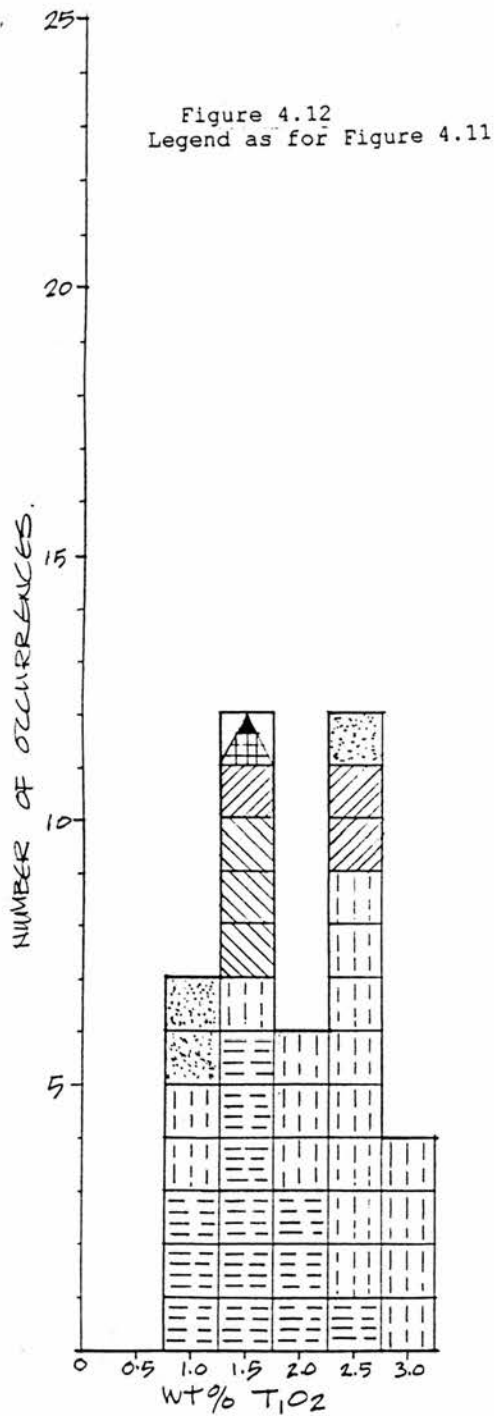
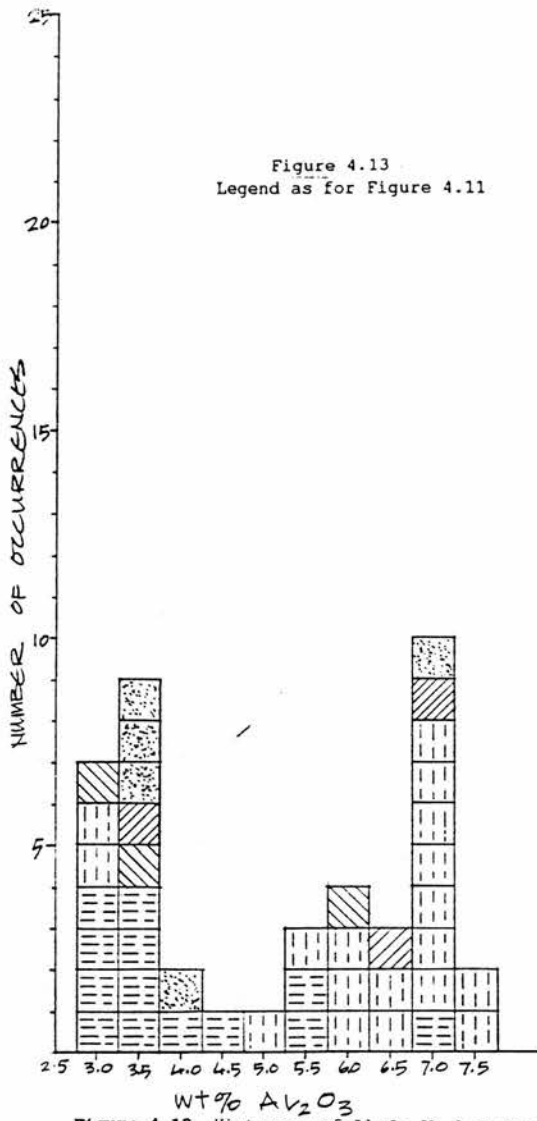


Figure 4.12 Histogram of TiO₂ Wt % content of comb-textured pyroxene from 174', 150' and 40'.

Figure 4.12a Histogram of TiO₂ Wt % content of comb-textured pyroxene from 74' (Walker 1985).



WT% Al₂O₃

Figure 4.13 Histogram of Al₂O₃ Wt % content of comb-textured pyroxene from 174', 150' and 40'.

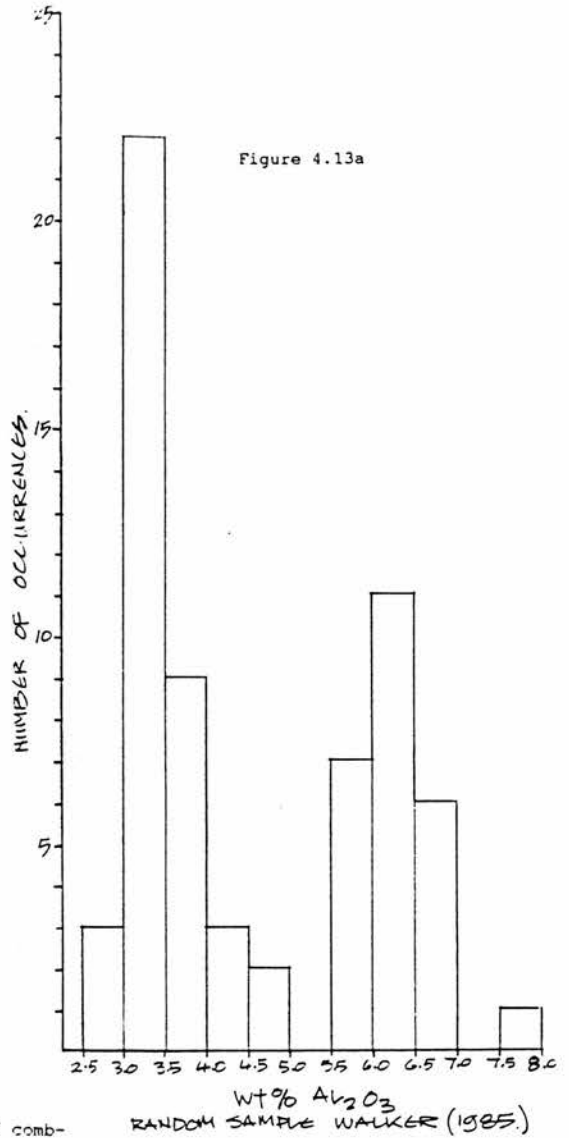


Figure 4.13a Histogram of Al₂O₃ Wt % content of comb-

WT% Al₂O₃

RANDOM SAMPLE WALKER (1985.)

calcium content bounded by low calcium sectors, the opposite of findings of this study.

Figures 4.11a-4.13a show Walker's data from the middle segment of the dyke for comparison with that from the northern and southern segments (this study). Walker (1985) does not give details of core and rim analyses, with his data covering a wider spread of compositions than those from this study, but shows a preference towards low-Ca sector analyses.

One comb-textured pyroxene crystal from 174' was analysed in detail. Plate 4.2 shows the birefringence variation of the crystal, with points of analyses. Results are highlighted on Figures 4.11-4.13. Figure 4.10a shows the tie-lines across transects of the crystal. With the exception of transect 4, the transects exhibit similar rim compositions, either side of the core. Core compositions exhibit clustering, showing compositional variation to be restricted to the rims. Transect 4 has a wide rim on one side, a wide core and a narrow rim on the opposite side. This exhibits a different trend to the other transects (Figure 4.10a). The core composition is enriched in CaO compared to other core compositions and rim analyses show varying MgO and FeO content. There is little variation in CaO content across the transect, unlike the other illustrated transects. Chemical variation in sector zoning is well displayed by Al_2O_3 wt% (Figure 4.13).

Most core compositions exhibit a restricted, low Al_2O_3 content compared to rim analyses.

There is little variation in the core composition along the length of the dendrite as shown in Figures 4.10a, 4.12 and 4.13, whereas high-CaO rims exhibit greater variation. The start of a dendrite contains more MgO and SiO_2 and less Al_2O_3 and TiO_2 than further along the dendrite.

4.5.4 Ophitic Pyroxene.

This form of matrix crystal was analysed from the Marginal, Intermediate and Central Units (Bands 6-11) of 174' and the Intermediate Units of 150' and 40'. These pyroxenes vary from En_{44} in the Intermediate Unit to En_{36} in Band 6/174', and show increasing magnesium content and compositional variation across the Marginal Unit, to a maximum in the Intermediate Units (Figure 4.7). These normally-zoned pyroxenes may exhibit differing amounts of zoning on opposite sides, one crystal exhibiting a wide, continuously-zoned rim on one side, whereas the opposite side is unzoned. Such uneven zoning may reflect the proximity of other crystals to the area of growth of the ophitic crystal.

4.6 Minor Element Variation within Pyroxene.

Only TiO_2 appears to have significant correlation with the enstatite content of the pyroxene. Figure 4.14 shows chemical variation of elements with enstatite content. TiO_2 displays a negative correlation with the magnesium-iron ratio of the pyroxenes, ranging from 0 to 4% across an enstatite variation of 20%.

Diopside-salite is the typical pyroxene in hypabyssal, alkali-olivine basalt magma e.g. Garbh Eilean Sill, Shiant Isles (Murray 1954, Gibb 1973). The dyke pyroxenes contain rather high amounts of Al_2O_3 , ranging from 1-6%, compared to published data for mildly alkaline intrusions which are in the range 1-3% (Deer et al 1965). These high values may reflect substitution of silicon by aluminium as those crystals with high Al_2O_3 contain lower amounts of SiO_2 . Pyroxenes within the dyke and sill also contain high amounts of TiO_2 (0.8-2.5%) compared to the average of 0.65% quoted by Deer et al (1965) for diopside-hedenbergite pyroxenes. These authors state that augites containing high amounts of titanium may contain higher levels of aluminium.

Figure 4.15 displays compositional variation with regard to texture. Phenocryst cores exhibit a greater variation in composition than their rims. This suggests that the phenocrysts may have nucleated in more than one location, then continued growth in the common conditions of the dyke. Matrix cores show a narrow range of

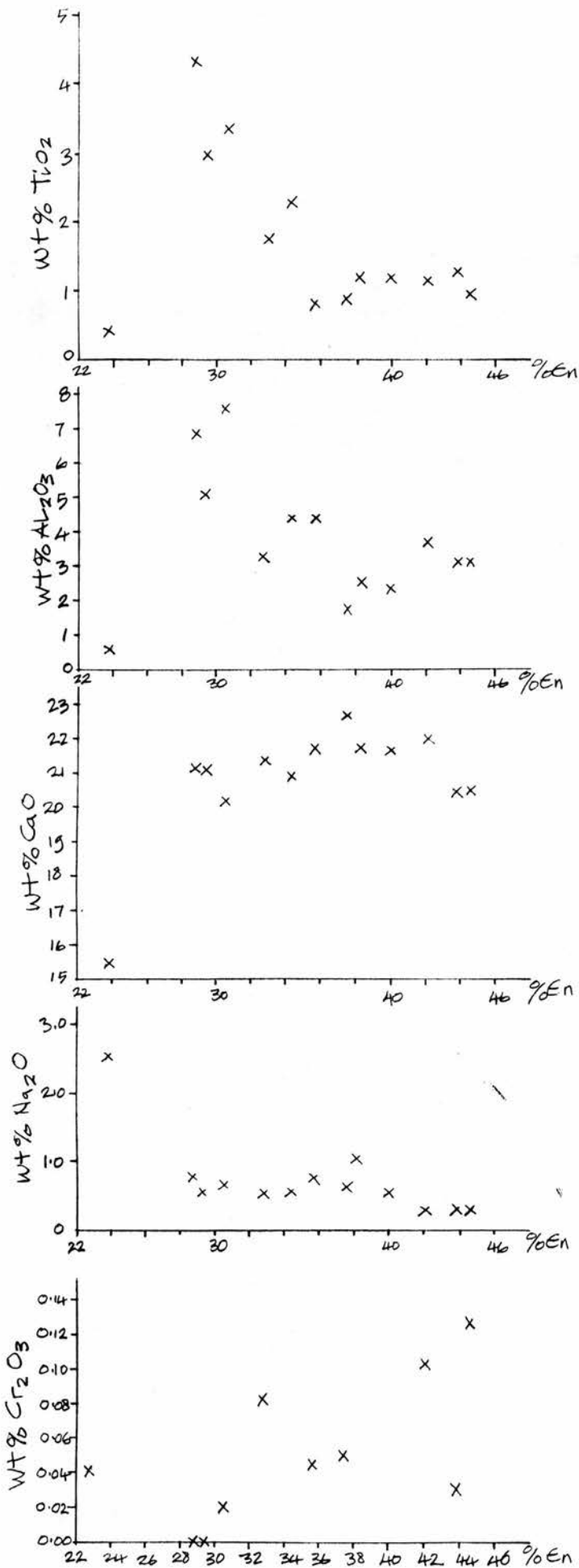


Figure 4.14 Variation of TiO₂, Al₂O₃, CaO, Na₂O and Cr₂O₃ against pyroxene enstatite content.

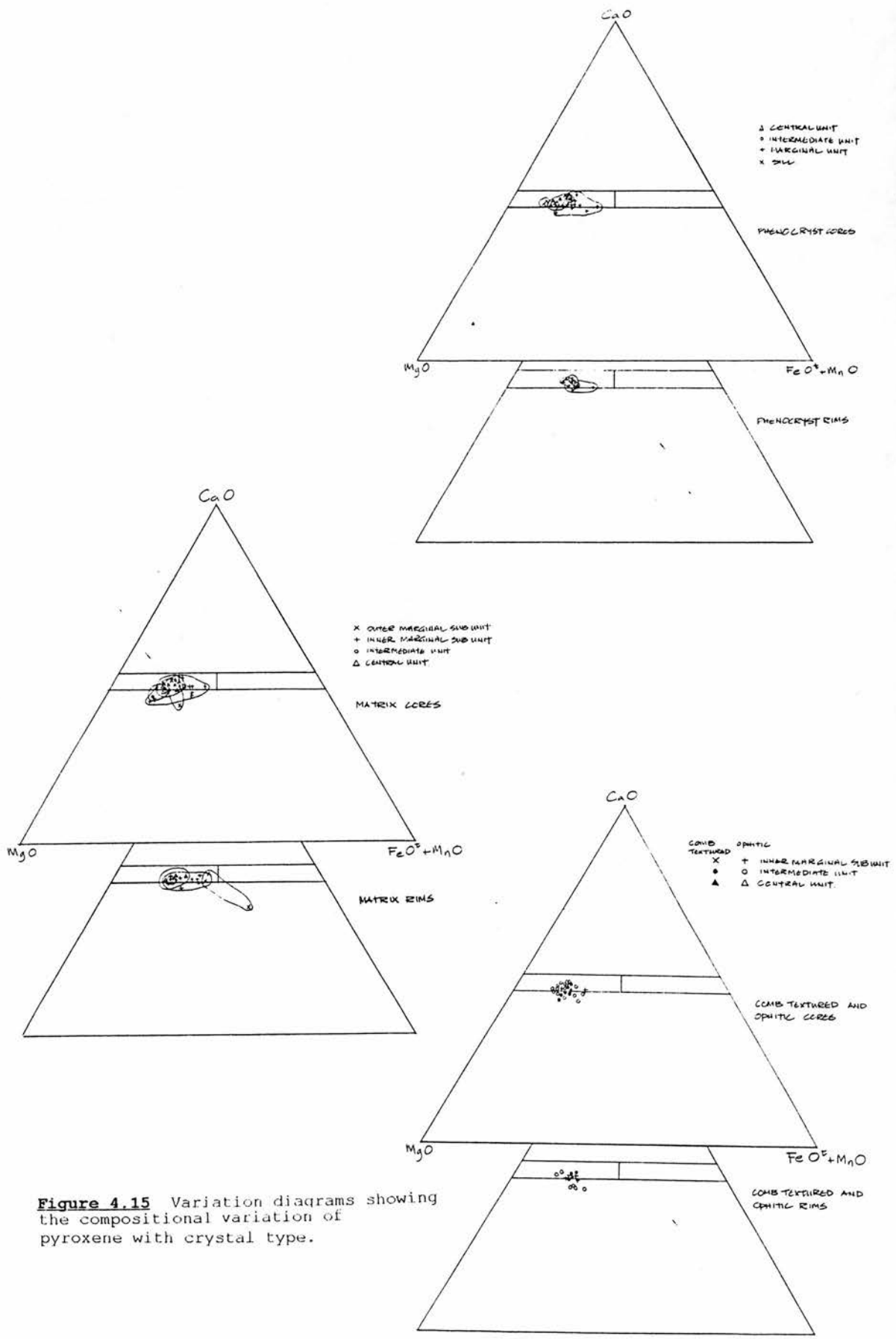


Figure 4.15 Variation diagrams showing the compositional variation of pyroxene with crystal type.

compositions, with rims displaying varying amounts of iron-enrichment, which may be considerable, as in the Outer Marginal Sub-Unit or slight as for those in the Central Unit. This decrease in zoning across the dyke may reflect slower cooling rates with distance into the dyke permitting a longer time for mineral-melt reactions to allow crystals to equilibrate. Smith and Lindsley (1971) found variation in pyroxene composition trends to depend on location (chill or interior of a flow). Figure 4.15 highlights crystallisation trends for typical pyroxenes from units of the dyke. Those from the chilled margin (Outer Marginal Sub-Unit) show a similar trend to that reported by Smith and Lindsley (1971), with Fe-Ca substitution, whilst those from the remainder of the intrusion exhibit little within-crystal calcium variation. Brown (1967) found pyroxene crystallisation from basaltic magmas depended mainly on silica content of the magma, and conditions under which it crystallised (particularly water pressure and oxygen fugacity).

Wass (1973) investigated hourglass sector zoning in matrix pyroxene crystals in Tertiary alkali-basalts. She noted that the opposing areas of the sector zoning were chemically and optically equivalent, and that TiO_2 and Al_2O_3 varied inversely with the SiO_2 content of the crystal. Dark sectors in PPL contained high amounts of TiO_2 and Al_2O_3 and low SiO_2 . The dark areas (in PPL) of the sector zoned comb-textured pyroxenes (this study)

contain high amounts of CaO, FeO, TiO₂ and Al₂O₃ and low amounts of SiO₂ and MgO, in agreement with Wass (1973).

B.V.S.P. (1981) states high Al₂O₃, TiO₂ and Na₂O in pyroxene is due to rapid cooling, while Carmichael et al (1974) state that high CaO and MgO in pyroxenes is consistent with crystallisation from alkali magma.

The pyroxenes studied by Wass (1973) were also concentrically zoned, proving that two compositions of pyroxene could be precipitated contemporaneously with similar rates of growth. The high- and low-Ca sectors of the comb-textured pyroxenes can grow simultaneously. Wass also states that rapid precipitation was required to initiate the growth of the two pyroxene compositions in different crystallographic planes, and continued rapid growth was probably required to allow the development of the sectors. She concluded that favourable kinetic conditions could be found under quenching conditions or in a melt supersaturated in the potential mineral.

Kouchi et al (1983) found experimentally that at degrees of supercooling above 55⁰C crystals developed dendritic morphology, whilst at $\Delta T=45^0$ C hopper morphology forms and at below $\Delta T=25^0$ C crystals have polyhedral morphologies. These authors also found growth rates for different crystallographic directions within a single crystal are different, and that growth rate in a particular direction increases as ΔT increases. TiO₂ and Al₂O₃ increase with increasing ΔT , while SiO₂ and MgO exhibit the reverse trend. No such trend was observed

for CaO, and the authors state that partitioning of elements is strongly controlled by growth kinetics.

4.7 Sill and Dyke Pyroxene Comparison.

Pyroxenes in the sill were analysed from 105' (Table 4.5 and Figure 4.7). Figures 4.7 and 4.15 show the compositional range of pyroxenes in the sill for comparison with those in the dyke. Phenocryst, matrix and ophitic pyroxenes were analysed, with the phenocryst core compositions in the sill having an enstatite content 1-2% in excess of that found in the dyke (En₄₄-En₄₅ compared to a maximum of En₄₃ for the dyke).

Representative samples of pyroxene in the sill complex (Gibson 1988) are reproduced in Table 4.5 and compare favourably with sill analyses in this study (Table 4.4). The ferrosilite, enstatite and wollastonite content of these representative pyroxenes in the sill fall within the range of the pyroxenes in the dyke. Major elements of pyroxenes in the sill complex generally fall within the range of those in the dyke, the Al₂O₃ and TiO₂ contents being towards the lower end of the dyke range, while the sill pyroxene SiO₂ content lies towards the higher end. Some chromium-rich samples are also enriched in magnesium. Wager and Mitchell (1951) found early formed (MgO-rich) pyroxenes in the Skaergaard

Table 4.5
 Representative analyses of
 Pyroxenes per principal lithology of
 the T.S.C.

(Gibson 1988)

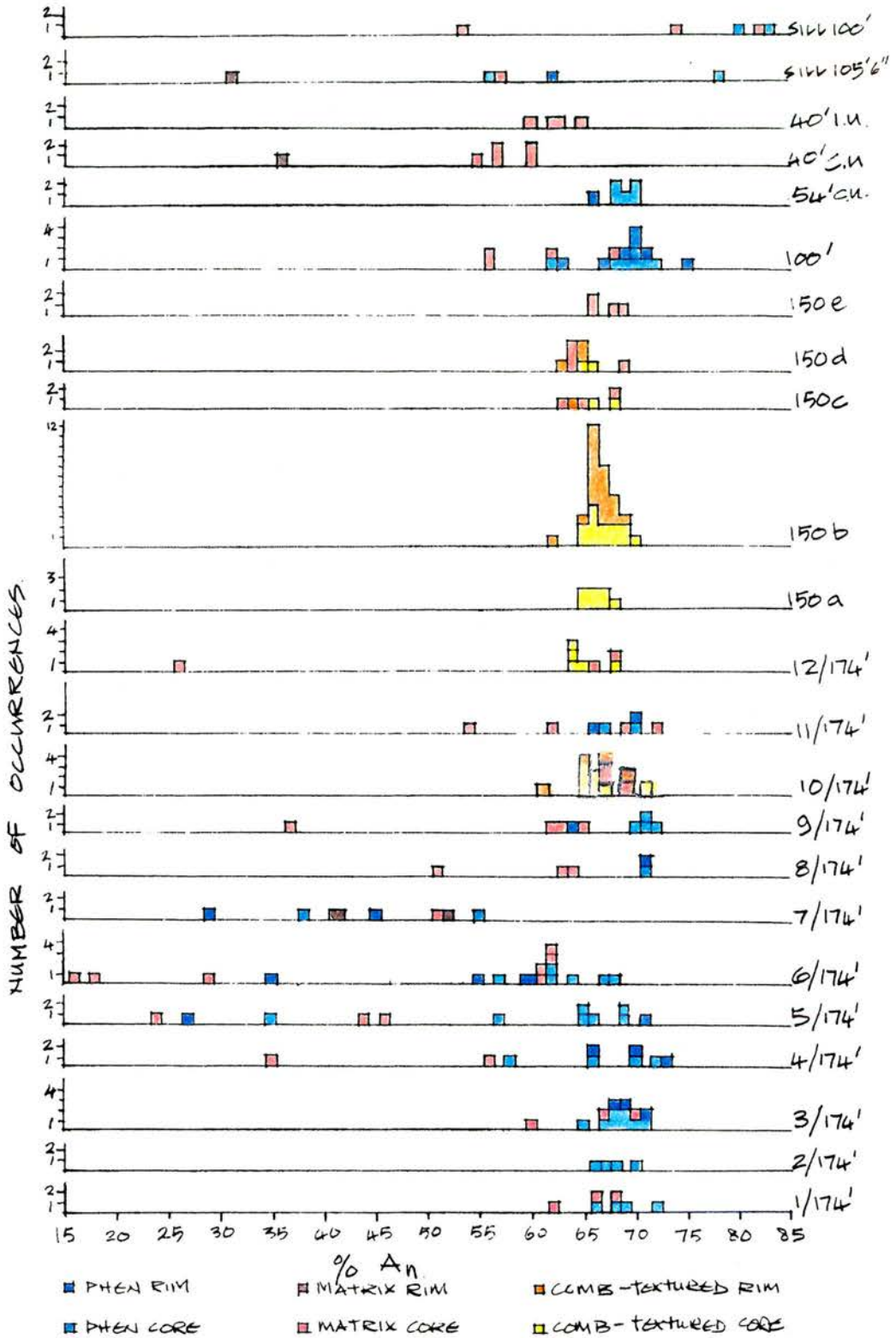
	Picro- dolerite	Picrite	Marginal Picrite	Crinanite
wt%				
SiO ₂	50.51	50.11	48.21	50.71
TiO ₂	1.15	0.55	2.09	1.17
Al ₂ O ₃	3.47	4.09	6.53	3.03
FeO t	7.27	5.71	8.99	10.44
MnO	0.18	0.13	0.26	0.42
MgO	14.40	15.89	11.86	12.64
CaO	20.29	20.29	21.11	20.31
Na ₂ O	0.90	1.95	1.03	0.08
Cr ₂ O ₃	0.37	1.20	0.09	n.d.
Total	98.54	99.84	100.17	99.52
Atoms per 6 Oxygens				
Si	1.90	1.86	1.81	1.91
Ti	0.03	0.02	0.06	0.03
Al	0.15	0.18	0.29	0.13
Fe t	0.23	0.18	0.28	0.33
Mn	0.01	0.00	0.01	0.01
Mg	0.81	0.88	0.66	0.71
Ca	0.82	0.81	0.85	0.82
Na	0.07	0.14	0.08	0.06
Cr	0.01	0.03	0.00	0.00
Fs Mol.%	12.34	9.51	15.64	17.74
En Mol.%	43.55	47.18	36.87	38.17
Wo Mol.%	44.12	43.31	47.49	44.09

contained higher amounts of several trace elements including chromium, therefore these sill crystals may represent the earlier formed pyroxenes. The elements content ranges are generally greater for the dyke than for the sill complex, suggesting that the dyke magma was more magnesian than the magma in the sill at the time that the sill pyroxenes analysed were crystallising.

4.7 Plagioclase Feldspar.

The plagioclase compositions range from Bytownite to Oligoclase (An_{75} - An_{16}), although the majority are Labradorite (Figures 4.2, 4.16 and 4.17). Some crystals are extensively zoned whilst others are homogeneous. Phenocryst cores range in composition from An_{72} to An_{35} , whilst matrix cores range from An_{69} to An_{16} (Figure 4.17). Comb-textured plagioclase has a much more restricted range of An_{71} - An_{64} . The most calcic phenocryst core composition (An_{75}) is found in the chilled margin (174' and 100') and Band 4/174', while the maximum matrix anorthite content (An_{70}) is found in comb-textured plagioclase in the Intermediate Unit at 150' (Figure 4.16). Orthoclase content is generally low with a maximum (Or_6) in a matrix core in Band 6/174' (Figure 4.16). Table 4.6 lists representative analyses for the dyke and sill.

Figure 4.16 Histogram of all plagioclase compositions of dyke and sill.



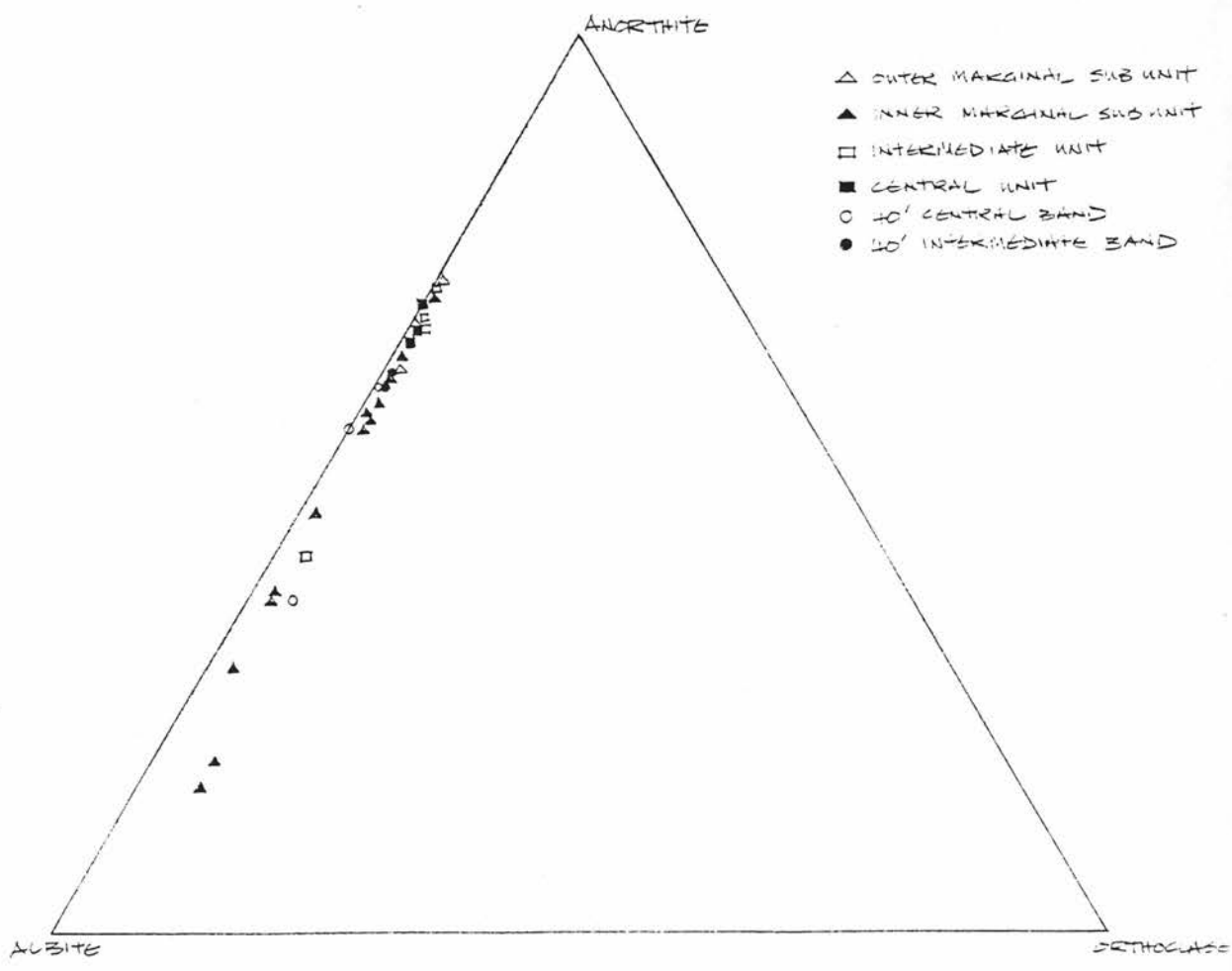


Figure 4.17 An-Ab-Or Variation Diagram for each unit of the dyke.

Table 4.6

Representative Plagioclase feldspar analyses from the dyke and sill.

Band	1/174'	2/174'	3/174'	4/174'	5/174'	6/174'	7/174'	8/184'	9/174'	10/174'
*Unit	O.M.S-U.	I.M.S-U.	I.M.S-U.	I.M.S-U.	I.M.S-U.	I.M.S-U.	I.M.S-U.	I.M.S-U.	I.M.S-U.	I.U.
Distance	2.29	4.24	7.77	11.49	13.94	15.42	16.95	24.19	27.75	28.56
across dyke in Gms										
wt%	phen core	phen core	phen core	gas core	phen core	phen core	phen rim	gas core	phen core	phen core
SiO ₂	49.93	49.86	50.38	53.99	51.51	51.72	55.78	51.03	49.42	50.67
TiO ₂	0.07	0.08	0.04	0.09	0.14	0.12	0.11	0.14	0.13	0.08
Al ₂ O ₃	31.33	30.87	30.80	28.56	29.08	29.87	27.17	29.41	30.67	30.32
FeO t	0.60	0.67	0.62	0.78	0.87	0.67	0.58	0.71	0.85	0.89
MnO	0.00	0.06	0.00	0.01	0.00	0.05	0.06	0.02	0.00	0.01
MgO	0.07	0.06	0.06	0.07	0.10	0.07	0.08	0.06	0.10	0.04
CaO	14.33	14.07	14.20	11.83	12.51	12.54	9.57	13.07	14.46	13.67
Na ₂ O	3.49	3.48	3.44	4.94	4.93	4.97	6.24	4.13	3.09	3.51
K ₂ O	0.06	0.10	0.15	0.20	0.16	0.23	0.26	0.15	0.08	0.13
Total:	99.87	99.24	99.70	100.47	99.28	100.23	99.83	98.71	98.79	99.30

Atoms per 32 Oxygens

Si	9.14	9.19	9.24	9.76	9.48	9.43	10.09	9.44	9.16	9.32
Ti	0.01	0.01	0.01	0.01	0.02	0.02	0.02	0.02	0.02	0.01
Al	6.76	6.70	6.65	6.09	6.31	6.42	5.79	6.41	6.70	6.57
Fe t	0.09	0.10	0.10	0.12	0.13	0.10	0.09	0.11	0.13	0.14
Mn	0.00	0.01	0.00	0.00	0.00	0.01	0.01	0.00	0.00	0.00
Mg	0.02	0.02	0.02	0.02	0.03	0.02	0.02	0.02	0.03	0.01
Ca	2.81	2.78	2.79	2.29	2.47	2.45	1.85	2.59	2.87	2.69
Na	1.24	1.24	1.22	1.73	1.76	1.76	2.19	1.48	1.11	1.25
K2	0.01	0.02	0.04	0.05	0.04	0.05	0.06	0.03	0.02	0.03
An Mol. %	69.18	68.67	68.89	56.32	57.88	57.53	45.13	63.08	71.78	67.77
Ab Mol. %	30.49	30.74	30.24	42.54	41.24	41.23	53.41	36.08	27.77	31.50
Or Mol. %	0.32	0.59	0.87	1.14	0.87	1.24	1.46	0.84	0.46	0.73

* Unit abbreviations:

O.M.S-U. Outer Marginal Sub-Unit

I.M.S-U. Inner Marginal Sub-Unit

I.U. Intermediate Unit

C.U. Central Unit

11/174'	12/174'	150'a	150'b	150'c	150'd	150'e	100'	54'	40'	40'
C.U.	I.U.	I.U.	I.U.	I.U.	I.U.	C.U.	I.M.S-U.	C.U.	C.U.	I.U.
60.83	63.14	33.37	35.53	40.73	42.66	48.20	0.251	53.94	56.30	78.31
phen core	phen core	c-t core	c-t core	c-t core	c-t core	gas core	phen rim	phen core	gas core	gas core
49.49	51.89	51.31	50.57	49.82	51.51	51.68	50.41	50.05	51.81	50.98
0.06	0.11	0.07	0.11	0.13	0.08	0.06	0.09	0.08	0.05	0.12
29.29	30.16	30.39	30.61	29.97	29.69	29.92	30.94	30.69	29.06	29.26
0.51	0.79	0.82	0.83	0.75	0.67	0.47	0.65	0.53	0.80	0.97
0.03	0.03	0.04	0.04	0.08	0.07	0.01	0.00	0.00	0.01	0.03
0.12	0.15	0.16	0.06	0.10	0.10	0.13	0.04	0.11	0.10	0.05
13.23	13.27	13.78	13.76	13.08	13.47	13.50	14.11	14.24	12.34	12.45
3.47	4.07	3.75	3.67	3.70	4.04	3.83	3.32	3.47	4.98	4.07
0.06	0.09	0.07	0.11	0.07	0.07	0.11	0.16	0.07	0.13	0.17
96.28	100.54	100.39	99.76	97.69	99.69	99.72	99.71	99.23	99.28	98.09
9.36	9.42	9.34	9.28	9.30	9.43	9.44	9.23	9.22	9.53	9.47
0.01	0.01	0.01	0.00	0.02	0.01	0.01	0.01	0.01	0.01	0.02
6.53	6.46	6.52	6.62	6.60	6.41	6.44	6.68	6.67	6.30	6.41
0.08	0.12	0.13	0.13	0.12	0.10	0.07	0.10	0.08	0.12	0.15
0.01	0.00	0.01	0.00	0.02	0.01	0.00	0.00	0.00	0.00	0.00
0.03	0.04	0.05	0.03	0.02	0.03	0.04	0.01	0.03	0.03	0.01
2.68	2.58	2.69	2.69	2.62	2.64	2.64	2.77	2.81	2.43	2.48
1.27	1.43	1.32	1.31	1.34	1.43	1.36	1.18	1.24	1.78	1.47
0.02	0.02	0.02	0.03	0.02	0.02	0.02	0.04	0.02	0.02	0.04
67.54	64.02	66.80	66.67	65.79	64.55	65.67	69.48	69.14	57.58	62.22
32.08	35.48	32.80	32.54	33.80	35.03	33.72	29.59	30.46	42.06	36.78
0.39	0.50	0.40	0.79	0.40	0.42	0.61	0.94	0.39	0.36	1.00

SILL	SILL
100'	105'

phen core	phen rim
47.67	50.91
0.07	0.08
32.02	30.08
0.48	0.60
0.00	0.05
0.02	0.09
16.38	12.89
2.13	4.11
0.15	0.12
98.93	98.92

8.86	9.38
0.01	0.01
7.01	6.53
0.07	0.09
0.00	0.01
0.00	0.02
3.26	2.54
0.77	1.47
0.04	0.03

80.27	62.97
18.85	36.36
0.87	0.67

Figure 4.18 shows the maximum anorthite content of phenocrysts across the banding of the dyke (matrix crystals have been included for 40' where no phenocrysts are present). With the exception of Band 7/174', maximum anorthite phenocrysts lie between An_{75} and An_{65} . The outer 12cms of the dyke show little variation in maximum anorthite content of phenocrysts, but Bands 6 and 7/174' show a decrease to An_{55} . Bands 8 and 9/174' contain phenocrysts with a similar composition to the outer 12cms of the dyke. The Intermediate Unit contains interstitial and comb-textured crystals whose compositions lie between the Marginal and Central Unit maximum anorthite compositions. Figure 4.19 shows plagioclase compositions for each area studied.

4.7.1 Phenocrysts.

The phenocrysts in the chilled margin have a composition of An_{75-62} and maximum zoning (oscillatory) of 6% An, with highest anorthite content in the rim. There is little change in composition across the dyke until Band 5/174' where a greater range of core compositions is found ($An_{69}-An_{35}$) (Figures 4.2, 4.16 and 4.17). Maximum zoning (normal) of 30% An is found in Band 5/174', with Bands 6 and 7/174' also containing highly, normally-zoned phenocrysts.

Figure 4.19 Variation in Plagioclase compositions per
area transect analysed:

- a) 174'
- b) 150'
- c) 100'
- d) 54'
- e) 40'.

Legend as for Figure 4.4

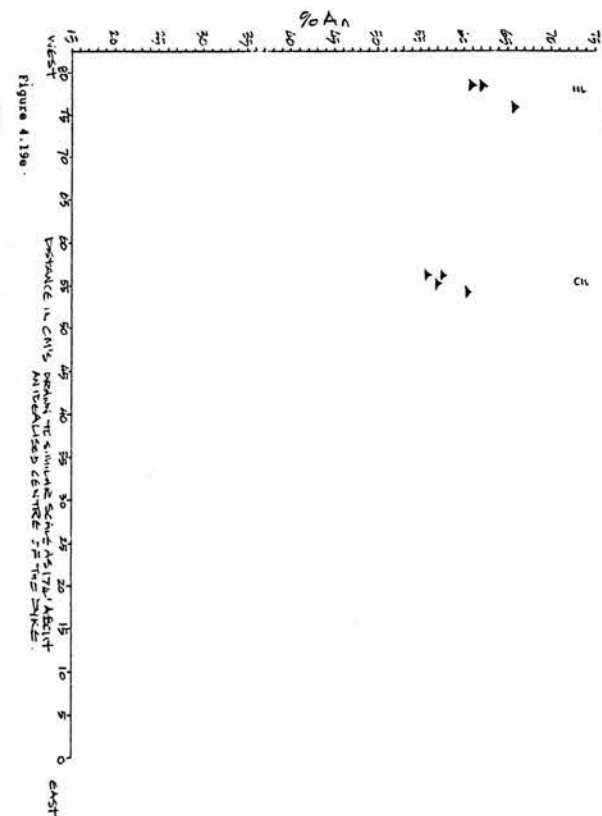
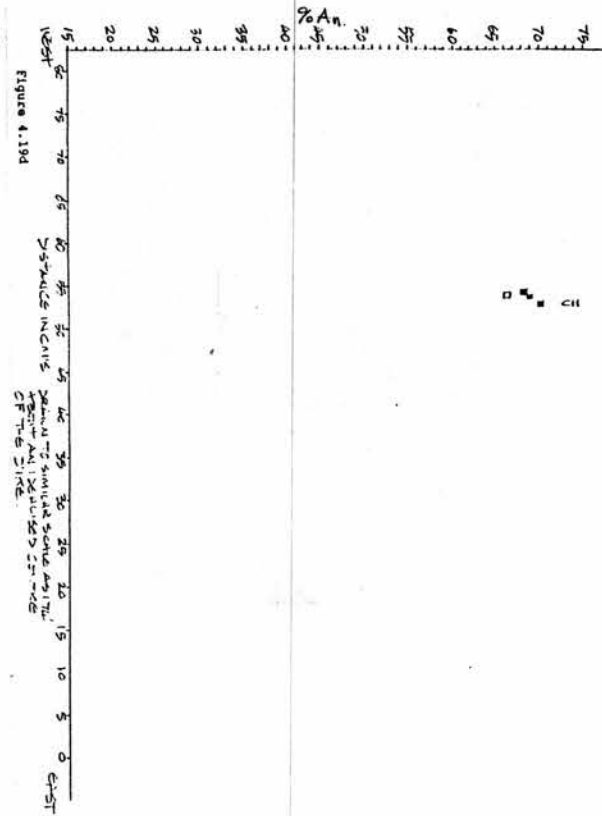
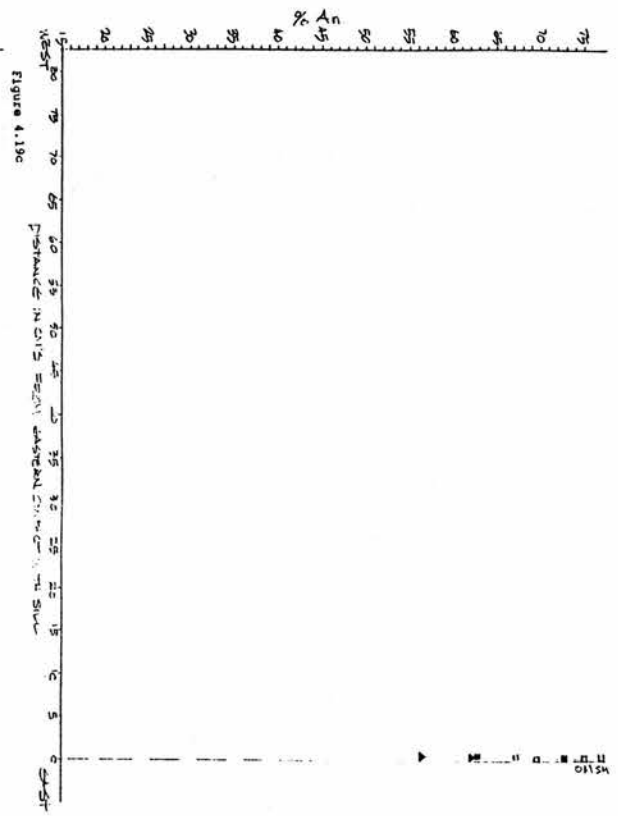
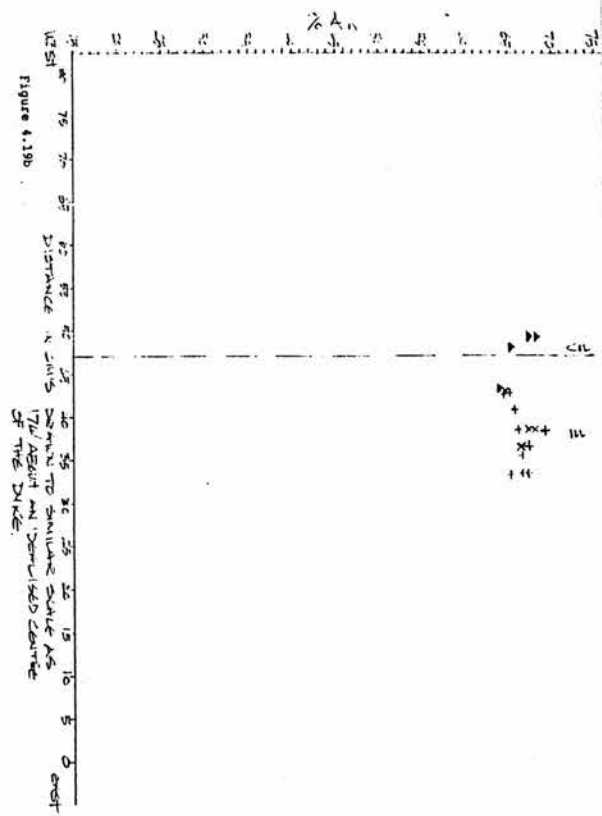
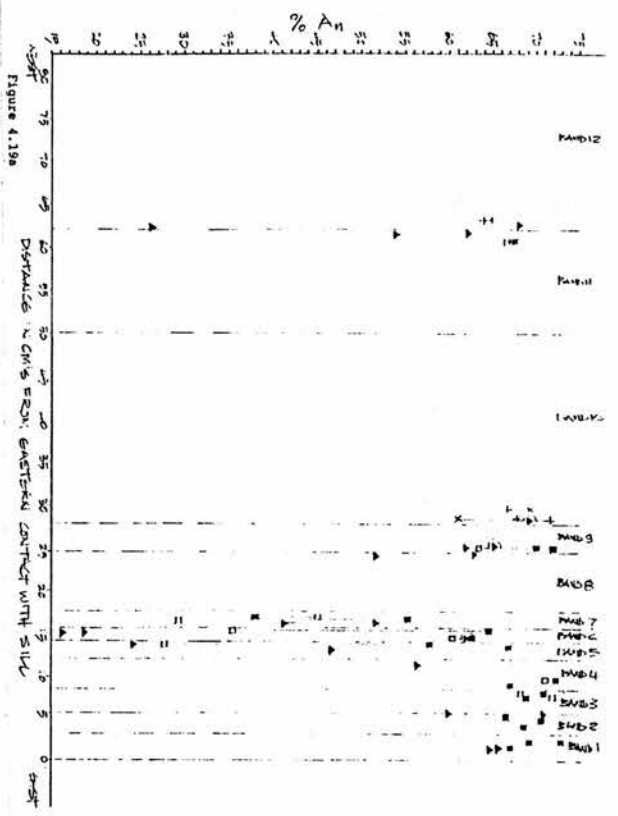


Figure 4.130.

4.7.2 Matrix.

Matrix crystals have a compositional range of An_{72} - An_{16} . There is a trend from a narrow to wide composition range across Bands 1-6/174', beyond which the range decreases until Band 10/174' (Figures 4.2 and 4.16). Band 12/174' shows a wide compositional variation due to one analysis of An_{26} (Figure 4.16). Matrix crystals and phenocrysts analysed from the Outer Marginal Sub-Unit (174' and 100'), are of similar composition (An_{68} - An_{62}). Differences between phenocryst and matrix cores exist in Band 3/174' (Figures 4.2, 4.16 and 4.19) and widen in Band 4/174', where the matrix crystals have a composition of An_{56} - An_{35} , while the phenocryst cores are An_{72} - An_{58} . This range in matrix composition increases across Bands 5 and 6/174' to An_{62} - An_{16} in Band 6/174'. Matrix crystals in Band 7/174' lie within the range of phenocryst compositions (Figure 4.2), but are not as anorthite-enriched as the phenocryst compositions in Band 8/174'. Matrix and comb-textured crystals were analysed from the Intermediate Unit, with both types having a similar composition at 174' (An_{69} - An_{66} , Figure 4.16). Walker (1985) gives matrix composition as An_{74} - An_{62} , with no obvious trends across the Intermediate Unit at 74'.

4.7.3 Comb-Textured Crystals.

Comb-textured plagioclases were analysed from the Intermediate Unit in the northern segment of the dyke

(174' and 150'). They have restricted compositions of An₇₁-An₆₁ (Figures 4.2 and 4.16), which is similar to the phenocrysts and matrix crystals in the Outer Marginal Sub-Unit. There is little variation along or across a crystal. A previous study of the comb-textured crystals in the Mystery Dyke by Walker (1985) found elongate (comb-textured) plagioclase had a consistent composition of An₇₀-An₆₆, and found no evidence of plagioclase-liquid fractionation having occurred during solidification.

4.8 Sill and Dyke Plagioclase Feldspar Comparison.

Phenocryst and matrix plagioclase feldspars were analysed from the sill (100' and 105'). Phenocryst cores have a composition of An₈₃ to An₅₆, the lower anorthite content being from a smaller phenocryst. A large phenocryst analysed from 105' was normally-zoned from An₇₉ to An₆₃ (Figure 4.16). Matrix crystals have core compositions between An₈₂-An₅₄, with one showing zoning from a core composition of An₅₇ to a rim composition of An₃₁. Crystals analysed are comparable to analyses given by Gibson (1988) for the Trotternish Sill Complex (An₈₉-An₆ -Table 4.7).

Plagioclase in the dyke shows a larger compositional range of An₇₅-An₁₆ compared to An₈₃-An₃₁ for the sill (this study), within the range quoted by Gibson (1988).

Table 4.7
Representative analyses of Plagioclase feldspar
from the T.S.C.

(Gibson 1988)

	Bytownite	Andesine	Oligoclase	Anorthoclase
	No data on crystal types.			
SiO ₂	48.54	53.40	58.59	64.28
Al ₂ O ₃	32.94	28.89	26.06	19.60
FeO t	1.51	1.01	0.53	1.53
CaO	16.42	11.03	5.23	1.21
Na ₂ O	1.12	5.29	9.05	8.52
K ₂ O	0.19	0.17	0.50	3.97
Total	100.71	99.79	99.96	99.11

	Atoms per 32 Oxygens			
Si	8.86	9.72	10.51	11.65
Al	7.09	6.20	5.51	4.19
Fe t	0.23	0.15	0.08	0.23
Ca	3.21	2.15	1.01	0.23
Na	0.40	1.87	3.15	2.99
K	0.04	0.04	0.11	0.92
Total	19.83	20.14	20.37	20.22

An Mol. %	88	53	24	6
Ab Mol. %	11	46	74	72
Or Mol. %	1	1	3	23

All major elements are comparable with the exception of FeO which has a higher range in the dyke than for the sill.

4.9 Oxide Minerals.

Oxide minerals were analysed from the dyke and the sill. Two types of oxide minerals are present within the dyke, chromium-rich spinels and titaniferous magnetite. These and ilmenite are present in the sill complex (Gibson 1988). Chrome-spinels are most abundant within the picrites (Gibson 1988) and are always enclosed by olivine (Gibson and Jones 1991).

In this study the Fe_2O_3 content was calculated from total FeO values according to the method described by Droop (1987).

In the dyke, oxide minerals are found in three environments: enclosed within olivine crystals, partially enclosed within olivine, clinopyroxene or plagioclase crystals and as isolated matrix crystals. Those found within olivine are chrome-spinels. These are indicative of a high-temperature environment and high $f\text{O}_2$ conditions where the oxide crystallises in preference to iron-rich silicates (Haggerty 1976b). The early-formed chrome-spinels are enriched in Cr, Al and Mg and relatively depleted in Fe and Ti compared to the titaniferous

magnetite (Table 4.8). Irvine (1967) states that chrome-spinels generally crystallise simultaneously with olivine and that their formation has in many instances been terminated by a peritectic (reaction) relation leading to the formation of pyroxene. This is in agreement with the modal proportions of spinel, olivine and pyroxene (Table 3.1), for high amounts of olivine and spinel give way to higher amounts of pyroxene (The Outer Marginal Sub-Unit and the Intermediate Unit). The crystallisation of olivine and pyroxene dominates the partitioning of magnesium, while plagioclase dominates the partitioning of aluminium, thus depleting oxides of these elements (Haggerty 1976b). Matrix oxide minerals are predominantly titaniferous-magnetites indicative of lower temperature conditions (Hill and Roeder 1974; Haggerty 1976b).

Haggerty (1976b), states that there are three trends that crystallising oxide minerals may follow. These are

- a) kimberlite or
- b) magmatic ore deposit or
- c) the xenolith and peridotite trends.

The changing composition from chrome-spinels enclosed by the olivine phenocrysts to the titaniferous magnetites in the groundmass indicates that oxide minerals in the dyke followed the magmatic ore deposit trend. This shows a trend upwards from the base of the spinel prism towards the Ti-Fe^{3+} apex, and from being magnesium-rich to iron-

Table 4.8
Representative oxide mineral compositions
in the dyke and sill.

	3/174'	3/174'	5/174'	Sill 105'	Sill 105'	Sill 105'
	Enclosed in Ol	Gas core	Enclosed in Ol	Enclosed in Ol	Enclosed in Ol	Enclosed in Ol
wt%						
TiO ₂	1.23	21.18	0.89	2.74	1.61	15.52
Al ₂ O ₃	32.14	1.45	33.98	19.60	26.85	7.14
FeO	17.03	38.97	17.69	22.87	19.92	33.17
Fe ₂ O ₃	9.02	29.27	8.42	10.81	10.91	10.69
MgO	13.53	2.73	13.39	8.99	10.78	8.05
Cr ₂ O ₃	24.30	0.00	24.01	31.51	25.55	19.06
Total	97.83	94.55	98.89	97.24	96.19	94.45
	Atoms per 4 Oxygens					
Ti	0.03	0.59	0.02	0.07	0.04	0.42
Al	1.16	0.14	1.18	0.76	1.00	0.30
Fe ⁺⁺	0.42	1.21	0.44	0.63	0.53	0.99
Fe ⁺⁺⁺	0.22	0.91	0.21	0.30	0.29	0.32
Mg	0.60	0.15	0.60	0.44	0.51	0.43
Cr	0.57	0.00	0.56	0.82	0.64	0.54

Cr-spinel Ti-magnet. Cr-spinel Cr-spinel Cr-spinel Cr-Ti-magn.

rich. This trend is visible in Figure 4.20, which shows the composition of oxide minerals in the dyke and sill.

4.10 Sill and Dyke Oxide Mineral Comparison.

Oxide minerals are enclosed within olivine phenocrysts and are predominantly spinels, which show a close similarity to those studied by Gibson (1988).

The titaniferous magnetite compositions of the dyke lie within the magnetite and titaniferous magnetite compositions in the sill given by Gibson (1988). Ridley (1973, 1977) gives details of spinels within the Rhum and Muck Tertiary basalts:- the former a transitional alkali olivine basalt, the latter an alkali olivine basalt. He states that the spinels are either wholly or partially enclosed by olivine with the latter possibly having undergone cation exchange with the melt (Ridley 1977). The spinels in the dyke (Table 4.8) show a close resemblance to those from Muck, which Ridley (1977) states began to crystallise prior to eruption of the magma, closely followed by the crystallisation of olivine. The two minerals grew in isothermal conditions prior to eruption, but then the zoned rims of the olivines indicate rapid crystal growth (Ridley 1977).

Oxide minerals in alkali olivine basalts have typically high $Cr/(Cr+Al)$ ratios (Haggerty 1976b),

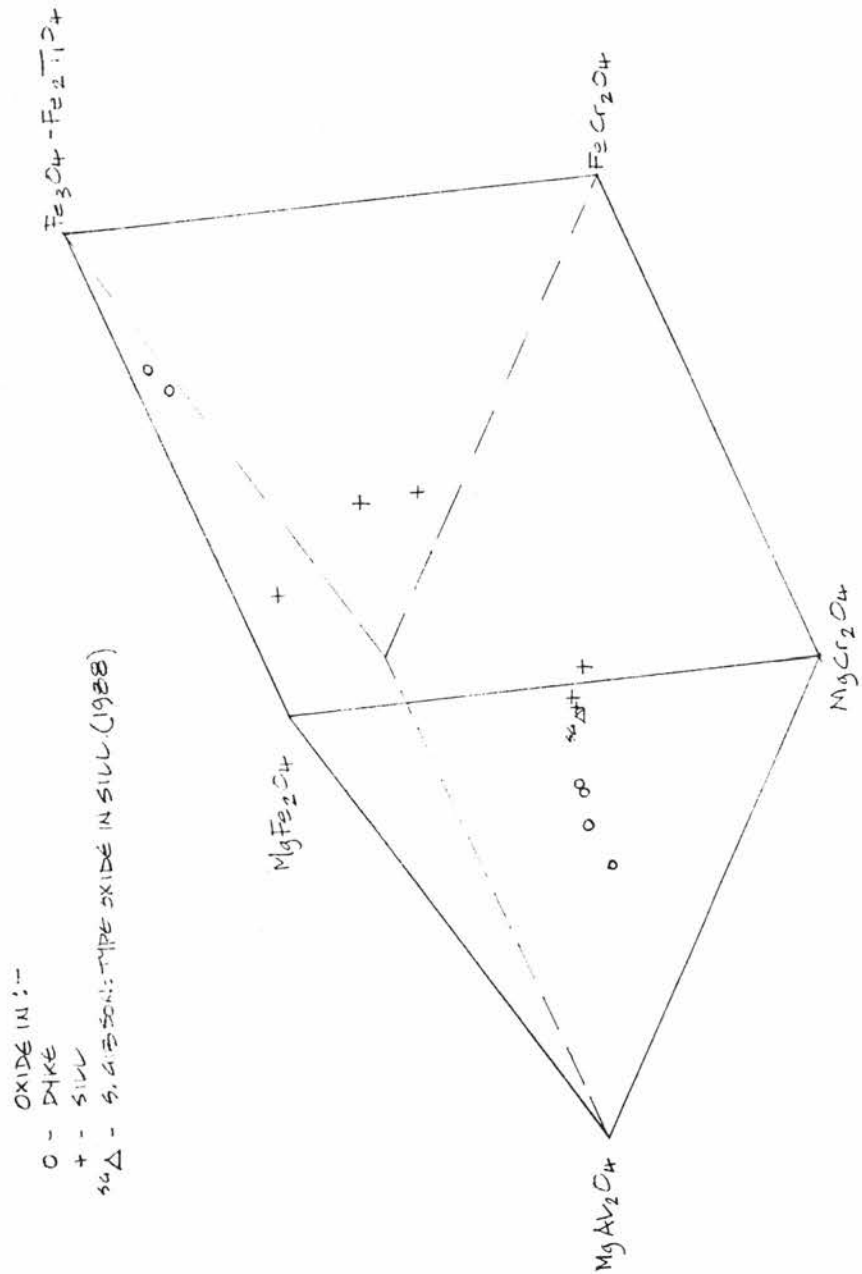


Figure 4.20 Oxide compositions in the dyke and sill.

whereas the dyke has ratios ranging from a maximum of 0.33 for the spinels enclosed by the olivine phenocrysts to zero for groundmass crystals. This compares with ratios ranging from 0.64 to 0.39 for oxide minerals within the sill (this study). The typical chrome-spinel analysis of Gibson (1988) (Table 4.9) has a ratio of 0.40. Ridley (1977) gives ratios of 0.67-0.24 and 0.37-0.11 for spinels from Muck and Rhum respectively. The ratios from the sill and the dyke fall within these ranges. Haggerty (1976b) states that variation in $Cr/(Cr+Al)$ ratios are related to variations in the initial bulk chemistry of the magma, the petrogenesis of Mg, Al and Fe-bearing silicates, and pressure and temperature of the crystallisation environment. Sigurdsson and Schilling (1976) state that the $Cr/(Cr+Al)$ ratio varies inversely with pressure.

Figure 4.20 shows the relationship between the oxide minerals in the dyke and the sill complex. The latter lie on the trend shown by the progression of the chrome-spinels (within olivine) to titaniferous magnetites (matrix crystals) within the dyke. The chemistry of the oxide minerals in dyke and sill suggests a common source but with differing crystallisation environments.

Table 4.9
 Representative chrome-spinel
 composition from the T.S.C.
 (Gibson 1988)

	Enclosed in Ol
wt%	
TiO ₂	1.96
Al ₂ O ₃	26.45
FeO	16.58
Fe ₂ O ₃	10.36
MgO	12.16
Cr ₂ O ₃	26.48
Total	93.99

	Atoms per 4 Oxygens
Ti	0.05
Al	0.97
Fe ⁺⁺	0.48
Fe ⁺⁺⁺	0.30
Mg	0.56
Cr	0.65

4.11 Accessory Minerals.

Accessory minerals analysed include zeolite and calcite. The zeolite may be mesolite, thomsonite or scolecite, and with one exception, all fibrous zeolites analysed are calcium-rich. The exception is sodium-enriched (Table 4.10). Mesolite, scolecite and thomsonite are all found in the Tertiary lavas of Skye (Deer et al 1963 Vol. 4). Gibson (1988) stated that the zeolites present within the sill complex were either analcime or thomsonite. No analcime was detected in the dyke. This variation in zeolite within the dyke and surrounding sill may be due to different thermal zones at the time of zeolitisation (Walker 1985).

4.12 Summary.

Mineral composition within each unit does not differ significantly along the dyke. Within units there is no compositional variation of similar crystal types with distance along the dyke (Figures 4.1, 4.2, 4.4). There is also little variation in olivine phenocryst core composition across the dyke (Fo₈₈-Fo₇₅) (Figures 4.1, 4.4) suggesting that phenocrysts did not crystallise in situ but were emplaced with the intruding magma. This is similar to the conclusions of Gibb and Henderson

Table 4.10
Representative Zeolite compositions from
the dyke.

Sample:	3/174'	12/174'	54'	54'
wt%				
SiO ₂	47.70	41.52	45.23	59.79
Al ₂ O ₃	24.03	28.91	32.37	33.70
CaO	9.07	11.23	12.55	1.38
Na ₂ O	0.92	1.11	1.33	3.58
K ₂ O	2.72	0.03	0.02	0.02
Total:	84.46	83.04	91.57	98.47

(1992), in their study of olivines within sill complexes. The extent of chemical zoning of olivine increases with distance into the dyke, indicating decreasing crystallisation rates, but with crystals not able to equilibrate with the melt.

With the exception of Bands 6-9/174', the phenocryst cores are more magnesian than matrix cores. Olivine groundmass crystals exhibit a wide range of compositions indicating changing thermal and chemical gradients. Comb-textured olivines have a restricted core composition (Fo_{75} - Fo_{68}) indicating crystallisation under constant conditions. Figures 4.1, 4.4 and 4.5 show a slight increase in forsterite content with distance into the dyke suggesting supercooling as the process responsible for comb-textured olivine crystallisation (Lofgren and Donaldson 1975, Kouchi et al 1983). The olivines in the Central Unit in the northern and southern segments may indicate an influx of hotter, more mafic magma.

The association of phenocrysts with high forsterite and high anorthite content suggests closely associated crystallisation of olivine and plagioclase. Comb-textured plagioclase, like the comb-textured olivine, exhibits a restricted composition (An_{71} - An_{61}). In the outer bands, phenocrysts and matrix crystals have similar compositions, but variation between crystal types increases to a maximum in Bands 4-6/174' (Figures 4.2, 4.16). Maximum zoning is exhibited by groundmass plagioclase suggesting precipitation of plagioclase

without sufficient time to allow crystals to react with the melt.

Pyroxene phenocryst and matrix crystals are of similar compositions (Figures 4.2, 4.7, 4.8 and 4.15), with the majority displaying slight, continuous normal zoning. Phenocrysts and matrix pyroxenes generally exhibit similar compositional variation within a band and similar zoning trends (Figure 4.7): both may be normally zoned or the phenocrysts may be zoned normally, with groundmass pyroxenes exhibiting reverse zoning (e.g. Band 5/174'). The latter situation can be explained due to phenocrysts being carried into the dyke by the magma and are zoned normally in response to decreasing temperature within the dyke conduit, whereas matrix crystals forming within the dyke are reverse-zoned due to increasing temperature and MgO content of the melt due to fresh influx of magma into the dyke. Reverse zoning of pyroxenes may also be due to decompression (Ewart et al 1975), the onset of magnetite precipitation (Gill 1981) or an increase in fO_2 due to pre-eruptive influx of H_2O (Luhr and Carmichael 1980).

A wide range of groundmass compositions are exhibited by olivine and pyroxene in Band 4/174'. Pyroxene matrix cores exhibit greater compositional variation than rims, suggesting crystallisation in different conditions and locations. Maximum zoning is exhibited by matrix pyroxenes in the outer bands of the dyke, with zoning decreasing with distance into the dyke.

The relationship between the amygdaloidal Central Unit and the non-amygdaloidal "central band" in the southern segment was investigated. Olivine and plagioclase from this "central band" have slightly lower forsterite and anorthite content respectively than those in the Intermediate Unit, indicative of continued cooling. No comparison can be made between 54' and 40' as only phenocrysts were analysed from 54' and mainly groundmass crystals from 40'. Olivine and pyroxene in the Intermediate Unit (40') are equivalent to matrix olivine and pyroxenes in the Intermediate Units at 150' and 174', with olivines in the Central Unit being equal to those in the Central Unit at 174'. Pyroxenes in the central band at 40' are of similar composition to those in the Central Unit (150' and 174') and phenocrysts at 54'. Groundmass plagioclase in the intermediate Unit at 40' has lower anorthite content than those in the Intermediate Unit in the northern segment, with those in the central band having compositions similar to those to less-anorthite plagioclases in the Central Unit (174').

Sill and dyke minerals show comparability suggesting related development. Olivines in both contain levels of CaO suggesting crystallisation in a high crustal environment. The sill contains phenocrysts with a lower forsterite content, but matrix crystals with higher forsterite content than comparable crystals in the dyke.

The abundant phenocrysts in the chilled margin of the dyke have not been scoured from the picrite sill by the intruding magma, as they are more forsteritic than the olivine phenocrysts in the adjacent sill. The concentration of the phenocrysts into the outer bands of the dyke may reflect the level of the magma chamber that was being tapped or the speed of the intruding magma.

Plagioclase in the dyke lies within the range of compositions for plagioclase in the sill. With the exception of FeO (plagioclase in the dyke contains higher amounts), there is overall similarity in chemical composition between the plagioclase in the sill and dyke.

Comparison between sill and dyke pyroxene compositions shows dyke pyroxenes to have a wider range than sill pyroxenes. Sill phenocryst cores have slightly higher enstatite content than dyke phenocryst cores. The olivine, plagioclase and pyroxene mineral chemistry shows no matching relationship between any one rock-type of the Little Minch Sill Complex and the dyke, but a general affinity between the dyke and the sill complex.

Unfortunately, insufficient data on the mineral chemistry in the Lava Series could be obtained, and no comment can therefore be made with respect to any relationship between these intrusions.

The mineral chemistry of the dyke indicates a more complicated history than can be explained by a single intrusive event. Variation of mineral compositions and

complex zoning patterns noted suggest cogenetic pulses of magma intruded within short periods of each other.

CHAPTER 5
GEOCHEMISTRY OF THE MYSTERY DYKE.

5.0 Introduction.

Whole-rock geochemical analysis was performed by X-ray fluorescence (XRF) spectrometry on fused discs for major oxides (except MnO) and on pressed powder pellets for trace elements and MnO. Ferrous iron was determined by traditional wet chemistry methods. A description of the methods and analytical error can be found in Appendix 5.1. Data for major and trace elements, together with selected element ratios for all dyke samples analysed are contained in Table 5.1.

The chemical compositions of the bands have been recalculated on a H₂O-free basis, to compensate for weathering of the samples obtained. A "dyke" composition based on the chemical compositions and proportions of each band for the half-width of the dyke at 174' is also shown, together with calculated compositions for each unit of the dyke at 174'. Band 10/174' has been defined as the Intermediate Unit composition as there is insignificant variation between it and a composition calculated with proportions of Bands 10 and 12/174'. Also shown is new data for the

Table 5.1

Whole-Rock Geochemistry of the Dyke and Sill, calculated for a dry sample with calculated iron ratios*

Band/Dist:	174'	174'	174'	174'	174'	1/174'	2/174'	3/174'	4/174'
**Unit:	'Dyke'	O.M.S-U.	I.M.S-U.	I.U.	C.U.	O.M.S-U.	I.M.S-U.	I.M.S-U.	I.M.S-U.
Wt%									
SiO ₂	46.70	45.99	47.08	46.81	45.43	45.99	46.17	46.58	47.79
TiO ₂	1.40	1.30	1.74	0.80	1.93	1.30	1.43	1.63	1.73
Al ₂ O ₃	16.60	14.11	15.30	19.23	14.64	14.11	13.83	14.68	15.32
Fe ₂ O ₃	2.90	3.00	3.24	2.30	3.43	3.00	2.95	3.15	3.25
FeO	8.66	9.71	9.43	7.42	9.63	9.71	9.96	9.86	9.26
MnO	0.18	0.21	0.19	0.15	0.19	0.21	0.19	0.19	0.20
MgO	9.10	12.21	8.16	9.69	9.49	12.21	12.48	9.31	7.27
CaO	10.40	10.09	10.73	9.97	10.19	10.09	9.62	10.34	10.77
Na ₂ O	3.30	2.39	3.33	3.26	4.25	2.39	2.19	3.03	3.22
K ₂ O	0.40	0.49	0.54	0.26	0.48	0.49	0.66	0.72	0.69
P ₂ O ₅	0.17	0.18	0.20	0.11	0.22	0.18	0.17	0.20	0.28
Total:	99.81	99.88	99.94	100.00	99.88	99.88	99.67	99.71	99.80
Total Fe	11.56	12.71	12.67	9.72	13.06	12.71	12.91	13.01	12.51
ppm									
Nb	2	2	3	1	4	2	4	5	5
Zr	79	80	101	40	114	80	74	106	135
Y	17	19	21	10	21	19	19	22	26
Sr	412	483	424	394	381	483	482	520	472
Rb	4	6	6	1	3	6	5	8	9
Th	1	0	1	0	1	0	4	4	0
Pb	2	1	3	0	0	1	6	2	4
Zn	70	81	78	57	73	81	81	83	85
Cu	74	86	97	42	76	86	82	89	88
Ni	166	287	135	185	170	287	314	189	102
Cr	336	609	313	271	298	609	634	455	335
V	300	359	373	175	385	359	328	348	368
Ba	65	77	97	26	61	77	87	70	138
Hf	2	2	2	1	2	2	2	2	3
Ca	5	0	9	1	1	0	0	14	19
La	4	3	5	4	5	3	6	8	8

*Calculated Iron Ratios following Irvine and Barager (1971)

**

O.M.S-U. Outer Marginal Sub-Unit
 I.M.S-U. Inner Marginal Sub-Unit
 I.U. Intermediate Unit
 C.U. Central Unit

Table 5.1 cont.

5/174' I.M.S-U.	6/174' I.M.S-U.	7/174' I.M.S-U.	8/174' I.M.S-U.	9/174' I.M.S-U.	10/174' I.U.	11/174' C.U.	12/174' I.U.	54' C.U.	40'-1 C.U.	40'-2 I.U.
48.00	47.51	46.38	46.49	47.63	46.81	45.43	46.73	45.39	46.74	47.41
1.78	1.62	2.06	2.05	1.73	0.80	1.93	0.72	1.81	2.36	1.46
15.45	15.60	14.54	15.12	17.42	19.23	14.64	20.21	14.47	14.32	16.27
3.28	3.12	3.56	3.55	3.23	2.30	3.43	2.22	3.31	3.86	2.96
9.18	9.65	10.50	9.85	6.68	7.42	9.63	7.18	10.19	10.28	7.73
0.20	0.21	0.21	0.19	0.16	0.15	0.19	0.13	0.21	0.22	0.16
7.06	7.83	7.77	6.73	8.93	9.69	9.49	9.50	10.95	6.10	7.92
10.39	9.70	10.21	11.40	11.34	9.97	10.19	9.62	8.44	10.97	11.59
3.49	3.75	3.82	3.83	2.90	3.26	4.25	3.14	4.30	4.10	3.61
0.68	0.53	0.52	0.39	0.30	0.26	0.48	0.29	0.47	0.57	0.56
0.33	0.26	0.16	0.17	0.13	0.11	0.22	0.10	0.23	0.29	0.18
99.84	99.78	99.73	99.77	100.45	100.00	99.88	99.84	99.77	99.81	99.85
12.46	12.77	14.06	13.40	9.91	9.72	13.06	9.40	13.50	14.14	10.69
5	4	1	2	0	1	4	0	5	4	1
148	130	86	96	57	40	114	31	108	143	71
27	25	19	20	14	10	21	11	20	27	17
391	319	370	395	407	394	381	526	258	413	606
6	4	8	4	3	1	3	1	4	3	3
0	0	0	1	0	0	1	0	2	0	3
4	2	3	1	6	0	0	1	4	3	4
78	88	91	73	63	57	73	53	76	91	60
87	73	96	134	60	42	76	30	73	96	62
84	136	132	75	145	185	170	183	230	49	107
296	423	338	254	378	271	298	185	340	180	395
351	297	358	469	277	175	385	150	301	464	312
154	151	105	77	56	26	61	16	63	115	37
2	2	2	2	2	1	2	2	2	2	2
13	6	0	6	14	1	1	0	6	24	20
5	9	1	1	3	4	5	0	8	6	4

fill samplefill samplefill samplefill sample

1a	1b	1c	2
41.60	41.94	41.65	49.73
0.77	0.81	0.75	3.82
2.22	2.02	2.07	14.72
2.27	2.31	2.25	5.32
12.56	12.93	12.80	4.89
0.20	0.20	0.21	0.15
26.66	26.34	27.13	4.70
5.31	5.23	5.22	8.62
1.43	1.40	1.29	4.91
0.22	0.27	0.13	2.58
0.09	0.07	0.07	0.56
99.49	99.58	99.57	100.06
14.83	15.24	15.05	10.21
0	0	2	11
55	52	50	377
10	12	12	49
193	174	157	215
3	5	5	38
2	1	2	0
0	0	2	5
91	93	85	80
62	62	62	49
1102	1106	1116	56
1929	1961	2018	73
209	212	205	469
18	19	14	254
1	1	1	6
0	0	0	84
5	5	4	21

sill adjacent to the dyke (this study). Analyses of the sill complex from Gibson (1988) are shown in Table 5.2 for comparison.

The dyke has been affected by zeolite-facies hydrothermal burial metamorphism which has also affected the sills and lavas (Gibson 1990, Morrison 1978 and Thompson 1982). Wood et al (1976), Morrison (1977, 1978) and Morrison et al (1980) suggest that immobile incompatible elements are relatively less mobile in transitional basalts than in tholeiites. Ratios of the immobile incompatible elements are therefore considered to be substantially unaffected by hydrothermal alteration.

One transect of the dyke was selected to be analysed in detail: 174'. This was chosen as a large unweathered sample could be collected in an area displaying relatively simple banding. Figures 2.1, 2.2 and Plate 3.1 show the relationship of this sample to the banding in the dyke. A section from East to West includes:

Table 5.2

Whole-Rock Geochemistry: of the Trottarnish Sill Complex.					Whole-Rock Geochemistry: Sill adjacent to the dyke.			
(Gibson, 1988)					(Gibson, 1988)			
Rock type:	Ficrite	Ficro-dolerite	Crinanite	Pegmatite	0m above S.L.	2m above S.L.	13m above S.L.	
Wt%					Wt%			
SiO ₂	42.10	48.81	50.71	47.83	42.10	41.33	42.13	
TiO ₂	0.67	1.08	1.67	2.73	0.67	0.67	0.83	
Al ₂ O ₃	6.90	12.26	15.03	13.46	6.90	6.95	8.28	
FeO t	13.97	9.32	10.35	13.11	13.97	13.91	15.48	
MnO	0.22	0.16	0.19	0.22	0.22	0.22	0.22	
MgO	30.46	12.11	5.97	3.34	30.46	29.24	26.78	
CaO	4.25	12.32	12.21	8.94	4.25	4.34	5.94	
Na ₂ O	0.99	2.05	3.20	3.33	0.99	1.14	1.81	
K ₂ O	0.11	0.34	0.49	2.30	0.11	0.10	0.19	
P ₂ O ₅	0.07	0.10	0.19	0.50	0.07	0.08	0.09	
Total:	99.74	98.55	100.01	95.76	Total:	99.74	97.98	101.75
ppm					ppm			
Nb	2	3	5	6	Nb	2	n.d.	n.d.
Zr	102	80	129	302	Zr	41	43	52
Y	7	12	18	45	Y	7	7	8
Sr	108	275	320	436	Sr	108	121	192
Rb	13	13	17	53	Rb	13	12	11
Th	0	0	1	3	Th	0	n.d.	n.d.
Zn	102	80	119	118	Zn	102	97	93
Cu	74	64	77	290	Cu	74	76	67
Ni	1272	227	68	38	Ni	1272	1248	1116
Cr	2491	939	162	8	Cr	2491	2373	2091
V	175	296	297	339	V	175	174	198
Ba	26	87	180	420	Ba	26	28	36
La	6	7	11	26	La	6	7	7

key:
n.d. not determined.

Sill	EAST	
Band:		
1	2.8cms	Outer Marginal Sub-Unit.
	(The inner 2.6cms sampled.)	
2	2.6cms	
3	3.0cms	
4	3.4cms	Inner Marginal Sub-Unit
5	2.2cms	Total width: 24.77cms.
6	1.5cms	
7	1.9cms	
8	7.3cms	
9	3.1cms	
10	22.1cms	Intermediate Unit.
	(The outer 12.8cms sampled.)	
11	12.0cms	Central Unit.
	(The western 11.8cms sampled.)	
12	20.0cms	Intermediate Unit.
	(The eastern 5.5cms sampled.)	
	22.0cms	Marginal Unit.
	(No sample obtained.)	
Sill	WEST	

Details of the banding at 174' can be found in Chapters 2 and 3. The hand sample was divided into bands, which were then measured and sawn out using a rock cutting saw. These bands were processed as detailed in Appendix 5.1.

Samples were also analysed from 54' (Central Unit) and 40' (Intermediate Unit and "Central band"). Samples of the sill (Sill sample 1 being adjacent to the dyke at 105', in the middle segment of the dyke at distances of a) 0.5', b) 3' and c) 25' from the dyke, while sill sample 2 was obtained from the southern side of the cove at a distance of approximately 200' from the southern end of the dyke.

Based on the total alkali-silica diagram of Schwarzer and Rogers (1974), the dyke lies within the mildly alkaline series of alkaline rocks. On the simple

classification diagram of Middlemost (1980), bands lie within the sub-alkalic basalt and alkalic basalt fields, with many plotting in the transitional basalt field. In Irvine and Baragar's diagram (1971) the dyke lies within the alkali olivine basalt (sodic) series. Average trace element abundances for basalts are given by Taylor (1964) and Krauskopf (1967). The Mystery Dyke is relatively enriched in Ni, Cr and V, and relatively depleted in Nb, Zr, Rb, Ba and Ce. Rubidium is soluble in seawater, and may have been leached out, whilst zirconium is resistant to alteration and may be useful for petrogenetic purposes (Cox et al 1979).

The bulk rock chemistry of the dyke shows certain affinities with the typical picrodolerite and pegmatite analyses for the Trotternish Sill Complex of Skye, as shown in Table 5.2, and with the basalt compositions of the S.M.L.S. given by Thompson et al (1972 and 1980) in Table 5.3. Moorbath and Thompson (1980) stated that their samples of the S.M.L.S., including those from the Trotternish Peninsula, had been variably affected by regional zeolite-facies metamorphism.

There is chemical variation across the units of the dyke. Al_2O_3 shows highest concentration in the Intermediate Unit, with this unit also containing the least TiO_2 , FeO^t , CaO and K_2O of the four units. The Outer Marginal Sub-Unit contains relatively high FeO^t and MgO and relatively low SiO_2 and Al_2O_3 compared to the estimated bulk dyke composition. The Inner Marginal

Table 5.3

Major and Trace Element Data for the S.M.L.S.

Data from:

Thompson, Esson and Dunham (1972) and

Thompson, Gibson, Marrison, Mathey and Morrison

Rock type:	B	B	B or H?	B	B	B	B	B	H	B
Rock No.:	891	892	894	921	925	928	929	932	934	970
Wt %										
SiO ₂	46.80	48.01	46.15	45.05	45.19	46.73	46.83	44.89	47.94	46.82
TiO ₂	1.65	1.27	1.42	2.15	2.03	1.60	1.44	2.05	2.23	1.64
Al ₂ O ₃	14.57	15.59	13.72	14.01	13.51	14.59	14.90	16.04	17.07	15.92
FeO ^t	12.98	11.70	11.25	13.94	13.32	12.00	11.67	14.76	14.28	12.27
MnO	0.18	0.17	0.18	0.20	0.16	0.17	0.16	0.21	0.20	0.19
MgO	10.99	7.63	11.73	11.47	12.27	10.16	9.86	9.97	4.57	7.20
CaO	9.03	10.29	9.20	9.04	8.30	9.06	9.63	9.29	6.56	9.34
Na ₂ O	2.78	2.59	2.47	2.70	2.89	2.53	2.92	2.81	4.91	2.73
K ₂ O	0.40	0.62	0.55	0.35	0.37	0.38	0.44	0.22	0.77	0.45
P ₂ O ₅	0.19	0.17	0.19	0.23	0.22	0.16	0.17	0.20	0.37	0.22
ppm										
Nb	8	4	7	8	9	6	9	6	20	3
Zr	127	50	86	134	125	123	100	133	311	115
Y	18	22	15	19	21	23	20	26	45	27
Sr	379	95	382	443	548	505	1210	332	813	711
Rb	3	0	8	1	4	4	4	3	17	1
Th	1.03	0	0.51	0.87	0.81	0.36	0.53	0.55	1.37	0.28
Ba	0	0	133	0	0	0	0	49	0	177
Hf	4.02	1.75	2.29	3.4	3.27	2.48	2.78	3.74	8.15	3.03
Ca	30.45	0	19.81	25.89	27.04	17.96	22.74	20.72	52.33	24.81
La	10.59	5.87	0	0	0	6.97	9.47	0	22.52	0

*Rock type B=Basalt
H=Hawaiite

Sub-Unit is relatively enriched in SiO_2 , TiO_2 , Al_2O_3 and Na_2O and relatively depleted in MgO compared to the Outer Marginal Sub-Unit. The Intermediate Unit shows relative enrichment in Al_2O_3 and MgO , and relative depletion in SiO_2 , TiO_2 , FeO^t , and CaO compared to the Inner Marginal Sub-Unit. The Central Unit shows similarities with the geochemistry of the Outer Marginal Sub-Unit (with many elements including SiO_2 , Al_2O_3 , FeO^t , CaO and K_2O being of similar amounts), and compared with the Intermediate Unit is relatively enriched in TiO_2 , FeO^t and Na_2O and depleted in SiO_2 and Al_2O_3 .

Thompson et al (1972) state that all Skye basalts with iron/magnesium ratios less than 0.54 and the majority of basalts with ratios less than 0.6 contain only olivine as a phenocryst phase. The ratios for all the bands within the dyke are all in excess of 1.0, suggesting more than one phenocryst phase can be expected. Sill sample 1, however, has ratios less than 0.6, suggesting that only olivine should be present as a phenocryst phase.

The petrography described in Chapter 3 portrays the dyke as an alkali basalt due to the mineralogy of olivine, clinopyroxene and plagioclase feldspar. However, the common variation diagram "total alkalis- SiO_2 " (Figure 5.1) shows a scatter of compositions for the bands within the dyke, with no obvious trends.

- DYKE 17A
- O.M.S.U. = BAND 1
- ▲ I.M.S.U.
- △ I.U. = BAND 10
- ▽ C.U. = BAND 11

- SILL
- 1a
- 1b
- 1c
- 2

ETC BANDS

- GIBSON (988)
- P PICRITE
- D P/DOUGERITE
- C CRINANITE
- G PEGAMITE

- SILL ADJACENT TO DYKE
- 0 ON ABOVE SILL
- 0 22M ABOVE SILL
- 0 13 13M ABOVE SILL

FRANK
WELTON
FRACTIONAL
CRYSTALLIZATION

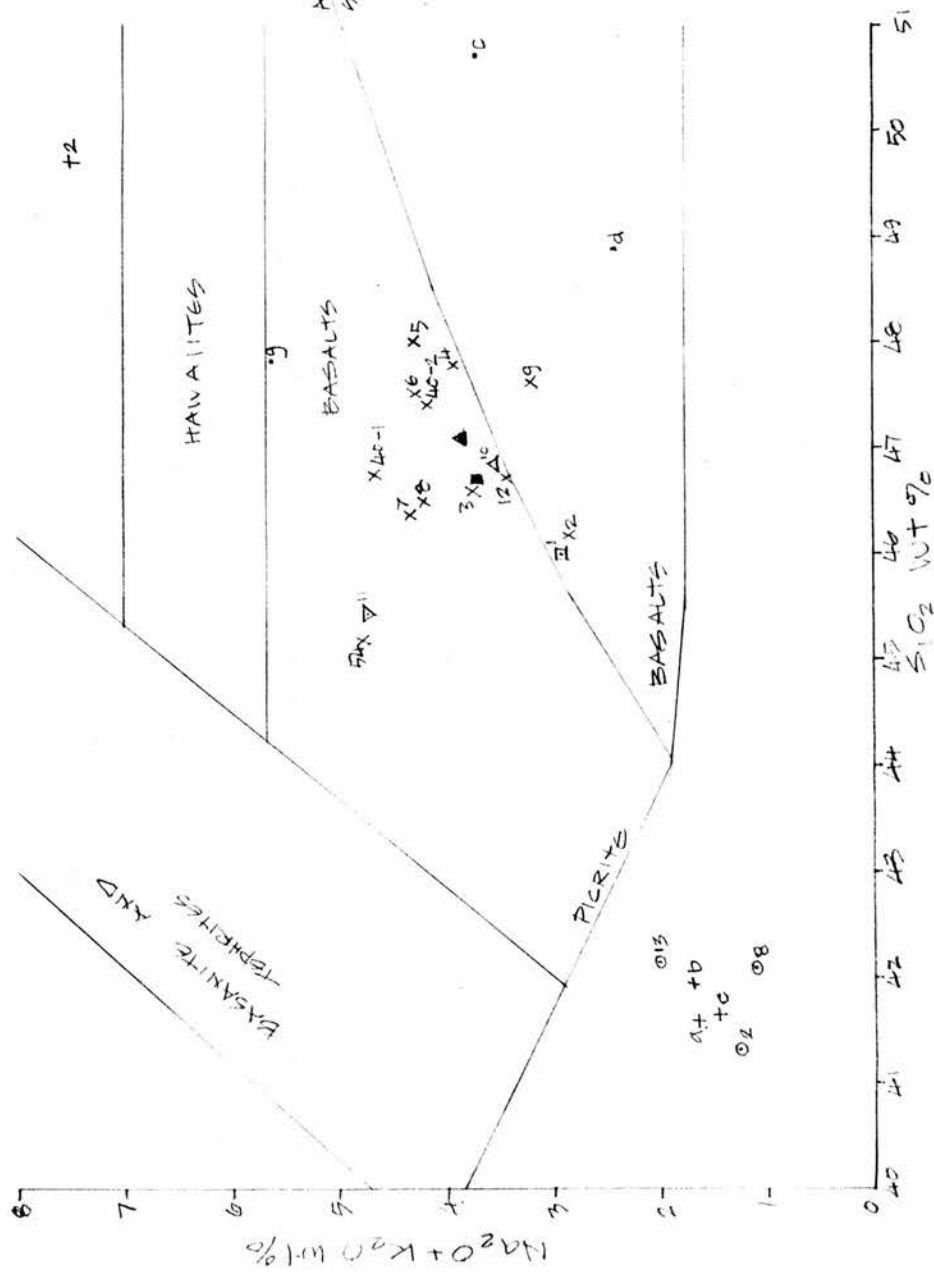


Figure 5.1 Total alkalis-SiO₂ Variation Diagram.

The 174' "dyke" sample lies within the basalt to picritic basalt fields in Figure 5.1. Sill sample 1 lies outwith the fields shown on the figure due to low SiO_2 and total alkali content. Sill sample 2 lies in the mugearite field, while the sill adjacent to the dyke (Table 5.2- Gibson 1988) plots close to the Sill 1 samples (this study). The typical analyses of picrite, picrodolerite, crinanite and pegmatite (Gibson 1988) are also shown.

The bands exhibit close correlation in the A.F.M. Diagram (Figure 5.2). Bands 1-8/174' show iron enrichment, Bands 9-10 magnesium enrichment and Bands 10-11/174' again exhibit iron enrichment. The sill samples lie removed from the dyke samples; Sill sample 1 lies on a trend from the dyke showing relative enrichment in MgO , Sill sample 2 shows no relation to the dyke and falls close to the mugearite field of Thompson et al (1972). The diagram also includes (Figure 5.2a) the area for analyses of the Skye lavas from Thompson et al (1972). These show a close major element correlation with the dyke samples. Figure 5.2b illustrates the area of analyses of the T.S.C. (Gibson 1988) together with selected other trends. The dyke lies within the area of picrodolerite-crinanite and stretches towards the pegmatite area of Gibson's data for the Trotternish Sill Complex (1988). These diagrams suggest a clear relationship between the dyke, Trotternish Sill Complex

and the Skye Main Lava Series. This will be discussed in greater detail later in this chapter.

The TiO_2 -Zr variation diagram (Figure 5.3) shows the dyke lying within both the tholeiitic and alkali fields as defined by Floyd and Winchester (1975). This was also the case for the T.S.C. as detailed by Gibson (1988), and the S.M.L.S. (Morrison 1978). As the S.M.L.S. contains both nepheline- and hypersthene-normative magmas, Morrison (1978) recommends the term "transitional basalts".

5.1 Major Element variation with distance across the dyke.

Figure 5.4. shows all major elements plotted against distance across the dyke and the computed "dyke" composition is marked on all figures. The half-transect of the dyke across Bands 1-11/174' will be discussed.

SiO_2

There is only slight variation in the silica content of the dyke varying from 45.4% in Band 11/174' to 48.0% in Band 5/174' and three groupings can be identified on Figure 5.4. Group A comprises of Bands 1-5/174' which have increasing SiO_2 content with distance into the dyke. Groups B and C (Bands 6-8/174' and 9-11/174')

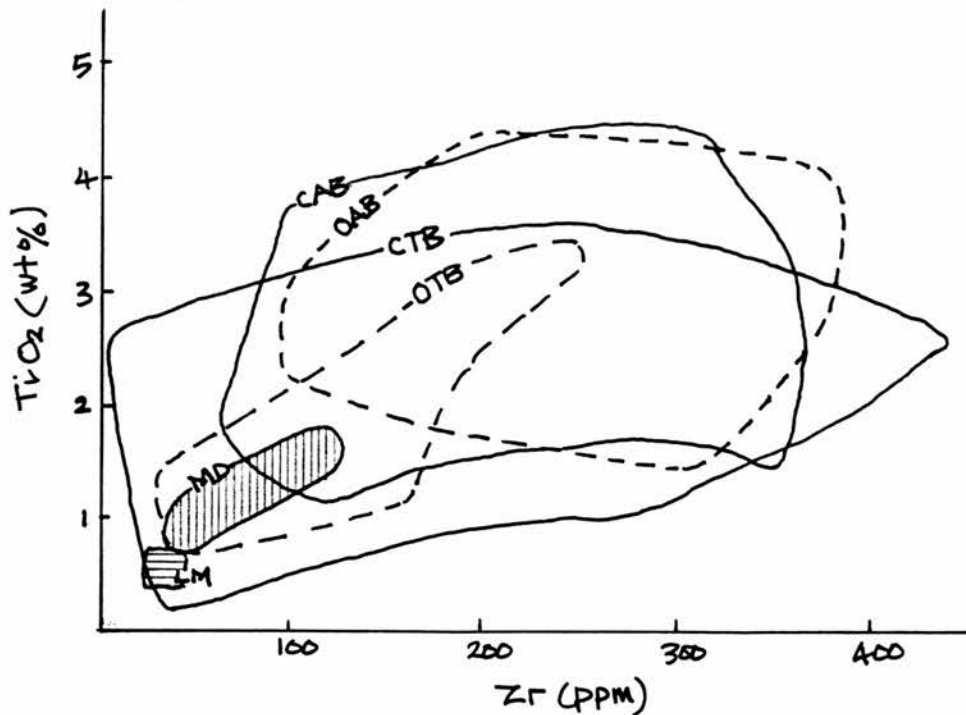
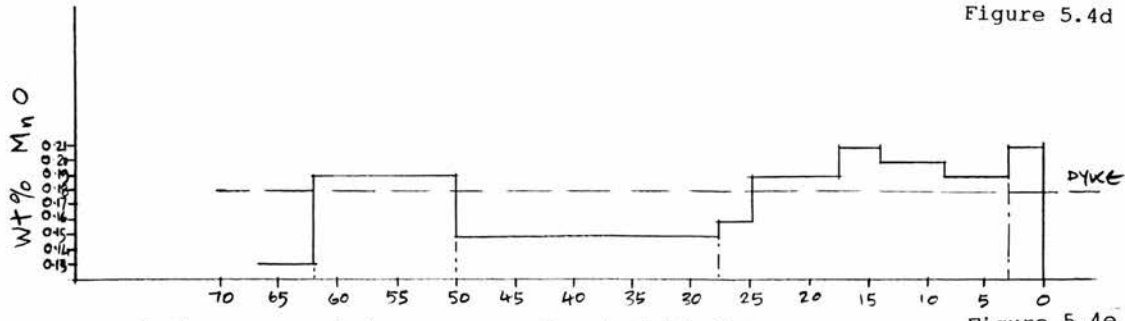
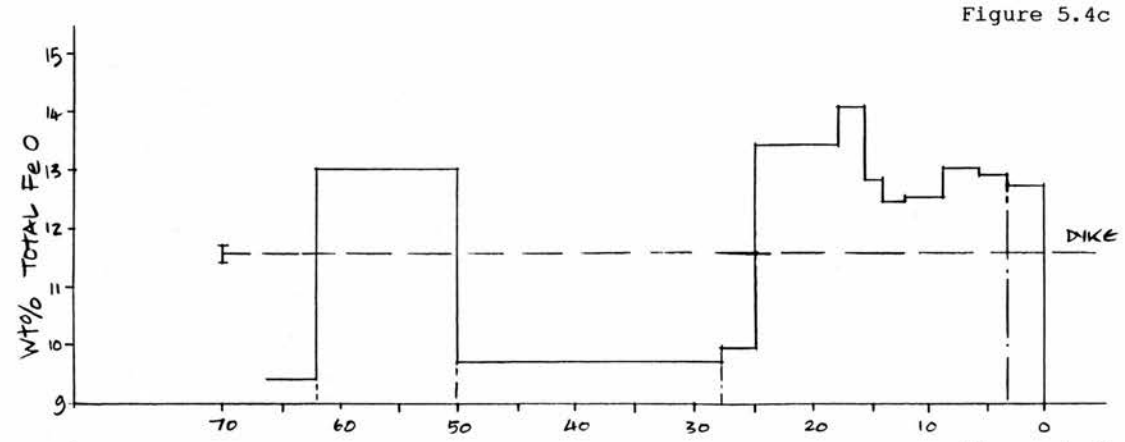
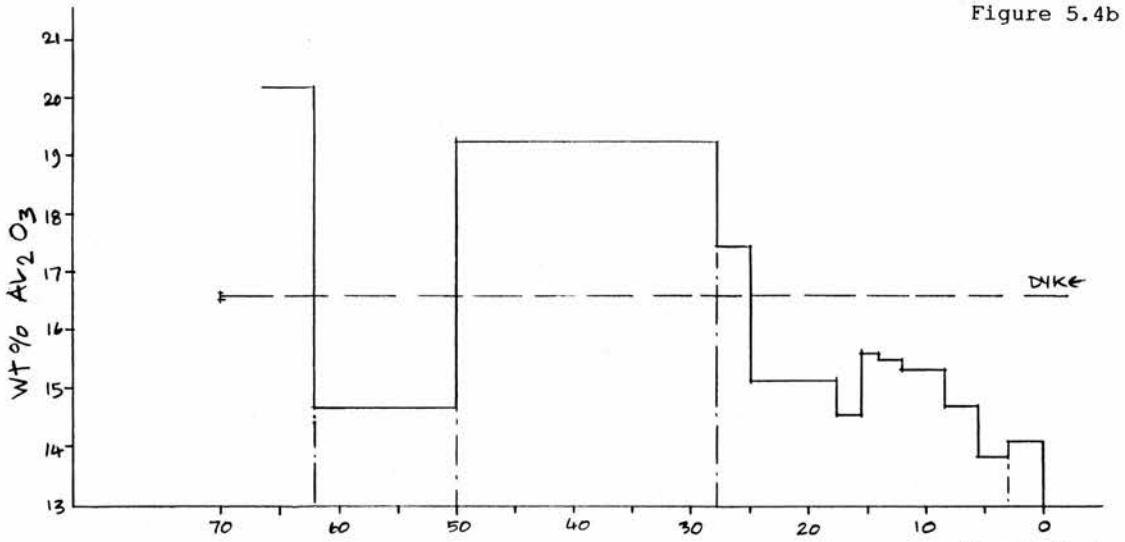
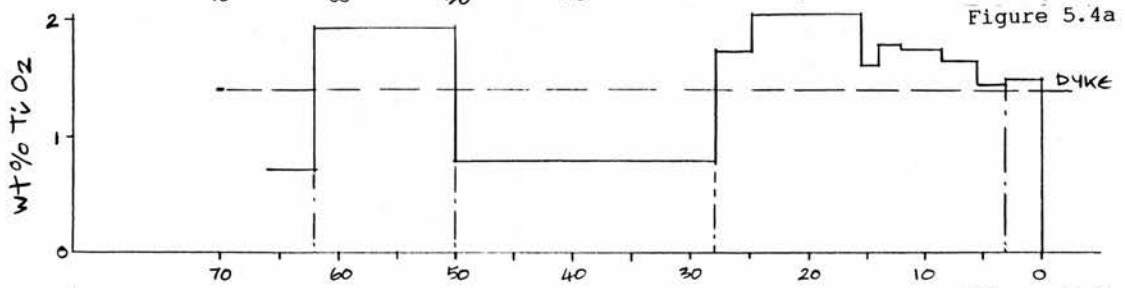
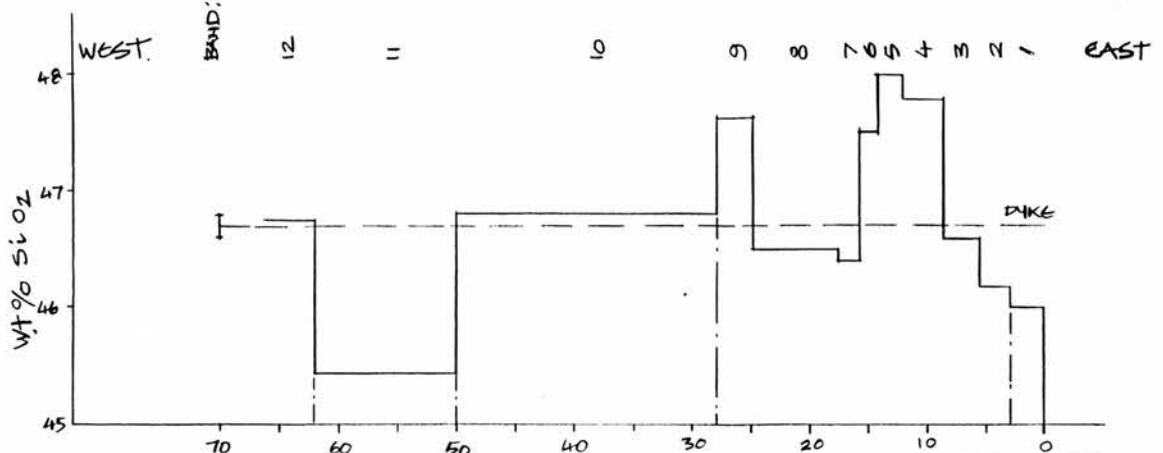


Figure 5.3 TiO₂-Zr Variation Diagram (from Floyd and Winchester, 1975)

- CAB - CONTINENTAL ALKALI BASALTS
- OAB - OCEANIC ALKALI BASALTS
- CTB - CONTINENTAL THOLEIITIC BASALTS.
- OTB - OCEANIC THOLEIITIC BASALTS
- MD - MYSTERY DIKE
- LM - LITTLE MINCH SILL COMPLEX.



DISTANCE IN CM'S FROM CONTACT WITH SILL

Figure 5.4 Major Element variation with distance across dyke.

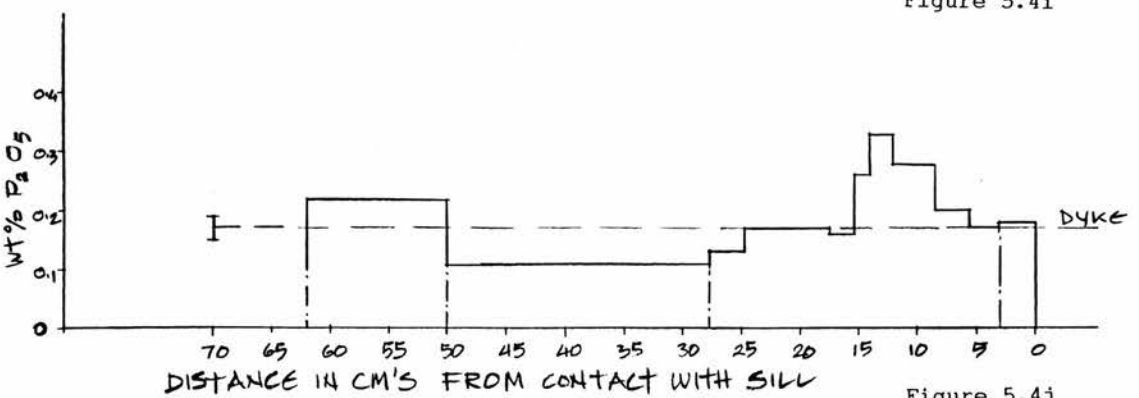
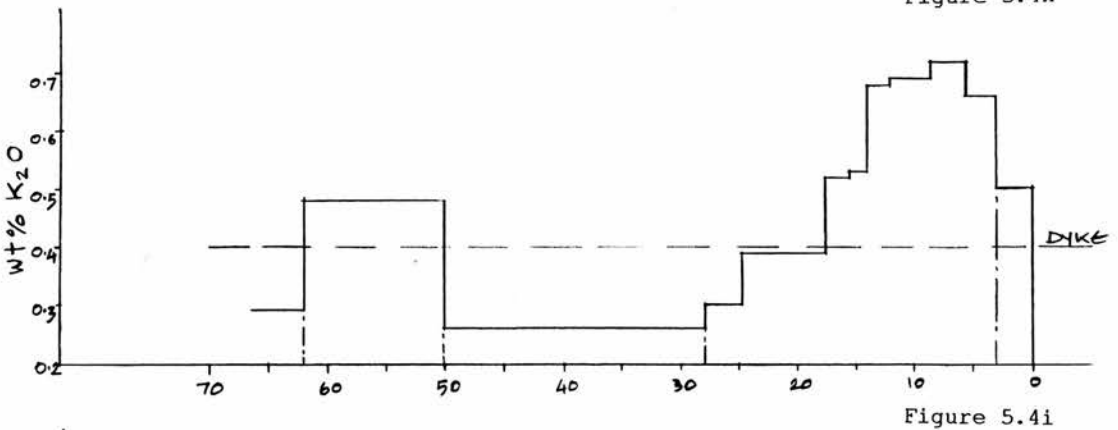
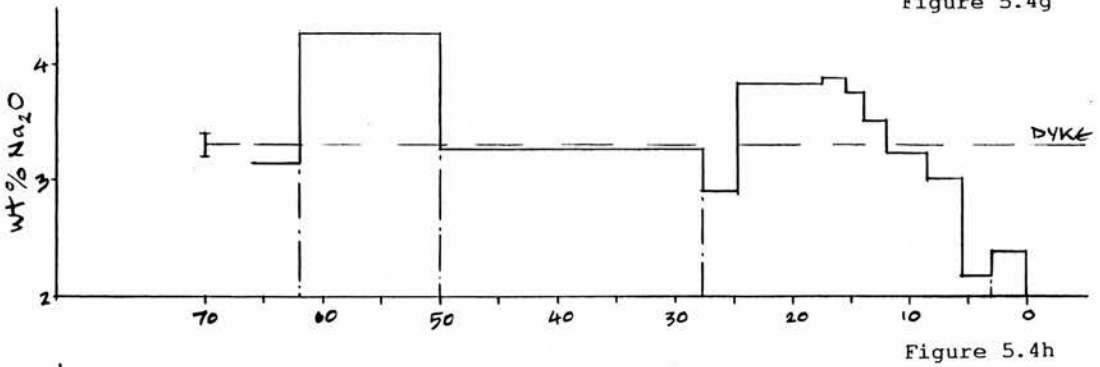
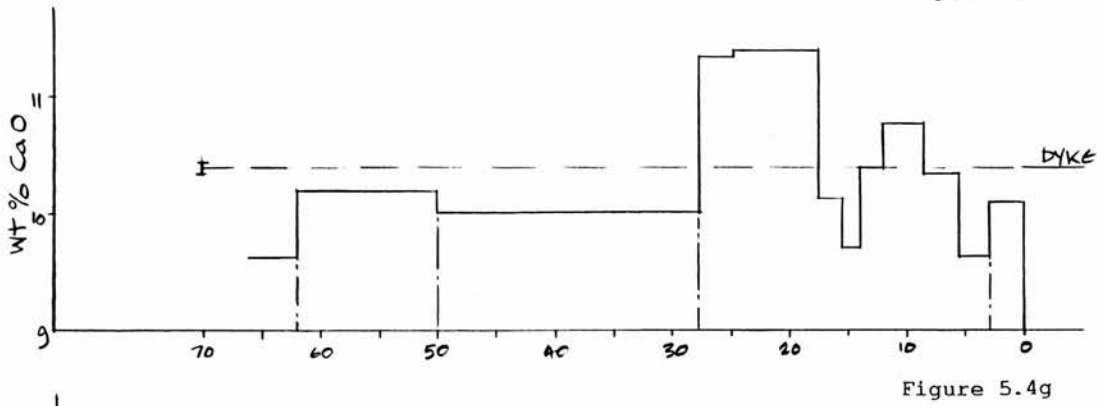
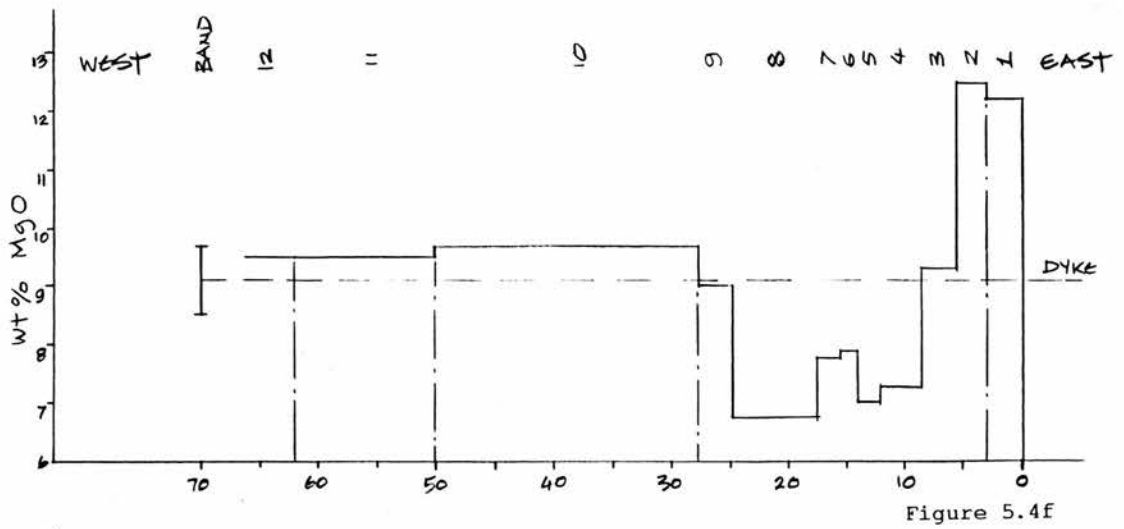


Figure 5.4 Major Element variation with distance across dyke. (cont)

respectively) both exhibit a decline in SiO_2 , with greater variation in Group C. Bands 4-6/174' and 9/174' are all relatively enriched in this element, whilst Bands 1,2 and 11/174' are relatively depleted.

Kennedy (1955) found that the precipitation of magnetite promoted SiO_2 enrichment; Bands 1-4/174' are enriched in opaque minerals and also exhibit an enrichment in SiO_2 . Bands 7-9/174' also show increasing SiO_2 which may indicate differentiation from primary magma to more evolved (silica-enriched) magmas was occurring across Bands 1-5 and 7-9/174'.

TiO₂

TiO₂ ranges from 0.7% to 1.7% in Bands 12/174' and 7/174' respectively. Four groupings are shown in Figure 5.4. Group A comprises Bands 1-5/174' inclusive, Group B: Bands 6-8/174', Group C: Bands 9-10/174', whilst Band 11/174' forms Group D.

Groups A and B exhibit enrichment, whilst Group C exhibits depletion. The Central Unit (Band 11/174') shows enrichment in this element compared to the Intermediate Unit. These groups closely relate to the total modal proportion of pyroxene (Figure 3.2), which increases across Bands 1-5/174'. Band 6/174' is relatively depleted in pyroxene and Bands 7-9/174' are relatively enriched. The Intermediate Unit contains little pyroxene or TiO₂, while the Central Unit contains proportionately more.

Al₂O₃

This oxide varies from 13.8% in Band 2/174' to 20.2% in Band 12/174'. Three groups can be highlighted in this transect. Group A consists of Bands 1-6/174' inclusive, Group B: Bands 7-10/174' and Group C: Band 11/174'. Group A shows increasing Al₂O₃ content inwards from the dyke margin, as does Group B, which shows a large variation in values from 14.5wt % to 19.2wt % Al₂O₃. Band 11/174' (Group C) is depleted in Al₂O₃ with regard to adjacent bands, containing approximately similar amounts to Band 7/174'.

Al₂O₃ is required by plagioclase, spinel and to a lesser degree by clinopyroxene. Modal plagioclase content (Figure 3.2) exhibits a similar pattern as that exhibited by Al₂O₃.

Total Iron

Iron is concentrated within olivine, spinel and pyroxene. The plot of Total Iron against distance across the dyke shows only slight variation (less than 5wt %). However, four groups have been identified. Bands 1-3/174', and 4-7/174' (Groups A and B) exhibit increasing iron. Group C (Bands 8-10/174') shows a decrease, whilst Band 11/174' (Group D) shows enrichment. The depletion of iron within the Intermediate Unit can not be explained modally, as Band 8/174' contains approximately similar amounts of total olivine and

pyroxene but contains significantly more total iron. Normative olivine is high within Band 10/174', although both the pyroxene and magnetite content are low.

MgO

Olivine and pyroxene also concentrate magnesium. Magnesium varies from 6.7wt % (Band 8/174') to 12.5wt % (Band 2/174') with three groups being identified on Figure 5.4. These contain the same bands as those described for SiO₂. Group A shows a decline in MgO but an increase in SiO₂, Group B in both cases shows a decline across the dyke, whilst Group C contains approximately constant amounts of MgO, and decreasing amounts of SiO₂.

CaO

There is only slight variation of CaO with distance across the dyke, with Bands 2 and 12/174' both containing the minimum (9.6wt %) and Band 8/174', the maximum (11.4wt %). Although concentrated in plagioclase feldspar and pyroxene, the irregular content of CaO across the dyke does not correspond to the modal plagioclase and pyroxene content variation previously identified (Figure 3.2). Band 1/174' forms Group A, whilst Bands 2-4/174' comprise Group B, which shows increasing CaO content and plagioclase and pyroxene content. Group C is made up of Bands 5-7/174', whilst Bands 8-9/174' form Group D. Group E contains Bands 10

and 11/174'. Groups B and D show increasing CaO whilst Groups C and D show decreasing CaO.

These selected plots of major element distribution with respect to distance across the dyke show common groupings. For a resume please see Table 5.10 in the Summary. These groups do not have consistent boundaries at specific bands, a feature which is investigated below.

5.2 Harker-type Plots of the Major Elements.

Due to restricted SiO_2 variation, MgO was taken as the abscissa. Wilson (1989) states that there are problems in using variation diagrams for phenocryst-rich rocks as the geochemical data does not actually represent the liquid magma composition. Bands 1-4 and 11/174' are all phenocryst-rich. Coherent trends on Harker Diagrams indicate chemical evolution. With the exception of K_2O -MgO and P_2O_5 -MgO, there are persistent groupings of bands in Figures 5.5a-i. Bands 1 and 2/174' plot together, Bands 4-8/174' lie together although Bands 7 and 8 may be slightly removed eg FeO-MgO and Bands 3 and 11/174' form a third group. Band 9/174' is frequently associated with Bands 10 and 12/174'. Table 5.10 in the Summary highlights the groupings of the bands.

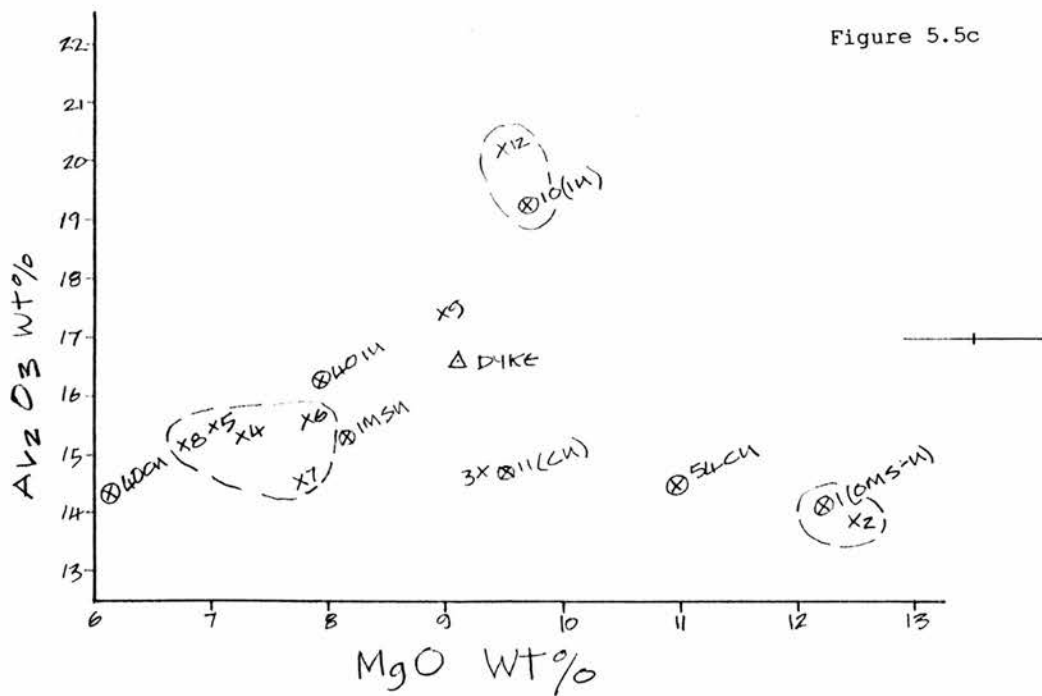
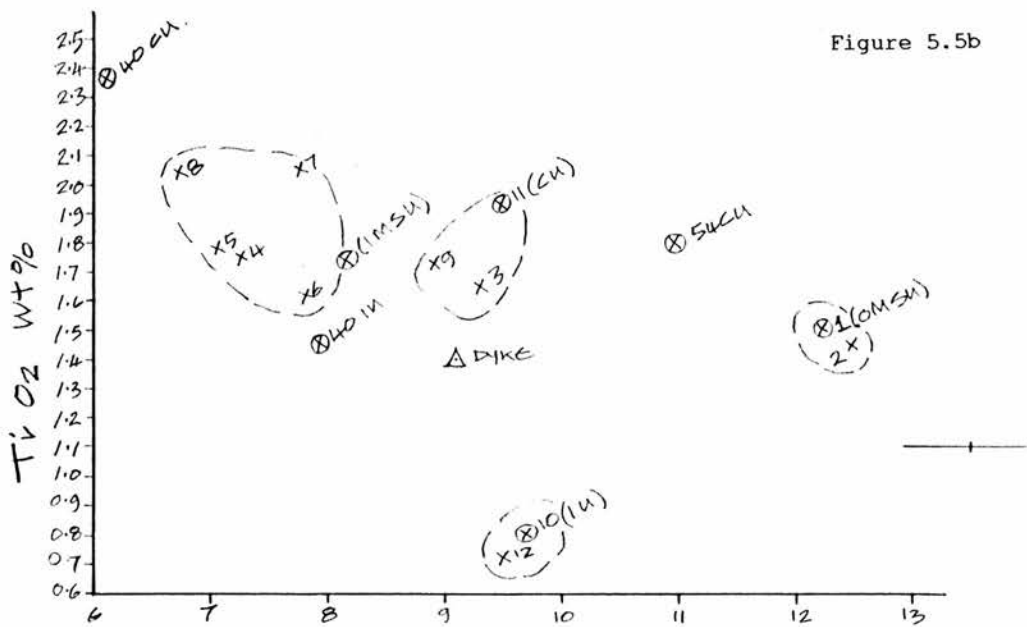
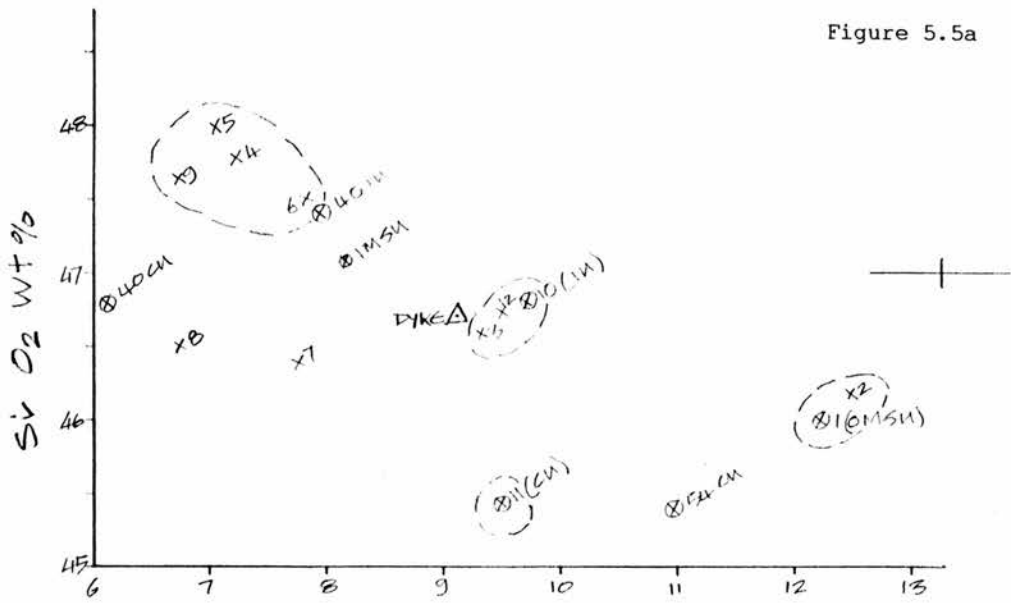


Figure 5.5

Figure 5.5d

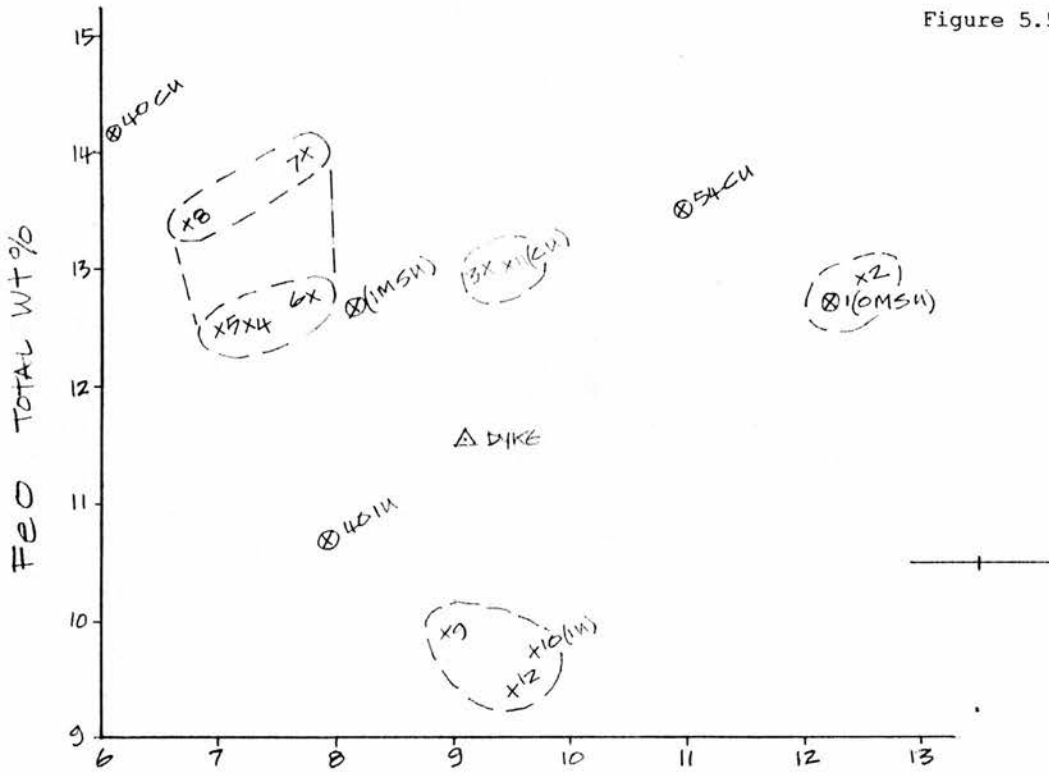


Figure 5.5e

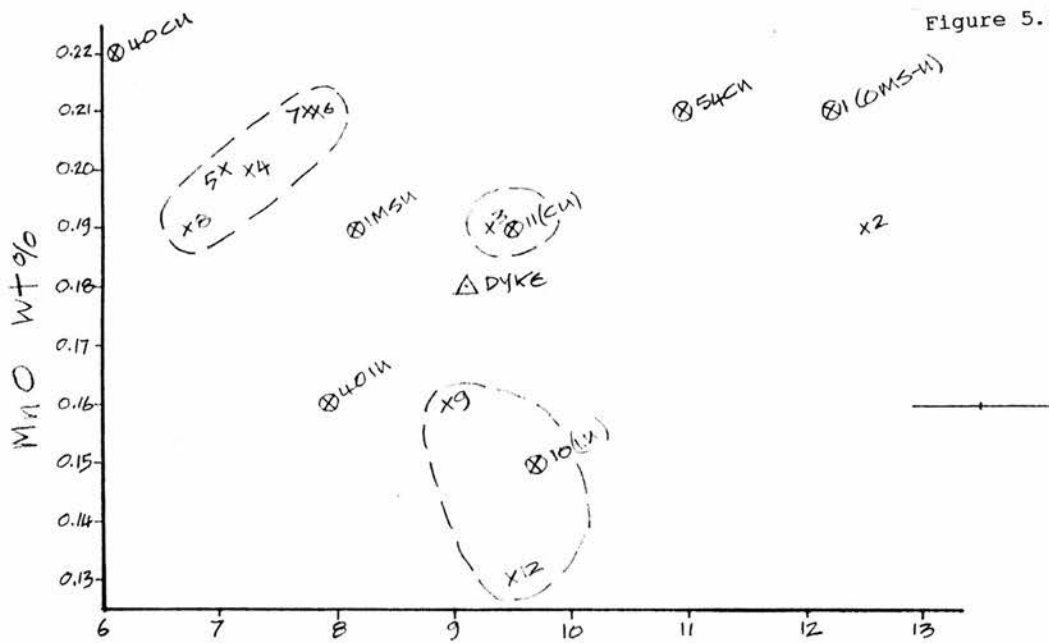


Figure 5.5f

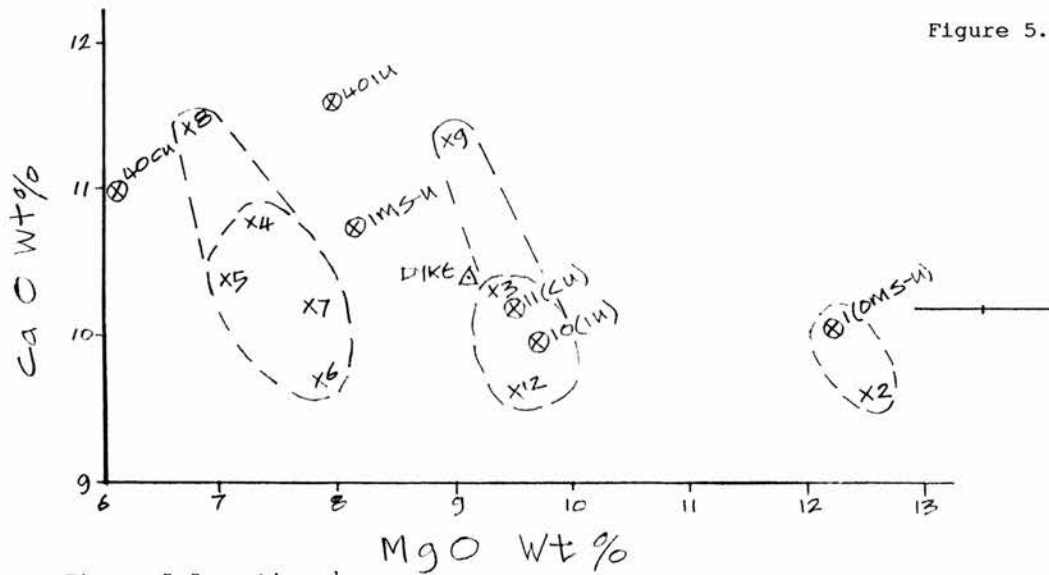


Figure 5.5 continued

Figure 5.5g

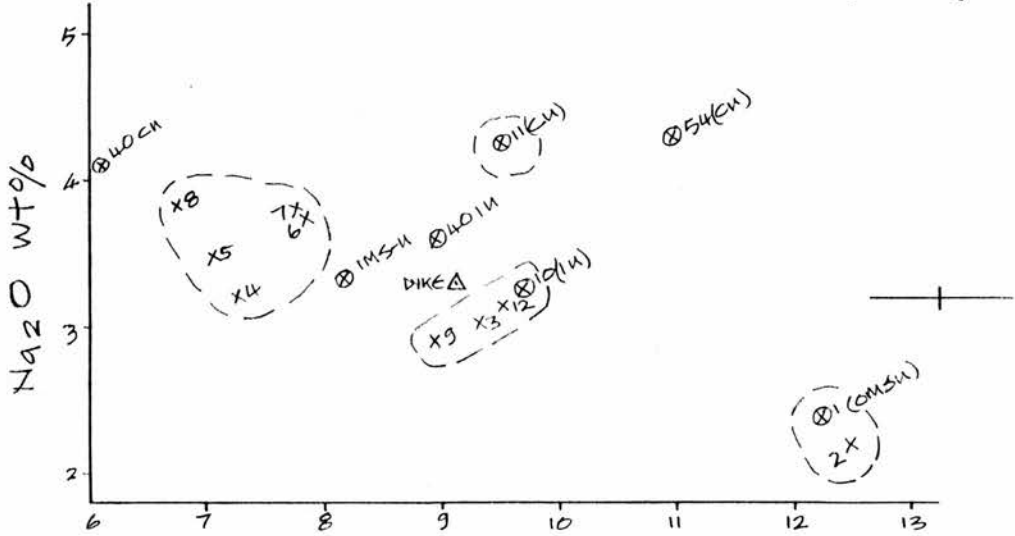


Figure 5.5h

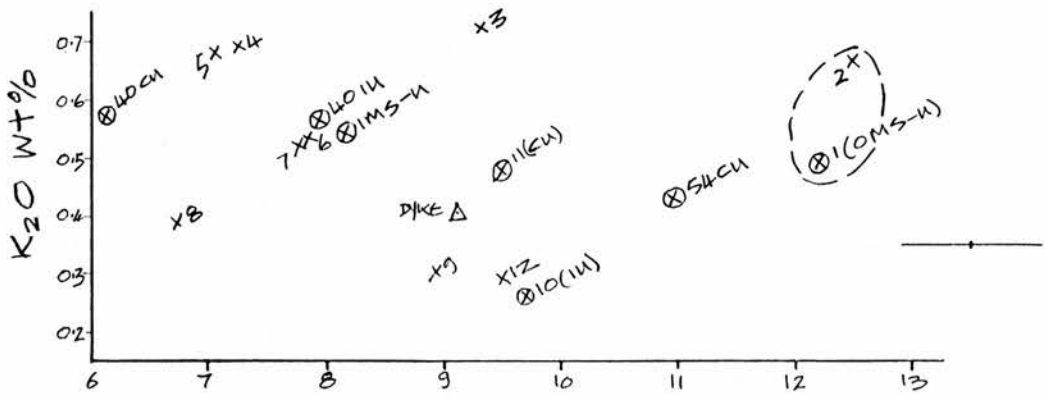


Figure 5.5i

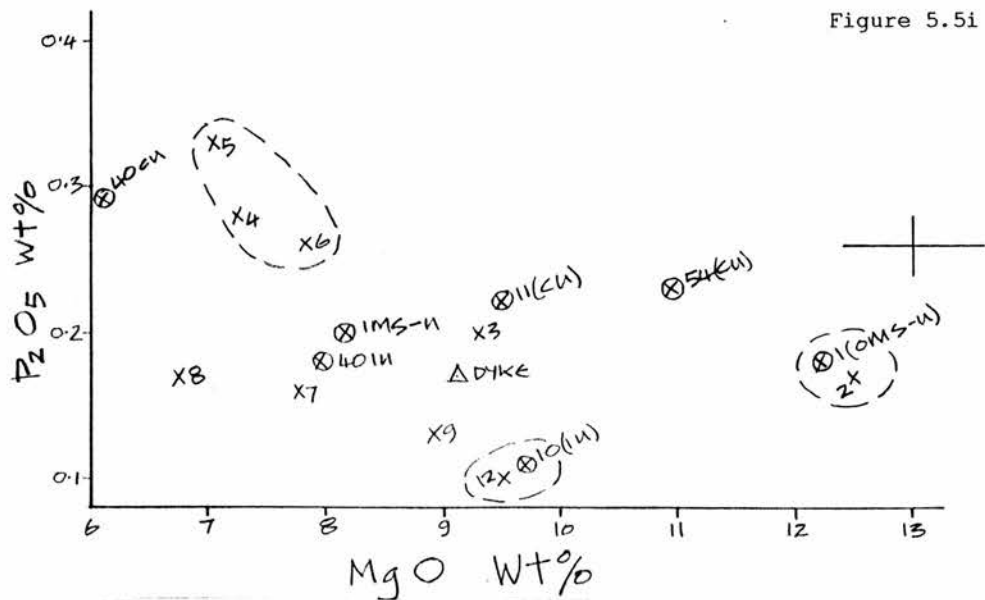


Figure 5.5 Harker Diagrams of Major Elements.

5.5a SiO₂/MgO

5.5b TiO₂/MgO

5.5c Al₂O₃/MgO

5.5d FeO^t/MgO

5.5e MnO/MgO

5.5f CaO/MgO

5.5g Na₂O/MgO

5.5h K₂O/MgO

5.5i P₂O₅/MgO

5.3 Trace Element Variation with distance across the dyke.

Several trace elements exhibit no obvious patterns across the dyke or the bands do not contain sufficient concentrations to allow discussion on the element. Elements considered in this section are Zr, Sr, Ni, Cr, V and Ba. The "dyke" concentration of each trace element is plotted on Figure 5.6 as a reference content. Table 5.10 details possible band groupings.

Zirconium

The concentration of Zr within the dyke transect varies from 31ppm in Band 12/174' to 148ppm in Band 5/174'. Four groups can be identified in Figure 5.6. Group A comprises of Bands 1-5/174' inclusive, Group B: Bands 6-7/174', Group C: Bands 8-10/174' whilst Group D is composed of Band 11/174'. This element is concentrated within magnetite and spinel minerals.

Group A exhibits a range of c70ppm showing an increase in Zr across Bands 1-5/174'. This trend is reversed in Group B, where the concentration of Zr in Band 7/174' falls to approximately that of Band 1/174' (also equivalent to the "dyke" concentration). Although Band 8/1174' exhibits a slight increase the depletion continues to Band 10/174' (The Intermediate Unit). Band 11/174', the Central Unit contains concentrations of Zr in excess of the dyke values. The concentrations of Zr

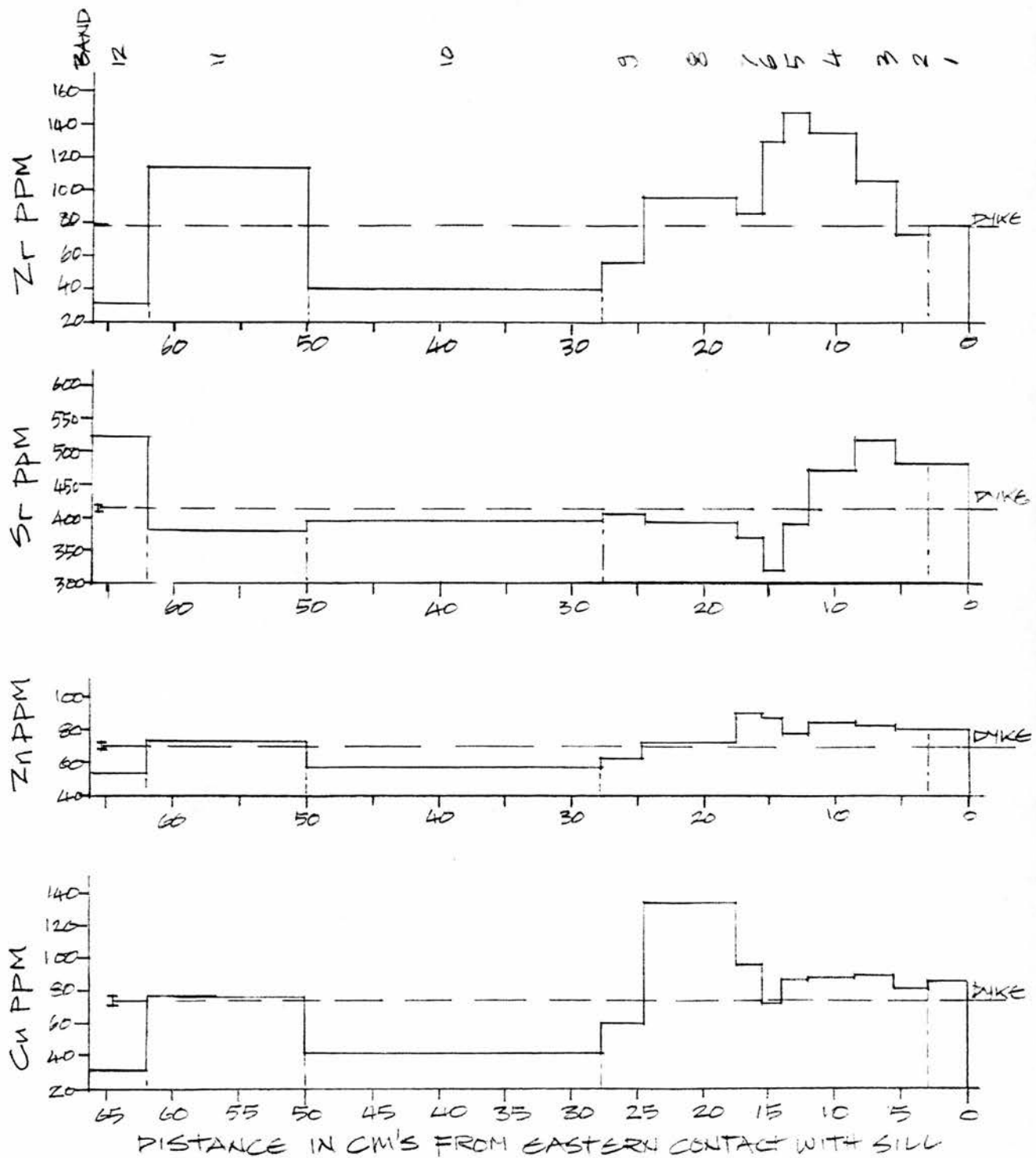


Figure 5.6 Trace Element variation with distance across the dyke.

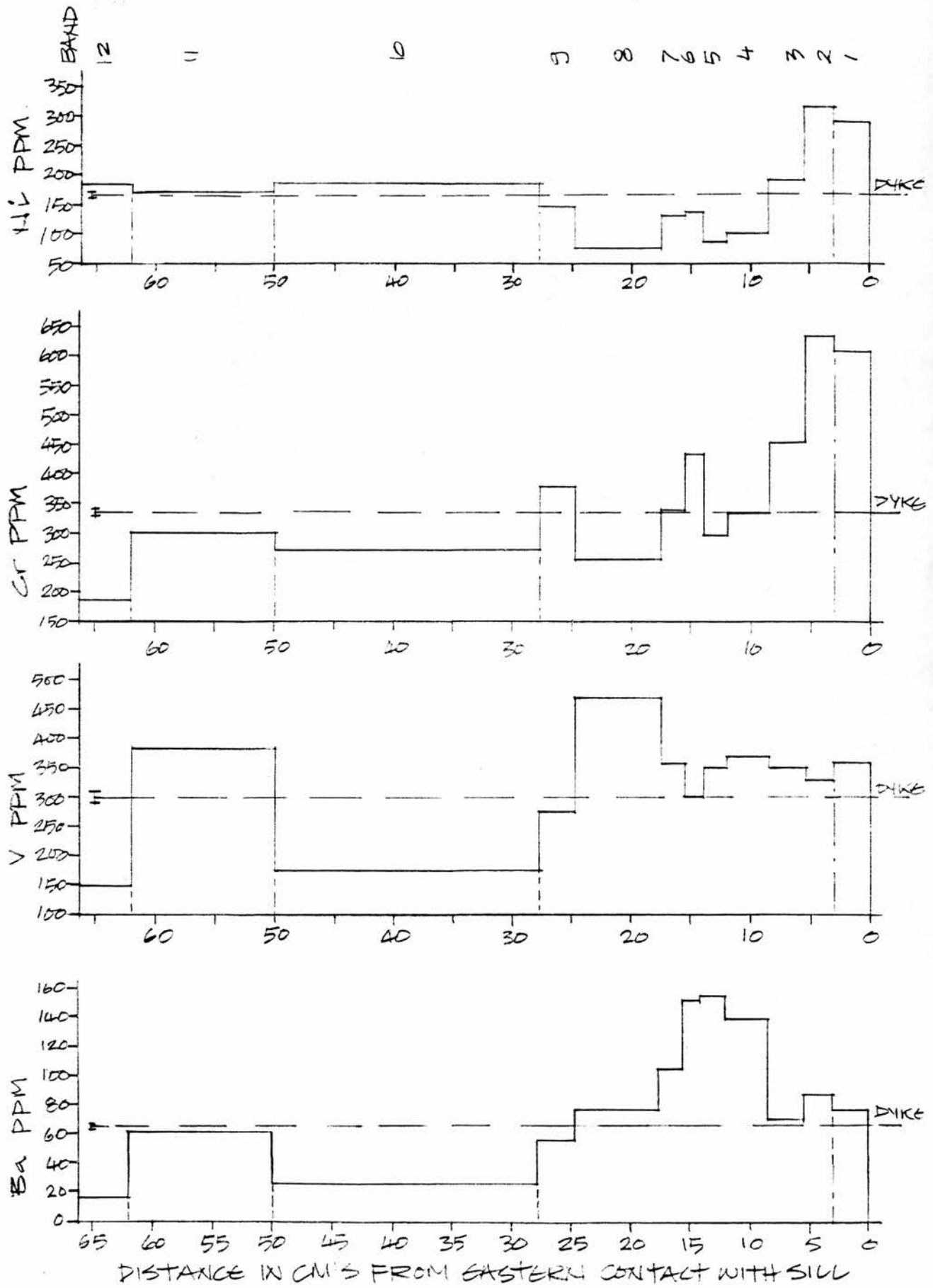


Figure 5.6 continued

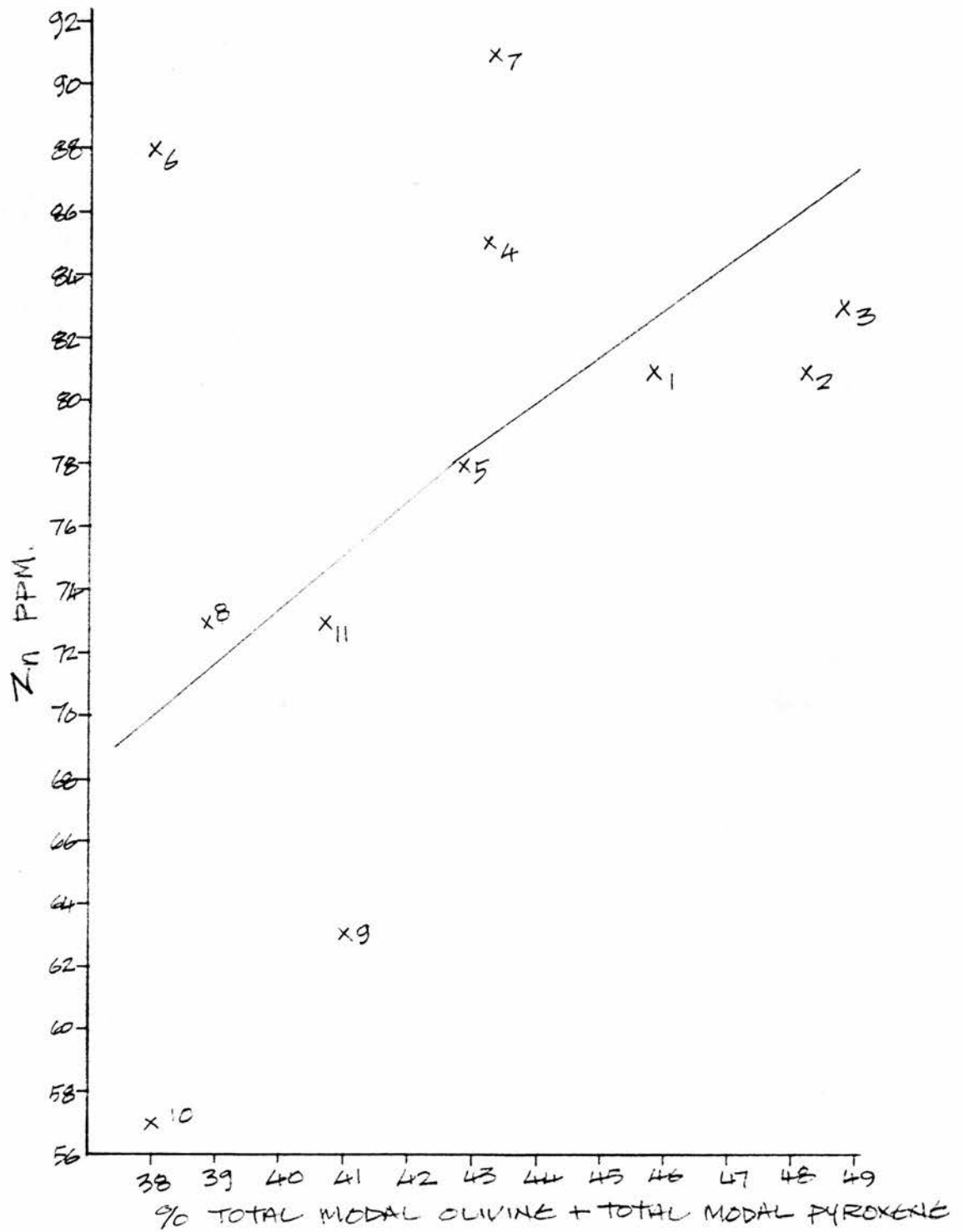


Figure 5.7 Zinc-Total Olivine+Pyroxene variation Diagram.

correlate closely with modal opaque content. The Zr content of the sill complex (Table 5.2) are comparable, but with the lavas having a slightly higher content (Table 5.3).

Strontium

Sr varies from 319ppm within Band 5/174' to 526ppm within Band 12/174'. This trace element is concentrated by plagioclase feldspar and, to a lesser extent, by magnetite. Three possible groupings are exhibited by strontium with distance across the dyke.

Group A contains Bands 1-3/174', Group B: Bands 4-6/174' and Group C: Bands 7-11/174'. Group A contains Sr in excess of the "dyke" concentration. Group B exhibits decreasing concentration of Sr, the reverse of modal and normative content of plagioclase. Group C shows little variation with distance across the dyke to the Central Unit, with all bands containing less than the "dyke" concentration of the element. This is not reflected in the modal concentration of plagioclase of Bands 8-10/174' and normative plagioclase of Bands 9-10/174'. Band 12/174' is enriched in Sr in comparison with Band 10/174' with the 130ppm variation being an unusual feature, as is the Central Unit (Band 11/174') plotting with Band 10/174'. This diversity across the Intermediate Unit reflects modal plagioclase variation from the outer contact (with the Inner Marginal Sub-Unit) to that with the Central Unit.

Nickel

This element varies from 75ppm in Band 8/174' to a maximum of 314ppm in Band 2/174'. Nickel is incorporated predominantly in olivine. Modal and normative olivine and Ni content per band exhibit covariation. Four groupings are shown on Figure 5.6. Group A is composed of Bands 1-2/174', which contain high amounts of Ni and olivine, Group B is formed by Bands 3-5/174' which show decreasing amounts of nickel and olivine. Bands 6-8/174' (Group C) contains decreasing amounts of Ni and olivine after an initial content in excess of Band 5/174'. Group D contains Bands 9 to 11/174', with Band 10/174' containing the greater amount of nickel and olivine (both normative and modal) of the bands within this group. The observed decreasing Ni content of Bands 2-5 and 6-8/174' suggest olivine fractionation could have been a mechanism of magma evolution for them (Cox et al 1979).

Chromium

Chromium values vary from 185ppm in Band 12/174' to 634ppm in Band 2/174'. Cr is concentrated in clinopyroxene and spinel minerals. Four groups are depicted in Figure 5.6. Group A includes Bands 1 to 5/174', which show decreasing Cr with distance across the dyke. Group B shows decreasing Cr across Bands 6 to 8/174', whilst Group C is composed of Bands 9 and 10/174', and Group D of Band 11/174'. There is a

general decline in Cr content across the dyke from margin to centre, with the exception of Bands 6 and 9/174'. Band 6/174' contains relatively low amounts of modal pyroxene and olivine. Normative opaques and pyroxene are relatively high for Band 6/174'. Band 9/174' contains a relatively high amount of modal pyroxene, but only equivalent to the "dyke" content of normative pyroxene.

Groups A and B show positive covariation with modal and normative olivine content-probably due to enclosed oxides in the olivines. Groups C and D show a positive correlation with the modal pyroxene content of Bands 9-12/174'. Bands 10 and 12/174' (the Intermediate Unit) exhibit variation in Cr content; the area in close contact to the Central Unit containing less Cr than the area further from the Central Unit. There is no significant variation in the total olivine+pyroxene+spinel for Bands 10 and 12/174'. Cox et al (1979) state that decreasing chromium suggests spinel and/or clinopyroxene fractionation. Bands 2-5, 6-8 and 9-10/174' show such a trend suggesting fractionation of clinopyroxene and/or spinel as a possible mechanism.

Vanadium

Vanadium varies from 150ppm (Band 12/174') to 469ppm (Band 8/174') and is preferentially concentrated by pyroxene. Three groupings are identified in Figure 5.6. Group A contains Bands 1 to 7/174', which exhibit little

variation in V content. Band 7/174' is equal to the "dyke" concentration of V, with all other bands containing in excess of the "dyke" concentration. Group B exhibits decreasing vanadium across Bands 8-10/174'. Band 10/174' shows a positive covariation between low pyroxene content and relatively low amounts of vanadium. Band 11/174', the Central Unit forms Group C, which contains relatively high amounts of V and pyroxene.

Barium

Ba variation within the dyke ranges from 16ppm to 154ppm in Bands 12 and 5/174' respectively. The trend shown in Figure 5.6 is similar to that exhibited by Zr and Y. Plagioclase preferentially concentrates barium within its crystal structure. Four groups are identified: Group A contains Bands 1 and 2/174'; Group B-Bands 3-5/174', with both of these groups showing increasing Ba across the dyke. Bands 6-10/174' (Group C) show decreasing barium, and Band 11/174' forms Group D. The trend in Group C does not agree with the trends shown by normative plagioclase content (Figure 5.9). Bands 5 and 6/174' both contain high amounts of modal and normative plagioclase and Ba, although the Intermediate Unit (Bands 10 and 12/174') also contains relatively high amounts of modal and normative plagioclase but low amounts of Ba, suggesting that other factors have influenced the concentration of this trace element.

5.4 Harker-type Plots of the Trace Elements.

Harker-type plots, using MgO as abscissa were produced for Zr, Sr, Zn, Cu, Ni, Cr, V and Ba (Figure 5.8a-h).

With the exception of Sr, Cr and Ni against MgO there are persistent groupings in Figures 5.8a-h (similar to those described for the major elements- Table 5.10). Bands 1 and 2/174' form one group as do Bands 3 and 11/174'. A third group is composed of Bands 4-8/174', although Bands 7 and 8/174' may form a sub-group slightly removed from the remainder eg Zr and Ba (Figures 5.8a and 5.8h). Bands 10 and 12/174' plot together in all figures but Sr-MgO (Figure 5.8b). Band 9/174' is associated with Bands 10 and 12/174' for Sr, Zr, Zn and Cu and with Bands 3 and 11/174' for Ba, V, Ni and Cr.

Prinz (1968) stated that trace elements including Ba, Cu, Rb, Sr, Y, V and Zr increase and Cr and Ni decrease with differentiation. Zr exhibits an increase across Bands 1-4 as does Rb. Y increases across Bands 1-5 while the amount of Sr increases across Bands 1-3 and 6-10. Ni and Cr both decrease across Bands 1-5 and 6-8. These consistent trends show that the dyke is differentiated across the outer bands of the dyke and possibly across Bands 6-8 or 10.

Figure 5.8a

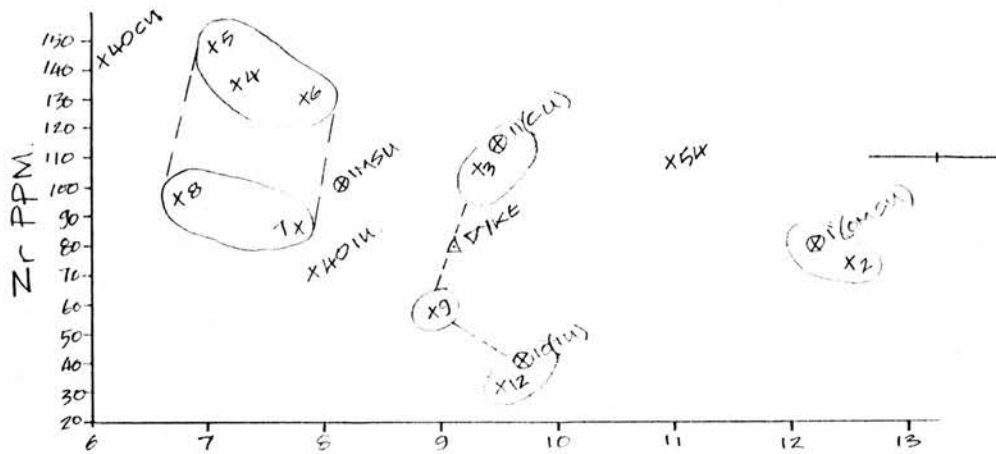


Figure 5.8b

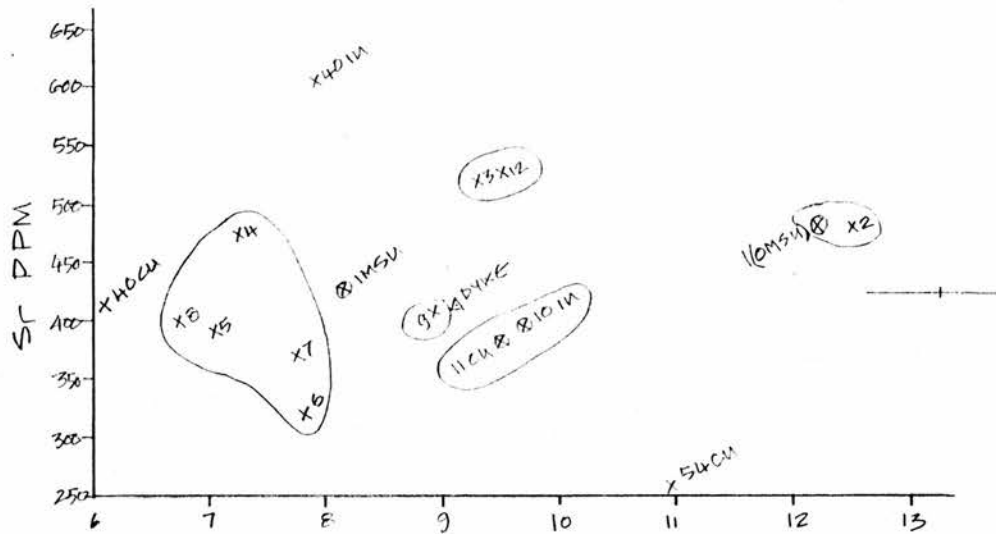


Figure 5.8c

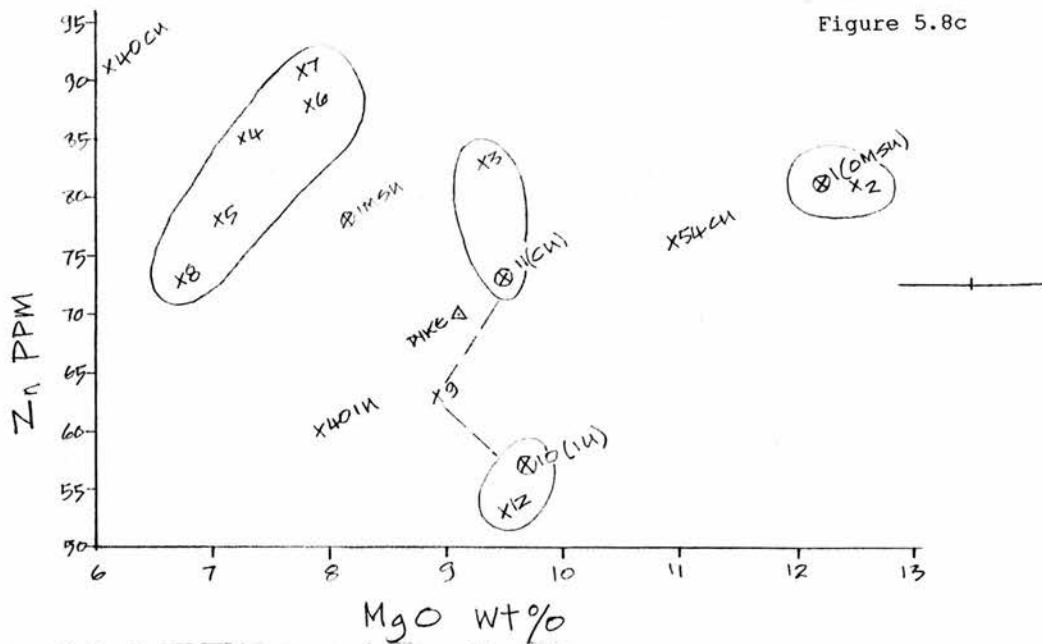


Figure 5.8 Harker Diagrams of Trace Elements.

- 5.8a Zr/MgO
- 5.8b Sr/MgO
- 5.8c Zn/MgO
- 5.8d Cu/MgO
- 5.8e Ni/MgO
- 5.8f Cr/MgO
- 5.8g V/MgO
- 5.8h Ba/MgO

Figure 5.8d

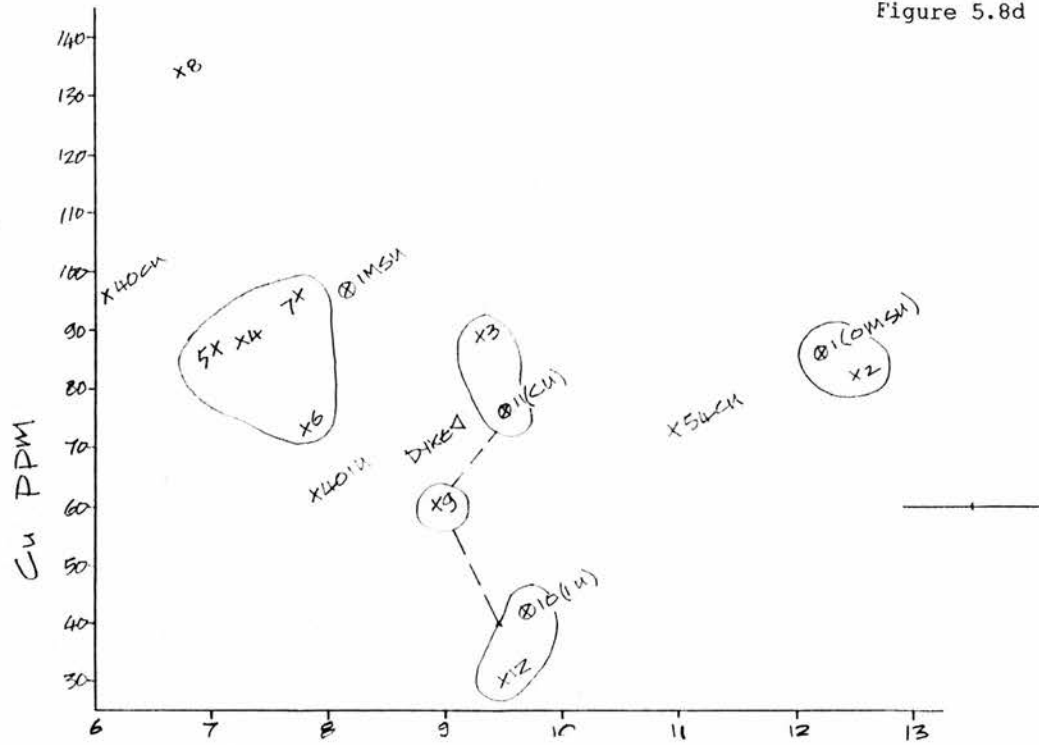


Figure 5.8e

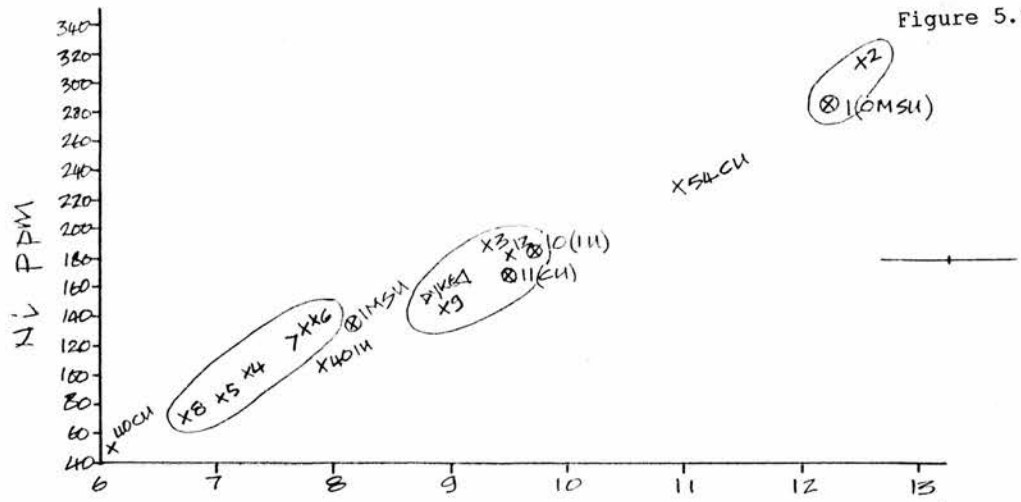


Figure 5.8f

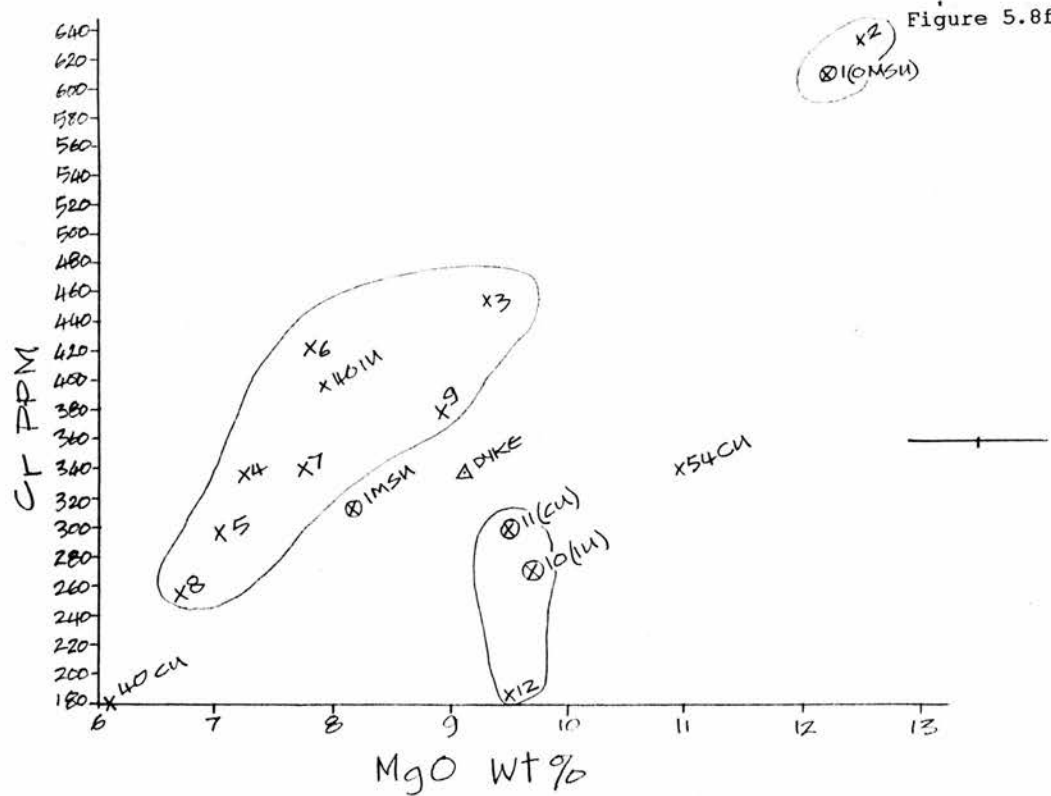


Figure 5.8 continued

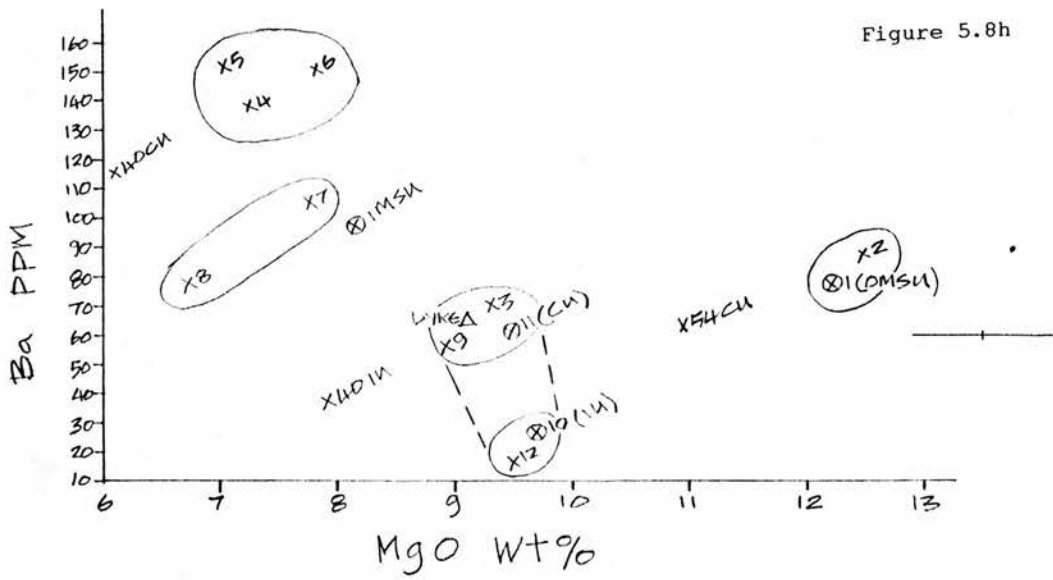
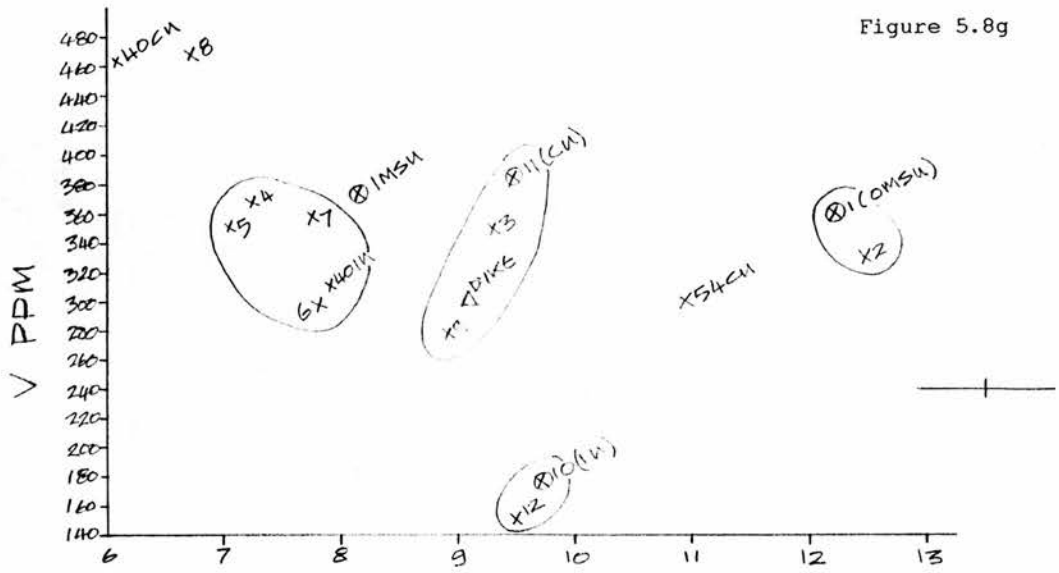


Figure 5.8 continued

5.5 Normative Mineralogy of the Dyke.

The norms of Bands 1-11/174' and the "dyke" composition were calculated using a H₂O- and zeolite-free whole-rock geochemistry (Table 5.4), and the NORM programme of MacGPP by Geist, McBirney and Baker (1982). Table 5.5 and Figure 5.9 show the results. Table 5.10 details persistent band groupings. The zeolite-free whole-rock geochemistry was used to reduce the influence of the chemical composition of this late-forming mineral. The volume of zeolite per band was calculated and its density taken as 2.3, compared to the density of dolerite of 3.0. The zeolite content was then removed from the band composition, which was recast to 100%.

Total Normative Plagioclase.

This varies from 35.2% to 61.4% in Bands 11 and 10/174' respectively. Four groups have been highlighted in Figure 5.9. Normative total plagioclase content mirrors the modal plagioclase content.

Normative Diopside.

This shows a variation from the minimum in Band 10/174' of 8.1% to the maximum of 27.2% in Band 8/174', with Figure 5.9 showing five groups. Generally, those bands relatively enriched in modal pyroxene are relatively enriched in normative diopside.

Table 5.4

Whole-Rock Geochemistry of the Dyke and Sill, calculated
for a Dry, Zeolite-free sample with Calculated Iron Ratios*

Band:	174'	174'	174'	174'	174'	1/174'	2/174'	3/174'	4/174'
**Unit:	Dyke	O.M.S-U.	I.M.S-U.	I.U.	C.U.	O.M.S-U.	I.M.S-U.	I.M.S-U.	I.M.S-U.
Wt%									
SiO ₂	46.64	45.98	46.98	46.81	45.29	45.98	46.25	46.49	46.63
TiO ₂	1.44	1.53	1.79	0.84	2.01	1.53	1.48	1.76	1.70
Al ₂ O ₃	16.07	13.78	14.74	18.80	13.80	13.78	13.47	13.38	14.21
Fe ₂ O ₃	3.06	3.05	3.42	2.38	3.58	3.05	3.02	3.37	3.24
FeO	8.92	9.89	9.66	7.49	10.04	9.89	10.18	10.55	10.14
MnO	0.18	0.21	0.19	0.14	0.20	0.21	0.19	0.20	0.20
MgO	9.53	12.43	8.41	9.99	9.90	12.43	12.76	9.96	9.58
CaO	10.26	10.04	10.65	9.89	10.06	10.04	9.58	10.16	10.29
Na ₂ O	3.42	2.41	3.39	3.27	4.38	2.41	2.21	3.15	3.08
K ₂ O	0.44	0.50	0.55	0.27	0.50	0.50	0.67	0.77	0.74
P ₂ O ₅	0.18	0.18	0.21	0.12	0.23	0.18	0.17	0.21	0.21
Total:	100.14	100.00	99.99	100.00	99.99	100.00	99.98	100.00	100.02
Total Fe	11.98	12.94	13.08	9.87	13.62	12.94	13.20	13.92	13.38
Wt% Zeolite removed	2.60	1.88	3.07	3.38	4.89	1.88	2.25	7.50	3.00

*Calculated Iron Ratios - Droop (1987)

**Unit:

O.M.S-U. Outer Marginal Sub-Unit

I.M.S-U. Inner Marginal Sub-Unit

I.U. Intermediate Unit

C.U. Central Unit

S.G.-Dolerite taken as 3.0

S.C.-Zeolite in dyke taken as 2.3

5/174'	6/174'	7/174'	8/174'	9/174'	10/174'	11/174'	12/174'
I.M.S-U.	I.M.S-U.	I.M.S-U.	I.M.S-U.	I.M.S-U.	I.U.	C.U.	I.U.
48.06	47.49	46.37	46.55	47.36	46.81	45.29	46.73
1.79	1.70	2.15	2.08	1.76	0.84	2.01	0.74
15.35	14.69	13.79	14.91	16.95	18.80	13.80	19.92
3.31	3.28	3.71	3.60	3.29	2.38	3.58	2.27
9.25	10.14	10.93	10.00	6.80	7.49	10.04	7.35
0.20	0.22	0.22	0.19	0.16	0.14	0.20	0.13
7.21	8.23	8.09	6.83	9.09	9.99	9.90	9.73
10.39	9.53	10.11	11.40	11.24	9.89	10.06	9.55
3.51	3.88	3.93	3.87	2.92	3.27	4.38	3.19
0.69	0.56	0.54	0.40	0.31	0.27	0.50	0.30
0.33	0.27	0.17	0.17	0.13	0.12	0.23	0.10
100.09	99.99	100.01	100.00	100.01	100.00	99.99	99.99
12.56	13.42	14.64	13.60	10.09	9.87	13.62	9.62
0.75	5.63	4.30	1.30	2.63	3.38	4.89	2.63

Table 5.5

Normative Mineralogy of sample 174' calculated for a dry, zeolite-free whole-rock geochemistry.

	'Dyke'					Band 1				Band 2				Band 3				Band 4			
	O.M.S-U.	I.M.S-U.	I.U.	C.U.		O.M.S-U.	I.M.S-U.	I.M.S-U.	I.M.S-U.												
Apatite	0.42	0.42	0.49	0.26	0.54	0.42	0.40	0.49	0.49	0.42	0.40	0.49	0.49	0.42	0.40	0.49	0.49	0.42	0.40	0.49	0.49
Ilmenite	2.74	2.91	3.41	1.50	3.83	2.91	2.82	3.35	3.24	2.91	2.82	3.35	3.24	2.91	2.82	3.35	3.24	2.91	2.82	3.35	3.24
Magnetite	4.44	4.43	4.97	3.38	5.20	4.43	4.39	4.90	4.71	4.43	4.39	4.90	4.71	4.43	4.39	4.90	4.71	4.43	4.39	4.90	4.71
Orthoclase	2.59	2.95	3.25	1.71	2.95	2.95	3.96	4.55	4.37	2.95	3.96	4.55	4.37	2.95	3.96	4.55	4.37	2.95	3.96	4.55	4.37
Albite	20.67	18.69	21.89	22.22	15.68	18.69	18.70	19.10	19.76	18.69	18.70	19.10	19.76	18.69	18.70	19.10	19.76	18.69	18.70	19.10	19.76
Anorthite	27.15	25.30	23.38	37.45	16.52	25.30	24.85	20.09	22.75	25.30	24.85	20.09	22.75	25.30	24.85	20.09	22.75	25.30	24.85	20.09	22.75
Diopside	18.19	18.79	22.82	8.08	25.80	18.79	17.38	23.48	21.84	18.79	17.38	23.48	21.84	18.79	17.38	23.48	21.84	18.79	17.38	23.48	21.84
Hypersthene	0.00	0.00	0.00	0.00	0.00	0.00	1.39	0.00	0.00	0.00	1.39	0.00	0.00	0.00	1.39	0.00	0.00	0.00	1.39	0.00	0.00
Olivine	19.35	25.59	16.12	22.64	17.91	25.59	26.12	19.95	19.44	25.59	26.12	19.95	19.44	25.59	26.12	19.95	19.44	25.59	26.12	19.95	19.44
Nepheline	4.45	0.92	3.68	2.76	11.58	0.92	0.00	4.08	3.41	0.92	0.00	4.08	3.41	0.92	0.00	4.08	3.41	0.92	0.00	4.08	3.41
Total:	100.00	100.00	100.01	100.00	100.01	100.00	100.01	99.99	100.01	100.00	100.01	99.99	100.01	100.00	100.01	99.99	100.01	100.00	100.01	99.99	100.01
Total Plag	50.41	46.94	48.52	61.38	35.15	46.94	47.51	43.74	46.88	46.94	47.51	43.74	46.88	46.94	47.51	43.74	46.88	46.94	47.51	43.74	46.88

Band 5	Band 6	Band 7	Band 8	Band 9	Band 10	Band 11
I.M.S-U.	I.M.S-U.	I.M.S-U.	I.M.S-U.	I.M.S-U.	I.U.	C.U.
0.77	0.63	0.40	0.40	0.30	0.26	0.54
3.40	3.24	4.09	3.96	3.35	1.50	3.83
4.80	4.77	5.39	5.23	4.78	3.38	5.20
4.07	3.31	3.19	2.36	1.83	1.71	2.95
26.12	25.31	20.99	20.23	23.64	22.22	15.68
24.06	31.01	18.39	22.13	32.22	37.45	16.52
20.60	19.98	25.02	27.24	18.13	8.08	25.80
0.00	0.00	0.00	0.00	0.00	0.00	0.00
14.25	17.70	15.90	11.67	15.17	22.64	17.91
1.92	4.07	6.64	6.78	0.57	2.76	11.58
99.99	110.02	100.01	100.00	99.99	100.00	100.01
54.25	59.63	42.57	44.72	57.69	61.38	35.15

O.M.S-U. Outer Marginal Sub-Unit
 I.M.S-U. Inner Marginal Sub-Unit
 I.U. Intermediate Unit
 C.U. Central Unit

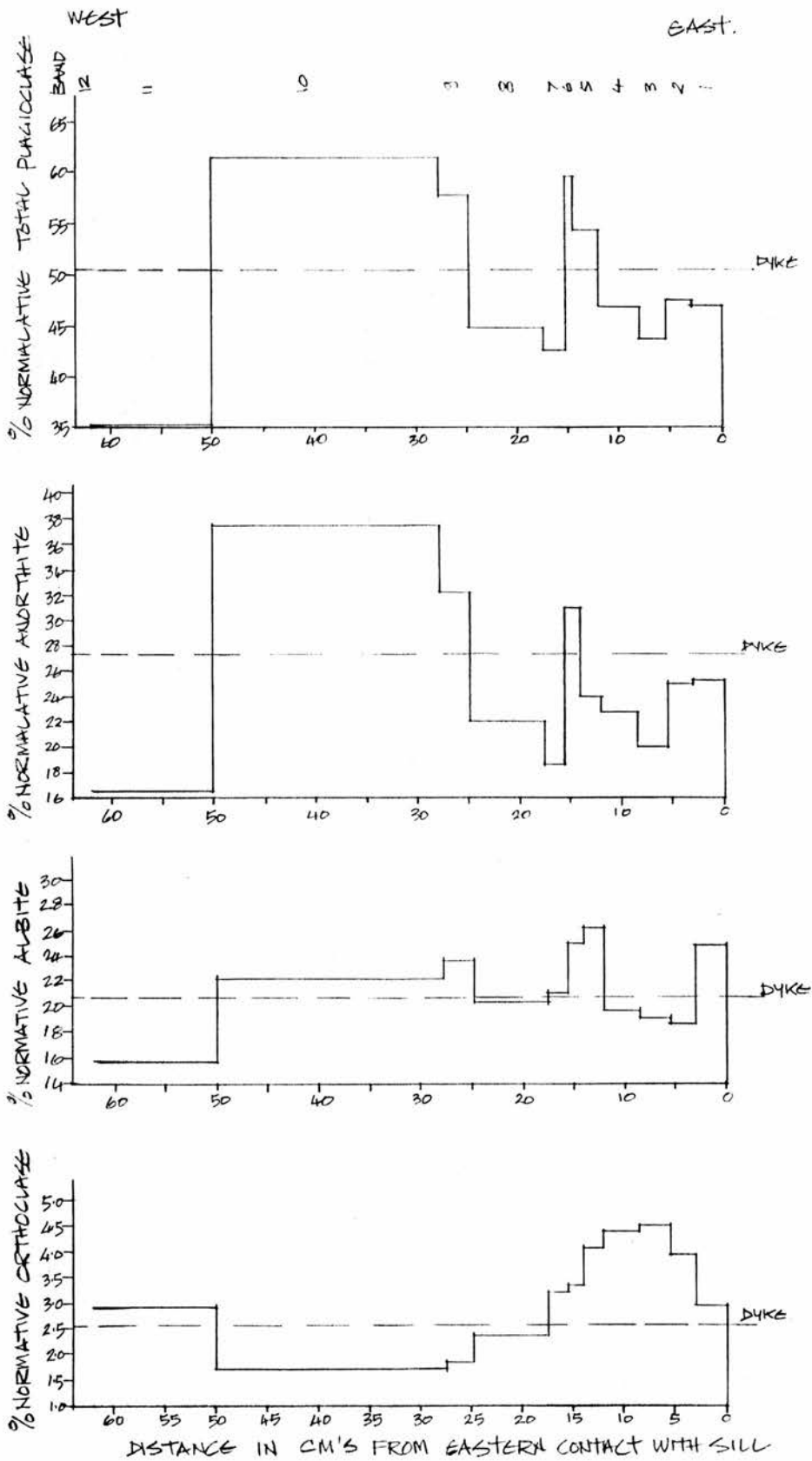


Figure 5.9 Normative mineralogy of the dyke.

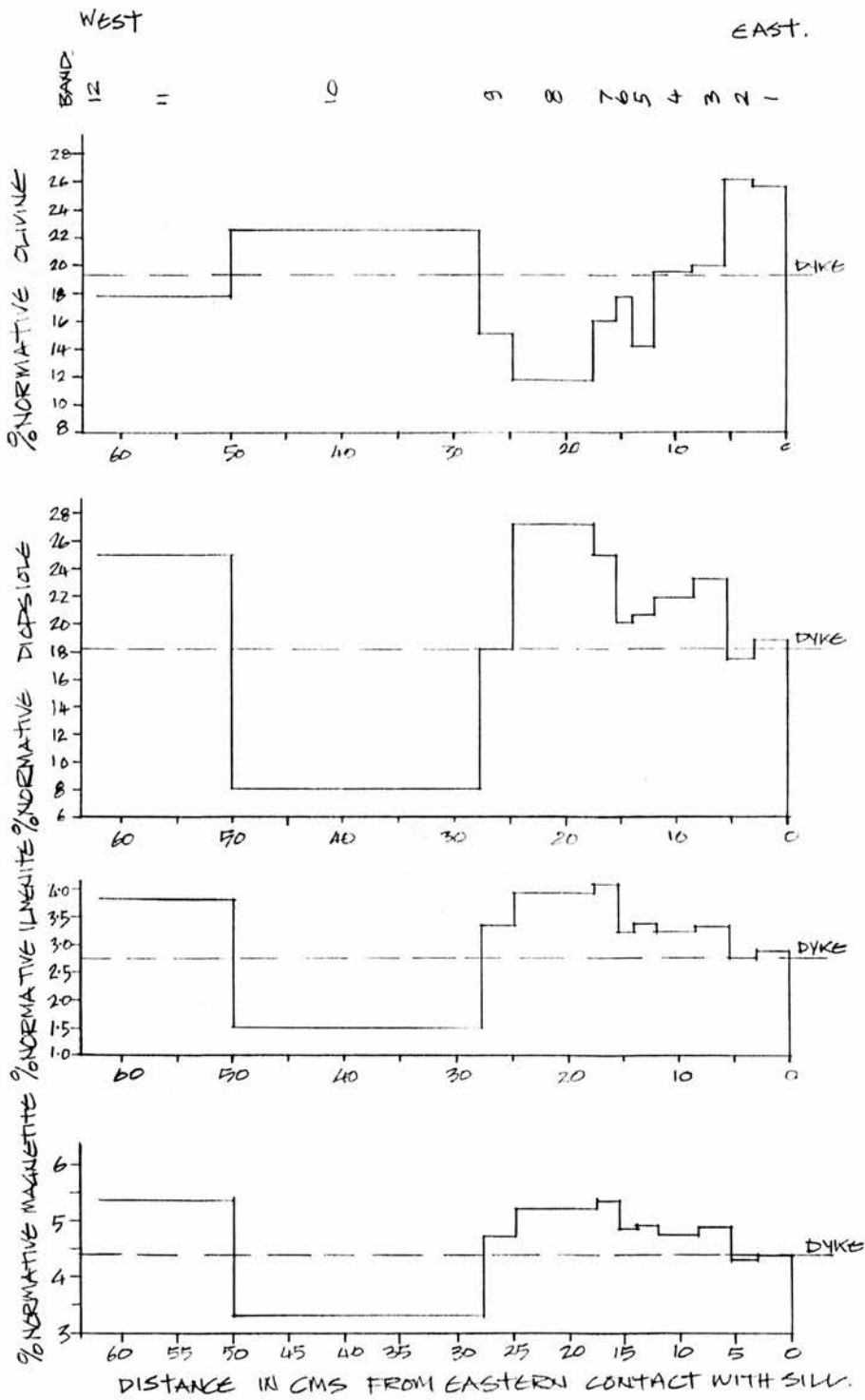


Figure 5.9 continued

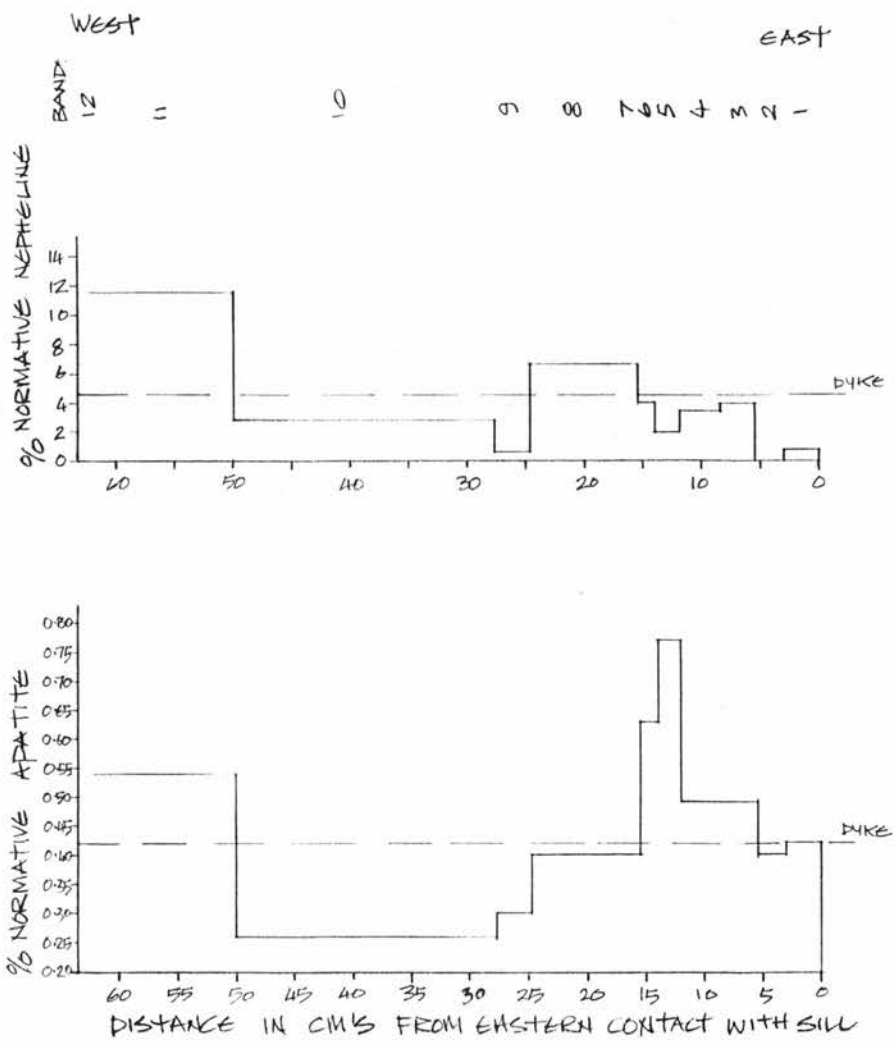


Figure 5.9 continued

Normative Hypersthene.

Only Band 2/174' is hypersthene normative (1.4%).

Normative Olivine.

Normative olivine is found in comparable amounts to normative diopside (11.7% to 26.1% in Bands 8 and 2/174' respectively). Normative and modal olivine content show comparable trends.

Normative Magnetite.

Normative magnetite content ranges from the minimum in Band 10/174' (3.4%) to the maximum in Band 7/174' (5.4%). Diopside and magnetite exhibit comparable trends across the dyke.

Normative Ilmenite.

Normative ilmenite is contained in smaller amounts than normative magnetite (1.5% in Band 10/174' to 4.1% in Band 7/174'). Normative ilmenite and magnetite exhibit identical trends across the transect.

Normative Apatite.

Normative apatite shows similar trends to normative ilmenite and magnetite. Normative apatite is present in very small amounts in the range 0.3% (Band 10/174') to 0.8% (Band 5/174'). Bands 6, 7 and 11/174' are relatively enriched in apatite. Apatite has a tendency to be more abundant in later solidified rocks due to P_2O_5

in the liquid increasing as fractionation proceeds. It can therefore be interpreted that Bands 6, 7 and 11 may be late fractionates.

Normative Nepheline.

Normative nepheline content across the dyke is irregular. Normative nepheline content varies from 0% in Band 2/174' to 11.6% in Band 11/174'.

Correlation between trace elements and host minerals do not show any consistent trends suggesting that fractionation by congelation, changing magma composition flowing past the walls and/or variation in the kinetics of crystallisation is taking place

Normative olivine, pyroxene and plagioclase feldspar were recalculated to 100% and plotted in Figure 5.10, the silica-poor part of the simple normative basalt system Ol-Cpx-Pl-SiO₂ projected for SiO₂ into Ol-Cpx-Pl. The figure shows approximate cotectic zones and expected areas of basalts equilibrating with olivine, clinopyroxene and plagioclase (Cox et al, 1979). This diagram is restricted by certain parameters, namely:

1. Normative plagioclase composition is >An50.
2. The ratio $\frac{\text{FeO}+\text{Fe}_2\text{O}_3}{\text{MgO}+\text{FeO}+\text{Fe}_2\text{O}_3} < 0.7$
3. K₂O content should be <1%

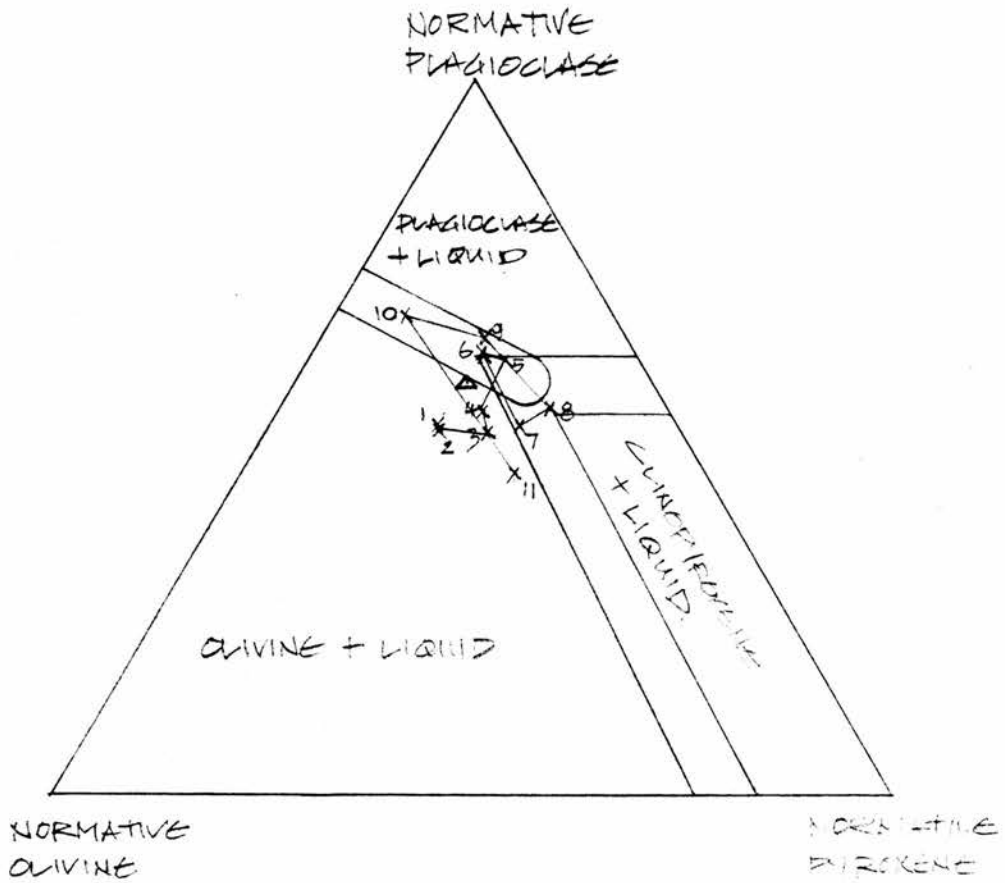
4. Basalts containing normative quartz >10 should be avoided.

The samples of the Mystery Dyke are considered to be of acceptable compositions as:

1. Normative plagioclase composition is >An50.
2. The ratio $\frac{\text{FeO} + \text{Fe}_2\text{O}_3}{\text{MgO} + \text{FeO} + \text{Fe}_2\text{O}_3} = 0.50 - 0.67$
3. The dyke has very low K₂O content
(0.27-0.77 wt%).
4. The dyke contains no normative quartz.

Figure 5.10 shows that many bands crystallised close to the eutectic of olivine, clinopyroxene and plagioclase, or close to a cotectic curve. This indicates that with the exception of Bands 1-2/174' (and to a lesser extent Bands 3,4 and 11/174'), the essential minerals should have commenced crystallisation at approximately the same time.

As the bands are traced from contact with the sill to centre of the dyke, trends can be followed. The outermost Bands (1 and 2/174') show that the initial magma should crystallise only olivine. As olivine continued to be precipitated in Bands 3 and 4/174', the magma composition shifted towards the eutectic of olivine, clinopyroxene and plagioclase, allowing all three minerals to crystallise together in Bands 5 and 6/174'. Pyroxene then dominated the precipitation



Δ DYKE
 X BAND COMPOSITIONS.

Figure 5.10 The Silica-poor part of the simple Normative basalt system Ol-Cpx-Pl-SiO₂ projected into Ol-Cpx-Pl, with bands from 174' marked. Areas of rocks with near-cotectic behaviour with regard to olivine, clinopyroxene and plagioclase of Cox and Bell (1972).

during Band 5/174', causing the liquid composition to move towards the plagioclase field. The plagioclase precipitated in Band 6/174' then caused the magma composition to become enriched in the components for pyroxene and olivine. Bands 7 and 8/174' crystallised olivine and pyroxene together, enriching the magma in felsic components. Bands 9 and 10/174' lie on the plagioclase and olivine cotectic. The Central Unit (Band 11/174') again lies within the olivine and liquid field.

In summary, Bands 1-4/174' are olivine cumulates, Bands 5-6/174' formed on the eutectic of olivine, plagioclase and pyroxene, while Bands 7-8/174' are olivine and pyroxene cumulates. Bands 9 and 10/174' are enriched in plagioclase and olivine and Band 11/174' is another olivine cumulate. The "dyke" composition falls within the olivine and liquid field close to the eutectic.

The average olivine phenocryst compositions per band (obtained from probe data-see Chapter 4) is shown on the overlay. Comb-texture olivine composition is shown for Band 10/174'. Bands 1-5/174' have relatively high forsterite phenocryst core values, which then decrease across Bands 6-9/174'. Band 9/174' contains the lowest value, which is in agreement with the positioning of Band 9/174' on Figure 5.10. Band 10/174' has an average comb-textured core composition of Fo₆₉, which increases to Fo₇₉ for phenocryst core composition in Band 11/174'.

This increase in magnesium content of the olivine phenocrysts in the Central Unit is in agreement with the position of Band 11/174' within the olivine and liquid field, compared to Band 10/174' lying on the olivine and plagioclase cotectic.

5.6 Computer Modelling.

The TEMP programme from MacGPP (Geist, McBirney and Baker 1989) was used to estimate temperatures of equilibrium crystallisation of minerals across the banding of sample 174'. This method was compiled by Tilley, Yoder and Schairer (1967) and is based on the relationship between the liquidus temperatures of natural mafic rocks and the ratio of $\text{FeO} + \text{Fe}_2\text{O}_3$ to $\text{MgO} + \text{FeO} + \text{Fe}_2\text{O}_3$ (applicable only to low pressure crystallisation of some mafic compositions).

The composition of each band was calculated on a H_2O -free, zeolite-free basis (Table 5.4). To try to minimise the effect caused by the volume of olivine phenocrysts in Band 1/174', the amount of olivine in this band was calculated and the chemical composition of this weight % of olivine removed from the Band 1/174' composition. Table 5.6 and Figure 5.11 display the crystallisation temperatures of a dry, zeolite-free, magma composition. Trends are apparent: namely Bands 1-

Table 5.6

Liquidus Temperatures calculated by TEMP (MacGPP)
for dry, Zeolite-free compositions.

	°C
Band 1/174'	1238
Band 1-12.98wt% Ol.	1190
Band 2/174'	1238
Band 3/174'	1202
Band 4/174'	1178
Band 5/174'	1177
Band 6/174'	1186
Band 7/174'	1174
Band 8/174'	1164
Band 9/174'	1231
Band 10/174'	1250
Band 11/174'	1205

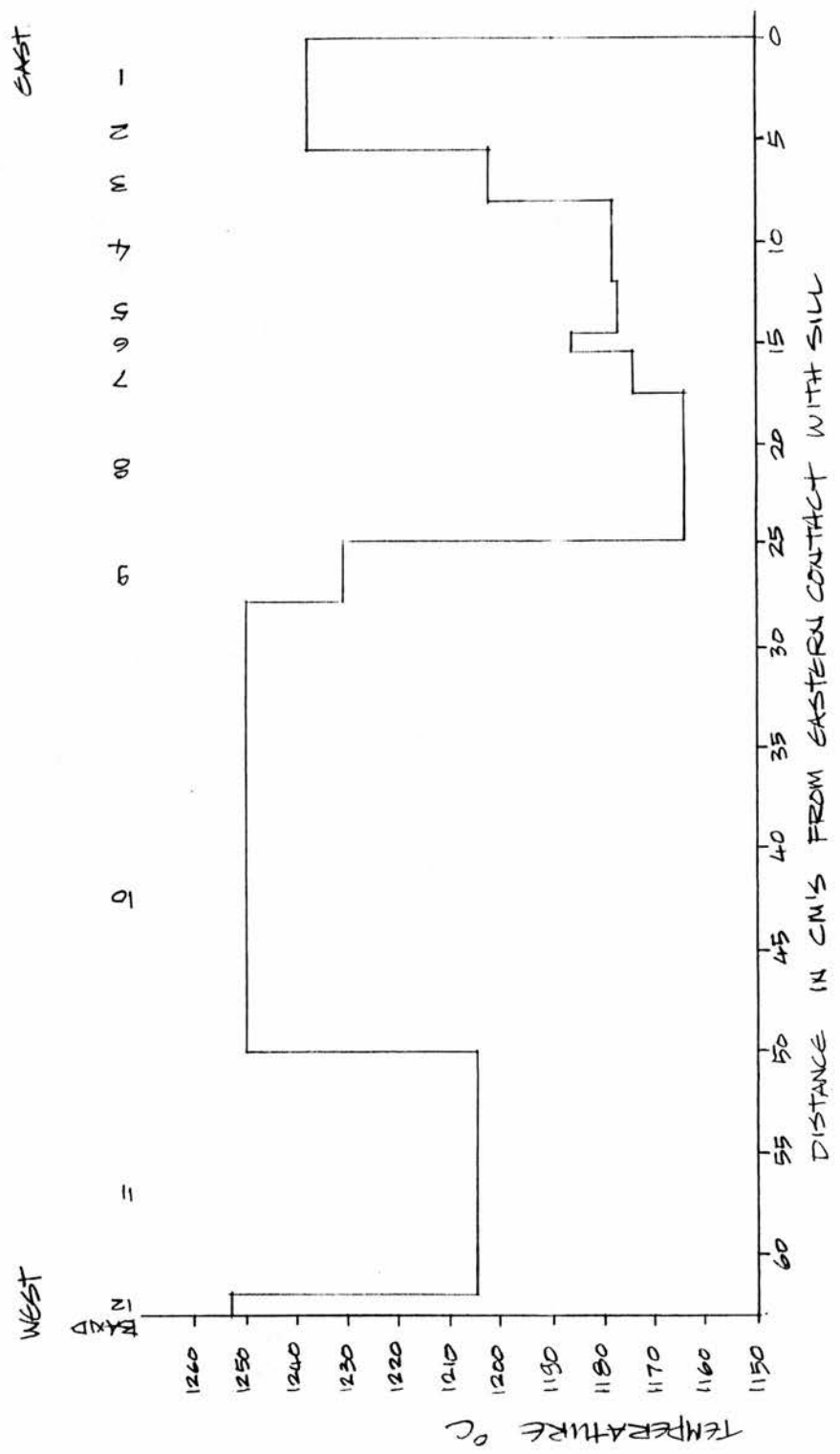


Figure 5.11 Crystallisation Temperatures of the bands at 174' as calculated by the TEMP programme of MacGPP.

5, 6-8, 8-10 and 10-11. With the exception of Bands 8-10, the trends display decreasing temperatures.

MAGMODEL was used to model the compositional changes resulting from equilibrium crystallisation of a basaltic magma, using the empirical equations derived by H.D. Nathan from experimental work. The equations are similar to those of Nathan and Van Kirk (1978) but have been updated by Geist et al (1989). Liquidus temperatures of olivine, Ca-rich pyroxene, Ca-poor pyroxene, plagioclase, quartz, Ti-magnetite, K-feldspar and nepheline are calculated from an original magma composition, together with the amounts of each and the solid solution compositions of the isomorphous series minerals during progressive computed crystallisation.

MAGMODEL was run for several compositions- all of which have been calculated on a water- and zeolite-free basis for 174' (Table 5.7). Options included no olivine phenocryst growth in the dyke through to all olivine phenocryst growth in the dyke. Similarly nil to all plagioclase phenocryst growth in the dyke was an option. Allowing for minor error in calculation, there was little variation in mineral composition for any of the options considered:

Olivine - Fo85-78:

Plagioclase - An80-67:

Magnetite - Mt54-51;

Augite - Di82-80.

Table 5.7

Various phenocryst growth options investigated in MAGMODEL

	Option A	Option B	Option C	Option D	Option E	Option F
Wt% Ol phen removed:	19 (all)	12.98	14.6	12	19 (all)	none
Wt% Ol phen growth in sit	0	5.9	5	6.9	0	19
Wt% Plag phen removed:	0	0	0	0	all	all
Wt% Plag phen growth in sit	all	all	all	all	0	0
Temp oC						
Olivine	1167	1200	1192	1207	1169	1309
Plagioclase	1218	1200	1205	1199	1187	1177
Magnetite	1176	1180	1180	1180	1179	1177
Augite	1170	1191	1191	1192	1172	1176
Min. Comp.						
Olivine	Fo 77-	85-80	83-81	83-81	83-78	83-80
Plagioclase	An 80-	77-71	78-72	78-72	78-67	78-73
Magnetite	Mag -	53	54-53	54-53	54-51	54-52
Augite	Au 82	82	82	82	82-80	82

The modelling was stopped once the last mineral had commenced crystallisation.

There was however, variation in the liquidus temperatures of the four minerals. If all olivine phenocrysts crystallised in situ: 1309°C, if none: 1167°C. All other options considered fell between these two values. The upper liquidus temperature for the first mineral to crystallise for most options was 1200°C (1192-1218°C). Olivine or plagioclase was always the first mineral to crystallise, with the others crystallising after only a few more degrees of cooling (excepting the unlikely options of all or no olivine phenocryst growth in situ). In the case of no olivine phenocrysts growth in situ, olivine was the last of the four essential minerals to commence crystallisation at 1167°C (after 25% crystallisation of the magma had occurred), whereas plagioclase commenced crystallisation at 1218°C.

The programme predicts that olivine and plagioclase will reach their liquidus temperatures almost together and that augite and magnetite will reach their liquidus temperatures together (augite has a slightly higher liquidus temperature than magnetite in most options considered). This prediction is in agreement with the findings of Figure 5.10, which shows olivine to crystallise alone initially, then plagioclase and pyroxene to have commenced crystallisation together with olivine.

These calculated initial olivine compositions are comparable with those analysed in Band 1/174', with the range of analysed olivine phenocryst core compositions being Fo₈₈₋₇₇. Analysed plagioclase phenocryst core compositions are lower than calculated (An₇₂₋₆₆ compared to the calculated range of An₇₈₋₆₇). There are no pyroxene phenocrysts in the Outer Marginal Sub-Unit for comparison. This agrees with the calculation showing that augite does not crystallise early in the cooling history of the dyke.

Both the TEMP and MAGMODEL programmes calculate liquidus temperatures of approximately 1200°C for olivine in Band 1/174' (Band 1/174'-12.98 wt% olivine phenocrysts to allow 5% modal, 5.9 wt% growth in situ: 1190°C-TEMP: 1200°C-MAGMODEL.) Temperatures calculated with no removal of phenocrysts for the phenocryst-rich bands will be in excess of actual temperatures due to the high percentage of crystals in the intruded magma.

A mass balance mixing calculation (MIX), based on the matrix inversion procedure devised by Bryan, Finger and Chayes (1969) was also run from MacGGP. The proportions of specified components, if added or subtracted to the parent magma composition, yields the best least-squares fit to a given daughter composition. This can test if fractionation, mixing or assimilation of given minerals

from one magma (the parent magma composition) to produce the daughter magma was a reasonable mechanism.

Only major elements were used in the calculations, with the weighting factors of all of the elements being equal. Representative olivine, plagioclase and spinel compositions from Band 1/174' were used together with a pyroxene from Band 2/174' (Table 5.8). The authors of the programme considered a square of the residuals (R^2) with a value less than 1 to be a reasonable fit, less than 0.3 to be a good fit and less than 0.1 to be excellent.

The parent composition was taken to be Band 1/174', with the daughter compositions to be Bands 2-11/174'. Table 4.8 details the lowest R^2 , amount of each mineral removed by crystallisation and any added to the magma to create the new rock composition.

Taking Band 1 as the parent magma, Bands 2-5 could be modelled as daughter magma compositions by fractionation. Band 6, having a R^2 of 1.2, was in excess of an acceptable figure as stated by the authors of the programme. Band 6 was then taken as a parent magma and the relationship of this composition to Bands 7-11 was investigated. Band 6 could be the parent magma to daughter Bands 7-10, but not to Band 11. Taking Band 10 as a parent magma, Band 11 could not be modelled as a daughter by fractionation, assimilation or mixing of the given mineral compositions.

Table 5.8

Representative Minerals used in
MAGMODEL calculations.

Band/Dist.	Olivine 1/174'	Plag. 1/174'	Augite 2/174'	Opaque 1/174'
wt%				
SiO ₂	39.8	49.9	46.5	1.1
TiO ₂	0.0	0.1	2.4	21.1
Al ₂ O ₃	0.1	31.3	6.9	1.7
FeO _t	13.9	0.6	8.6	66.2
MnO	0.1	0.0	0.2	1.6
MgO	46.4	0.1	12.3	1.3
CaO	0.3	14.3	21.5	0.2
Na ₂ O	0.0	3.5	0.5	0.0
K ₂ O	0.0	0.1	0.0	0.0
Total:	100.6	99.84	98.9	93.24

5.7 Relationships between Bands in the Southern Segment of the Dyke.

The Central bands from 54' and 40' were analysed and plotted on variation diagrams (Figures 5.1, 5.2, 5.5 and 5.8) together with the Intermediate Unit from 40'. Chemically the Central Unit at 54' lies between the Outer Marginal Sub-Unit and the Central Unit of 174', and contains relatively more FeO^t , MnO and Ni and relatively less CaO , Sr and V than the Central Unit, 174'. The Central Unit at 54' contains 16 modal% olivine compared to 10 modal% in the Central Unit at 174', with both units containing approximately similar amounts of plagioclase and pyroxene.

The Central band and Intermediate Unit at 40' are associated with the grouping of Bands 4,5,6,7 and 8/174' (with the exception of Ba and Zn where 40' Intermediate Unit lies closer to Band 9/174'). The Central band contains relatively more TiO_2 , FeO^t , MnO , Zr , Zn , Ba , V and Cu and less Al_2O_3 , MgO , Sr , Cr and Ni than the Intermediate Unit at 40'. Modally, the two bands are distinct- the Intermediate Unit contains 12% comb-textured pyroxene, while this texture is not present in the Central band. The Central band contains more total and matrix pyroxene and opaques, and less total and matrix plagioclase than the Intermediate Unit. This is in agreement with the geochemical data.

The Central Units at 40', 54' and 174' were compared. Geochemically, the only variation is in the amounts of MgO and CaO. The Central band at 40' contains less MgO and the Central Unit at 54' contains slightly less CaO than the others. However there are differences in modal mineralogy. The Central band at 40' contains the greatest volume of groundmass crystals (olivine, pyroxene and plagioclase). A marked decrease in the amount of pyroxene phenocrysts and an increase in opaques with distance down the dyke from 174' to 40' is noted. The Central band at 40' contains significantly less plagioclase phenocrysts and zeolite than the Central Unit further north. The Central Unit at 54' contains the greatest amount of olivine phenocrysts. The Central band at 40' is considered to be the Central Unit based on comparisons with the Central Unit elsewhere in the dyke.

The ratio: $(\text{FeO} + \text{Fe}_2\text{O}_3) / (\text{FeO} + \text{Fe}_2\text{O}_3 + \text{MgO})$ was investigated to help define the relationship of the banding at 40' to that elsewhere in the dyke. This did not clarify the relationship of the banding as the Intermediate Unit (40') has a ratio of 0.58, comparable with that of Bands 3 and 11/174' and the Central Unit at 54', while the Central Unit has a ratio of 0.70, the highest of any sample analysed from the dyke. The ratio Zr/TiO_2 was also compared. The Central Units at 174', 54' and 40' all have comparable values, as do the Intermediate Units at 174' and 40'.

5.8 The Relationship between "Mystery Dyke", Little Minch Sill Complex and the Skye Main Lava Series.

As stated earlier in this chapter these three groups of igneous rocks appear to be related with obvious overlap on the AFM Diagram (Figure 5.2). Comparatively little whole-rock geochemistry has been published on the Little Minch Sill Complex (Trotternish and Shiant Isles-Walker 1930,1931,1932, Mohammed 1982, Gibson 1988,1990 and Gibb and Henderson 1989). Certain ratios of elements were investigated, notably elements that are relatively immobile (K_2O/Rb , Zr/Y , Rb/Sr and Nb/Y). These are shown in Table 5.9. Ratios from the dyke, sills and lavas exhibit similarities and comparable ranges of values. Anderson and Dunham (1966) suggest that olivine-rich dykes present in the region, may represent injections of olivine cumulus from the sill system.

The Mystery Dyke is relatively enriched in some trace elements and depleted in others compared to a typical basalt. The sill adjacent to the dyke is enriched or depleted in the same elements.

Bell and Harris (1986) show the northern Trotternish Peninsula to be the Beinn Edra Group of lavas, although the peninsula could also be within the area covered by the Beinn Totaig Group. The Beinn Edra group consists of non-porphyrific basalts with minor porphyritic flows (Anderson and Dunham 1966), the lower lavas seen in Uig

Table 5.9

Comparison of Selected Element Ratios
of the Dyke, Sill and Lavas.

	K ₂ O/Rb	Zr/Y	Rb/Sr	Nb/Y
"Dyke"	1100	4.7	0.010	0.12
O.M.S-U.	817	4.2	0.012	0.11
I.M.S-U.	900	4.8	0.014	0.14
I.U.	2600	4.0	0.003	0.10
C.U.	1600	5.4	0.008	0.19
Band 1/174'	817	4.2	0.012	0.11
Band 2/174'	1320	3.9	0.010	0.21
Band 3/174'	900	4.8	0.015	0.23
Band 4/174'	767	5.2	0.019	0.19
Band 5/174'	1133	5.5	0.015	0.19
Band 6/174'	1325	5.2	0.013	0.16
Band 7/174'	650	4.5	0.022	0.05
Band 8/174'	975	4.8	0.010	0.10
Band 9/174'	1000	4.1	0.007	0.00
Band 10/174'	2600	4.0	0.003	0.10
Band 11/174'	1600	5.4	0.008	0.19
Sill sample 1a	733	5.5	0.015	0.00
Sill sample 1b	540	4.3	0.028	0.00
Sill sample 1c	260	4.2	0.032	0.04
Sill sample 2	679	7.7	0.170	0.03
T.S.C.:				
Picrite	85	14.6	0.120	0.29
Picrodolerite	262	6.7	0.050	0.25
Crinanite	288	7.2	0.050	0.28
Pegmatite	434	6.7	0.120	0.13
(Gibson, 1988)				
Sill nr dyke:				
OM above S.L.	85	5.9	0.120	0.29
2M above S.L.	83	6.1	0.100	0.00
13M above S.L.	173	6.5	0.060	0.00
(Gibson, 1988)				
S.M.L.S.:				
Basalt range	688-4500	2.3-7.1	0-0.020	0.11-0.47
Hawaiite	453	6.9	0.020	0.44
(Thompson et al, 1972 & 1979)				

Bay being undifferentiated basalts. The Beinn Totaig Group may have covered much of the Trotternish Peninsula, and contains composite mugearite lava flows: the lower section being non-porphyrific, the upper porphyritic (Anderson and Dunham 1966).

There have been two stages to the olivine crystallisation in the lavas- phenocrysts emplaced with the lava and later growth in situ. Anderson and Dunham (1966) calculated 17.5wt% of the olivine in the sills to have been emplaced as phenocrysts with less than 10wt% olivine growth in situ. In the dyke, 6wt% olivine phenocryst growth is suggested as growth within the dyke, with 13wt% of the olivine to have been emplaced as phenocrysts.

Gibson (1988) and Gibson and Jones (1991) state that in the sill complex, the picrites with 18-30wt% MgO are olivine cumulates and crinanites (3-8wt% MgO) are olivine-poor fractionates of an alkali olivine basalt (10wt% MgO).

In Figure 5.12: $TiO_2 - (FeO + Fe_2O_3) / (FeO + Fe_2O_3 + MgO)$ from Moorbath and Thompson (1980), the Central Unit at 40' lies with the hawaiite and mugearite samples of the S.M.L.S., with the Intermediate Unit (40') and all other samples (with the exception of Band 8/174') lying in the basalt field. Band 8/174' lies between these two fields.

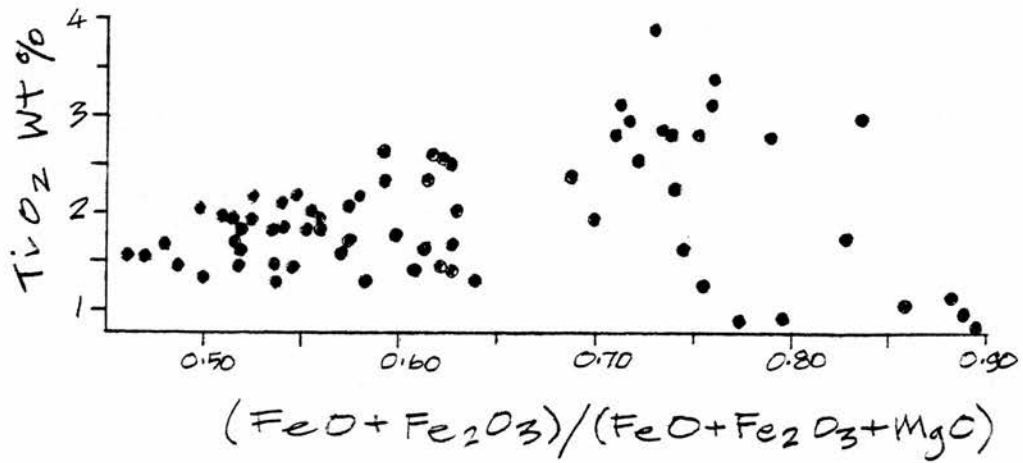


Figure 5.12 $TiO_2 - (FeO + Fe_2O_3) / (FeO + Fe_2O_3 + MgO)$ (from Moorbath and Thompson 1980).

5.9 Summary.

The major element geochemistry indicates that the dyke is alkaline in composition, and consists of more than one intrusive pulse. Trace element geochemistry supports the evidence of the major elements, although band groupings chosen are not always exactly comparable (Table 5.10).

The evolution from primary (parental) magma to more evolved (differentiated) magmas can be shown by increasing SiO_2 content of the magma. Bands 1-5 and 7-9/174' exhibit increasing SiO_2 content, while Bands 5-7 and 9-11/174' have decreasing silica content. This is in agreement with concentration of olivine or pyroxene and/or spinel as detailed below. The reversal of olivine fractionation processes at Bands 5 and 9/174' is also in agreement with this. Morrison (1978) states that high Zr/TiO_2 ratios are often indicative of magmatic differentiation. This ratio increases across Bands 2-5/174', 7-8/174' and 9-11/174' and decreases across Bands 5-7/174' and 8-9/174'. The above two trends are in agreement with the exception of Bands 9-11/174'.

There are problems in using variation diagrams with phenocryst-rich rocks, as the whole-rock geochemistry does not necessarily give the actual magma composition. This has to be considered in the case of Bands 1-4 and 11/174' which are phenocryst-rich. Comb-textured bands

Table 5.10

Summary of groupings

	1/174'	2/174'	3/174'	4/174'	5/174'	6/174'	7/174'	8/174'	9/174'	10/174'	11/174'
Major Element-Distance											
Summary:	A	A	A	A	A	B	B	B	C	C	C/D
Trace Element-Distance											
Summary:	A	A	A	A	A/B	B	B	C	C	C	D
Norms-Distance											
Summary:	A	A	A/B	B	B	B	C	C	C/D	C/D	D/E
Major- Harker Diagrams											
Summary:	1	1	2	3	3	3	3	3	4	4	2
Trace-Harker Diagrams											
Summary:	1	1	2	3	3	3	3	3	2/4	4	2

are also problematic, as they may be crystal concentrates.

Figure 5.2 displays trends of iron or magnesium enrichment. Increasing iron content suggests early crystallisation of Mg-rich minerals (normal olivine fractionation trend). Bands 1-8/174' and 10-11/174' exhibit iron enrichment, while Bands 8-10/174' show magnesium enrichment, indicating other processes occurring, including possible new magma intrusion and assimilation.

The Harker-type variation diagrams exhibit three distinct and common groupings. Bands 1 and 2/174' form one, with Bands 4,5,6,7 and 8/174' forming another (Table 5.10). Lying between these two groups are Bands 3,9,10 and 11/174'. Coherent trends on the Harker Diagrams represent steady chemical evolution (including fractionation trends). $\text{SiO}_2\text{-MgO}$ and Ni-MgO both suggest olivine fractionation across Bands 2-5/174', while CaO-MgO suggests olivine fractionation across Bands 2-4/174'.

$\text{SiO}_2\text{-MgO}$ and $\text{Na}_2\text{O-MgO}$ both show the reverse trend of olivine fractionation from Band 5-6/174' suggesting olivine accumulation or addition to the magma. Ni-MgO exhibits the olivine fractionation trend from Band 6-8/174', while $\text{SiO}_2\text{-MgO}$ exhibits the olivine fractionation trend from Band 7-8/174', and the reverse trend from Band 9-10/174'. Chromium can be used as an indicator of pyroxene and/or spinel fractionation. Cr-MgO (Figure

5.8f) suggests that pyroxene and/or spinel was fractionated across Bands 2-5, 6-8 and 9-10/174'.

Accepting Band 1/174' as the initial magma intruded into the dyke fissure, all other bands in a simple intrusion should relate to this composition. The chilled margin (Band 1/174') is relatively enriched in olivine and its components and relatively depleted in felsic elements including SiO_2 and Al_2O_3 compared to the "dyke" composition. Olivine fractionation has taken place to produce the comparable Band 2/174'.

Band 3/174' shows increasing SiO_2 indicating differentiation occurring, and is relatively depleted in MgO, Ni and Cr due to continued olivine fractionation.

The SiO_2 content of the rock continues to rise in Band 4/174', with continued differentiation. Olivine fractionation has continued together with commencement of pyroxene and/or spinel fractionation.

Continued differentiation into Band 5/174' increases SiO_2 content. This band is relatively enriched in plagioclase and pyroxene compared to Band 4. Fractionation of olivine may have ceased.

Band 6/174' is depleted in SiO_2 , relatively enriched in plagioclase and depleted in olivine compared to Band 5. Various figures suggest continued olivine, pyroxene and/or spinel fractionation.

Band 7 contains less plagioclase, SiO_2 , TiO_2 and Al_2O_3 and is relatively enriched in pyroxene, FeO, MgO and CaO compared to the previous band. The decreasing

silica content may indicate fresh magma being mixed with magma in the dyke, with various figures suggesting continued olivine, pyroxene and/or spinel fractionation.

Compared with Band 7, Band 8/174' is rich in plagioclase, with decreasing FeO, MgO, Ni and Cr together with increasing SiO₂ indicating continued differentiation and fractionation of olivine, pyroxene and/or spinel.

Band 9 continues the trends outlined for Band 8/174', but is becoming relatively depleted in pyroxene components of TiO₂, FeO and V.

The Intermediate Unit (Band 10) is enriched in olivine and plagioclase and depleted in pyroxene, SiO₂, TiO₂ and Al₂O₃ compared to Band 9/174'. Decreasing silica indicates continued differentiation.

Fresh magma is suggested by the change in geochemistry of the Central Unit (Band 11), due to a decrease in SiO₂, and an increase in TiO₂, FeO and CaO. However, the band is relatively depleted in olivine and plagioclase and enriched in pyroxene compared to Band 10/174'.

Computer modelling suggests either three or four pulses of intruding magma. TEMP highlights four pulses: namely Bands 1-5, 6-8, 9-10 and 11, whereas MIX highlights Bands 1-5, and Band 11, but has Bands 6-10 as a single event. Possible hypotheses developed from these computer modelling programmes will be discussed in Chapter 6: the petrogenesis of the dyke.

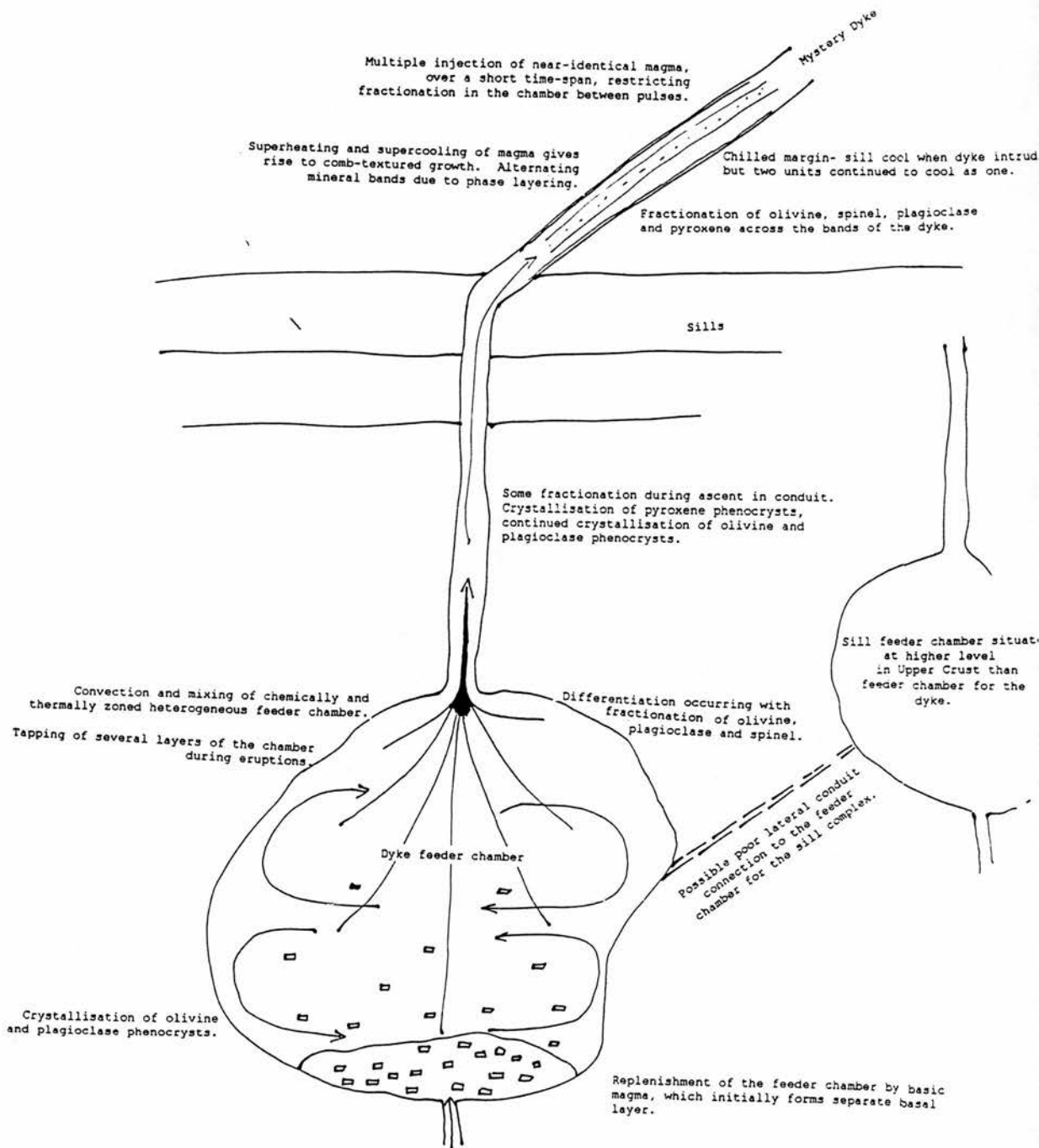


Figure 6.3 A possible Magmatic System responsible for the development of the Mystery Dyke

Chapter 6

Petrogenesis

6.0 Introduction.

The "Mystery Dyke" displays extensive heterogeneity based on evidence from field relations, petrography, mineral chemistry and geochemistry. Any petrogenetic model must account for the features summarised below:

- a) Lateral and longitudinal variation in the banding.
- b) Modal variation across and along the dyke.
- c) Textural variation with the development of specific textures, eg comb-texture within certain bands.
- d) Near-constant olivine phenocryst core compositions.
- e) Complex zoning of matrix crystals, especially pyroxene.
- f) Persistent chemical associations and trends shown by groupings of bands.

Features of general interest are discussed first and petrogenetic schemes are considered in the latter part of the chapter.

6.1 Direction and Type of Flow.

The curved, concentric banding displays a constant flow direction from the north, with banding in the south also indicating an upward vector.

Laminar flow is envisaged due to smooth contacts between bands and the curved, concentric banding exhibiting no erosion due to turbulent eddying. In addition, certain textures including trachytic, poikilitic and comb-texture indicate smooth flow or possibly crystal growth in stagnant magma.

Olivines in the chilled margin are elongate parallel to the dyke walls, while in Band 2/174', they are sub-horizontal across the dyke, suggesting that magma flowed more quickly against the walls or that magma shearing here aligned the crystals. Bands 4-6/174' again show vertical, elongate olivines parallel to the dyke walls, suggesting smooth flow, whereas the orientation of olivines varies across Band 7/174'. The outer area contains vertically elongate olivines (cf Band 6) but further in contains sub-horizontal olivines that plunge to the south and towards the walls of the dyke, indicating some variation in flow regime. The comb-textured crystals in the Intermediate Unit probably crystallised from stagnant or slow-moving magma to allow growth of delicate dendrites.

The proportion of suspended particles in the melt increases the "effective" viscosity of magma and renders

turbulent flow unlikely (Cox et al 1979). This remark applies to several bands including the chilled margin. The Reynolds no. (Re) has to exceed 2300 to allow turbulent flow, and this requires the velocity of magma flow in the dyke to exceed 26.5m/s. Since the dyke shows no sign of erosion of lumpy incision type, it is presumed it enjoyed laminar flow with a flow rate of less than 26.5m/s.

6.2 Cooling Time and Propagation of the Dyke.

Average velocity of lava has been calculated at 1m/s (Thorarinsson 1968) to 500m/s (Kinoshito et al 1969). Delaney and Pollard (1982) calculated that magmas flowing more than a few kilometres from an upper crustal source, with initial velocities of 1m/s in dykes 2m thick would solidify within a few hours, with general thinning of the conduit due to solidification on its walls causing decreased flow rates, and conclude that magma flow in narrow dykes and at low Re can only last for a few hours, or perhaps a day, before solidification stifles flow.

Using the calculations of Jaeger (1968) to calculate the cooling time for a vertical sheet of magma intruded into cold country rock, with the following assumptions: temperature of magma = 1100°C and the intrusion undergoing crystallisation to 800°C by conductive heat loss through

the walls, a single-pulse intrusion of 1m thickness would solidify in 5 days. A longer cooling time is indicated by the calculations of Cox et al (1979) which suggests that a 1.2m thick dyke intruded as a single pulse would have undergone substantial cooling at the centre by 3 weeks, be substantially solid by 4 weeks and solidified by 6 weeks from intrusion.

Just ahead of the dyke-tip, the wall rock is under tension due to leverage exerted by magma flowing into the tip (Lister et al 1991). Jackson et al (1975) and Brandsdottir and Einarrson (1979) estimate velocity of dyke propagation between 0.4 and 0.5m/s. Dykes will continue to propagate provided density differences continue to cause magma to flow to the dyke-tip. The amygdaloidal Central Unit of the Mystery Dyke failed to reach the southernmost tip of the dyke, and resulting in cessation of dyke propagation in this direction.

The simplest way to separate crystals from melt is for them to settle by gravitational differences. Crystal settling rates depend on crystal size, viscosity of the liquid and the density contrast between liquid and crystal. Cox et al (1979) state that phenocrysts of 1mm radius can settle 20 to 500 metres per year for plagioclase and magnetite respectively, with olivine and pyroxene having rates intermediate to these. This form of fractional crystallisation is therefore of limited

importance to magmatic evolution within the dyke as the time-scales are inappropriate.

6.3 Variation in Band/Unit Thickness.

The Central and Intermediate Units are of almost constant thickness, whereas the Marginal Unit (especially the Outer Marginal Sub-Unit) varies in thickness. As the magma was intruded approximately central to the dyke (the weakest plane in solidifying magma), the pressure of intruding magma maintained the force on the outer volumes against the sill, emphasising the angular deviations in the outermost bands, but with increasing distance from the angular contact with the sill, bands became increasingly more linear and of near-constant thickness.

The constriction at 66' reduces the thickness of all units, while the constrictions at 168' and 188', are obvious due to reduction in thickness of the Central Unit. The northern constrictions may be due to the sill not separating as easily at these points as it did elsewhere, while the whole dyke has been constricted at 66', possibly due to conditions as suggested above, or to later movements causing the sill to squash the dyke before it had completely solidified, as the bands can be traced smoothly around the constriction. The slight

skew, may be due to uneven movements in this squeezing associated with the hexagonal cooling joints.

6.4 Mineral layering across the Dyke.

The high volume of olivine phenocrysts within the chilled margin requires consideration, as the Bagnold effect, due to dispersive pressure being highest at the walls of the dyke (Komar 1972a,b) should cause crystals to move from the area of high shear rate (close to the walls) inwards to areas of low rates of shear. Drever and Johnston (1958) and Battacharji (1967) found small crystals abundant close to intrusion walls. Smaller phenocrysts are abundant in the Outer Marginal Sub-Unit and Central Unit, while phenocrysts in the Inner Marginal Sub-Unit are considerably larger (1-2mm diameter compared to 0.3-0.4mm in the Outer Marginal Sub-Unit and Central Unit).

Wager (1959) suggested varying crystal nucleation rates in a supercooled magma as a possible cause of rhythmic layering in igneous intrusions, rather than external influences such as successive pulses of magma. Equilibrium conditions and non-equilibrium supersaturated conditions alternate in his hypothesis. Experimental evidence shows that olivine and magnetite usually

crystallise easily, while complex silicates do not (Goldsmith 1953, Eitel 1954, Wager 1959). McBirney and Noyes (1979) state that rhythmic supersaturation during crystallisation of a magma saturated with one or more minerals can account for alternating compositional layers. However, not all layering can be explained in this way, and some involve periodic injections of magma.

6.5 Textural implications.

Systematic variation in crystal morphology with cooling rate has been documented by many authors (Walker et al 1976, Donaldson 1976). Walker et al (1976) found that phenocrysts become more equant with slower cooling rates and that skeletal phenocrysts developed at runs in excess of 50°C/Hr, while olivine phenocrysts have a platy, skeletal form and pyroxenes form elaborate, dendritic sprays at cooling rates greater than 500°C/Hr. Cooling rate experiments of Lofgren and Donaldson (1975) on plagioclase of An40 composition produced tabular crystals at cooling rate <10°C/Hr, elongate at 16°C/Hr, curved crystals at 32°C/Hr and complex branching crystals at 130°C/Hr. This suggests that the simple dendrites at 151' formed under slightly lower cooling rates than those in the Intermediate Unit at 174'.

Branches develop on a dendrite because unstable interfaces form when crystal growth rates increases with distance into the melt, and any perturbation can grow quickly (Weston and Rogers 1978). The impurity-rich layer adjacent to the crystal growth-front has an equilibrium melting temperature lower than that of the melt as a whole, such that the effective supercooling increases from the interface into the melt (Weston and Rogers 1978, Rutter and Chalmers 1953, Tashiro et al 1975, Lofgren and Donaldson 1975). With less supercooling immediately adjacent to the crystal, and a decrease in the supercooling gradient between the fibres, lateral growth between the fibres is inhibited, favouring elongate crystals.

A growing olivine crystal must preferentially incorporate magnesium and to a lesser degree iron while rejecting other elements of the melt. High cooling rates suggest high diffusion rates, although with extreme cooling rates, skeletal protrusions may penetrate (and sample) "fresh" melt without the requirement of long-range diffusion occurring. These protrusions may therefore propagate rapidly, yielding a skeletal olivine crystal with near-equilibrium Fe/Mg ratios, as is the case in Band 10/174'.

Variation in crystal morphology and groundmass crystal diameter indicate changing cooling rates across

the dyke. Skeletal olivine phenocrysts in Bands 1-2/174' and the Central Unit indicate rapid cooling of the magma. Matrix crystal diameter increases across Bands 2-7/174 suggesting slowing cooling rates, with Bands 9 and 10/174' cooling rapidly for comb-texture to develop.

6.6 Comb-layering.

Moore and Lockwood (1973) noted the close relationship between comb-layering and orbicular layering in granitoid intrusions and argued similar conditions were required for the development of these textures. This relationship has also been noted elsewhere (Enz et al 1979, Elliston 1984, Vernon 1985).

Conditions required for development of comb-layering include zero or only a small proportion of suspended crystals of the comb-layered phase present in the magma (Donaldson 1977). This absence of nuclei delays crystallisation and allows supercooling, which promotes dendritic growth and the constitutional supercooling responsible for development of compositional layering (Lofgren and Donaldson 1975, Lofgren 1980).

Lofgren (1983) and Donaldson (1979) have shown experimentally that slight superheating can destroy nuclei of a particular phase (especially framework silicates), inhibiting crystallisation of that phase on

later cooling. Comb-layered rocks may have crystallised from previously superheated magma.

Sudden intrusion of hot mafic magma into felsic or intermediate magma can cause superheating, especially at higher confining pressures, which depress the water-saturated liquidus (Whitney 1975), although more mafic magmas at lower confining pressures and with low-water contents would be less likely to undergo superheating in this way (Vernon 1985). A more probable mechanism is introduction of water into a water-undersaturated magma (Moore and Lockwood 1973), which lowers the liquidus temperature causing effective superheating.

Water content of the magma may be responsible for layering, as hydrous magma may undergo effective superheating while less-hydrous parts still contain crystal nuclei (Vernon 1985). Removal of nuclei by superheating can promote later supercooling, and if the melt becomes water-saturated, local pressure-release could induce further supercooling (Lofgren and Donaldson 1975).

The delay in olivine nucleation increases systematically with decreasing supercooling, cooling rate, olivine content of the melt and increasing melt viscosity (Donaldson 1979). Increased superheating increases the delay in nucleation at a given degree of supercooling (Donaldson 1979), but does not alter significantly the nucleation temperature, with olivine-

rich melts nucleating at smaller degrees of supercooling (Donaldson 1979).

An olivine may nucleate in a crystal-free melt:

- 1) by heterogeneous nucleation on a foreign particle,
- 2) by heterogeneous nucleation on an alumino-silicate polymeric unit of the melt structure and
- 3) by homogeneous nucleation (Donaldson 1979).

Suggestion 1 is unlikely to be the normal type as both the cooling rates and amount of superheating affect the delay in nucleation. Suggestion 2 is unlikely, as the required number of polymer units is unlikely to be present. Furthermore, if this was the case, the viscous terrestrial basalts would be expected to nucleate olivine more readily than the less-viscous lunar basalts. Donaldson (1979) has proved this not to be the case and concludes that olivine nucleation is homogeneous.

Several authors (Kirkpatrick 1975, 1981, Lofgren 1980, Donaldson 1976, 1979) state that crystal morphology is related to supercooling and supersaturation. Dendritic growth requires supercooled liquid ahead of the solidification front (Rutter and Chalmers 1953, Lofgren 1974a), which occurs when heat is extracted from the liquid faster than the rate of solidification (thermal supercooling) or when liquidus depression of the melt attains a steeper profile than the thermal profile towards the solid/liquid interface (constitutional supercooling) (Tiller et al 1953). Moore and Lockwood

(1973) state that water-undersaturated magma may be effectively superheated by rapid movement of the magma upwards. Lofgren (1980) found comb-texture developed readily under moderate to high degrees of supercooling, with curvature of the dendrite due to kinetic factors.

Comb-texture may have been initiated due to the magma in the dyke being superheated by intrusion of water-bearing magma into a water-undersaturated magma, causing effective superheating by lowering the liquidus temperatures. Superheating may destroy crystal nuclei thereby causing the magma to contain few crystals. Superheating delays nucleation and can promote supercooling. Due to lack of crystals in the melt, minerals crystallise onto crystals forming the walls of the dyke.

Where one mineral nucleates on another mineral (comb-textured olivine on comb-textured plagioclase, comb-textured pyroxene on comb-textured olivine or comb-textured pyroxene on matrix plagioclase in the dyke) it has done so in the static boundary layer and indicates constitutional supercooling for the nucleating mineral. In this context, supercooling equals supersaturation.

The comb-textured olivines exhibit slight, normal zoning along the branches of the dendrites but no zoning along the dendrite itself (cf Preston 1963, Walker 1985), suggesting steady state conditions prevailing during

growth. The forsterite content of the olivine dendrites increases across Band 10/174' (cf Walker 1985), possibly due as temperature rises in stagnant magma on release of latent heat of crystallisation (cf Wilson 1989).

Alternating layers of comb-textured olivine- and plagioclase and comb-textured pyroxene have developed due to oscillating chemical reactions in the crystallisation front of the solidifying magma (McBirney and Noyes 1979). This is achieved by supersaturation of one or more minerals in the boundary layer of a growing crystal. Before the comb-textured pyroxene in Band 9/174' and adjacent to the Central Unit, there has been abundant plagioclase and olivine crystallising, enriching the melt in pyroxene components. Assuming isothermal crystallisation, as the cooling melt nucleates and crystallises olivine and plagioclase (Phase A in Figure 6.1), the latent heat of crystallisation is removed through the solidified crystals. Only crystals orientated with their fastest growing axis normal to the thermal and supersaturation gradients will be able to keep pace with the initial growth rate and continue crystallising, while less favourably orientated crystals gradually cease growing (Petersen 1985). Continued crystallisation of olivine and plagioclase drives the composition of the chemical boundary layer (which has a lower liquidus temperature than the bulk melt) towards the left until it becomes supersaturated in pyroxene

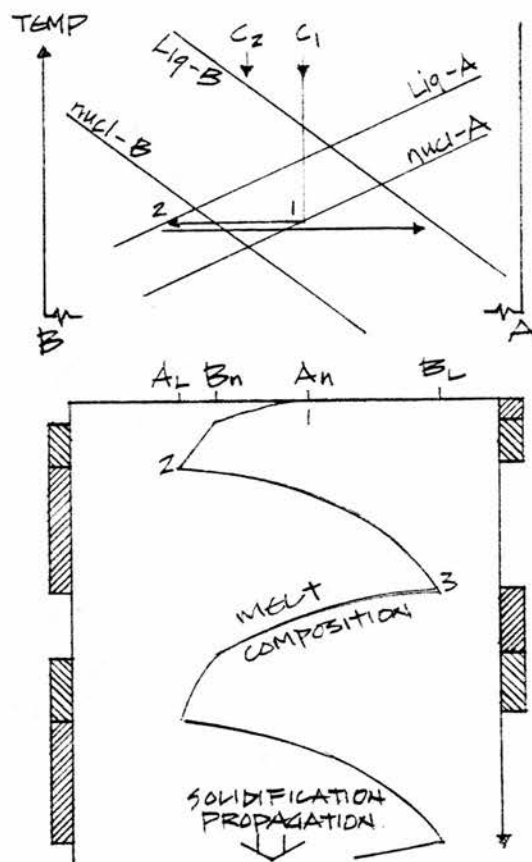


Figure 6.1 Alternating phase-layering of comb-textured minerals interpreted as the result of competitive nucleation and growth of successive liquidus phases in supersaturated conditions. (From Petersen 1985)



Monophase layers



Two-phase (transitional) layers

A_L

A_n Liquidus and nucleation temperatures for A and B respectively.

B_L

B_n

components (Phase B) and passes Phase B nucleation curve, allowing pyroxene to nucleate and crystallise. This reduces the concentration of Phase B components in the melt. If Phase B has a higher growth rate than Phase A, it takes over the nucleation front and encloses nuclei of the slower growth phase (Phase A-olivine and plagioclase), preventing their further growth. Phase A components then accumulate in the boundary layer liquid, driving its composition towards the right.

The melt then passes the nucleation curve for Phase A, which once more nucleates and grows. Prevention of Phase B (pyroxene) nucleation may be achieved if latent heat of crystallisation is not removed rapidly enough along the olivine dendrites, causing the interface temperature to rise above the liquidus temperature for Phase B (pyroxene), but allowing continued growth of Phase A (olivine and plagioclase). The cycle can then commence as before.

Comb-textured olivine- and pyroxene may overlap (0.5-4mm in width), indicating that both minerals can precipitate contemporaneously before growth of olivine is prevented (Figure 6.1). Comb-textured olivine often crystallises from a plagioclase crystal, while comb-textured pyroxene frequently anchors onto comb-textured olivine. Pyroxene frequently grows along the olivine crystal indicating this direction to be perpendicular to the thermal and supersaturation gradients. Petersen (1985) states that the inner margin of the slower growing

mineral tends to be gradational (uneven), with the relationship between comb-textured olivine and pyroxene in the overlap region of the alternating layers suggesting olivine is the slower growing mineral phase.

6.7 Relationship between Amygdales (zeolite) and Pyroxene.

Kushiro (1964) noted olivine and plagioclase decreasing at the expense of augite and zeolite in the Atumi Dolerite, Japan. This is similar to north to south lateral variation in the banding of the dyke (Chapter 2). Magma flow from the north to the south is in agreement with this. Kushiro (1964) states that zeolite crystallises as late differentiates from residual liquids of the magma. Crystallisation temperature of analcite is less than 550°C with H₂O pressures <1000 bars as inferred from experiments by Yoder (1950) (Kushiro 1964).

The banded Atumi dolerite contains bands of more- or less-resistance to weathering. The less-resistant bands are areas where volatiles were concentrated during solidification of magma (Kushiro 1964), with concentration of volatiles causing cavities, which weather preferentially. This is similar to the Mystery Dyke, where the non-amygdaloidal Intermediate Unit forms

upstanding ridges and the amygdaloidal Central Unit is preferentially eroded.

Iddings (1887) ascribed alternating bands of dense glassy rhyolite and highly vesicular pumiceous rhyolite to be the result of fluid flow, but concluded that the differences in texture were due to unequal concentrations of volatiles that had been drawn out by flowage. Fuller (1927) considered unequal concentrations of volatiles to be due to preferential partitioning of volatile components as a result of fluid flow.

As crystallisation proceeds, the dyke cools from both contacts towards the centre, with volatiles being concentrated in the residual liquid. Kushiro (1964) states that these volatiles could begin to separate at certain temperatures and pressures (so called second boiling). As second boiling proceeds, vapour pressure increases, but if pressure on the magma is released- in the case of the dyke possibly by extension of the dyke southwards, the pressure would not rise beyond a certain limit. If pressure was periodically released, (possibly by extension of the dyke), this allows periodic rise and fall in volatile content, causing vesicle concentration within certain bands.

Shaw (1969) noted that thermal feedback (where the temperature of the magma could theoretically increase over a short-time period) may be an important factor in

vesiculation. If heat is generated in the liquid faster than it can be conducted away (eg latent heat of crystallisation) the energy balance approaches the adiabatic case, and local temperatures can increase over a shorter or longer period (minutes to days). Decreasing viscosities result in increasing strain rates, causing more heat to be generated. Thus, if heat is not conducted away fast enough, further temperature increases ensue until a runaway situation occurs.

Nelson (1981) considered that thermal feedback could play a role in the formation of alternating vesicular and non-vesicular banding in a laminar-flowing acid magma. Solubility of a volatile phase at low pressure decreases with increasing temperature, thus, if the liquid is near-saturated with H_2O , increasing temperature due to fluid flow could cause the separation of a gaseous phase, resulting in vesiculation of the lava. The increased temperature within such a layer would further aid vesiculation since diffusion coefficients, bubble-nucleation rates and bubble growth rates all increase with increasing temperature (Shaw 1974, Murase and McBirney 1973, Sparks 1978,). Concentration of interstitial liquid expelled from the cumulus pile may also have accumulated locally as veins.

6.8 Olivine and Melt Equilibrium Compositions.

Interpretation of the crystallisation record of porphyritic rocks often proves to be equivocal due to possible two-stage crystallisation history. Although many porphyries do have a two-stage cooling history, the presence of phenocrysts does not necessarily mean a two-phase cooling history (Bowen 1914, Lofgren et al 1974, Walker et al 1976).

Roeder and Emslie (1970) and Walker et al (1976) state that olivine composition is virtually independent of temperature, depending strongly on the magnesium to ferrous iron ratio of the melt in which the olivine is crystallising. Roeder and Emslie (1970) produced the data for Figure 6.2, showing the relationship between equilibrium olivine and magma composition. This figure can also be used to determine whether an olivine of particular composition could crystallise from a liquid with a particular magnesium:ferrous iron ratio. Mole % fractions were calculated per band at 174', for "melts" including all olivine phenocrysts and "melts" minus all olivine phenocrysts. It was assumed all iron in the olivine was FeO. Results are shown in Figure 6.2 and Table 6.1. Also shown is the calculated composition of olivine in equilibrium with a "melt" composition equivalent to Band 1/174' minus 13wt% olivine phenocrysts.

Table 6.1

Equilibrium Temperatures and Olivine compositions for Banding at 174'
as calculated from Mole% MgO and FeO in the liquid.
(after Roeder and Emslie, 1970)

Band:	Calculations of melt including all olivine phenocrysts			Calculations of melt being olivine phenocryst-free		
	Temp. °C	Oliv. compn. (Phen.) Fo	Range of Oliv. phen compn. (from Ch 4) Fo	Temp. °C	Oliv. compn. (Gms) Fo	Range of Oliv. gms compn. (from Ch 4) Fo
Band 1/174'	1305	88	88-77	1100	74	61-58
Band 2/174'	1310	88	85-84	1140	78	no data
Band 3/174'	1255	85	88-83	1200	81	60
Band 4/174'	1200	82	85-82	1080	71	62-54
Band 5/174'	1190	82	87-78	1160	80	59-57
Band 6/174'	1220	83	86-64	1150	77	57
Band 7/174'	1220	82	86-82	1160	77	no data
Band 8/174'	1180	81	87-62	1180	80	63-58
Band 9/174'	1230	88	64	1225	88	66-58
Band 10/174'	1250	89	no phen.	1250	89	69-67
Band 11/174'	1250	86	84-75	1175	82	58-46

Calculation of melt minus
12.98wt% Oliv. phen.

Temp.	Oliv. compn. (Phen) Fo
1205	84

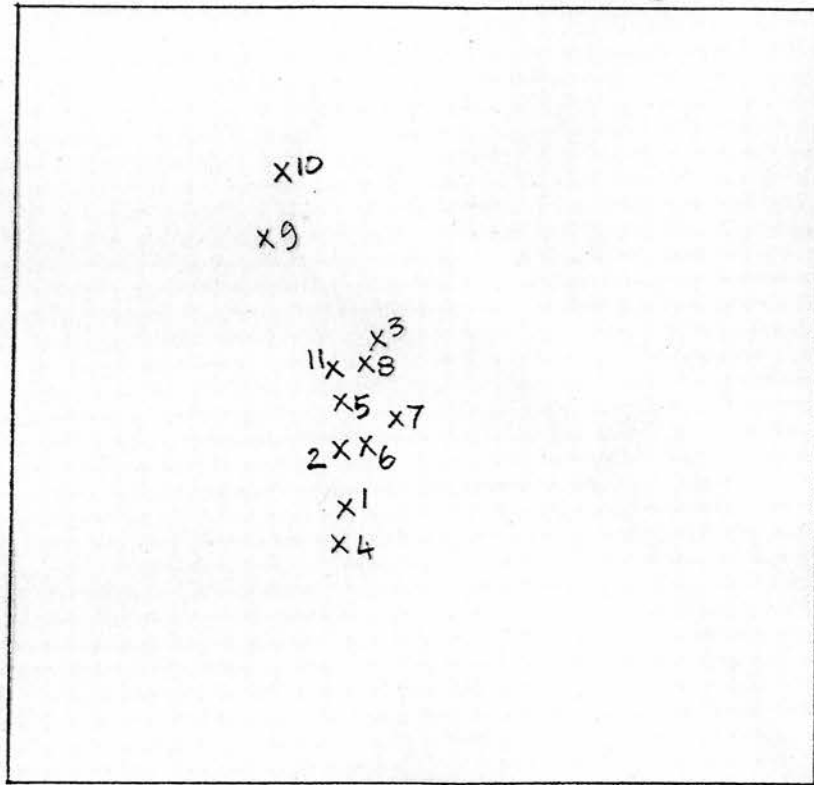


Figure 6.2b Olivine Groundmass Crystal Composition per band in equilibrium with the melt (calculated for a dry, zeolite-free, olivine phenocryst-free whole-rock composition). (From Roder and Emslie 1970) All iron in the olivine was taken as FeO.

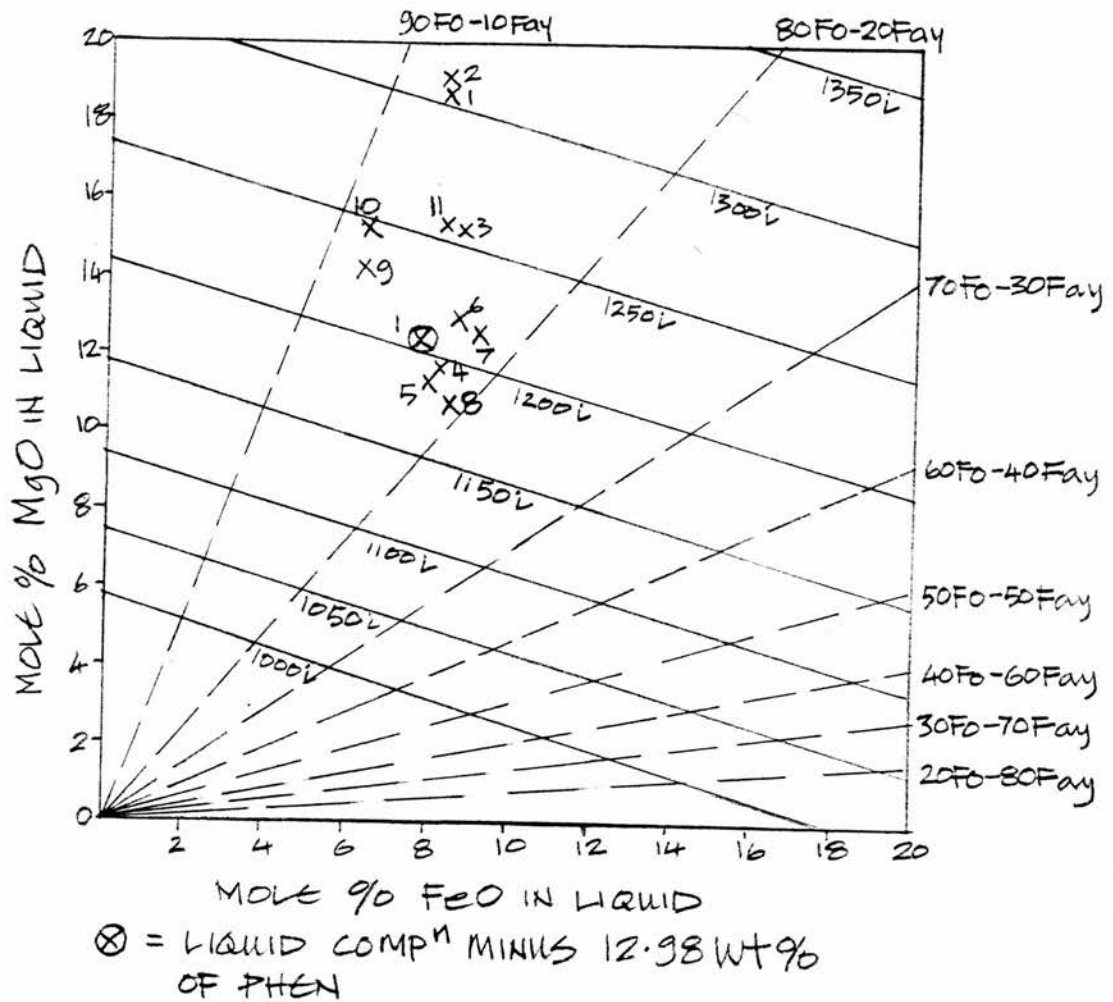


Figure 6.2a Olivine Phenocryst Composition per band in equilibrium with the melt (calculated for a dry, zeolite-free, whole-rock composition). (From Roder and Emslie 1970) All iron in the olivine was taken as FeO.

Calculated olivine compositions are generally within the phenocryst compositional ranges, with the exceptions of Bands 2, 9 and 11. Bands 2 and 11 have calculated olivine compositions slightly in excess of analysed values, possibly due to analytical and calculation errors. This suggests that the olivine phenocrysts could have crystallised from the melt represented by each band composition with the exception of Band 9/174'.

The liquid FeO:MgO ratio per band was calculated. Band 10/174' (olivine phenocryst-free) was the only band to have an actual FeO:MgO ratio similar to calculated (1:2.36 compared to 1:2.32) proving that some phenocryst growth took place outwith the band that the phenocrysts are found in.

Calculated groundmass olivine composition (Table 6.1, Figure 6.2) is higher than analysed compositions, implying that groundmass crystals are not in equilibrium with the melt or more probably olivine phenocrysts growth continued in the dyke.

6.9 Mineral Chemistry.

Irvine (1975,1978) states that each inflow of magma to an intrusion is marked by setback of fractionation marked by Mg/Fe ratios in olivine (Cameron 1980). Matrix olivines in the dyke show a gradual decrease

across Bands 1-6/174', then the Fo content increases across Bands 8-10/174', with a marked decrease in Band 11/174'.

Phenocrysts close to the sill are unzoned due to rapid chilling of the magma, but with increasing distance into the dyke, compositional zoning is evident (Figures 4.1, 4.2, 4.4). In the outer bands, matrix crystals and phenocrysts are of similar composition but diversity widens to a maximum in Bands 4-6/174'. Band 5/174' contains both zoned and unzoned olivine phenocrysts of similar core composition. These two types suggest that zoned phenocrysts were cooling in the dyke from the first pulse of magma, whereas the unzoned ones may represent the initiation of flow of a fresh pulse of magma, and slight mixing with the melt already in the dyke. Plagioclase phenocryst composition varies little until Band 5/174', where a greater range of core compositions is found, in agreement with the suggestion of another pulse of intruding magma. Association of high forsterite and high anorthite phenocrysts indicates associated crystallisation of olivine and plagioclase.

Olivine groundmass crystals exhibit a wide range of core compositions across the width of the dyke, and have narrow, normally zoned rims indicating changing thermal and chemical gradients. Groundmass olivines in Bands 4 and 8/174' are of comparable compositions to the iron-rich phenocryst rims indicating that both were in

equilibrium with the melt. However, in Band 9/174' they may be more magnesian than the phenocrysts, with magnesium content of matrix crystals continuing to increase into Band 10/174'. This indicates that the phenocrysts did not form in the dyke and are not in equilibrium with the melt. Increasing forsterite composition of the matrix olivines may be due either to latent heat of crystallisation allowing crystals to form at slightly higher temperatures than adjacent ones or to changing thermal and chemical conditions accompanying integration of new magma into the dyke.

The high CaO content of olivine phenocrysts is indicative of unequilibrated growth or growth in high crustal conditions (Simkin and Smith 1970), and may be explained by crystallisation in a high-level crustal magma chamber prior to eruption of the magma and crystal mush into the dyke conduit (cf Gibson 1988, 1990).

No patterns of zoning of pyroxene are seen across or along the dyke. Maximum zoning is found in matrix crystals in the chilled margin, while those in the Central Unit are unzoned. Phenocryst cores exhibit greater variation in composition than rims, having nucleated in more than one location but continued growth under common conditions. Pyroxene phenocrysts may be normally or reversely zoned. Band 4/174' contains reversely zoned phenocrysts and matrix pyroxenes while in

Band 5/174', phenocrysts are normally zoned, and matrix pyroxenes reversely zoned, both to a comparable composition. Sudden reverse zoning of phenocrysts may indicate increasing magma temperature due to another pulse of magma or to decompression (Ewart et al 1975) caused by sudden propagation of the dyke fissure, or to magnetite crystallisation (Gill 1981) though this is unlikely as the modal percentage of oxides remains constant over the outer 4 bands, or to an increase in fO_2 due to a pre-eruptive influx of H_2O (Luhr and Carmichael 1980).

The dyke pyroxenes contain high contents of Al_2O_3 , which due to substitution of SiO_2 by Al_2O_3 , and high TiO_2 (as do sill pyroxenes). Wass (1973) found TiO_2 and Al_2O_3 varied inversely with SiO_2 content of sector-zoned pyroxenes. B.V.S.P. (1981) states that high Al_2O_3 , TiO_2 and Na_2O are due to rapid cooling while Kouchi et al (1983) found Ti and Al increased with increased supercooling. Wass (1973) envisaged rapid growth for development of sector zoning (cf conditions for comb-textured growth), due possibly to quenching of a melt supersaturated in a mineral.

Plagioclase exhibits maximum zoning (An30%) in Band 5/174' with Bands 6 and 7/174' also containing highly zoned (normal) crystals. Matrix plagioclase shows a widening compositional range across Bands 1-6/174' due to slower cooling with distance into the dyke. Comb-textured plagioclase has a restricted composition with no

chemical variation along or across crystals, suggesting crystallisation under constant conditions.

6.10 Whole-Rock Geochemistry.

The dyke is mildly alkaline in composition, and consists of more than one pulse of magma. Trace element geochemistry supports major element evidence and shows the dyke to be relatively enriched in Ni, Cr and V and depleted in Nb, Zr, Rb, Ba and Ce compared to average basalts (Taylor 1964, Krauskopf 1967).

Differentiation of the melt has occurred across Bands 1-5 and 7-9/174', with SiO_2 content of these bands increasing, while Bands 5-7/174' have decreasing silica content. This is in agreement with concentration of olivine, pyroxene and/or spinel. SiO_2 -MgO and Na_2O -MgO variation diagrams (Figures 5.5a and 5.5g) suggests fractionation of olivine across Bands 2-5, and CaO-MgO (Figure 5.5f) across Bands 2-4/174'. Ni-MgO (Figure 5.8e) exhibits an olivine fractionation trend across Bands 6-8/174. Reversal of this trend across Bands 5-6 and 9-10/174' suggests olivine accumulation in the melt, possibly due to a fresh pulses of magma being intruded.

Chromium is an indicator of pyroxene and/or spinel fractionation, and its variation in the dyke suggests fractionation occurred across Bands 2-5, 6-8 and 9-

10/174' (Figure 5.8f). Spinel and olivine have associated crystallisation histories, therefore fractionation of spinel and olivine is reflected in the trends seen in the variation diagrams.

In the dyke, (Figure 5.11) olivine, plagioclase then pyroxene is expected to reach their liquidus. Computer modelling (MAGMODEL) also calculated that olivine and plagioclase should reach the liquidus first followed after a few degrees of cooling by augite and magnetite, is in agreement with the phenocryst phases present.

Computer modelling suggests that olivine and plagioclase crystallise first at approximately 1200°C, and augite and magnetite start to precipitate slightly later. The Mass Balance Mixing programme (MIX) indicates that Band 1/174' can be the parent to Bands 2-5/174' by removal of olivine, plagioclase, pyroxene and oxide respectively, and Band 6/174' could be the parent magma to Bands 7-10/174', predominantly by addition of plagioclase and pyroxene to Band 6 composition. This suggests at least three intrusive pulses of magma.

6.11 Magma evolution in a chamber beneath the dyke.

A unique feature of liquid fractionation by differentiation involving compositional convection resulting from crystallisation or melting of the walls of a shallow chamber is the ability to segregate highly differentiated liquids without gravitational settling of large proportions of crystals (McBirney et al 1985). The densities of the liquids are a function of temperature and composition, both of which may alter during crystallisation (McBirney et al 1985), with the convection of basaltic magma in the chamber depending on changes caused by density changes in the magma as it crystallises (Sparks and Huppert 1984). Density of the magma decreases during the fractionation of olivine, olivine-pyroxene and pyroxene assemblages, but plagioclase may lead to the melt becoming denser (Sparks and Huppert 1984).

Magma chambers must be assumed to be open systems (Turner and Campbell 1986, O'Hara and Mathews 1981). O'Hara (1977) states that there is no requirement for a magma chamber ever to be large, as inflow could equal outflow. Turner and Campbell (1986) state that high-level chambers are vertically stratified with regard to composition, density and temperature. Immediately after an injection of magma into a chamber, there may be turbulent convection, with this diminishing with

crystallisation, due to increased viscosity, decreasing temperature and chamber size (Turner and Campbell 1986). Hildreth (1979) agrees with compositional and thermal zoning in chambers but also states that there may be variation in trace element concentration throughout the chamber, with little variation in major element concentration (cf Table 5.1).

An influx of hot, dense, ultrabasic magma into a chamber containing a lighter, fractionated basaltic magma will not mix, but spread over the floor forming a distinct layer (Huppert & Sparks, 1980, Sparks et al 1980, Stolper & Walker 1980; Huppert & Turner 1981 and O'Hara & Mathews 1981). Both layers convect as heat transfer to the upper layer proceeds until both layers they are of approximately equal temperature, with equilibrium fractionation of olivine. Only at this time do olivines begin to settle from the melt. These olivines should be of uniform composition due to formation in a well-mixed, convecting magma.

An influx may act as a mechanism for eruption (Brown 1956, Sparks et al 1977). O'Hara (1968) states that if the chamber was replenished with primitive magma, this may trigger eruption of porphyritic magma.

Weissberg (1962) stated that a Newtonian fluid in a flat-topped chamber would approach a cylindrical conduit in the roof from all directions, not just directly from below it. Velocity varies from fastest immediately

below the pipe to slowest nearer the roof. Due to volumes erupted, the chamber may be tapped 2-5km below the roof, with the deeper layers contributing greater amounts of magma than shallow layers. Blake (1981) states that approximately half of erupted lavas represent material from the deepest part of the magma chamber, with little chemical variation across basalt flows due to turbulent currents in the magma chamber and erupted magma representing a mixture of several horizons of the chamber. Once eruption has started to tap basal layers, this flows more rapidly than silicic melt, causing mafic material to be over-represented in the flow (Blake 1981).

With laminar flow, physically distinct magmas will be sheared out into thin sheets parallel to the walls suppressing homogenization. This process may have assisted in the development of the banding along the dyke. Phenocryst-poor and phenocryst-rich bands are suggested to be evidence of the sampling of heterogeneous magma chamber.

Olivine phenocrysts have near-constant core compositions (Figures 4.1, 4.2, 4.4), indicating formation in a well mixed, convecting magma chamber. However, there are two groups of phenocrysts depicted in Band 8/174' (Figures 4.1, 4.4), proving the magma chamber was not entirely homogeneous, and possibly representing two distinct layers within the chamber, or, as the lower

forsterite group are smaller phenocrysts, later formation at slightly lower temperatures.

McBirney (1979) stated that crustal contamination was greatest when wall-rock differed from magma. In the case of the dyke, this must have been lessened due to similarity between it and sills and the lavas into which it intruded, although it is significantly different to underlying Jurassic rocks. Laminar flow allows little contamination as magma crystallises along the conduit, walls preventing contamination.

6.12 Relationship between the Dyke and Sills.

The dyke has intruded along the sill's hexagonal cooling joints, and continuance of some joints across both sill and dyke suggests that the sill was still warm when the dyke intruded, with both intrusions thereafter cooling as one. The irregular contact between the sill and the dyke could be better understood if visible in three-dimensions.

Gibson (1988) and Gibson and Jones (1991) state that the picrites, picrodolerites and crinanites in the Little Minch Sill Complex are genetically related, resulting from multiple intrusions from a zoned magma chamber in

the upper crust. They conclude that picrites with 18-30wt% MgO are olivine cumulates and crinanites (3-8wt% MgO) are olivine-poor fractionates of an alkali olivine basalt (10wt% MgO). Gibson (1988, 1990) states that the sills were emplaced as a series of multiple intrusions, but with isotopic evidence suggesting that their genetic relationship with the overlying lavas (S.M.L.S.) is more complicated than previously thought.

Gibb and Henderson (1989) noted chills within the Shiant Isles Sill indicating multiple intrusion of near-identical magmas, although continuous columnar jointing indicates that the sill later cooled as a single unit.

Donaldson (1977) and Thompson et al (1980) conclude that substantial magma reservoirs did not exist below Skye but were in the form of numerous sub-volcanic conduits and fissures with poor lateral connections.

The sill complex has greater chemical variation (picrite-picrodolerite-crinanite and pegmatite) than the dyke suggestive of a larger and possibly zoned chamber. Extended periods between extrusion of pulses would allow greater time for differentiation to occur in the chamber, rather than the dyke having formed by pulses of almost identical magma.

The petrogenesis of the Little Minch Sill Complex was summarised by Gibson (1988) to include partial melting of the mantle to produce alkali basaltic magma, which then ascended with some fractionation to a magma chamber in the crust, where some fractionation of olivine

and spinel took place, together with some crustal assimilation. The magma was then intruded at high discharge rates into the Jurassic sediments, in the form of a multiple intrusion. In situ differentiation and filter pressing caused interstitial liquid to form pegmatite veins.

The petrogenetic model proposed by Thompson et al (1972) for the S.M.L.S. was for nepheline-normative basalts to represent minimal partial melts of a phlogopite-garnet-peridotite mantle, while hypersthene-normative basalts represent greater partial melt fractions of the same rock.

The sill contains olivine with lower forsterite content and which contain oxides with higher SiO_2 and TiO_2 and lower FeO^t than those in the dyke. This suggests that the feeder chamber for the sill was situated at a higher -level than the feeder chamber for the dyke.

6.13 Petrogenetic Processes.

Several petrogenetic schemes have been examined and applied to the "Mystery Dyke" in an attempt to explain observed features. These include closed and open system behaviour. Band 1/174' composition (the chilled margin)

is assumed to represent the parental magma at the initiation of magma flow into the dyke.

The schemes examined were:

- 1) Closed system, in situ fractionation of a single intrusion of magma in stagnant conditions.
- 2) A closed system with differentiation by fractional crystallisation. Compositional convection is assumed to be the dominant fractional crystallisation mechanism, together with congelation fractionation.
- 3) An open system with continuous flow of magma from a single magma chamber.
- 4) An open system with through flow of magma as pulses. This is a composite/multiple intrusion scheme of which there are possible sub-categories.

Scheme 1) The simplest possible history is formation by one pulse of magma and crystallisation under closed system conditions. Variations across the dyke must then be caused by processes operating within the dyke itself. Changes in chemical composition across the dyke would be caused by fractional crystallisation, involving material transport in the magma at right angles to the wall. Fractionation arises by crystals of early-formed bands being isolated from the magma by crystals of younger bands.

The earlier section relating to calculated cooling times show that the dyke would have substantially cooled

within a very short-time span, meaning that processes acting within the dyke must occur quickly.

Several features are inconsistent with fractional crystallisation of a stagnant sheet of magma, which would be expected to result in a steady change in magma composition, mirrored by systematic variation in mineral composition from band to band. This mechanism cannot account for the existence of discrete bands, as no sudden variation in magma composition should occur.

If fractional crystallisation of stagnant magma is the origin of the dyke, the "dyke" composition of Bands 1-1/211/174' should equal Band 1/174'. The "dyke" composition was calculated by weighting band compositions based on the thicknesses of each band. The compositions are as follows:

Band 1/174'		Band 1-1/211/174'	
composition:		composition:	
SiO ₂	45.99 wt%	46.70 wt%	
TiO ₂	1.50	1.40	
Al ₂ O ₃	14.11	16.60	
FeO ^t	12.71	11.56	
MnO	0.21	0.18	
MgO	12.21	9.18	
CaO	10.09	10.40	
Na ₂ O	2.39	3.30	
K ₂ O	0.49	0.40	
P ₂ O ₅	0.18	0.17	

The discrepancy between the two compositions in Al, Fe, Mg and Na is too great to be attributed to analytical and calculation errors. The "dyke" bulk composition is enriched in normative plagioclase and nepheline and depleted in olivine relative to Band 1/174' (Table 5.5).

Mass Balance Mixing Calculations (MIX) were considered in Chapter 5. Table 5.8 details the lowest R^2 for various combinations of mineral extracts. For the single pulse, closed system scheme, there should be no addition to the solution. Only Bands 2-5/174' are acceptable daughter compositions from a parent magma of Band 1/174', with an $R^2 < 1$.

Curved, concentric banding implies some movement of magma during formation of the dyke and rules out fractional crystallisation of a stagnant magma. Furthermore, the internal chill developed within the comb-textured pyroxene lamina along the contact of the Intermediate and Central Units, may implicate more than one pulse of magma. Thus geochemically and petrographically this hypothesis is unsatisfactory and can be discounted.

Scheme 2) In this scheme, a closed system is again envisaged with differentiation by fractional crystallisation and compositional convection being the dominant mechanism. In compositional convection, growth of a crystal on the wall of the intrusion produces a film

of solute-depleted melt around the crystal, with the melt having a different density to more distant melt and will move up or down relative to the crystal. Sparks et al (1984) found compositionally and density-graded film around growing crystals in a basaltic magma chamber to be unstable and continual convection of differentiated liquid should occur away from the growing crystals (convective fractionation). As a result, there will be enrichment-depletion of the melt in contact with the mush on the walls with respect to the various minerals. This could trigger the appearance or disappearance of minerals and generate modal layering. Once again, fractionation arises by crystals of early-formed bands being isolated from the magma by crystals of younger bands. This is stated to be a closed system, but there is enhanced vertical transport of melt constituents occurring.

Strictly, this hypothesis is untestable, because there is no access to the rock below or that which lay above current level of exposure; thus no mass-balance calculations can be performed as was possible for hypothesis 1. Nonetheless, time relations are not encouraging. Thermal diffusion is relatively rapid compared to chemical diffusion ($3-5 \times 10^{-3} \text{cm}^2 \text{ s}^{-1}$ and $10^{-5}-10^{-10} \text{cm}^2 \text{ s}^{-1}$ respectively (McBirney et al 1985). As a result, the thermal boundary layer tends to be wider than the compositional boundary layer. It is difficult to believe that in less than 24 hours (cooling time of the

dyke based on the calculations of Jaeger 1968) compositional convection could be effective.

Scheme 3) This is an open system with a constant flow of magma through the dyke. Two sub-categories are considered:

a) Each band represents frozen magma, with one source chamber supplying all magmas required to achieve the noted banding. Ways of achieving the necessary changes in magma composition include a zoned magma chamber or differentiation having occurred in the dyke at deeper levels than currently exposed. A zoned magma chamber was proposed by Gibson (1988, 1990) as the source of the multiple intrusions that compose the Little Minch Sill Complex. Constant through-flow of magma from a simple magma chamber being drained from top to bottom should initially show low liquidus temperatures followed by higher temperatures as lower levels of the chamber are drained. This is not the case for the dyke, where initial magma (Outer Marginal Sub-Unit) is olivine phenocryst-rich (Fo_{88-76}). Since the most forsterite-rich olivine phenocrysts analysed from the adjacent sill have a composition of Fo_{85} (this study), the abundant olivine phenocrysts have not been scoured from the sill and assimilated into the molten dyke on intrusion, but were intruded with the molten lava of the dyke, having crystallised either in the magma chamber itself or in the dyke conduit. The volume of olivine phenocrysts in Band

1 suggests crystallisation within the magma chamber, suggesting an olivine phenocryst-rich mush forming the lower levels of the magma chamber. The phenocryst-rich chilled margin requires this low level, phenocryst-rich horizon of the chamber to be drained early.

In detail, the intrusion might have formed as follows. The enrichment in olivine phenocrysts of the magma is attributed to crystal settling in the magma chamber. Bands 1 and 2/174' show high liquidus temperatures in MgO thermometry calculations (Temp) of 1238°C, with mean olivine phenocryst composition of Fo₈₆. Bands 1 and 2/174' are comparable but with increasing groundmass crystal diameter, increasing pyroxene and decreasing olivine content in Band 2/174' (Table 3.1), suggesting formation from similar magma with slower cooling rates for Band 2.

Band 3/174' shows a decrease in Fo content of the olivine phenocrysts to Fo₈₄, and a lower liquidus temperature of 1202°C. Pyroxene (matrix) has increased substantially and total olivine (both phenocryst and matrix) has decreased from Band 2. This decrease in olivine phenocryst content suggests that the band may have been formed from similar magma to Bands 1-2 that has undergone some degree of filter pressing reducing the volume of olivine phenocrysts, or alternatively, continuing flow from the chamber drained a slightly higher level, containing less cumulus olivine crystals

immediately after the initial expulsion of phenocryst-rich magma. Band 4/174' is modally very similar to Band 3 and may have formed from magma derived from the same horizon.

Plagioclase is the only abundant phenocryst phase in Band 5, suggesting continued tapping of the same horizon, or of a slightly higher layer in which plagioclase had been concentrated by gravitational floating.

The next band (6) is enriched in plagioclase compared to Band 5 and also contains more olivine phenocrysts. This may represent mixing of an influx of magma (containing some olivine phenocrysts) into the magma chamber. Bands 7-8 may represent continued flow from a single horizon, with decreasing olivine phenocryst content due to gravity settling, and increased plagioclase phenocryst content due to flotation in the chamber.

Band 9/174' contains few phenocrysts, mainly of plagioclase, suggesting a higher layer in the chamber being tapped. The Intermediate Unit (Band 10/174') contains comb-textured olivine, pyroxene and plagioclase, with no phenocrysts, possibly due to filter pressing. Mass balance calculations (MIX-Chapter 5) suggests a similar parent magma to that for Band 9/174'.

The Central Unit (Band 11/174') contains abundant phenocrysts, including notably the first abundant pyroxene phenocrysts. The calculated liquidus temperature is high (1205°C) and with the high phenocryst

content suggests magma again being drawn from a low horizon in the chamber. Phenocrysts have relatively high forsterite, anorthite and enstatite content (75-84% Fo compared to 77-88% Fo in Band 1/174', 67-70% An compared to 66-72% An in Band 1 and 39-42% En compared to 37%En in Band 2/174').

If there was a constant flow of similar magma, there should be little variation in liquidus temperatures calculated in the computer modelling programme TEMP, which varies from 1250°C (Band 10/174') to 1164°C (Band 8/174'), although the chemically and thermally zoned magma chamber as suggested to explain variations in the banding would show variation in liquidus temperatures.

This complex pattern of magma chamber draining required to produce the banding, petrology and mineralogy of the dyke make this hypothesis unacceptable.

b) In this sub-category, the banding represents differentiation of a continually flowing magma of a constant composition. This can be disregarded due to variations in the phenocryst compositions. Also the poor sum of the residuals squared calculated in the Mass Balance Calculations (MIX) from a parent Band 1/174' composition to daughter compositions of Bands 6-8 and 11/174' suggest that the banding cannot be explained by fractionation of a magma of constant composition.

Scheme 4) This is an open system with pulses of magma giving a composite or multiple intrusion hypothesis of which two sub-categories are discussed:

a) Four groups of bands are considered to represent four compositionally distinct pulses of magma, based on several lines of evidence, including whole-rock geochemistry, mineralogy, variations in R^2 in MIX calculations, variations in weight fractions of the mixing components in the previous calculations and calculated temperatures from the MgO geothermometry computer programme.

Pulse 1 represents Bands 1-5/174'

Pulse 2 represents Bands 6-8/174'

Pulse 3 represents Bands 9-10/174'

Pulse 4 represents Band 11/174'.

Each pulse is considered to be a closed system, although the dyke as a whole acts as an open system. Evidence of pulses include the chilled margin of the Central Unit and variations in mineral chemistry and whole-rock geochemistry. In this scheme, each pulse is intruded and forms a stagnant pool. This can be discounted due to reasons given in category 1 as movement has occurred within the dyke after intrusion of the magma. Furthermore, the daughter compositions are not equal to parent composition compositions (ie Bands 2-5 do not equal Band 1).

b) This is equivalent to 3b, but now there are several pulses rather than one, with each pulse continuing to flow along the conduit. The pulses noted in Scheme 4a are accepted also to be present here. This scheme has been accepted as a possible explanation for the development of the dyke, as it supports the evidence of magma movement, mineral zoning reflecting magma feeder chamber conditions, pulses of magma intruding into the dyke reflected in the zoning of matrix pyroxene crystals and major and trace element trends. Figure 6.3 shows a proposed view of the magmatic system.

In this scheme, magma is intruded into the dyke fissure and quenches forming a chilled margin (Band 1/174'). This is rich in olivine phenocrysts, and contains some plagioclase phenocrysts; both minerals have crystallised in the feeder magma chamber or at lower depths in the dyke fissure. Anderson and Dunham (1966) calculated that 17.5wt% olivine in the sills was emplaced as phenocrysts, with <10wt% phenocryst growth in situ. In the present study, computer modelling was carried out on several possible magma compositions allowing differing amounts of phenocryst growth in situ. In the case of the dyke, the considered acceptable composition required 13wt% olivine phenocryst growth prior to emplacement into the dyke, with 6wt% continued growth in situ.

Due to the high concentration of cumulus olivine phenocrysts in Band 1, a deep horizon of the magma chamber is proposed as the portion of the feeder chamber

initially drained. The phenocryst-rich pulse may have been triggered due to replenishment of the chamber itself (Brown 1956, Sparks et al 1977). As phenocrysts in the dyke are of approximately constant composition, they probably crystallised in a convecting environment in the chamber (Huppert and Sparks 1980).

Band 2 is considered equivalent to Band 1, but crystallisation at slightly lower temperatures and slower rates gave rise to slightly different characteristics.

Computer modelling programme MIX shows that Band 3 composition can be a daughter of Band 1 parent composition by fractionation of olivine (Table 5.*). SiO_2 -MgO and Ni-MgO variation diagrams (Figures 5.5a, 5.8e) also support continued fractionation of olivine. Figure 6.4 shows 4 possible extract mixes that could produce Band 3 from Band 1 composition, and places olivine, plagioclase then pyroxene in order of importance (average 47% olivine, 35% plagioclase, 18% pyroxene). These diagrams were produced following procedures in Chapter 6, Cox et al (1979). The three-phase triangles for the lever-rule figures cannot be reproduced in this thesis due to their complexity, and only the three-phase triangles showing possible best-fit mineral extracts, which were drawn using information obtained in the lever-rule figures have been reproduced. The term "mineral extract" may be misleading as the minerals may be added to, or subtracted from the parent composition to obtain the daughter composition.

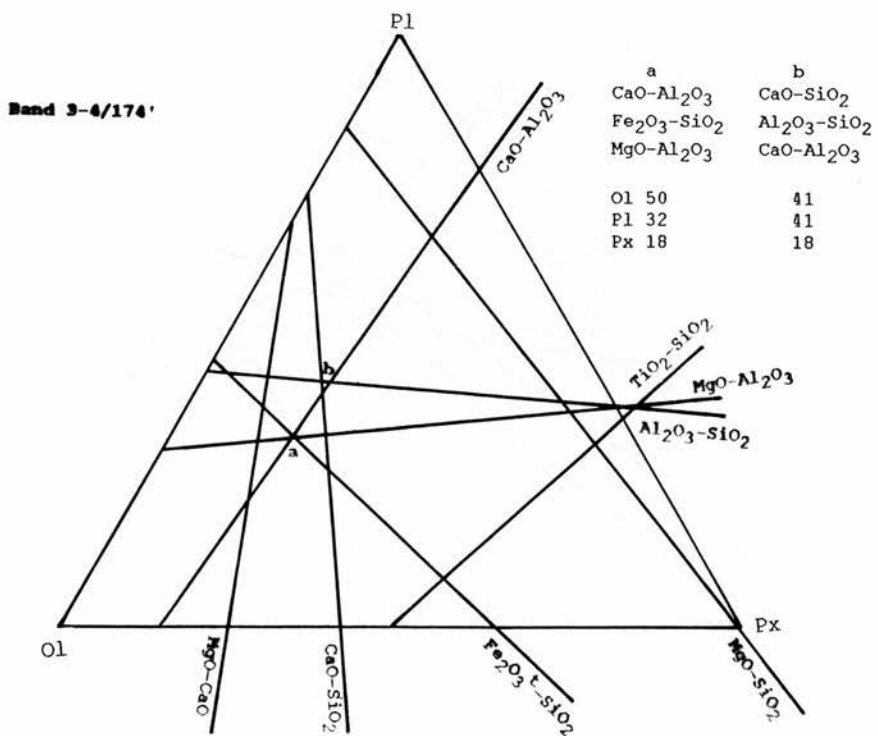
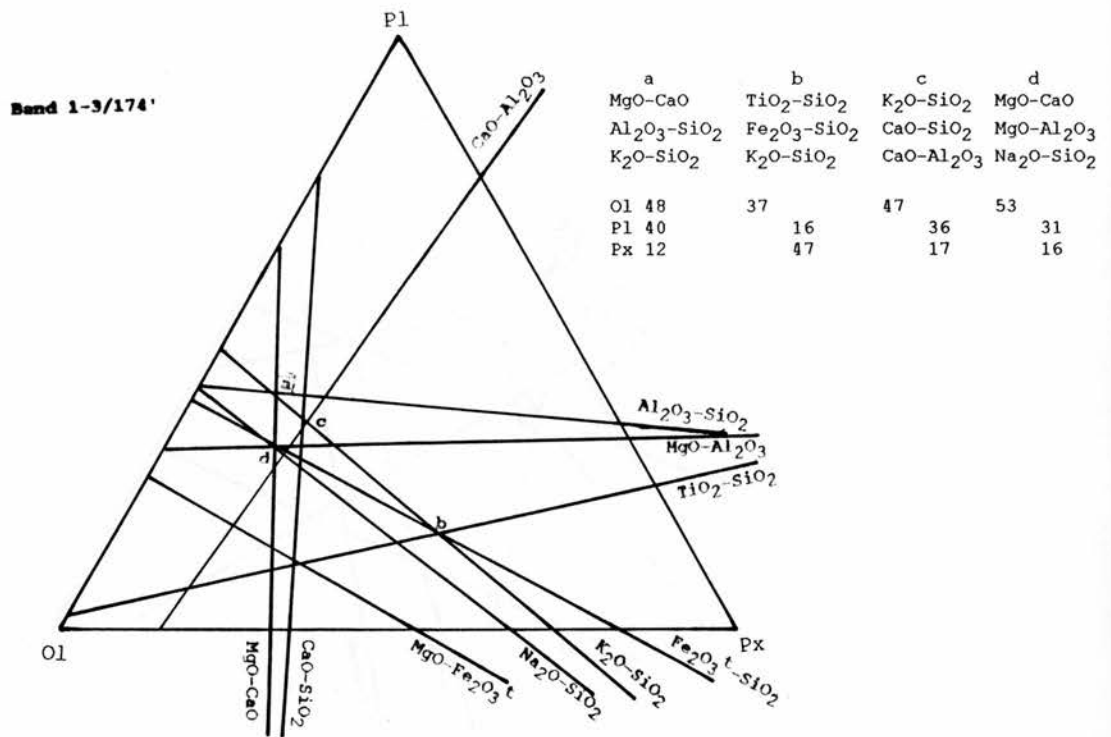


Figure 6.4 Olivine-Plagioclase-Pyroxene three-phase triangles for the determination of best-fit extracts from Parent band to Daughter band composition across the dyke. (Method for their compilation from Cox et al 1979).

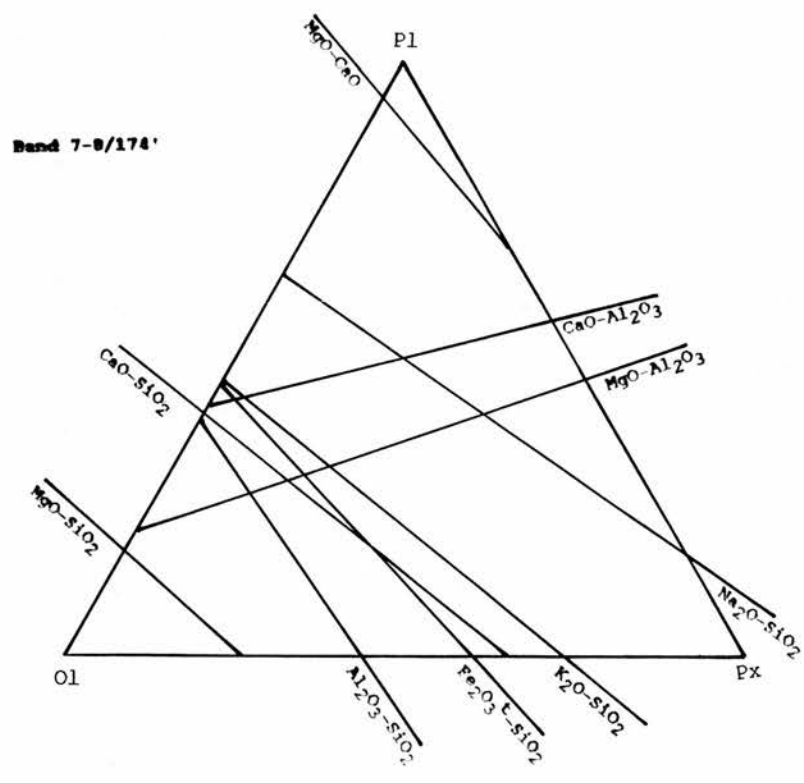
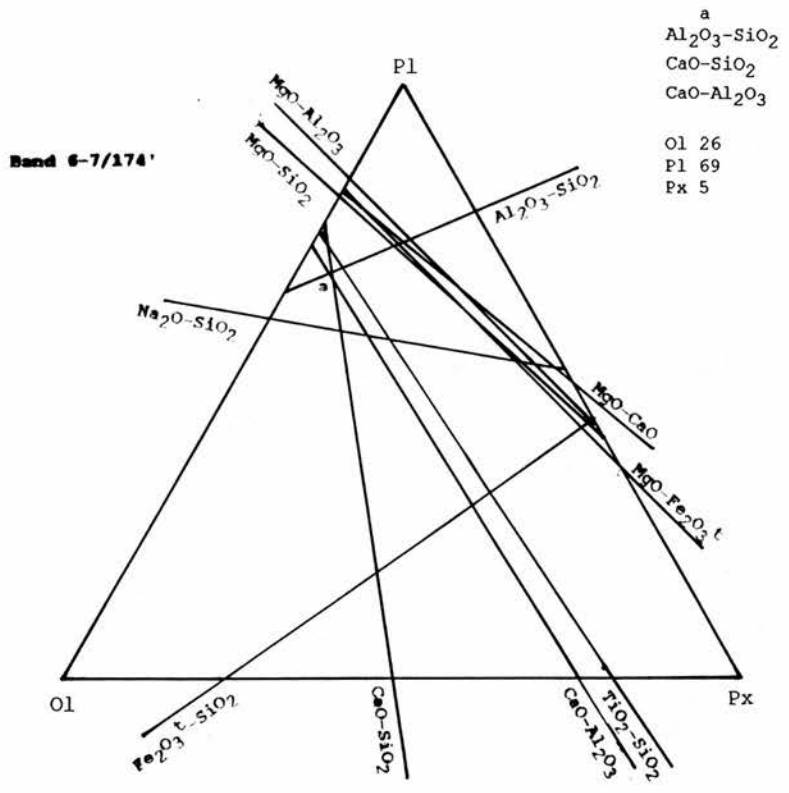


Figure 6.4 Cont.

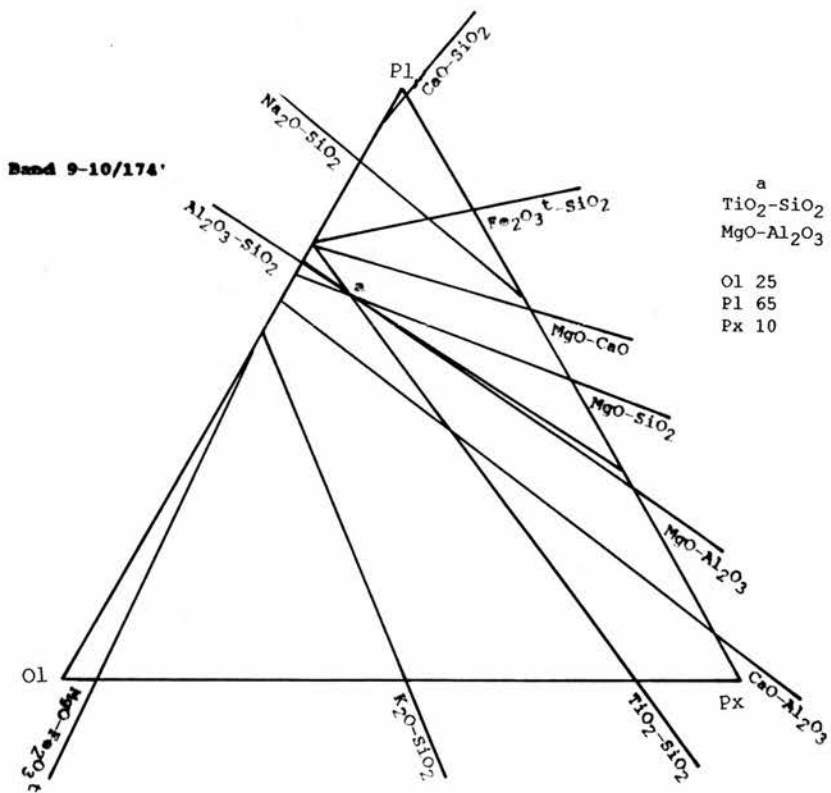
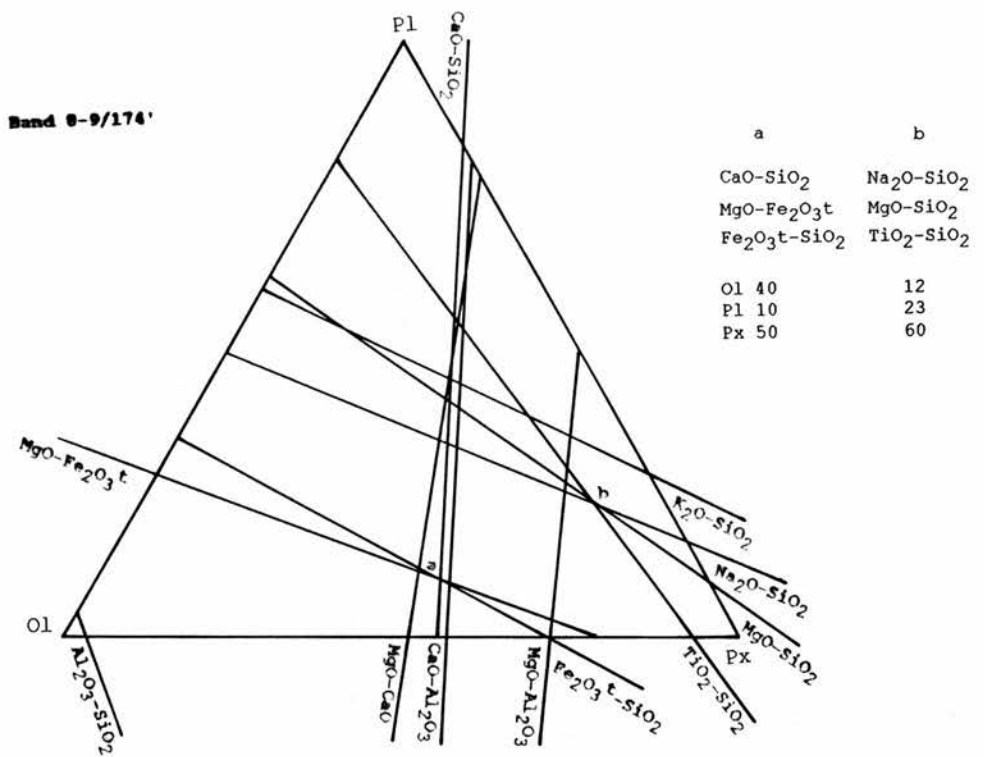


Figure 6.4 Cont.

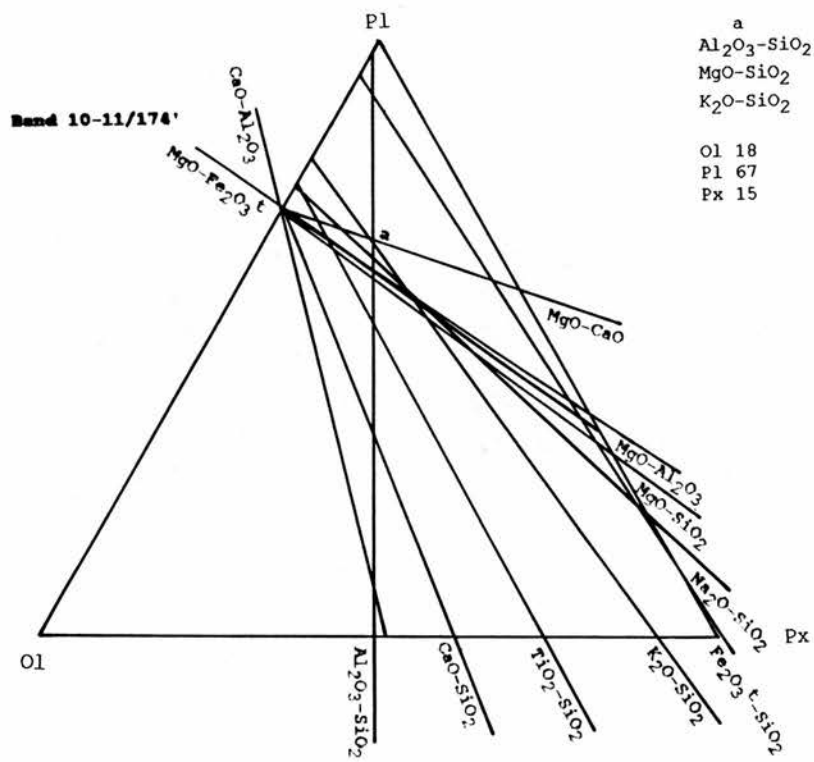


Figure 6.4 Cont.

Continuing magma movement is shown by tangential orientation of groundmass crystals around olivine phenocrysts in Bands 2-4.

Band 4 can be a daughter of a Band 1 composition parent according to calculations of MIX by continued fractionation of olivine. Increasing SiO_2 content of the rock suggests differentiation. This is supported by Figures 5.5a and 5.8e, SiO_2 -MgO and Ni-MgO variation diagrams, together with increasing iron content of the magma indicating continued MgO-rich olivine crystallisation. Spinel fractionation may also be occurring. Figure 6.4 continues the trend for band 1-3 for Band 3-4 development of 50-41% olivine, 32-41% plagioclase and 18% pyroxene for a best-fit extract. Plagioclase phenocrysts display trachytic texture parallel to the walls of the dyke indicating flowing magma. Matrix olivines are of comparable composition to iron-rich phenocryst rims indicating both were in equilibrium with the melt. Pyroxene phenocrysts and matrix crystals are reversely zoned in this band, suggesting complex nucleation and crystallisation conditions.

Silica and iron content of the rock continue to increase into Band 5 suggesting continued differentiation. Fractionation of olivine was still continuing, with possibly some fractionation of pyroxene taking place (Figures 5.8e-f). Figure 6.4 shows 36-48% plagioclase, 54-20% pyroxene and 10-32% olivine as a

best-fit extract mixture. Modally, the sample is enriched in plagioclase and pyroxene compared to Band 4 (Table 3.1). Band 5 contains both zoned and unzoned olivine phenocrysts, the normally zoned variety have rims that are in equilibrium with the melt, while the unzoned variety may represent pyroxene growth during initiation of new magma flow into the fissure. Plagioclase core composition varies little until this band, again suggesting another pulse of magma has come into the dyke. Phenocryst pyroxenes are normally zoned, while matrix ones are reversely zoned to a comparable composition, suggesting the former nucleated in a hotter environment, while the latter formed in the dyke prior to the next magma pulse and are reversely zoned due to increasing magma temperature in the dyke.

Band 6 is taken to represent a fresh pulse of magma intruded along the fissure. It cannot be modelled from a Band 1 composition by mass balancing techniques. As there is no chill developed between Bands 5 and 6, the first pulse may still have been flowing, or separated by a very short period. Whole-rock geochemistry of Band 6 is similar to Band 5 (with the exception of Band 6 being slightly depleted in SiO_2) with both bands lying within the same group on variation diagrams eg Figures 5.5 and 5.8 suggesting similar horizons of the feeder magma chamber continued to be drained, although the reduced volume of olivine phenocrysts may suggest higher layers are being sampled in greater volumes. The higher volume

compositions. Two groups of olivine phenocrysts are contained in Bands 6-9, supporting the idea of pulses of magma, probably with some mixing occurring in the dyke fissure.

MIX shows a R^2 of 0.21 for Band 8 as a daughter of Band 6 composition. Pyroxene and plagioclase were important crystallising phases. Band 8 can be produced by olivine fractionation and addition of plagioclase to the Band 7 composition. The best-fit extract involves approximately 49% olivine 31% plagioclase and 20% pyroxene components.

In this scheme, Bands 9 and 10 formed from another pulse of magma, despite Mix allowing these bands to be acceptable daughter compositions from a Band 6 parent composition. This suggests pulses of near-identical magma. The calculated equilibrium temperatures for Bands 9 and 10 increase from that for Band 8. MgO shows increasing content across Bands 8-10, supporting the proposal of a fresh pulse of magma.

The best-fit extract (Figure 6.4) involves 40:10:50% or 12:23:65% olivine:plagioclase:pyroxene, with pyroxene and olivine being removed and plagioclase added to the melt. Comb-textured pyroxene is present in Band 9, indicating that superheated magma became supercooled.

The "reverse" trend of olivine fractionation is shown from Bands 9 to 10, by the SiO_2 -MgO variation diagram (Figure 5.5a), suggesting olivine accumulation in the magma, with modal olivine increasing across Bands 9-

10. Cr-MgO (Figure 5.8f) shows pyroxene and/or spinel fractionation across Bands 9-10, with the former band relatively enriched in both these minerals. Figure 6.4 shows plagioclase, olivine then pyroxene in order of importance in development of Band 10 from Band 9 (65% plagioclase, 25% olivine and 10% pyroxene). The lever rule figures used in the preparation of Figure 6.4 show addition of olivine and possible fractionation of plagioclase and pyroxene to be occurring.

Comb-texture is present in the Intermediate Unit along the length of the dyke. At 174' it is predominantly olivine- and plagioclase, with a lamina of pyroxene. The precipitation of olivine and plagioclase enriched (possibly supersaturated) the melt in pyroxene components and allowing this mineral to crystallise (see Figure 6.1).

Band 11 cannot be modelled by MIX from a parent Band 10 composition, and must represent a pulse of magma. Geochemically, it is a separate phase (Chapter 5). Figure 6.4 shows a best-fit extract involving 67% plagioclase, 18% olivine and 15% pyroxene, with the lever rule diagrams showing addition of pyroxene and removal of plagioclase. Intrusion of a fresh pulse of magma into the dyke is supported by the internal chill developed in the comb-textured pyroxene lamina adjacent to the Central Unit. The calculated liquidus temperature however shows a decrease from that for Band 10. The first significant amount of pyroxene phenocrysts are found in the

amygdaloidal Central Unit. This unit is amygdaloidal possibly due to formation from water-bearing magma together with high volatile content. This suggests that the magma possibly represents a higher horizon of the magma chamber than previous pulses.

6.14 Summary.

Petrogenesis of the Mystery Dyke can be summarised as the partial melting of the mantle and intrusion of fractionated alkali basaltic magma into a relatively small, replenished magma chamber situated in the upper crust. It is reasonable to assume some contamination occurred (Carter et al 1978, Thompson et al 1984), as the magma underwent fractionation of olivine, spinel and plagioclase. The magma was discharged from the shallow-level feeder chamber at high rates as a multiple intrusion of near-identical magma, with only short times separating each pulse of magma, restricting possible further fractionation. However, fractionation of olivine, plagioclase and pyroxene within the dyke continued across several bands between the intrusive pulses of magma. Concentration and filter pressing of volatiles and residual liquids formed amygdaloidal bands and veins. The sill and dyke continued cooling together allowing joints to cut uninterrupted both rock types.

The spectacular comb layers are caused by magma superheating causing destruction of nuclei, followed by supercooling promoting competitive, columnar crystal growth.

The relationship of the dyke to the sill complex and the lavas requires further investigation. Despite, comparabilities, the dyke was not formed from residual liquids from the sill complex, and the sill and dyke did not share the same feeder chamber, due to olivine phenocrysts in the dyke having a higher forsterite content than those in the sill complex. The feeder chambers for the sill and dyke may however, have been laterally connected, as Donaldson (1977) and Thompson et al (1980) suggested numerous sub-volcanic conduits with poor lateral connections to be present on Skye. This inter-connected system of feeder chambers could allow the closely related lavas, sill and dyke to develop independently of each other.

Only one transect (174') was studied in detail in this study, and due to the length, and complex banding of the dyke, further work on the whole of the dyke is required to fully document the variations and aid the understanding of the processes responsible for the variations in banding (both across and along the dyke), mineral chemistry and the geochemistry of the dyke.

Appendix 5.1

Rock samples for geochemical analysis were the freshest possible material. All obviously weathered surfaces were removed using a grinding wheel before the pieces were split using a Lake and Elliot hydraulic splitter with steel jaws. These blocks were then passed through a Sturtevant jaw crusher to reduce the rock into small chippings, which were then ground in a Tema swing mill with tungsten carbide discs until the powder is less than the 200 mesh.

XRF Analysis.

X-ray fluorescence spectrometry (XRF) analysis was conducted on a PHILLIPS PW1212 automatic spectrometer linked to an on-line computer.

Major oxides were determined following the conditions of Norrish and Hutton (1968) and Norrish and Chappell (1977). Analyses were performed on fused beads of 0.5g sample powder and 2.5 Spectroflux 105 and ammonium nitrate as oxidant prepared after the method of Harvey et al (1973) and adapted for use at St. Andrew by R. Batchelor (Int. Pub. 1980).

Accuracy and precision.

The instrument precision c.v.% calculated for the X.R.F. machine at St. Andrews was accepted as a working standard for the calculation of the standard deviation for the dyke compositions. These precision estimates are based on six replicates and the statistics are derived in the manner described by Harvey et al (1973). Appendix 5.1, Table 5.1 shows the dyke composition, standard deviation and range of the dyke composition. Appendix 5.1, Table 5.2 shows the accepted values given by Abbey, Geological Survey of Canada (1977) Paper 77-34, together with those for St. Andrews for comparison of accuracy.

FeO Determination.

This was performed by titration following the procedures of Batchelor (1980) adapted from Wilson (1955). To ensure accuracy, U.S.G.S. standards were also analysed and if necessary, corrections applied to the samples.

Samples were digested in HF and then oxidised by the addition of ammonium metavanadate, any excess of which was removed by adding excess ferrous ammonium sulphate. Any excess ferrous iron was titrated with potassium dichromate and sodium diphenylamine sulphonate indicator.

Appendix 5.1, Table 5.2

Accuracy and precision of the dyke composition, 174'.

Element	Dyke composition	Instrument c.v. %	Standard deviation	Range for Dyke composition:		Detection limits
				Minimum	Maximum	
wt%						
SiO ₂	46.70	0.22	0.103	46.60	46.80	
TiO ₂	1.40	0.33	0.005	1.40	1.41	
Al ₂ O ₃	16.60	0.36	0.060	16.54	16.66	
Fe ₂ O ₃ ^t	11.56	0.53	0.061	11.50	11.62	
MnO	0.18	0.29	0.0005	0.18	0.18	
MgO	9.10	6.73	0.612	8.49	9.71	
CaO	10.40	0.18	0.019	10.38	10.42	
Na ₂ O	3.30	3.27	0.108	3.19	3.41	
K ₂ O	0.40	0.10	0.0004	0.40	0.40	
P ₂ O ₅	0.17	14.02	0.024	0.15	0.19	
ppm						
Nb	2	4.30	0.086	2	2	0.9
Zr	79	0.43	0.340	79	79	0.8
Y	17	3.43	0.583	16	18	0.3
Sr	412	0.45	1.854	410	414	0.3
Rb	4	0.85	0.034	4	4	0.4
Th	1	12.42	0.124	1	1	1.2
Pb	2	4.08	0.082	2	2	1.2
Zn	70	1.19	0.833	69	71	0.5
Cu	74	1.94	1.436	73	75	0.5
Ni	166	0.68	1.129	165	167	0.6
Cr	336	1.04	3.494	333	339	0.9
V	300	2.27	6.810	293	307	1.0
Ba	65	0.96	0.624	64	66	3.7
Hf	2	6.00	0.120	2	2	2.0
Ce	5	1.63	0.082	5	5	4.0
La	4	1.25	0.050	4	4	1.3

H₂O Determination.

Total H₂O was determined by loss-on-ignition during fused bead preparation at T>800°C, (Batchelor 1980).

Trace Element XRF analysis.

Trace elements (Nb, Zr, Y, Sr, Rb, Th, Pb, Zn, Cu, Ni, Cr, V, Ba, Hf, Ce and La) were analysed separately following the conditions of Leake et al (1970) and Norrish and Chappell (1977). Analysis was performed on pressed powder pellets, the powder for which had been homogenised in a TEMA ball mill.

References:

- Abbey S. (1977) Studies in "standard samples" for use in the general analysis of silicate rocks and minerals. Part 5: 1977 edition of "usable" values. Geological Survey of Canada. Paper 77-34.
- Anderson D.L. (1989) Theory of the Earth. Blackwell Scientific Publications.
- Anderson F.W., Dunham K.C. (1966) The Geology of Northern Skye. Memoirs of the geological Survey, Scotland. H.M.S.O. Edinburgh.
- Anderton R., Bridges P.H., Leeder M.R., Sellwood B.W. (1979) A Dynamic Stratigraphy of the British Isles. George Allen and Unwin.
- Bhattacharji S. (1964) Mechanics of flow differentiation in ultramafic and mafic sills. J. Geol. 75:101-112.
- Barriere M. (1976) Flowage differentiation: limitations to the "Bagnold Effect" to the narrow intrusions. Contrib. Mineral. Petrol. 55:139-145.
- Basaltic Volcanism Study Project (1981) Basaltic Volcanism on the Terrestrial Planets. Pergamon Press Inc. New York.
- Batchelor R.A. (1980) Analysis of major, minor and selected trace elements in silicate rocks and minerals. Internal Publication No 80/1, Univ. St. Andrews.
- Batemann P.C., Lockwood J.P., Lyndon P.A. (1963) Geological map of the Kaiser Peak quadrangle, Central Sierra Nevada, California. Prof. Paper U.S. Geol. Survey 414D.
- Bell B.R., Harris J.R. (1986) An Excursion Guide to the Geology of the Isle of Skye. The Geological Society of Glasgow.
- Blake S. (1981) Volcanism and the dynamics of open magma chambers. Nature 289:783-785.

- Blake S. and Ivey G.N. (1986) Density and viscosity gradients in zoned magma chambers, and their influence on withdrawal dynamics. *Jour. Volcanol. and Geotherm. Res.* 30:201-223.
- Blanchard J.P.L., Boyer P., Gagny C. (1979) Un nouveau critere de sens de mise en place dans une caisse filonienne le "pincement" des mineraux aux epontes. *Tectonophysics* 53:1-25.
- Bowen N.L. (1914) The Ternary system: Diopside-Forsterite-Silica. *Amer. J. Sci.* 38:207-264.
- Brandsdottir B. and Einarrson P. (1979) Seismic activity associated with the September, 1977 deflation of the Krafla Central Volcano in northeastern Iceland. *Jour. Volcanol. and Geotherm. Res.* 6:197-212.
- Brown G.M. (1956) The layered ultrabasic rocks of Rhum, Inner Hebrides. *Phil. Trans. Roy. Soc. London. Ser. B.* 240:1-53.
- Brown G.M. (1967) Mineralogy of basaltic rocks. In Hess H.H & Poldervaart A. (eds) *Basalts 1*, New York: Interscience pp103-62.
- Bryan W.B. (1972) Morphology of Quench crystals in submarine basalts. *J. Geophys. Res.* 77:5812-5819.
- Bryan W.B., Finger L.W., Chayes F. (1969) Estimating proportions in petrographic mixing equations by least squares approximation. *Science* 163:926-927.
- Cameron E.N. (1980) Evolution of Eastern Bushveld Complex. *Econ Geol.* 75:845-871.
- Carmichael I.S.E., Turner F.J., Verhoogen J. (1974) *Igneous Petrology*. McGraw-Hill Book Co.
- Carter S.R., Evensen N.M., Hamilton P.J. and O'Nions R.K. (1978) Nd- and Sr- isotope evidence for crustal contamination of continental volcanics. *Science* 202:743-747.
- Cas R.A.F. and Wright J.V. (1987) *Volcanic Successions modern and ancient*. Allen and Unwin.
- Chalmers B. (1964) *Principles of Solidification*. Wiley and Sons, New York.

- Cox K.G., Bell J.D. and Pankhurst R.J. (1979) The Interpretation of Igneous Rocks. George Allen and Unwin. London.
- Deer W.A., Howie R.A., Zussman J. (1962) Rock-Forming Minerals. Volume One: Ortho- and Ring Silicates. Longmans, Green and Co. Ltd. London.
- Deer W.A., Howie R.A., Zussman J. (1965) Rock-Forming Minerals. Volume Two: Chain Silicates. Longmans, Green and Co. Ltd. London.
- Deer W.A., Howie R.A., Zussman J. (1975) Rock-Forming Minerals. Volume Four: Framework Silicates. Longman Group Ltd. London.
- Deer W.A., Howie R.A., Zussman J. (1982) An Introduction to the Rock Forming Minerals. Longman (13th Impression).
- Deer W.A., Howie R.A., Zussman J. (1982) Rock Forming Minerals: Volume 1A: Orthosilicates. Second Edition. John Wiley and Sons.
- Delaney P.T. and Pollard D.F. (1982) Solidification of basaltic magma during flow in a dike. Am. J. Sci. 282:856-885.
- Donaldson C.H. (1975) A Petrogenetic Study of Harrisite in the Isle of Rhum Pluton, Scotland. PhD Thesis (Unpub.) University of St. Andrews.
- Donaldson C.H. (1976) An experimental investigation of olivine morphology. Contr. Min. and Pet. 57:187-213.
- Donaldson C.H. (1977) Laboratory duplication of comb layering in the Rhum pluton. Min. Mag. 41:323-336.
- Donaldson C.H. (1979) An experimental investigation of the delay in nucleation of olivine in mafic magmas. Contrib. Mineral. and Petrol. 69:21-32.
- Donaldson C.H. (1983) Tertiary igneous activity in the Inner Hebrides. Proc. Roy. Soc. Edin. 83B:65-81.
- Donaldson C.H., Reid A.M. (1982) Multiple Intrusion of a Kimberlite Dyke. Trans. Geol. Soc. S. Afr. 85:1-12.

- 109
- Drever H.I. (1963) A Note on the Field Relations of the Shiant Isle's Picrite. *Geol. Mag.* 90:159-60.
- Drever H.I. (1969) The alkali olivine dolerite-picrodolerite-picrite sills and the banded alkali dolerite dyke in Northern Trotternish. In *Geologists' Association Guides No. 13: The Tertiary Igneous Geology of the Isle of Skye.* pp9-15.
- Drever H.I., Johnston R. (1957) Crystal growth of forsteritic olivine in magmas and melts. *Trnas R. Soc Edin.* 63:287-315.
- Drever H.I., Johnston R. (1958) The petrology of picritic rocks in minor intrusions- A Hebridean group. *Trans R. Soc. Edin.* 63:459-497.
- Drever H.I., Johnston R. (1967) Picritic minor intrusions. In *Wyllie P.J. (ed) Ultramafic and Related Rocks.* John Wiley and Sons pp71-86.
- Drever H.I., Johnston R. (1972) Metastable Growth Patterns in some Terrestrial and Lunar Rocks. *Meteoritics* 7:327-340.
- Droop G.T.R. (1987) A general equation for estimating Fe³⁺ concentrations in ferromagnesian silicates and oxides from microprobe analyses, using stoichiometric criteria. *Min. Mag.* 51:431-435.
- Dunham A.C., Wadsworth W.J. (1978) Cryptic variation in the Rhum layered intrusion. *Min Mag* 42:347-356.
- Ehlers E.G., Blatt H. (1982) *Petrology Igneous, Sedimentary and Metamorphic.* W.H. Freeman and Company.
- Eitel W. (1954) *The Physical Chemistry of the Silicates.* Uni of Chicago Press.
- Elliston J.N. (1984) Orbicules: An indication of the crystallisation of hydrosilicates 1. *Earth Sci. Rev.* 20:265-344.
- Emeleus C.H. (1983) Tertiary Igneous Geology. In *Craig G.Y. (Ed) Geology of Scotland.* Scottish Academic Press. Edinburgh.
- Enz R.D., Kudo A.M. and Brookins D.G. (1979) Igneous origin of the orbicular rocks of the Sandia

- Mountains, New Mexico: Summary. Geol. Soc. Am. Bull. 90:138-140.
- Evans A.L., Fitch F.J., Miller J.A. (1973) K-Ar determinations on some British Tertiary rocks. J. Geol. Soc. London. 129:419-443.
- Ewart A., Hildreth W. and Carmichael I.S.E. (1975) Quaternary acid magma in New Zealand. Contrib. Mineral. and Petrol. 51:1-27.
- Fisk M.R., Bence A.E. (1980) Experimental crystallization of chrome spinel in Famous Basalt 527-1-1. Earth Planet Sci Lett. 48:111-123.
- Fleet M.E. (1975) Growth Habits of Clinopyroxene. Canadian Mineralogist Vol 13:336-341.
- Floyd P.A., Winchester J.A. (1975) Magma type and tectonic setting discrimination using immobile elements. Earth Planet Sci Lett 27:211-218.
- Fuller R.E. (1927) The mode of origin of the colour of certain varicolored obsidians. J. Geol. 35:570-573.
- Geist D.J., McBirney A.R., Baker B.H. (1989) MacGPP: A Program Package for Creating and Using Geochemical Data Files.
- Geikie A. (1897) The Ancient Volcanoes of Great Britain. Vol 2. London.
- Gibb F.G.F. (1968) Flow differentiation in the xenolithic ultrabasic dykes of the Cuillins and the Strathaird Peninsula, Isle of Skye, Scotland. Jour. Pet:9:411-443.
- Gibb F.G.F. (1973) The Zoned Clinopyroxenes of the Shiant Isles Sill, Scotland. J of Petrol 14(2):203-230.
- Gibb F.G.F., Gibson S.A. (1989) The Little Minch Sill Complex. Scot. J. Geol. 25:367-370.
- Gibb F.G.F., Henderson C.M.B. (1989) Discontinuities between picritic and crinaitic units in the Shiant Isles Sill: evidence of multiple intrusion. Geol. Mag. 126:127-137.

- 182
- Gibb F.G.F., Henderson C.M.B. (1992) Convection and crystal settling in sills. *Contrib. Mineral. Petrol.* 109(4):538-545.
- Gibson S.A. (1988) The geochemistry, mineralogy and petrology of the Trotternish Sill Complex, northern Skye, Scotland. Kingston Polytechnic Ph.D. thesis (unpubl.)
- Gibson S.A. (1990) The Geochemistry of the Trotternish sills, Isle of Skye: crustal contamination in the British Tertiary Volcanic Province. *J Geol Soc London* 147:1071-1081.
- Gibson S.A., Henderson C.M.B. (1989) Discontinuities between picritic and crinaitic units in the Shiant Isles Sill: evidence of multiple intrusion. *Geol Mag* 126:127-137.
- Gibson S.A., Jones A.P. (1991) Igneous stratigraphy and internal structure of the Little Minch Sill Complex, Trotternish Peninsula, northern Skye, Scotland. *Geol. Mag.* 128:51-66.
- Gill J. (1981) *Orogenic Andesites and Plate Tectonics.* Springer-Verlag.
- Goldsmith J.R. (1953) A "simlexity principle" and its relation to "ease" of crystallisation. *J. Geol.* 61:439-451.
- Haggerty S.E. (1976a) Oxidation of Opaque Mineral oxides in Basalts. In: *Oxide Minerals. Mineral Soc Am Short Course Notes Vol. 3.*
- Haggerty S.E. (1976b) Opaque mineral oxides in terrestrial Igneous rocks. In: *Oxide Minerals. Mineral Soc Am Short Course Notes Vol. 3.*
- Hall A.L. (1932) The Bushveld Igneous Complex of the Central Transvaal. *Mem. Geol. Surv. S. Afr.* 28:554.
- Harker A. (1904) *The Tertiary Igneous Rocks of Skye.* Mem. Geol. Survey United Kingdom. H.M.S.O. Edinburgh.
- Harry W.T., Pulvertaft T.C.R. (1963) The Nunarssuit Intrusive Complex, South Greenland. *Medd. om Gronland,* 169:No.1:4-136.

- Harvey P.K., Taylor D.M., Hendry R.D. and Bancroft F.
(1973) An accurate fusion method for the analysis
of rocks and chemically related materials by X-ray
fluorescence spectrometry. X-ray Spectro. 5:33-44.
- Henderson P. (1982) Inorganic Geochemistry. Pergamon
Press.
- Henderson P., Suddaby P (1971) The nature and origin of
the chrome-spinel of the Rhum layered intrusion.
Contrib Mineral. Petrol. 33:21-31.
- Hess H.H. (1949) Chemical composition and optical
properties of common clinopyroxenes. Amer. Min.
34:621-666.
- Hildreth W. (1979) The Bishop Tuff: evidence for the
origin of compositional zonation in silicic magma
chambers. Geol. Soc. Am. Sp. Paper 180:43-75.
- Hill R., Roeder P. (1974) The crystallisation of spinel
from basaltic liquid as a function of oxygen
fugacity. J. Geol. 82:pp709.
- Hughes (1982) Igneous Petrology. Elsevier, New York,
U.S.A.
- Huppert H.E. and Sparks R.S.J. (1980) The fluid
dynamics of a basaltic magma chamber replenished by
influx of hot, dense ultrabasic magma. Contrib.
Mineral. and Petrol. 75:279-289.
- Huppert H.E. and Turner J.S. (1981) A laboratory model
of a replenished magma chamber. Earth and Planet.
Sci. Lett. 54:144-152.
- Hutchinson C.S. (1974) Laboratory Handbook of
Petrographic Techniques. Wiley-Interscience
Publications.
- Iddings J.P. (1887) The nature and origin of
lithophysae and the lamination of acid lavas. Am.
J. Sci. 33:36-45.
- Irvine T.N. (1967) Chromian Spinel as a Petrogenetic
Indicator. Part 2. Petrologic Applications.
Canadian Jour Earth Sciences. 4:71-103.
- Irvine T.N. (1975) Olivine-Pyroxene-plagioclase
relations in the system Mg_2SiO_4 - $CaAl_2Si_2O_8$ -
 $KAlSi_3O_8$ - SiO_2 and their bearing on the

differentiation of stratiform intrusions. Carnegie Inst. Washington Yearbook 74:492-500.

Irvine T.N. (1978) Infiltration mechanism, adcumulus growth, and secondary differentiation in the Muskox Intrusion. Carnegie Inst. Washington Yearbook 77:743-751.

Irvine T.N. (1979) Rocks whose composition is determined by crystal accumulation and sorting. in H.S.Yoder (ed) The Evolution of Igneous Rocks. Fiftieth Anniversary Perspectives. Princeton Univ. Press, 245-306.

Irvine T.N. (1982) Terminology for layered intrusions. J. Petrol. 23:127-62.

Irvine T.N. (1987) Glossary of Terms for Layered Intrusions. Appendix 1. in: Parsons I.(ed) Origins of Igneous Layering pp641-647 D. Reidel Publishing Co.

Irvine T.N., Baragar W.R.A. (1971) A Guide to the Chemical Classification of the Common Volcanic Rocks. Canadian Jour Earth Sciences 8:523-543.

Jackson D.B., Swanson D.A., Koyanagi K.Y and Wright T.L. (1975) The August and October 1968 East Rift eruptions of Kilauea Volcano, Hawaii. U.S. Geol. Survey Prof. Paper 890:pp33.

Jaeger J.C. (1968) Cooling and solidification of igneous rocks. In: Basalts Vol 2. Ed by Hess H.H. and Poldervaart A. Interscience Publishers.

Judd J.W. (1874) The Secondary Rocks of Scotland. Second Paper. On the Ancient Volcanoes of the Highlands and the Relations of their Products to the Mesozoic Strata. Quart. Jour. Geol. Soc. 30:220-301.

Kennedy G.C (1955) Some aspects of the role of water in rock melts. Geol. Soc. Am. Special Paper 62:489-503.

Kinoshito W.T, Koyanagi R.Y., Wright T.L. and Fiske R.S. (1969) Kilauea Volcano: The 1967-68 summit eruption. Science 1:459-468.

Kirkpatrick R.J. (1975) Crystal growth from the melt: a review. Am. Miner. 60:798-814.

- Kirkpatrick R.J. (1981) Kinetics of crystallisation of igneous rocks. In A.C. Lasaga and R.J. Kirkpatrick (Eds) Kinetics of geochemical processes. Min. Soc. Am. Reviews in Mineralogy. 8:321-398.
- Komar P.D. (1972a) Mechanical interactions of phenocrysts and flow differentiation of igneous dikes and sills. Geol. Soc. Am. Bull. 83:973-988.
- Komar P.D. (1972b) Flow differentiation of igneous dikes and sills: Profiles of velocity and phenocryst concentration. Geol. Soc. Am. Bull. 83:3443-3448.
- Kouchi A., Sugawara J., Kashima K., Sunagawa I. (1983) Laboratory growth of sector zoned clino-pyroxene in the system Ca Mg Si₂ O₆ - Ca Ti Al₂O₆. Contrib. Mineral. Petrol. 83:177-184.
- Krauskopf K.B. (1967) Introduction to Geochemistry. McGraw-Hill Book Co.
- Kushiro I. (1964) Petrology of the Atumi Dolerite, Japan. Jour. Fac. Sci. Uni. of Tokyo. SecII, Vol 15:135-202.
- Leake B.E., Hendry G.L., Kemp A., Plant A.G., Harry P.K., Wilson J.R., Coats J.S., Ancott J.W. Lunel and Howarth R.J. (1970) The chemical analysis of rock powders by automatic X-ray fluorescence. Chem Geol. 5:7-86.
- Leveson D.J. (1966) Orbicular Rocks: A Review. Geol. Soc. Am Bull. 77:409-426.
- Leveson D.J. (1973) Origin of Comb Layering and Orbicular Structure, Sierra Nevada Batholith, California: Discussion. Bull. Geol. Soc. Am. 84:4005-4006.
- Lister J.R., Campbell I.H. and Kerr R.C. (1991) The eruption of komatiites and picrites in preference to primitive basalts. Earth and Planet Sci. Lett. 105:343-352.
- Lofgren G.E. (1974) An isotherma study of plagioclase crystal morphology: Isothermal crystallisation. Am. Jour. Sci. 274:243-273.
- Lofgren G.E. (1980) Experimental studies on the dynamic crystallisation of silicate melts. In R.B.

- Hargraves, (Ed) Physics of magmatic processes 487-551. Princeton University Press, Princeton, New Jersey.
- Lofgren G.E. (1983) Effect of heterogeneous nucleation on basaltic textures: A dynamic crystallisation study. Jour. Petrol. 24:229-255.
- Lofgren G. E., Donaldson C.H. (1975) Curved branching crystals and differentiation in comb-layered rocks. Contrib. Mineral Petrol. 49:309-319.
- Lofgren G. E., Donaldson C.H., Williams R.J., Mullins O. & Usselman T.M. Experimentally reproduced textures and mineral chemistry of Apollo 15 Qz-normative basalts. Proc.5th Lunar Sci. pp549-567.
- Loomis A.A. (1963) Noritic anorthositic bodies in the Sierra Nevada batholith. Mineral. Soc. Am. Spec. Paper 1:62-68.
- Luhr J.F., Carmichael I.S.E. (1980) The Colima Volcanic Complex, Mexico 1. Post-caldera andesites from Volcan Colima. Contrib. Mineral Petrol. 71:343-372.
- Maaloe S., Tumyr O., James D. (1989) Population density and zoning of olivine phenocrysts in tholeiites from Kauai, Hawaii. Contrib. Mineral. Petrol. 101:176-186.
- MacKenzie W.S., Donaldson C.H., Guilford C. (1982) Atlas of Igneous Rocks and their Textures. Longman.
- Marsh B.D. (1989) On convection style and vigor in sheet-like magma chambers. Jour. Petrol. 30:479-530.
- Martin D., Griffiths R.W and Campbell I.H. (1987) Compositional and thermal convection in magma chambers. Contrib. Mineral. Petrol. 96:465-475.
- McBirney A. R. (1979) Effects of assimilation. In Yoder H.S. (Ed) The Evolution of the Igneous Rocks. 50th Anniversary Perspectives. Princeton University Press, Princeton, New Jersey, U.S.A.
- McBirney A. R., Noyes R.M. (1979) Crystallisation and layering of the Skaergaard Intrusion. Jour. of Petrol. 20:487-554.

- McBirney A. R., Baker B.H. and Nilson R.H. (1985)
Liquid fractionation Part 1: Basic principles and
experimental simulation. Jour. Volcanol. Geotherm.
Res. 24:1-24.
- Middlemost E.A.K. (1975) The Basalt Clan. Earth
Science Reviews 11:337-364.
- Middlemost E.A.K. (1980) A Contribution to the
nomenclature and classification of volcanic rocks.
Geol. Mag. 117:51-57.
- Middlemost E.A.K. (1985) Magmas and Magmatic Rocks.
Longman.
- Mohammed A.R.O. (1982) Mineralogy and Petrology of
Eilean Mhuire, Shiant Islands. PhD Thesis
(unpubl), University of Cambridge.
- Moorbath S., Thompson R.N. (1980) Strontium Isotope
Geochemistry and Petrogenesis of the Early Tertiary
Lava Pile of the Isle of Skye, Scotland, and other
Basic Rocks of the British Tertiary Province: an
Example of Magma-Crust Interaction. J Petrol
21:295-321.
- Moore J.G., Lockwood J.P. (1973) Origin of comb
layering and orbicular structure, Sierra Nevada
batholith, California. Bull. Geol. Soc. Am. 84:1-
20.
- Morimoto N. (1988) Nomenclature of Pyroxenes.
Subcommittee on Pyroxenes, IMA. Min. Mag. 152:535-
550.
- Morrison M.A. (1977) Interactions between water and
Palaeocene basalt, Mull, NW Scotland. Abstracts of
IASPEI/IAVCEI meeting, Durham, 250.
- Morrison M.A. (1978) The use of immobile trace elements
to distinguish palaeotectonic affinities of
metabasalts: applications to the Palaeocene basalts
of Mull and Skye, NW Scotland. Earth and Planet Sci
Lett 39:407-416.
- Morrison M.A., Thompson R.N., Gibson S.A., Marriner G.F.
(1980) Lateral chemical heterogeneity in the
Palaeocene upper mantle beneath the Scottish
Hebrides. Phil Trans Roy Soc London. A297:229-244.

- Morse S.A. (1980) Basalts and Phase Diagrams: An Introduction to the quantitative use of phase diagrams in Igneous Petrology. Springer-Verlag, New York, U.S.A.
- Mueller R.F., Saxena S.K. (1977) Chemical Petrology with applications to The Terrestrial Planets and Meteorites. Springer-Verlag.
- Murase T. and McBirney A.R. (1973) Properties of some common igneous rocks and their melts at high temperature. Geol. Soc. Am. Bull. 84:3563-3592.
- Murray R.J. (1954) The Clinopyroxenes of the Garbh Eilean Sill, Shiant Isles. Geol. Mag 91:17-31.
- Mussett A.E. (1986) ^{40}Ar - ^{39}Ar step-heating ages of the Tertiary igneous rocks of Mull, Scotland. Jour of the Geol. Soc. 143: 887-896.
- Nakamura K (1972) Intrusion vector of dike magmas, its field criteria (Abstr.) Bull. Volcanol. Soc. Jpn. 17:115.
- Nathan H.N., Van Kirk C.K. (1978) A model of magmatic crystallisation. Jour. Petrol. 19:66-94.
- Nelson S.A. (1981) The possible role of thermal feedback in the eruption of siliceous magmas. Jour. Volcanol. Geotherm. Res. 11:127-137.
- Norrish K. and Chappell B.W. (1977) Pages 201-272 in "Physical methods in Determinative mineralogy". Ed Zussman J. Academic Press.
- Norrish K. and Hutton (1968) An accurate X-ray spectrographic method for analysis of a wide range of geological samples. Geochem et Cosmochim Acta 33:431-453.
- O'Hara M.J. (1968) The bearing of phase equilibria studies on the origin and evolution of basic and ultrabasic rocks. Earth Sci. Rev 4:69-133.
- O'Hara M.J. (1977) Geochemical evolution during crystallisation of a periodically refilled magma chamber. Nature 266:503-507.
- O'Hara M.J., Mathews R.E. (1981) Geochemical evolution in an advancing, periodically replenished,

- periodically tapped, continuously fractionated magma chamber. *J. Geol. Soc. London* 138:237-277.
- Pearce T.H. (1984) The analysis of zoning in magmatic crystals with emphasis on olivine. *Contrib Mineral Petrol.* 86:149-154.
- Petersen J.S. (1985a) Columnar-Dendritic Feldspars in the Lardalite Intrusion, Oslo Region, Norway:1. Implications for Unilateral Solidification of a Stagnant Boundary Layer. *J Petrology* 26:223-252.
- Petersen J.S. (1985b) The Directional Solidification of Silicate melts: Crystallization Kinetics and Macrosegregation. In: *Ten Papers in the Exact Sciences and Geology being Part One of Sixteen Research Reports by the Niels Bohr Fellows of the Royal Danish Academy of Sciences and Letters published on the Occasion of the Centenary of Niels Bohr.* Det Kongelige Danske Videnskabernes Selskab Matematisk-fysiske Meddelelser 41, Copenhagen.
- Petersen J.S. (1981) Solidification contraction: another approach to cumulus processes and the origin of igneous layering. In I. Parsons (Ed) *Origins of igneous layering.* D.Reidel Publishing Co.
- Petersen J.S. and Lofgren G.E. (1986) Lamellar and patchy intergrowths in feldspars: Experimental crystallisation of eutectic silicates. *American Mineralogist* 71:343-355.
- Platten I.M., Watterson J.S. (1969) Orientated crystal growth in some Tertiary dykes. *Nature* 223:286-287.
- Poldervaart A., Taubeneck W.H. (1959) Willow-Lake type layered intrusions. *Bull. Geol. Soc. Am.* 70:1393-8.
- Preston J. (1963) A Columnar Growth of Dendritic Pyroxene. *Geol. Mag.* 103:548-557.
- Prinz M. (1968) *Geochemistry of Basaltic Rocks: Trace Elements In Basalts: The Poldervaart Treatise on Rocks of Basaltic Composition Volume 1.* Ed by Hess H.H. & Poldervaart A. Interscience Publishers-John Wiley & Sons.
- Richey J.E. (1961) *British Regional Geology. Scotland: The Tertiary Volcanic Districts. (Third Edition)* H.M.S.O. Edinburgh.

- Ridley W.I. (1973) The Petrology of volcanic rocks from the Small Isles of Inverness-shire. Inst. Geol. Sci. London. Report 73/10. 55pp.
- Ridley W.I. (1977) The Crystallisation Trends of Spinels in Tertiary Basalts from Rhum and Muck and Their Petrogenetic Significance. Contrib. Mineral. Petrol. 64:243-255.
- Ringwood A.E. (1975) Composition and Petrology of the Earth's Mantle. McGraw-Hill Book Company.
- Roeder P.L. and Emslie R.F. (1970) Olivine-Liquid Equilibrium. Contr. Mineral. and Petrol. 29:275-289.
- Rutter J.W. and Chalmers B. (A prismatic substructure formed during solidification of metals Can. J. Phys. 31:15-39.
- Schwarzer R.R., Rogers J.J.W. (1974) A Worldwide Comparison of Alkali Olivine Basalts and their Differentiation Trends. Earth Planet Sci Lett 23:286-296.
- Shannon J.R., Walker B.M., Carter R.B., Geraghty E.P. (1982) Unidirectional solidification textures and their significance in determining relative ages of intrusion at the Henderson Mine, Colorado. Geology 10:293-7.
- Shaw H.R. (1969) Rheology of basalt in the melting range. J. Petrol. 10:510-535.
- Shaw H.R. (1974) Diffusion of H₂O in granitic liquids. Part 1: Experimental data. Part 2: Mass transfer in magma chambers. In Hoffman A.W., Gileti B.J. Yoder H.S. Jr. Yund R.A. (Eds) Geochemical Transport and Kinetics. Carnegie Inst. Washington Publication 634:139-170.
- Shelley D. (1985) Determining paleo-flow directions from groundmass fabrics in the Lyttelton radial dykes, New Zealand. J. Volcano. Geotherm. Res. 25:69-79.
- Sigurdsson H., Schilling J.G. (1976) Spinels in mid-Atlantic ridge basalts: Chemistry and occurrence. Earth Planet Sci Lett 29:7-20.

- Simkin T. (1965) The Picritic Sills of North Skye, Scotland. PhD Thesis, Princeton University (unpublished).
- Simkin T. (1967) Flow Differentiation in the Picritic Sills of North Skye. In: Ultramafic and Related Rocks. Ed: P.J. Wyllie John Wiley and Sons.
- Simkin T., Smith J.V. (1970) Minor element distribution in olivine. J Geol 78:304-325.
- Smith D., Lindsley D.H. (1971) Stable and metastable augite crystallisation trends in a single basalt flow. Am Mineral 56:225-233.
- Sparks R.S.J. (1978) The dynamics of bubble formation and growth in magmas: a review and analysis. Jour. Volcanol. Geotherm. Res. 3:1-37.
- Sparks R.S.J., Sigurdsson H. and Wilson L. (1977) Magma mixing: a mechanism of triggering acid explosive eruptions. Nature 267:315-318.
- Sparks R.S.J., Huppert H.E and Turner J.S. (1984) The fluid dynamics of evolving magma chambers. Phil. Trans. R. Soc. Lond. A310:511-534.
- Sparks R.S.J. and Huppert H.E. (1984) Density changes during the fractional crystallisation of basaltic magmas: implications for the evolution of layered intrusions. Contr. Mineral. Petrol. 85:300-309.
- Stolper E and Walker D. (1980) Melt density and the average composition of basalt. Contr. Mineral. Petrol. 74:7-12.
- Tarshis L.A., Tiller W.A. (1967) The Effect of interface-attachment kinetics on the morphological stability of a planar interface during solidification. In: Crystals Growth, Peiser H.S. (ed) pp709-719 Pergamon Oxford.
- Tashiro M., Kobubo T., Ito S. and Arioka M. (1975) Bull. Inst. Chem. Res. Kyoto University 53:471-488.
- Taubeneck W.H., Poldervaart A. (1960) Geology of the Elkhorn mountains, Northeastern Oregon: Part 2. Willow Lake Intrusion. Bull. Geol. Soc. Am. 71:1295-1322.

- Taylor S.R. (1964) Abundance of chemical elements in the continental crust. *Geochem et Cosmochim Acta* 28:1280-1281.
- Thompson R.N. (1974) Primary basalts and magma genesis 1. Skye, north-west Scotland. *Contrib. Mineral. Petrol.* 45:317-341.
- Thompson R.N. (1982) Magmatism of the British Tertiary Volcanic Province. *Scot. Jour. Geol.* 18:49-107.
- Thompson R.N., Esson J., Dunham A.C. (1972) Major Element Chemical Variation in the Eocene Lavas of the Isle of Skye, Scotland. *J of Petrol* 13:219-253.
- Thompson et al (1974) Origin of magmas and hydrothermal systems associated with Skye centre ?????
- Thompson R.N., Gibson I.L., Marriner G.F., Matthey D.P., Morrison M.A. (1980) Trace-element evidence of multistage mantle fusion and polybaric fractional crystallization in the Palaeocene lavas of Skye, N.W. Scotland. *J of Petrol* 21:265-293.
- Thompson R.N., Morrison M.A., Hendry G.L. and Perry S.J. (1984) An Assessment of the relative roles of a crust and mantle in magma genesis: an elemental approach. *Phil. Trans. R. Soc. Lond.* A310:549-590.
- Thorarinsson S. (1968) On the rate of lava and tephra production and the upward migration of magma in four Icelandic eruptions. *Geol. Rundschau.* 57:705-718.
- Tiller W.A., Jackson K.A., Rutter J.W. and Chalmers B. (1953) The redistribution of solute atoms during the solidification of metals. *Acta Metallurgica* 1:428-437.
- Tilley, Yoder, Schairer (1964) *Carnegie Inst. Washington Yearbook* 63:92.
- Turner J.S. and Campbell I.H. (1980) Convection and mixing in magma chambers. *Earth Sci. Rev.* 23:255-352.
- Upton B.G.J. (1988) History of Tertiary igneous activity in the N. Atlantic borderlands. In: Morton A.C. and Parson L.M. (eds) *Early Tertiary Volcanism and the opening of the N.E. Atlantic.* *Geol. Soc. Spec. Publ.* 39:429-454.

- Vernon R.H. (1985) Possible role of superheated magma in the formation of orbicular granitoids. *Geology* 13:843-845.
- Wada Y. (1992) Magma flow directions inferred from preferred orientations of phenocryst in a composite feeder dike, Miyake-Jima, Japan. *J Volc Geothermal Res* 49:119-126.
- Wager L.R. (1959) Differing powers of crystal nucleation as a factor producing diversity in layered igneous intrusions. *Geol. Mag.* 96:75-80.
- Wager L.R., Brown G.M. (1951) A note on Rhythmic Layering in the ultrabasic rocks of Rhum. *Geol. Mag.* 88:166-168
- Wager L.R., Brown G.M. (1968) *Layered Igneous Rocks.* Oliver and Boyd.
- Wager L.R., Deer W.A (1939) *Geological Investigations in East Greenland, Part III. The petrology of the Skaergaard Intrusion, Kangerlugssuaq, East Greenland.* *Meddr. Gronland*, 105:1-352
- Wager L.R., Mitchell R.L. (1951) The distribution of trace elements during strong fractionation of basic magma—a further study of the Skaergaard intrusion, East Greenland. *Geochim. et Cosmochim. Acta*, 13:81-6.
- Walker F. (1930) The geology of the Shiantis Isles (Hebrides). *Quart Jour Geol Soc of London* 86:355-398
- Walker F. (1931) The dolerite isles of the North Minch. *Trans Roy Soc Edinburgh* 56:753-766.
- Walker F. (1932) Differentiated sills of Northern Trotternish (Skye). *Trans Roy Soc Edinburgh* 57:241-257.
- Walker F.D.L. (1985) Electron Microprobe analysis of dendritic pyroxene, columnar olivine and plagioclase within the banding of the Mystery Dyke, North Isle of Skye. Carnegie Vacation Scholarship Report, University of St. Andrews (Unpubl).
- Walker D., Kirkpatrick R.J., Longhi J. & Hays J.F. (1976) Crystallisation history of lunar picrite basalt

- sample 12002: phase equilibria and cooling rate studies. Bull. Geol. Soc. Am. 87:646-656.
- Wass S. Y. (1973) The origin and petrogenetic significance of hour-glass zoning in titaniferous clinopyroxenes. Min. Mag. 39:133-144
- Weissberg H.L. (1962) End correction for slow viscous flow through long tubes. Phys. Fluids 5:1033-1036.
- Weston R.M. and Rogers P.S. (1978) The growth of calcium metasilicate polymorphs from supercooled melts and glasses. Min. Mag. 42:325-335.
- White R.S. (1988) A hot-spot model for early Tertiary volcanism in the N. Atlantic. In: Morton A.C. and Parson L.M. (eds) Early Tertiary Volcanism and the opening of the N.E. Atlantic. Geol. Soc. Spec. Publ. 39:429-454.
- Whitney J.A. (1975) The effect of pressure, temperature, and XH_2O on phase assemblages in four synthetic rock compositions. Jour. Geol. 83:1-31.
- Wilson A.D. (1955) A new method for determination of ferrous iron in rocks and minerals. Gt Britain Geol. Surv. Bull. 9:56-58.
- Wilson M. (1989) Igneous Petrogenesis. A Global Tectonic Approach. Unwin Hyman London.
- Windley B.F. (1977) The Evolving Continents. Wiley.
- Wood D.A., Gibson I.L., Thompson R.N. (1976) Elemental mobility during zeolite facies metamorphism of the Tertiary basalts of eastern Iceland. Contrib. Mineral. Petrol. 55:241-254.
- Yoder H.S. (1950) The Jadeite problem- Part 2. Am. Jour. Sci. 248:312-334.
- Zussman J. (1977) (ed) Physical methods in determinative mineralogy. Second edition. Academic Press.